Advanced Courses in Mathematics CRM Barcelona

Jaume Llibre
Richard Moeckel
Carles Simó

Central Configurations, Periodic Orbits, and Hamiltonian Systems

CENTRE DE RECERCA MATEMÀTICA

Birkhäuser

Advanced Courses in Mathematics
CRM Barcelona

Centre de Recerca Matemàtica

Managing Editor:
Enric Ventura

More information about this series at http://www.springer.com/series/5038

Jaume Llibre • Richard Moeckel • Carles Simó

Central Configurations, Periodic Orbits, and Hamiltonian Systems

Editors for this volume:
Montserrat Corbera, Universitat de Vic
Josep Maria Cors, Universitat Politècnica de Catalunya
Enrique Ponce, Universidad de Sevilla

Birkhäuser

Jaume Llibre
Departament de Matemàtiques
Universitat Autònoma de Barcelona
Barcelona, Spain

Richard Moeckel
School of Mathematics
University of Minnesota
Minneapolis, MN, USA

Carles Simó
Dept Matemàtica Aplicada i Anàlisi
Universitat de Barcelona
Barcelona, Spain

ISSN 2297-0304 ISSN 2297-0312 (electronic)
Advanced Courses in Mathematics - CRM Barcelona
ISBN 978-3-0348-0932-0 ISBN 978-3-0348-0933-7 (eBook)
DOI 10.1007/978-3-0348-0933-7

Library of Congress Control Number: 2015956332

Mathematics Subject Classification (2010): 34C29, 34C25, 37J10, 37J15, 37J40, 37J45, 37M05, 37N05, 47H11, 70F07, 70F10, 70F15

Springer Basel Heidelberg New York Dordrecht London
© Springer Basel 2015
This work is subject to copyright. All rights are reserved by the Publisher, whether the whole or part of the material is concerned, specifically the rights of translation, reprinting, reuse of illustrations, recitation, broadcasting, reproduction on microfilms or in any other physical way, and transmission or information storage and retrieval, electronic adaptation, computer software, or by similar or dissimilar methodology now known or hereafter developed.
The use of general descriptive names, registered names, trademarks, service marks, etc. in this publication does not imply, even in the absence of a specific statement, that such names are exempt from the relevant protective laws and regulations and therefore free for general use.
The publisher, the authors and the editors are safe to assume that the advice and information in this book are believed to be true and accurate at the date of publication. Neither the publisher nor the authors or the editors give a warranty, express or implied, with respect to the material contained herein or for any errors or omissions that may have been made.

Printed on acid-free paper

Springer Basel AG is part of Springer Science+Business Media (www.birkhauser-science.com)

Foreword

This book collects the notes of lectures given by Jaume Llibre, Richard Moeckel, and Carles Simó at Centre de Recerca Matemàtica (CRM) in Bellaterra, Barcelona, from January 27th to 31st, 2014. The activity, in the framework of the Research Program on *Central Configurations, Periodic Orbits and Beyond in Celestial Mechanics*, hosted at CRM from January to July 2014, was a joint collaboration with the winter school in dynamical systems *Recent Trends in Nonlinear Science* (RTNS2014), promoted by the DANCE (Dinámica, Atractores y Nolinealidad: Caos y Estabilidad) Spanish network.

The Advanced Course on *Central Configurations, Periodic Orbits and Hamiltonian Systems* aimed at training their participants both theoretically and in applications in the field of nonlinear science; in this area as in many others, the theoretical and the applications points of view clearly reinforce each other.

There were three series of lectures and, accordingly, the material is distributed in three chapters in the book. The first series, delivered by Jaume Llibre, was dedicated to the study of periodic solutions of differential systems in $\mathbb{R}^n$ via Averaging Theory. Roughly speaking, in Averaging Theory one replaces a vector field by its average (over time or an angular variable) with the goal of obtaining asymptotic approximations to the original system that will be capable of guaranteeing the existence of periodic solutions. The corresponding notes in Chapter 1 start with an introduction of the classical, first order averaging theory followed by the main results of the theory for arbitrary order and dimension. The theory is applied next to the study of periodic solutions of some well known differential equations, like the van der Pol differential equation, the Liénard differential systems, or the Rossler differential system, among others. Some Hamiltonian systems are also studied.

The second series of lectures, given by Richard Moeckel, focused on methods for studying central configurations, in Chapter 2. A Central Configuration is a special arrangement of point masses interacting by Newton's law of gravitation, and with the following property: the gravitational acceleration vector produced on each mass by all the others should point toward the center of mass and be proportional to the distance to the center of mass. Central Configurations play an important role in study of the Newtonian n-body problem. For example, they lead to the only explicit solutions of the equations of motion, they govern the behavior of solutions near collisions, and they influence the topology of integral manifolds. The

lectures dealt with questions about the existence and enumeration of various types of Central Configurations, including algebraic-geometrical approaches to Smale's Sixth Problem: is the number of Central Configurations always finite?

Chapter 3 is devoted to the last series of lectures, given by Carles Simó. They describe the main mechanisms leading to a fairly global description of the dynamics in conservative systems, either in the continuous version described by a Hamiltonian, or in the discrete version. The Newtonian n-body problem belongs to the general class of Hamiltonian systems. The chapter starts with several simple but paradigmatic examples in the 2D case, from which it is easier to grasp the main underlying ideas, also useful in higher dimension. Next, general theoretical results are presented and applied to different problems in Celestial Mechanics, with a rich variety of goals.

We would like to express our gratitude to the director and staff of the Centre de Recerca Matemàtica for making possible this activity. Finally, our special thanks to the three lecturers, Jaume Llibre, Richard Moeckel and Carles Simó, for the enthusiasm they showed during the course and for their fine preparation of these notes. It is our hope that with their publication we may contribute to the spreading of the interest of actual and future researchers for the exciting world of dynamical systems.

Montserrat Corbera, Josep M. Cors and Enrique Ponce

Contents

Chapter 1

The Averaging Theory for Computing Periodic Orbits

Jaume Llibre

1.1 Preface

The method of averaging is a classical tool allowing us to study the dynamics of the non-linear *differential systems* under periodic forcing. The method of averaging has a long history starting with the classical works of Lagrange and Laplace, who provided an intuitive justification of the method. The first formalization of this theory was done in 1928 by Fatou [34]. Important practical and theoretical contributions to the averaging theory were made in the 1930's by Bogoliubov–Krylov [8], in 1945 by Bogoliubov [7], and by Bogoliubov–Mitropolsky [9] (english version 1961). For a more modern exposition of the averaging theory, see the book Sanders–Verhulst–Murdock [78].

Every orbit of a differential system is homeomorphic either to a point, or to a circle, or to a straight line. In the first case it is called a *singular point* or an *equilibrium point*, and in the second case it is called a *periodic orbit*. The third case does not have a name. These notes are dedicated to studying analytically the periodic orbits of a given differential system.

We consider differential systems of the form

$$\dot{\mathbf{x}} = F_0(t, \mathbf{x}) + \varepsilon F_1(t, \mathbf{x}) + \varepsilon^2 R(t, \mathbf{x}, \varepsilon), \tag{1.1}$$

with $\mathbf{x}$ in some open subset D of $\mathbb{R}^n$, $F_i \colon \mathbb{R} \times D \to \mathbb{R}^n$ of class C^2 for $i = 1, 2$, $R \colon \mathbb{R} \times D \times (-\varepsilon_0, \varepsilon_0) \to \mathbb{R}^n$ of class C^2 with $\varepsilon_0 > 0$ small, and with the functions F_i and R being T-periodic in the variable t. Here, the dot denotes derivative with respect to the time t.

© Springer Basel 2015

J. Llibre et al., *Central Configurations, Periodic Orbits, and Hamiltonian Systems*,
Advanced Courses in Mathematics - CRM Barcelona, DOI 10.1007/978-3-0348-0933-7_1

In general, to obtain analytically periodic solutions of a differential system is a very difficult problem, many times a problem impossible to solve. As we shall see when we can apply the averaging theory, this difficult problem for differential systems (1.1) is reduced to finding the zeros of a non-linear function of dimension at most n, i.e., now the problem has the same difficulty as the problem of finding the singular or equilibrium points of a differential system.

An important problem for studying periodic solutions of differential systems of the form

$$\dot{\mathbf{x}} = F(t, \mathbf{x}), \quad \text{or} \quad \dot{\mathbf{x}} = F(\mathbf{x}), \tag{1.2}$$

using averaging theory is to transform them into systems written in the *normal form of the averaging theory*, i.e., as a system (1.1). Note that systems (1.2), in general, are not periodic in the independent variable t and do not have any small parameter ε. So, we must find changes of variables which allow us to write the differential systems (1.2) into the form (1.1), where F_0 can eventually be zero.

The present chapter is divided in three sections. Section 1.2 is dedicated to the averaging theory of first order; we present in it three main results for studying the periodic solutions of differential systems, see Theorems 1.2.1, 1.2.9 and 1.2.18. We develop four applications of Theorems 1.2.1, namely to the van der Pol equation, to the Liénard differential system, to study the zero-Hopf bifurcation in $\mathbb{R}^n$, and to a class of Hamiltonian systems. We present three applications of Theorem 1.2.9; in the first we study the Hopf bifurcation of the Michelson system, in the second the periodic solutions of a third-order differential equation, and in the third one we analyze the periodic solutions of the Vallis system which models the "El Niño" phenomenon. Finally, we do an application of Theorem 1.2.18 to a class of Duffing differential equations.

In Section 1.3, the most theoretical one, we present averaging theory for studying periodic solutions of a differential system in $\mathbb{R}^n$ at any order in the small parameter. This theory is developed using weaker assumptions.

Finally, in Section 1.4, we present some applications of averaging theory of order higher than one. More concretely, using averaging theory of second order we study periodic solutions of the Hénon–Heiles Hamiltonian, and using averaging theory of third order we study first the limit cycles of the quadratic polynomial differential systems, and of the linear with cubic homogeneous non-linearities polynomial differential systems; and finally, we analyze the periodic solutions of the generalized Liénard polynomial differential equations.

1.2 Introduction: the classical theory

1.2.1 A first order averaging method for periodic orbits

We consider the differential system

$$\dot{\mathbf{x}} = \varepsilon F(t, \mathbf{x}) + \varepsilon^2 R(t, \mathbf{x}, \varepsilon), \tag{1.3}$$

with $\mathbf{x} \in D \subset \mathbb{R}^n$, D a bounded domain, and $t \geq 0$. Moreover we assume that $F(t, \mathbf{x})$ and $R(t, \mathbf{x}, \varepsilon)$ are T-periodic in t.

The *averaged system* associated to the system(1.3) is defined by

$$\dot{\mathbf{y}} = \varepsilon f^0(\mathbf{y}), \tag{1.4}$$

where

$$f^0(\mathbf{y}) = \frac{1}{T} \int_0^T F(s, \mathbf{y}) ds. \tag{1.5}$$

The next theorem says under what conditions the singular points of the averaged system (1.4) provide T-periodic orbits for the system (1.3). The proof presented here comes from [85].

Theorem 1.2.1. *We consider system* (1.3) *and assume that the vector functions F, R, $D_{\mathbf{x}}F$, $D^2_{\mathbf{x}}F$ and $D_{\mathbf{x}}R$ are continuous and bounded by a constant M (independent of ε) in $[0, \infty) \times D$, with $-\varepsilon_0 < \varepsilon < \varepsilon_0$. Moreover, we suppose that F and R are T-periodic in t, with T independent of ε.*

(i) *If $p \in D$ is a singular point of the averaged system* (1.4) *such that*

$$\det(D_{\mathbf{x}} f^0(p)) \neq 0 \tag{1.6}$$

then, for $|\varepsilon| > 0$ sufficiently small, there exists a T-periodic solution $\mathbf{x}(t, \varepsilon)$ of system (1.3) *such that $\mathbf{x}(0, \varepsilon) \to p$ as $\varepsilon \to 0$.*

(ii) *If the singular point $\mathbf{y} = p$ of the averaged system* (1.4) *has all its eigenvalues with negative real part then, for $|\varepsilon| > 0$ sufficiently small, the corresponding periodic solution $\mathbf{x}(t, \varepsilon)$ of system* (1.3) *is asymptotically stable and, if one of the eigenvalues has positive real part $\mathbf{x}(t, \varepsilon)$, it is unstable.*

Theorem 1.2.1 is proved in Subsection 1.2.6. Before its proof we shall present some applications of it in Subsection 1.2.2.

For each $\mathbf{z} \in D$ we denote by $\mathbf{x}(\cdot, \mathbf{z}, \varepsilon)$ the solution of (1.3) with initial condition $\mathbf{x}(0, \mathbf{z}, \varepsilon) = z$. We consider also the function $\zeta \colon D \times (-\varepsilon_0, \varepsilon_0) \to \mathbb{R}^n$ defined by

$$\zeta(\mathbf{z}, \varepsilon) = \int_0^T \left[\varepsilon F(t, \mathbf{x}(t, \mathbf{z}, \varepsilon)) + \varepsilon^2 R(t, \mathbf{x}(t, \mathbf{z}, \varepsilon), \varepsilon) \right] dt. \tag{1.7}$$

From (1.3) it follows that, for every $\mathbf{z} \in D$,

$$\zeta(\mathbf{z}, \varepsilon) = \mathbf{x}(T, \mathbf{z}, \varepsilon) - \mathbf{x}(0, \mathbf{z}, \varepsilon). \tag{1.8}$$

The function ζ can be written in the form

$$\zeta(\mathbf{z}, \varepsilon) = \varepsilon f^0(\mathbf{z}) + O(\varepsilon^2), \tag{1.9}$$

where f^0 is given by (1.5). Moreover, under the assumptions of Theorem 1.2.1, the solution $\mathbf{x}(t, \varepsilon)$, for $|\varepsilon|$ sufficiently small, satisfies that $\mathbf{z}_\varepsilon = \mathbf{x}(0, \varepsilon)$ tends to be an isolated zero of $\zeta(\cdot, \varepsilon)$ when $\varepsilon \to 0$. Of course, due to (1.8) the function ζ is a *displacement function* for system (1.3), and its fixed points are initial conditions for the T-periodic solutions of system (1.3).

1.2.2 Four applications

We recall that a *limit cycle* of a differential system is a periodic orbit isolated in the set of all periodic orbits of the system.

The van der Pol differential equation

Consider the *van der Pol differential equation* $\ddot{x} + x = \varepsilon(1 - x^2)\dot{x}$, which can be written as the differential system

$$\begin{aligned} \dot{x} &= y, \\ \dot{y} &= -x + \varepsilon(1 - x^2)y. \end{aligned} \tag{1.10}$$

In polar coordinates (r, θ), where $x = r\cos\theta$, $y = r\sin\theta$, this system becomes

$$\begin{aligned} \dot{r} &= \varepsilon r(1 - r^2\cos^2\theta)\sin^2\theta, \\ \dot{\theta} &= -1 + \varepsilon\cos\theta(1 - r^2\cos^2\theta)\sin\theta, \end{aligned}$$

or, equivalently,

$$\frac{dr}{d\theta} = -\varepsilon r(1 - r^2\cos^2\theta)\sin^2\theta + O(\varepsilon^2).$$

Note that the previous differential system is in the normal form (1.3) for applying the averaging theory described in Theorem 1.2.1 if we take $\mathbf{x} = r$, $t = \theta$, $T = 2\pi$ and $F(t, \mathbf{x}) = -r(1 - r^2\cos^2\theta)\sin^2\theta$.

From (1.5) we get that

$$f^0(r) = -\frac{1}{2\pi}\int_0^{2\pi} r(1 - r^2\cos^2\theta)\sin^2\theta d\theta = \frac{1}{8}r(r^2 - 4).$$

The unique positive root of $f^0(r)$ is $r = 2$. Since $(df^0/dr)(2) = 1$, by Theorem 1.2.1 (i), it follows that system (1.10) has, for $|\varepsilon| \neq 0$ sufficiently small, a limit cycle bifurcating from the periodic orbit of radius 2 of the unperturbed system (1.10) with $\varepsilon = 0$. Moreover, since $(df^0/dr)(2) = 1 > 0$, by Theorem 1.2.1 (ii), this limit cycle is unstable.

The Liénard differential system

The following result is due to Lins–de Melo–Pugh [53]. Here, we provide an easy and shorter proof with respect to the initial proof given by the mentioned authors.

Proposition 1.2.2. *The Liénard differential systems of the form*

$$\begin{aligned} \dot{x} &= y - \varepsilon(a_1 x + \cdots + a_n x^n), \\ \dot{y} &= -x, \end{aligned}$$

with ε sufficiently small and $a_n \neq 0$ have at most $[(n-1)/2]$ limit cycles bifurcating from the periodic orbits of the linear center $\dot{x} = y$, $\dot{y} = -x$, and there are examples with exactly $[(n-1)/2]$ limit cycles; here, $[\cdot]$ denotes the integer part function.

Proof. We write the system

$$\dot{x} = y - \varepsilon(a_1 x + \cdots + a_n x^n), \quad \dot{y} = -x,$$

in polar coordinates (r, θ), where $x = r\cos\theta$, $y = r\sin\theta$, and we obtain

$$\dot{r} = -\varepsilon \sum_{k=1}^{n} a_k r^k \cos^{k+1}\theta,$$
$$\dot{\theta} = -1 + \varepsilon \sin\theta \sum_{k=1}^{n} a_k r^{k-1} \cos^k \theta$$

or, equivalently,

$$\frac{dr}{d\theta} = -\varepsilon \sum_{k=1}^{n} a_k r^k \cos^{k+1}\theta + O(\varepsilon^2).$$

Again, taking $\mathbf{x} = r$, $t = \theta$, $T = 2\pi$ and $F(t, \mathbf{x}) = -\sum_{k=1}^{n} a_k r^k \cos^{k+1}\theta$, the previous differential system is in the normal form (1.3) for applying the averaging theory described in Theorem 1.2.1.

We have that

$$f^0(r) = -\frac{1}{2\pi} \sum_{k=1}^{n} a_k r^k \int_0^{2\pi} \cos^{k+1}\theta \, d\theta = -\frac{\varepsilon}{2\pi} \sum_{\substack{k=1 \\ k \text{ odd}}}^{n} a_k b_k r^k = p(r),$$

where $b_k = \int_0^{2\pi} \cos^{k+1}\theta \, d\theta \neq 0$ if k is odd, and $b_k = 0$ if k is even. Now we apply Theorem 1.2.1, since the polynomial $p(r)$ has at most $[(n-1)/2]$ positive roots, and we can choose the coefficients a_k with k odd in such a way that $p(r)$ has exactly $[(n-1)/2]$ simple positive roots; the proposition follows. □

Zero-Hopf bifurcation in $\mathbb{R}^n$

In this example we study a zero-Hopf bifurcation of C^3 differential systems in $\mathbb{R}^n$ with $n \geq 3$. These results come from Llibre–Zhang [58].

We assume that these systems have a singularity at the origin, whose linear part has eigenvalues $\varepsilon a \pm bi$, with $b \neq 0$ and εc_k for $k = 3, \ldots, n$, where ε is a small parameter. Since the eigenvalues of the linearization at the origin when $\varepsilon = 0$ are $\pm bi \neq 0$ and 0 with multiplicity $n-2$, if an infinitesimal periodic orbit bifurcates from the origin when $\varepsilon = 0$, we call such kind of bifurcation a *zero-Hopf*

bifurcation. Such systems can be written into the form

$$\begin{aligned}
\dot{x} &= \varepsilon a x - b y + \sum_{i_1+\cdots+i_n=2} a_{i_1\ldots i_n} x^{i_1} y^{i_2} z_3^{i_3} \cdots z_n^{i_n} + \mathcal{A},\\
\dot{y} &= b x + \varepsilon a y + \sum_{i_1+\cdots+i_n=2} b_{i_1\ldots i_n} x^{i_1} y^{i_2} z_3^{i_3} \cdots z_n^{i_n} + \mathcal{B},\\
\dot{z}_k &= \varepsilon c_k z_k + \sum_{i_1+\cdots+i_n=2} c^{(k)}_{i_1\ldots i_n} x^{i_1} y^{i_2} z_3^{i_3} \cdots z_n^{i_n} + \mathcal{C}_k, \quad k = 3, \ldots, n,
\end{aligned} \tag{1.11}$$

where $a_{i_1\ldots i_n}$, $b_{i_1\ldots i_n}$, $c^{(k)}_{i_1\ldots i_n}$, a, b and c_k are real parameters, $ab \neq 0$, and $\mathcal{A}$, $\mathcal{B}$ and $\mathcal{C}_k$ are the Lagrange expression of the error function of third order in the expansion of the functions of the system in Taylor series.

Theorem 1.2.3. *There exist C^3 systems* (1.11) *for which $l \in \{0, 1, \ldots, 2^{n-3}\}$ limit cycles bifurcate from the origin at $\varepsilon = 0$, i.e., for ε sufficiently small the system has exactly l limit cycles in a neighborhood of the origin, and these limit cycles tend to the origin when $\varepsilon \searrow 0$.*

As far as we know, Theorem 1.2.3 was the first result proving that the number of limit cycles that can bifurcate in a Hopf bifurcation increases exponentially with the dimension of the space. We recall that a *Hopf bifurcation* takes place when one or several limit cycles bifurcate from an equilibrium point.

From the proof of Theorem 1.2.3 we get immediately the following result.

Corollary 1.2.4. *There exist quadratic polynomial differential systems* (1.11) *(i.e., with $\mathcal{A} = \mathcal{B} = \mathcal{C}_k = 0$) for which $l \in \{0, 1, \ldots, 2^{n-3}\}$ limit cycles bifurcate from the origin at $\varepsilon = 0$, i.e., for ε sufficiently small the system has exactly l limit cycles in a neighborhood of the origin and these limit cycles tend to the origin when $\varepsilon \searrow 0$.*

Proof of Theorem 1.2.3. Doing the cylindrical change of coordinates

$$x = r\cos\theta, \quad y = r\sin\theta, \quad z_i = z_i, \quad i = 3, \ldots, n, \tag{1.12}$$

in the region $r > 0$ the system (1.11) becomes

$$\begin{aligned}
\dot{r} &= \varepsilon a r + \sum_{i_1+\cdots+i_n=2} (a_{i_1\ldots i_n}\cos\theta + b_{i_1\ldots i_n}\sin\theta)(r\cos\theta)^{i_1}(r\sin\theta)^{i_2} z_3^{i_3}\cdots z_n^{i_n} + O(3),\\
\dot{\theta} &= \frac{1}{r}\left[b r + \sum_{i_1+\cdots+i_n=2} (b_{i_1\ldots i_n}\cos\theta - a_{i_1\ldots i_n}\sin\theta)(r\cos\theta)^{i_1}(r\sin\theta)^{i_2} z_3^{i_3}\cdots z_n^{i_n} + O(3)\right],\\
\dot{z}_k &= \varepsilon c_k z_k + \sum_{i_1+\cdots+i_n=2} c^{(k)}_{i_1\ldots i_n}(r\cos\theta)^{i_1}(r\sin\theta)^{i_2} z_3^{i_3}\cdots z_n^{i_n} + O(3), \quad k = 3, \ldots, n,
\end{aligned} \tag{1.13}$$

where $O(3) = O_3(r, z_3, \ldots, z_n)$.

As usual, $\mathbb{Z}_+$ denotes the set of all non-negative integers. Taking $a_{00e_{ij}} = b_{00e_{ij}} = 0$ where $e_{ij} \in \mathbb{Z}_+^{n-2}$ has the sum of the entries equal to 2, it is easy to show that in a suitably small neighborhood of $(r, z_3, \ldots, z_n) = (0, 0, \ldots, 0)$ we

have $\dot{\theta} \neq 0$. Then, choosing θ as the new independent variable system (1.13), in a neighborhood of $(r, z_3, \dots, z_n) = (0, 0, \dots, 0)$ it becomes

$$\begin{aligned}
\frac{dr}{d\theta} &= \frac{r\left(\varepsilon a r + \sum\limits_{i_1+\cdots+i_n=2} (a_{i_1\dots i_n}\cos\theta + b_{i_1\dots i_n}\sin\theta)(r\cos\theta)^{i_1}(r\sin\theta)^{i_2} z_3^{i_3}\cdots z_n^{i_n} + O(3)\right)}{br + \sum\limits_{i_1+\cdots+i_n=2} (b_{i_1\dots i_n}\cos\theta - a_{i_1\dots i_n}\sin\theta)(r\cos\theta)^{i_1}(r\sin\theta)^{i_2} z_3^{i_3}\cdots z_n^{i_n} + O(3)}, \\
\frac{dz_k}{d\theta} &= \frac{r\left(\varepsilon c_k z_k + \sum\limits_{i_1+\cdots+i_n=2} c^{(k)}_{i_1\dots i_n}(r\cos\theta)^{i_1}(r\sin\theta)^{i_2} z_3^{i_3}\cdots z_n^{i_n} + O(3)\right)}{br + \sum\limits_{i_1+\cdots+i_n=2} (b_{i_1\dots i_n}\cos\theta - a_{i_1\dots i_n}\sin\theta)(r\cos\theta)^{i_1}(r\sin\theta)^{i_2} z_3^{i_3}\cdots z_n^{i_n} + O(3)},
\end{aligned} \tag{1.14}$$

for $k = 3, \dots, n$. We note that this system is 2π periodic in the variable θ.

In order to write system (1.14) in the normal form of the averaging theory we rescale the variables

$$(r, z_3, \dots, z_n) = (\rho\varepsilon, \eta_3\varepsilon, \dots, \eta_n\varepsilon). \tag{1.15}$$

Then the system (1.14) becomes

$$\begin{aligned}
\frac{d\rho}{d\theta} &= \varepsilon f_1(\theta, \rho, \eta_3, \dots, \eta_n) + \varepsilon^2 g_1(\theta, \rho, \eta_3, \dots, \eta_n, \varepsilon), \\
\frac{d\eta_k}{d\theta} &= \varepsilon f_k(\theta, \rho, \eta_3, \dots, \eta_n) + \varepsilon^2 g_k(\theta, \rho, \eta_3, \dots, \eta_n, \varepsilon), \quad k = 3, \dots, n,
\end{aligned} \tag{1.16}$$

where

$$\begin{aligned}
f_1 &= \frac{1}{b}\left(a\rho + \sum_{i_1+\cdots+i_n=2} (a_{i_1\dots i_n}\cos\theta + b_{i_1\dots i_n}\sin\theta)(\rho\cos\theta)^{i_1}(\rho\sin\theta)^{i_2} z_3^{i_3}\cdots z_n^{i_n}\right), \\
f_k &= \frac{1}{b}\left(c\eta_k + \sum_{i_1+\cdots+i_n=2} c^{(k)}_{i_1\dots i_n}(\rho\cos\theta)^{i_1}(\rho\sin\theta)^{i_2} z_3^{i_3}\cdots z_n^{i_n}\right).
\end{aligned}$$

We note that the system (1.16) is in the normal form (1.3) of the averaging theory, with $\mathbf{x} = (\rho, \eta_3, \dots, \eta_n)$, $t = \theta$, $F(\theta, \rho, \eta_3, \dots, \eta_n) = (f_1(\theta, \rho, \eta_3, \dots, \eta_n), f_3(\theta, \rho, \eta_3, \dots, \eta_n), \dots, f_n(\theta, \rho, \eta_3, \dots, \eta_n))$, and $T = 2\pi$. The averaged system of (1.16) is

$$\dot{y} = \varepsilon f^0(y), \quad y = (\rho, \eta_3, \dots, \eta_n) \in \Omega, \tag{1.17}$$

where Ω is a suitable neighborhood of the origin $(\rho, \eta_3, \dots, \eta_n) = (0, 0, \dots, 0)$, and

$$f^0(y) = (f_1^0(y), f_3^0(y), \dots, f_n^0(y)),$$

with

$$f_i^0(y) = \frac{1}{2\pi}\int_0^{2\pi} f_i(\theta, \rho, \eta_3, \dots, \eta_n)d\theta, \quad i = 1, 3, \dots, n.$$

After some calculations we have that

$$f_1^0 = \frac{1}{2b}\rho\left(2a + \sum_{j=3}^{n}(a_{10e_j} + b_{01e_j})\eta_j\right),$$

$$f_k^0 = \frac{1}{2b}\left(2c_k\eta_k + \left(c^{(k)}_{20\mathbf{0}_{n-2}} + c^{(k)}_{02\mathbf{0}_{n-2}}\right)\rho^2 + 2\sum_{3\le i\le j\le n} c^{(k)}_{00e_{ij}}\eta_i\eta_j\right), \quad k = 3,\dots,n,$$

where $e_j \in \mathbb{Z}_+^{n-2}$ is the unit vector with the j-th entry equal to 1, and $e_{ij} \in \mathbb{Z}_+^{n-2}$ has the sum of the i-th and j-th entries equal to 2 and the other equal to 0.

Now we shall apply Theorem 1.2.1 for studying the limit cycles of system (1.16). Note that these limits, after the rescaling (1.15), will become infinitesimal limit cycles for system (1.14), which will tend to the origin when $\varepsilon \searrow 0$; consequently, they will be bifurcated limit cycles of the Hopf bifurcation of system (1.14) at the origin.

From Theorem 1.2.1 for studying the limit cycles of system (1.16) we only need to compute the non-degenerate singularities of system (1.17). Since the transformation from the cartesian coordinates $(r, z_3, \dots, z_n)$ to the cylindrical ones $(\rho, \eta_3, \dots, \eta_n)$ is not a diffeomorphism at $\rho = 0$, we deal with the zeros having the coordinate $\rho > 0$ of the averaged function f^0. So, we need to compute the roots of the algebraic equations

$$\begin{aligned} &2a + \sum_{j=3}^{n}(a_{10e_j} + b_{01e_j})\eta_j = 0,\\ &2c_k\eta_k + \left(c^{(k)}_{20\mathbf{0}_{n-2}} + c^{(k)}_{02\mathbf{0}_{n-2}}\right)\rho^2 + 2\sum_{3\le i\le j\le n} c^{(k)}_{00e_{ij}}\eta_i\eta_j = 0, \quad k = 3,\dots,n. \end{aligned} \tag{1.18}$$

Since the coefficients of system (1.18) are independent and arbitrary, in order to simplify the notation we write it as

$$a + \sum_{j=3}^{n} a_j\eta_j = 0, \quad c_0^{(k)}\rho^2 + c_k\eta_k + \sum_{3\le i\le j\le n} c_{ij}^{(k)}\eta_i\eta_j = 0, \quad k = 3,\dots,n, \tag{1.19}$$

where $a_j, c_0^{(k)}, c_k$ and $c_{ij}^{(k)}$ are arbitrary constants.

Denote by $\mathcal{C}$ the set of algebraic systems of form (1.19). We claim that there is a system belonging to $\mathcal{C}$ which has exactly 2^{n-3} simple roots. The claim can be verified by the example:

$$a + a_3\eta_3 = 0, \tag{1.20}$$

$$c_0^{(3)}\rho^2 + c_3\eta_3 + \sum_{3\le i\le j\le n} c_{ij}^{(3)}\eta_i\eta_j = 0, \tag{1.21}$$

$$c_k\eta_k + \sum_{3\le i\le j\le k} c_{ij}^{(k)}\eta_i\eta_j = 0, \quad k = 4,\dots,n, \tag{1.22}$$

with all the coefficients being non-zero. Equations (1.22) can be treated as quadratic algebraic equations in η_k. Substituting the unique solution η_{30} of η_3 in (1.20) into (1.22) with $k = 4$, this last equation has exactly two different solutions, namely η_{41} and η_{42} for η_4, choosing conveniently c_4. Introducing the two solutions (η_{30}, η_{4i}), $i = 1, 2$, into (1.22) with $k = 5$ and choosing conveniently the values of the coefficients of equation (1.22) with $k = 5$ and $(\eta_3, \eta_4) = (\eta_{30}, \eta_{4i})$, we get two different solutions η_{5i1} and η_{5i2} of η_5 for each i. Moreover, playing with the coefficients of the equations, the four solutions $(\eta_{30}, \eta_{4i}, \eta_{5ij})$ for $i, j = 1, 2$, are distinct. By induction, we can prove that for suitable choice of the coefficients, equations (1.20) and (1.22) have 2^{n-3} different roots $(\eta_3, \dots, \eta_n)$. Since $\eta_3 = \eta_{30}$ is fixed, for any given $c_{ij}^{(3)}$ there exist values of c_3 and $c_0^{(3)}$ such that equation (1.21) has a positive solution ρ for each of the 2^{n-3} solutions $(\eta_3, \dots, \eta_n)$ of (1.20) and (1.22). Since the 2^{n-3} solutions are different, and the number of the solutions of (1.20)–(1.22) is the maximum that the equations can have (by the Bezout Theorem, see for instance [80]), it follows that every solution is simple, and consequently the determinant of the Jacobian of the system evaluated at it is not zero. This proves the claim.

Using the same arguments which allowed us to prove the claim, we can also prove that we can choose the coefficients of the previous system in order to have $0, 1, \dots, 2^{n-3} - 1$ simple real solutions.

Taking the averaged system (1.17) with f^0 having the convenient coefficients as in (1.20)–(1.22), the averaged system (1.17) has exactly $k \in \{0, 1, \dots, 2^{n-3}\}$ singularities with the components $\rho > 0$. Moreover, the determinants of the Jacobian matrix $\partial f^0/\partial y$ at these singularities do not vanish because all the singularities are simple. In short, by Theorem 1.2.1 we get that there are systems of the form (1.11) which have $k \in \{0, 1, \dots, 2^{n-3}\}$ limit cycles. This proves the theorem. □

An application to Hamiltonian systems

The results of this subsubsection come from the paper Guirao–Llibre–Vera [39].

We consider the following class of Hamiltonians in the action-angle variables

$$\mathcal{H}(I_1, \dots, I_n, \theta_1, \dots, \theta_n) = \mathcal{H}_0(I_1) + \varepsilon \mathcal{H}_1(I_1, \dots, I_n, \theta_1, \dots, \theta_n), \tag{1.23}$$

where ε is a small parameter. For more details on the action-angle variables see, for instance, [1].

As usual, the *Poisson bracket* of the functions $f(I_1, \dots, I_n, \theta_1, \dots, \theta_n)$ and $g(I_1, \dots, I_n, \theta_1, \dots, \theta_n)$ is

$$\{f, g\} = \sum_{i=1}^{n} \left(\frac{\partial f}{\partial \theta_i} \frac{\partial g}{\partial I_i} - \frac{\partial f}{\partial I_i} \frac{\partial g}{\partial \theta_i} \right).$$

The next result provides sufficient conditions for computing periodic orbits of the Hamiltonian system associated to the Hamiltonian (1.23).

Theorem 1.2.5. *We define*

$$\langle \mathcal{H}_1 \rangle = \frac{1}{2\pi} \int_0^{2\pi} \mathcal{H}_1(I_1, \dots, I_n, \theta_1, \dots, \theta_n) d\theta_1,$$

and we consider the differential system

$$\begin{aligned} \frac{dI_i}{d\theta_1} &= \varepsilon \frac{\{I_i, \langle \mathcal{H}_1 \rangle\}}{\mathcal{H}_0'(\mathcal{H}_0^{-1}(h^*))} = \varepsilon f_{i-1}(I_2, \dots, I_n, \theta_2, \dots, \theta_n), \quad i = 2, ..., n, \\ \frac{d\theta_i}{d\theta_1} &= \varepsilon \frac{\{\theta_i, \langle \mathcal{H}_1 \rangle\}}{\mathcal{H}_0'(\mathcal{H}_0^{-1}(h^*))} = \varepsilon f_{i+n-2}(I_2, \dots, I_n, \theta_2, \dots, \theta_n), \quad i = 2, \dots, n, \end{aligned} \tag{1.24}$$

restricted to the energy level $\mathcal{H} = h^*$ with $h^* \in \mathbb{R}$. The value h^* is such that the function $\mathcal{H}_0^{-1}$ in a neighborhood of h^* is a diffeomorphism. The system (1.24) *is a Hamiltonian system with Hamiltonian $\varepsilon \langle \mathcal{H}_1 \rangle$. If $\varepsilon \neq 0$ is sufficiently small then for every equilibrium point $p = (I_2^0, \dots, I_n^0, \theta_2^0, \dots, \theta_n^0)$ of system* (1.24) *satisfying that*

$$\det \left(\frac{\partial(f_1, \dots, f_{2n-2})}{\partial(I_2, \dots, I_n, \theta_2, \dots, \theta_n)} \Big|_{(I_2, \dots, I_n, \theta_2, \dots, \theta_n) = (I_2^0, \dots, I_n^0, \theta_2^0, \dots, \theta_n^0)} \right) \neq 0,$$

there exists a 2π-periodic solution $\gamma_\varepsilon(\theta, \dots, I_n(\theta_1, \varepsilon), \theta_2(\theta_1, \varepsilon), \dots, \theta_n(\theta_1, \varepsilon))$ of the Hamiltonian system associated to the Hamiltonian (1.23)*, taking as independent variable the angle θ_1 such that $\gamma_\varepsilon(0) \to (\mathcal{H}_0^{-1}(h^*), I_2^0, \dots, I_n^0, \theta_2^0, \dots, \theta_n^0)$ when $\varepsilon \to 0$. The stability or instability of the periodic solution $\gamma_\varepsilon(\theta_1)$ is given by the stability or instability of the equilibrium point p of system* (1.24)*. In fact, the equilibrium point p has the stability behavior of the Poincaré map associated to the periodic solution $\gamma_\varepsilon(\theta_1)$.*

Now we clarify some of the notations used in the statement of Theorem 1.2.5. The function $\mathcal{H}_0$ is only a function of the variable I_1, i.e., $\mathcal{H}_0 \colon J \to \mathbb{R}$ where J is an open subset of $\mathbb{R}$ (the domain of definition of $\mathcal{H}_0$), and consequently $\mathcal{H}_0(I_1) \in \mathbb{R}$. Therefore, $\mathcal{H}_0'$ means derivative with respect to the variable I_1.

The differential system (2) is defined on the energy level $\mathcal{H}(I_1, \dots, I_n, \theta_1, \dots, \theta_n) = h^*$ with $h^* \in \mathbb{R}$, and we assume that the value h^* is such that the function $\mathcal{H}_0^{-1}$ in a neighborhood of h^* is a diffeomorphism. Therefore, the expression $\mathcal{H}_0'(\mathcal{H}_0^{-1}(h^*))$ is well defined.

On the other hand, every periodic solution of a differential system has defined in its neighborhood a return map F usually called the Poincaré map. The periodic solution provides a fixed point of the map F. The stability or instability of this fixed point for the map F is what we call the stability behavior of the Poincaré map associated to the periodic solution in the statement of Theorem 1.2.5. For more details on the Poincaré map see, for instance, [76].

Theorem 1.2.5 will be proved later on.

The next goal is to study the periodic orbits of the Hamiltonian system with the *perturbed Keplerian Hamiltonian* of the form

$$\mathcal{H} = \frac{1}{2}\left(P_1^2 + P_2^2 + P_3^2\right) - \frac{1}{\sqrt{Q_1^2 + Q_2^2 + Q_3^2}} + \varepsilon \mathcal{P}_1(Q_1^2 + Q_2^2, Q_3). \tag{1.25}$$

Note that the perturbation is symmetric with respect to the Q_3-axis. It is easy to check that the third component $K = Q_1P_2 - Q_2P_1$ of the angular momentum is a first integral of the Hamiltonian system associated to the Hamiltonian (1.25). We use this second first integral to simplify the analysis of the given axially symmetric Keplerian perturbed system.

In the following we use the *Delaunay variables* for studying easily the periodic orbits of the Hamiltonian system associated to the Hamiltonian (1.25), see [23, 71] for more details on the Delaunay variables. Thus, in Delaunay variables, the Hamiltonian (1.25) has the form

$$\mathcal{H} = -\frac{1}{2L^2} + \varepsilon \mathcal{P}(l, g, k, L, G, K) = -\frac{1}{2L^2} + \varepsilon \mathcal{P}(l, g, L, G, K), \tag{1.26}$$

where l is the *mean anomaly*, g is the *argument of the perigee* of the unperturbed elliptic orbit measured in the invariant plane, k is the *longitude of the node*, L is the *square root of the semi-major axis* of the unperturbed elliptic orbit, G is the *modulus of the total angular momentum*, and K is the *third component of the angular momentum*. Moreover, $\mathcal{P}$ is the perturbation obtained from the perturbation $\mathcal{P}_1$ using the transformation to Delaunay variables, namely

$$\begin{aligned} Q_1 &= r\left(\cos(f+g)\cos k - c\sin(f+g)\sin k\right), \\ Q_2 &= r\left(\cos(f+g)\sin k + c\sin(f+g)\cos k\right), \\ Q_3 &= rs\sin(f+g), \end{aligned} \tag{1.27}$$

with

$$c = \frac{K}{G}, \qquad s^2 = 1 - \frac{K^2}{G^2}.$$

The *true anomaly* f and the *eccentric anomaly* E are auxiliary quantities defined by the relations

$$\sqrt{1-e^2} = \frac{G}{L}, \quad r = a(1 - e\cos E), \quad l = E - e\sin E.$$

$$\sin f = \frac{a\sqrt{1-e^2}\sin E}{r}, \quad \cos f = \frac{a(\cos E - e)}{r},$$

where e is the eccentricity of the unperturbed elliptic orbit.

Note that the angular variable k is a cyclic variable for the Hamiltonian (1.26) and, consequently, K is a first integral of the Hamiltonian system as we already knew.

The family of Hamiltonians (1.26) is a particular subclass of the Hamiltonians (1.23) with $\mathcal{H}_1 = \mathcal{P}$. We denote by $\langle \mathcal{P} \rangle$ the averaged map of $\mathcal{P}$ with respect to the mean anomaly l, i.e.,

$$\langle \mathcal{P} \rangle = \frac{1}{2\pi} \int_0^{2\pi} \mathcal{P}(l, g, L, G, K) dl = \frac{1}{2\pi} \int_0^{2\pi} \mathcal{P}(E - e \sin E, g, L, G, K)(1 - e \cos E) dE.$$

We remark that the map $\langle \mathcal{P} \rangle$ only depends on the angle g and the three action variables L, G, K. We claim that $\mathcal{H}_0'(\mathcal{H}_0^{-1}(h^*)) = (-2h^*)^{3/2}$. Indeed, $\mathcal{H}_0(L) = -1/(2L^2) = h^*$ so, $\mathcal{H}_0^{-1}(h^*) = (-2h^*)^{1/2}$. Since $\mathcal{H}_0'(L) = 1/L^3$, the claim follows. From the definition of Poisson parenthesis, we also have that

$$\{G, \langle \mathcal{P} \rangle\} = -\frac{\partial G}{\partial G} \frac{\partial \langle \mathcal{P} \rangle}{\partial g} = -\frac{\partial \langle \mathcal{P} \rangle}{\partial g},$$

$$\{g, \langle \mathcal{P} \rangle\} = \frac{\partial g}{\partial g} \frac{\partial \langle \mathcal{P} \rangle}{\partial G} = \frac{\partial \langle \mathcal{P} \rangle}{\partial G},$$

$$\{k, \langle \mathcal{P} \rangle\} = \frac{\partial k}{\partial k} \frac{\partial \langle \mathcal{P} \rangle}{\partial K} = \frac{\partial \langle \mathcal{P} \rangle}{\partial K}.$$

Then, by Theorem 1.2.5 at the energy level $\mathcal{H} = h^*$ with $h^* < 0$ (because $\mathcal{H}_0(L) = -1/(2L^2)$) and with angular momentum $K = k^*$, the differential system (1.24) with respect to the mean anomaly l is

$$\begin{aligned}
\frac{dG}{dl} &= \varepsilon \frac{\{G, \langle \mathcal{P} \rangle\}}{\mathcal{H}_0'(\mathcal{H}_0^{-1}(h^*))} = -\varepsilon (-2h^*)^{3/2} \frac{\partial \langle \mathcal{P} \rangle}{\partial g} = -\varepsilon f_1(g, G, K), \\
\frac{dg}{dl} &= \varepsilon \frac{\{g, \langle \mathcal{P} \rangle\}}{\mathcal{H}_0'(\mathcal{H}_0^{-1}(h^*))} = \varepsilon (-2h^*)^{3/2} \frac{\partial \langle \mathcal{P} \rangle}{\partial G} = \varepsilon f_2(g, G, K), \\
\frac{dk}{dl} &= \varepsilon \frac{\{k, \langle \mathcal{P} \rangle\}}{\mathcal{H}_0'(\mathcal{H}_0^{-1}(h^*))} = \varepsilon (-2h^*)^{3/2} \frac{\partial \langle \mathcal{P} \rangle}{\partial K} = \varepsilon f_3(g, G, K).
\end{aligned} \tag{1.28}$$

Note that we do not write the differential equation $dK/dt = 0$ because we are working in the invariant set $\mathcal{H} = h^*$ and $K = k^*$.

Now, we are ready to state a corollary of Theorem 1.2.5 providing sufficient conditions for the existence and the kind of stability of the periodic orbits in the perturbed Kepler problems with axial symmetry.

Corollary 1.2.6. *System* (1.28) *is the Hamiltonian system taking as independent variable the mean anomaly l of the Hamiltonian* (1.25) *written in Delaunay variables on the fixed energy level $\mathcal{H} = h^* < 0$ and on the fixed third component of the angular momentum $K = k^*$. If $\varepsilon \neq 0$ is sufficiently small then, for every solution $p = (g_0, G_0, k^*)$ of the system $f_i(g, G, K) = 0$ for $i = 1, 2, 3$ satisfying*

$$\det \left(\left. \frac{\partial (f_1, f_2, f_3)}{\partial (g, G, K)} \right|_{(g,G,K)=(g_0,G_0,k^*)} \right) \neq 0, \tag{1.29}$$

and all $k_0 \in [0, 2\pi)$ *there exists a* 2π*-periodic solution*

$$\gamma_\varepsilon(l) = \big(g(l,\varepsilon), k(l,\varepsilon), L(l,\varepsilon), G(l,\varepsilon), K(l,\varepsilon) = k^*\big)$$

such that $\gamma_\varepsilon(0) \to (g_0, k_0, \sqrt{-2h^*}, G_0, k^*)$ *when* $\varepsilon \to 0$*. The stability or instability of the periodic solution* $\gamma_\varepsilon(l)$ *is given by the stability or instability of the equilibrium point* p *of system* (1.28)*. In fact, the equilibrium point* p *has the stability behavior of the Poincaré map associated to the periodic solution* $\gamma_\varepsilon(l)$*.*

We remark that having a periodic solution for every $k_0 \in [0, 2\pi)$ with the same initial conditions for all of the other variables, means that we really have a two dimensional torus foliated by periodic solutions.

There are many papers studying periodic orbits of different perturbed Keplerian problems, see for instance [42, 47, 79] and the papers quoted therein.

In what follows we shall study the spatial generalized van der Waals Hamiltonian system modeling the dynamical symmetries of the perturbed hydrogen atom.

The generalized *van der Waals Hamiltonian* system was proposed in the paper [3] via the following Hamiltonian with $\beta \in \mathbb{R}$

$$\mathcal{H} = \frac{1}{2}\left(P_1^2 + P_2^2 + P_3^2\right) - \frac{1}{\sqrt{Q_1^2 + Q_2^2 + Q_3^2}} + \varepsilon\left(Q_1^2 + Q_2^2 + \beta^2 Q_3^2\right). \tag{1.30}$$

Note that this Hamiltonian is of the form (1.25). For more references, see the ones quoted in [38].

Theorem 1.2.7. *On every energy level* $\mathcal{H} = h^* < 0$*, and for the third component of the angular momentum* $K = k^*$*, the spatial van der Waals Hamiltonian system associated to the Hamiltonian* (1.30) *for* $\varepsilon \neq 0$ *sufficiently small has:*

(i) *For* $K = k^* = 0$*, two* 2π*-periodic solutions* $\gamma_\varepsilon^{\pm}(l) = \big(g(l,\varepsilon), k(l,\varepsilon)), L(l,\varepsilon), G(l,\varepsilon), K(l,\varepsilon)\big)$ *such that*

$$\gamma_\varepsilon^{\pm}(l)(0) \to \left(\pm\frac{1}{2}\arccos\left(\frac{3(\beta^2+1)}{5(\beta^2-1)}\right), k_0, \frac{1}{\sqrt{-2h^*}}, \frac{1}{\sqrt{-2h^*}}, 0\right)$$

when $\varepsilon \to 0$*, for each* $k_0 \in [0, 2\pi)$ *if* $\beta \in (-\infty, -2) \cup (-1/2, 1/2) \cup (2, \infty)$*. These periodic orbits have a stable manifold of dimension* 2 *and an unstable one of dimension* 1 *if* $\beta \in (-1/2, 1/2)$*, and have a stable manifold of dimension* 1 *and an unstable one of dimension* 2 *if* $\beta \in (-\infty, -2) \cup (2, \infty)$*. Consequently, these periodic orbits are unstable.*

(ii) *For* $K = k^* \neq 0$*, four* 2π*-periodic solutions* $\gamma_\varepsilon^{\pm,\pm}(l) = \big(g(l,\varepsilon), k(l,\varepsilon)), L(l,\varepsilon), G(l,\varepsilon), K(l,\varepsilon)\big)$ *such that*

$$\gamma_\varepsilon^{\pm,\pm}(0) \to \left(\pm\frac{\pi}{2}, k_0, \frac{1}{\sqrt{-2h^*}}, \frac{1}{2}\sqrt{\frac{5}{-2h^*}}, \pm\frac{1}{4}\sqrt{\frac{5(1-4\beta^2)}{-2h^*(1-\beta^2)}}\right)$$

when $\varepsilon \to 0$*, for each* $k_0 \in [0, 2\pi)$ *if* $\beta \in (-1, -1/2) \cup (1/2, 1)$*.*

Theorem 1.2.7 is proved later on. The result in statement (i) was already obtained using cylindrical coordinates in [38].

The stability or instability of the four periodic orbits in statement (ii) can be determined analyzing the eigenvalues of the corresponding Jacobian matrices, but since the expression of these eigenvalues are huge and depend on the two parameters h^* and β, this study is a long task we are not going to do here.

We remark that, when $(\beta^2-1)(\beta^2-4)(\beta^2-1/4)=0$, i.e., for the values that the averaging theory for finding periodic orbits do not provide any information, it is known that the van der Waals Hamiltonian system is integrable, see [33]. Therefore the averaging method, when it cannot be applied for finding periodic orbits, provides a suspicion that for such values of the parameter the system could be integrable.

The Hamiltonian system associated to the Hamiltonian (1.23) can be written as

$$\begin{aligned}
\frac{dI_i}{dt} &= \varepsilon\{I_i,\mathcal{H}_1\} = -\varepsilon\frac{\partial \mathcal{H}_1}{\partial \theta_i}, \quad i=1,\dots,n,\\
\frac{d\theta_i}{dt} &= \varepsilon\{\theta_i,\mathcal{H}_1\} = \varepsilon\frac{\partial \mathcal{H}_1}{\partial I_i}, \quad i=2,\dots,n,\\
\frac{d\theta_1}{dt} &= \mathcal{H}_0'(I_1)+\varepsilon\{\theta_1,\mathcal{H}_1\} = \mathcal{H}_0'(I_1)+\varepsilon\frac{\partial \mathcal{H}_1}{\partial I_1}.
\end{aligned} \tag{1.31}$$

Lemma 1.2.8. *Taking as new independent variable the variable θ_1, we have in the fixed energy level $\mathcal{H}=h^*<0$ that the differential system* (1.31) *becomes*

$$\begin{aligned}
\frac{dI_i}{d\theta_1} &= \varepsilon\frac{\{I_i,\mathcal{H}_1\}}{\mathcal{H}_0'(\mathcal{H}_0^{-1}(h^*))}+O(\varepsilon^2), \quad i=2,\dots,n,\\
\frac{d\theta_i}{d\theta_1} &= \varepsilon\frac{\{\theta_i,\mathcal{H}_1\}}{\mathcal{H}_0'(\mathcal{H}_0^{-1}(h^*))}+O(\varepsilon^2), \quad i=2,\dots,n,
\end{aligned} \tag{1.32}$$

with $I_1=\mathcal{H}_0^{-1}(h^*)+O(\varepsilon)$ if $\mathcal{H}_0'(\mathcal{H}_0^{-1}(h^*))\neq 0$.

Proof. Taking as new independent variable θ_1, equations (1.31) become

$$\begin{aligned}
\frac{dI_i}{d\theta_1} &= \frac{\varepsilon\{I_i,\mathcal{H}_1\}}{\mathcal{H}_0'(I_1)+\varepsilon\{\theta_1,\mathcal{H}_1\}} = \varepsilon\frac{\{I_i,\mathcal{H}_1\}}{\mathcal{H}_0'(I_1)}+O(\varepsilon^2), \quad i=1,\dots,n,\\
\frac{d\theta_i}{d\theta_1} &= \frac{\varepsilon\{\theta_i,\mathcal{H}_1\}}{\mathcal{H}_0'(I_1)+\varepsilon\{\theta_1,\mathcal{H}_1\}} = \varepsilon\frac{\{\theta_i,\mathcal{H}_1\}}{\mathcal{H}_0'(I_1)}+O(\varepsilon^2), \quad i=2,\dots,n.
\end{aligned}$$

Fixing the energy level of $\mathcal{H}=h^*<0$, we obtain $h^*=\mathcal{H}_0(I_1)+\varepsilon\mathcal{H}_1(I_1,\dots,I_n,\theta_1,\dots,\theta_n)$. Using the Implicit Function Theorem and the fact that $\mathcal{H}_0'(\mathcal{H}_0^{-1}(h^*))\neq 0$, for ε sufficiently small, we get $I_1=\mathcal{H}_0^{-1}(h^*)+O(\varepsilon)$, and the equations are reduced to (1.32). □

Proof of Theorem 1.2.5. The averaged system in the angle θ_1 obtained from (1.32) is

$$\begin{aligned}\frac{dI_i}{d\theta_1} &= -\frac{1}{2\pi}\frac{\varepsilon}{\mathcal{H}_0'(\mathcal{H}_0^{-1}(h))}\int_0^{2\pi}\frac{\partial\mathcal{H}_1}{\partial\theta_i}d\theta_1, \quad i=2,\dots,n,\\ \frac{d\theta_i}{d\theta_1} &= \frac{1}{2\pi}\varepsilon\frac{\{\theta_i,\mathcal{H}_1\}}{\mathcal{H}_0'(\mathcal{H}_0^{-1}(h))}\int_0^{2\pi}\frac{\partial\mathcal{H}_1}{\partial I_i}d\theta_1, \quad i=2,\dots,n.\end{aligned} \tag{1.33}$$

Since

$$\frac{\partial\langle\mathcal{H}_1\rangle}{\partial\theta_i} = \frac{1}{2\pi}\int_0^{2\pi}\frac{\partial\mathcal{H}_1}{\partial\theta_i}d\theta_1, \quad i=2,\dots,n,$$

$$\frac{\partial\langle\mathcal{H}_1\rangle}{\partial I_i} = \frac{1}{2\pi}\int_0^{2\pi}\frac{\partial\mathcal{H}_1}{\partial I_i}d\theta_1, \quad i=2,\dots,n,$$

the differential system (1.33) becomes

$$\begin{aligned}\frac{dI_i}{d\theta_1} &= -\frac{\varepsilon}{\mathcal{H}_0'(\mathcal{H}_0^{-1}(h))}\frac{\partial\langle\mathcal{H}_1\rangle}{\partial\theta_i} = \varepsilon\frac{\{I_i,\langle\mathcal{H}_1\rangle\}}{\mathcal{H}_0'(\mathcal{H}_0^{-1}(h))}, \quad i=2,\dots,n,\\ \frac{d\theta_i}{d\theta_1} &= \frac{\varepsilon}{\mathcal{H}_0'(\mathcal{H}_0^{-1}(h))}\frac{\partial\langle\mathcal{H}_1\rangle}{\partial I_i} = \varepsilon\frac{\{\theta_i,\langle\mathcal{H}_1\rangle\}}{\mathcal{H}_0'(\mathcal{H}_0^{-1}(h))}, \quad i=2,\dots,n,\end{aligned}$$

which coincides with (1.24).

Once we have obtained the averaged system (1.24), it is immediate to check that it satisfies the assumptions of Theorem 1.2.1, then applying the conclusions of this theorem the rest of the statement of Theorem 1.2.5 follows immediately. □

Proof of Theorem 1.2.7. For the generalized van der Waals Hamiltonian system, the function $\mathcal{P}(E,g,h,G,K)$ is equal to

$$\begin{aligned}&\frac{\left(\beta^2G^2+G^2+K^2-K^2\beta^2\right)(e\cos E-1)^2L^4}{2G^2}\\ &-\frac{L^4(G^2-K^2)(\beta^2-1)(e-\cos E)^2\cos^2 g}{2G^2}\\ &+\frac{L^4(G^2-K^2)(\beta^2-1)(e-\cos E)^2\sin^2 g}{2G^2}\\ &-\frac{2L^3(G^2-K^2)(\beta^2-1)(e-\cos E)\cos g\sin E\sin g}{G}\\ &+\frac{1}{2}L^2(G^2-K^2)(\beta^2-1)\cos^2 g\sin^2 E\\ &-\frac{1}{2}L^2(G^2-K^2)(\beta^2-1)\sin^2 E\sin^2 g.\end{aligned}$$

Its averaged function with respect to the mean anomaly is

$$\langle \mathcal{P} \rangle = \frac{1}{2\pi} \int_0^{2\pi} \mathcal{P}(E, g, h, G, K)(1 - e\cos E)dE = \frac{B}{4G^2},$$

where $B = L^2\big(5(G^2 - K^2)(G^2 - L^2)(\beta^2 - 1)\cos(2g) - (3G^2 - 5L^2)(G^2 + K^2 + (G^2 - K^2)\beta^2)\big)$.

Equations (1.28) are the averaged equations of the Hamiltonian system with Hamiltonian (1.30)

$$\begin{aligned}
\frac{dG}{dl} &= \varepsilon \frac{5(1 + 2h^*G^2)(G^2 - K^2)(\beta^2 - 1)\sin(2g)}{2G^2\sqrt{-2h^*}} = -\varepsilon f_1(g, G, K),\\
\frac{dg}{dl} &= -\varepsilon \frac{C}{2G^3\sqrt{-2h^*}} = \varepsilon f_2(g, G, K),\\
\frac{dk}{dl} &= \varepsilon \frac{K(\beta^2 - 1)(-5 - 6h^*G^2 + 5(1 + 2h^*G^2)\cos(2g))}{2G^2\sqrt{-2h^*}} = \varepsilon f_3(g, G, K),
\end{aligned}$$

where $C = 5K^2(\beta^2 - 1) + 6h^*G^4(\beta^2 + 1) - 5(2h^*G^4 + K^2)(\beta^2 - 1)\cos(2g)$; here, $L = 1/\sqrt{-2h^*} + O(\varepsilon)$. The equilibrium solutions (g_0, G_0, k^*) of this averaged system satisfying (1.29) give rise to periodic orbits of the Hamiltonian system with Hamiltonian (1.30) for each $\mathcal{H} = h^* < 0$ and $K = k^*$, see Theorem 1.2.1. These equilibria (g_0, G_0, k^*) are

$$\left(\pm\frac{1}{2}\arccos\left(\frac{3(\beta^2 + 1)}{5(\beta^2 - 1)}\right), \frac{1}{\sqrt{-2h^*}}, 0\right), \left(\pm\frac{\pi}{2}, \frac{1}{2}\sqrt{\frac{5}{-2h^*}}, \pm\frac{1}{4}\sqrt{\frac{5(1 - 4\beta^2)}{-2h^*(1 - \beta^2)}}\right).$$

The first two equilibria exist if $3(\beta^2 + 1)/(5(\beta^2 - 1)) \in [-1, 1]$, i.e., if $\beta \in (-\infty, -2] \cup [-1/2, 1/2] \cup [2, \infty)$.

The Jacobian (1.29) of the first equilibrium is equal to $J = 16\sqrt{-2h^*}(\beta^2 - 1)(\beta^2 - 4)(\beta^2 - 1/4)$. So, when $\beta \in (-\infty, -2) \cup (-1/2, 1/2) \cup (2, \infty)$, each of these equilibria provides one periodic orbit of the Hamiltonian system with Hamiltonian (1.30) for each $\mathcal{H} = h^* < 0$ and $K = k^* = 0$. Since $k^* = 0$, these periodic orbits bifurcate from an elliptic orbit ($g_0 \neq 0$) of the Kepler problem living in the plane of motion of the two bodies of the Kepler problem. Moreover, since the eigenvalues of the Jacobian matrix at these equilibra are $\pm 2\sqrt{(\beta^2 - 4)(4\beta^2 - 1)}$ and $\sqrt{-2h^*}(\beta^2 - 1)$, these periodic orbits have a stable manifold of dimension 2 and an unstable one of dimension 1 if $\beta \in (-1/2, 1/2)$, and have a stable manifold of dimension 1 and an unstable one of dimension 2 if $\beta \in (-\infty, -2) \cup (2, \infty)$. This proves statement (i) of the theorem.

The last four equilibria exist if $\beta \in (-1, -1/2] \cup [1/2, 1)$ and have Jacobian equal to $J = -15\sqrt{-2h^*}(\beta^2 - 1)(4\beta^2 - 1)$. So, for each value of $k \in [0, 2\pi)$ these four equilibria when $\beta \in (-1, -1/2) \cup (1/2, 1)$ provide four periodic orbits

of the Hamiltonian system with Hamiltonian (1.30) for each $\mathcal{H} = h^* < 0$ and $K = k^* = \pm\frac{1}{4}\sqrt{\frac{5(1-4\beta^2)}{-2h^*(1-\beta^2)}} \neq 0$. Since $k^* \neq 0$ these periodic orbits bifurcate from elliptic orbits ($g_0 \neq 0$) of the Kepler problem which are not in the plane of motion defined by the two bodies. This proves statement (ii) of the theorem. □

1.2.3 Other first order averaging methods for periodic orbits

We consider the problem of bifurcation of T-periodic solutions from the differential system

$$\dot{\mathbf{x}} = F_0(t, \mathbf{x}) + \varepsilon F_1(t, \mathbf{x}) + \varepsilon^2 R(t, \mathbf{x}, \varepsilon), \tag{1.34}$$

with $\varepsilon = 0$ to $\varepsilon \neq 0$ sufficiently small. Here, the functions $F_0, F_1 \colon \mathbb{R} \times D \to \mathbb{R}^n$ and $R \colon \mathbb{R} \times D \times (-\varepsilon_0, \varepsilon_0) \to \mathbb{R}^n$ are $\mathcal{C}^2$ functions, T-periodic in the first variable, and D is an open subset of $\mathbb{R}^n$. One of the main assumptions is that the unperturbed system

$$\mathbf{x}' = F_0(t, \mathbf{x}), \tag{1.35}$$

has a submanifold of periodic solutions.

Let $\mathbf{x}(t, \mathbf{z})$ be the solution of the unperturbed system (1.35) satisfying that $\mathbf{x}(0, \mathbf{z}) = \mathbf{z}$. We write the linearization of the unperturbed system along the periodic solution $\mathbf{x}(t, \mathbf{z})$ as

$$\mathbf{y}' = D_{\mathbf{x}} F_0(t, \mathbf{x}(t, \mathbf{z}))\mathbf{y}. \tag{1.36}$$

In what follows we denote by $M_{\mathbf{z}}(t)$ some fundamental matrix of the linear differential system (1.36), and by $\xi \colon \mathbb{R}^k \times \mathbb{R}^{n-k} \to \mathbb{R}^k$ the projection of $\mathbb{R}^n$ onto its first k coordinates, i.e., $\xi(x_1, \ldots, x_n) = (x_1, \ldots, x_k)$.

The next result goes back to Malkin [29] and Roseau [76]. Here, we shall present the shorter proof given by A. Buică–Françoise–Llibre [12].

Theorem 1.2.9. *Let $V \subset \mathbb{R}^k$ be open and bounded, and let $\beta_0 \colon \operatorname{Cl}(V) \to \mathbb{R}^{n-k}$ be a $\mathcal{C}^2$ function. We assume that*

(i) *$\mathcal{Z} = \{\mathbf{z}_\alpha = (\alpha, \beta_0(\alpha)) : \alpha \in \operatorname{Cl}(V)\} \subset \Omega$ and that for each $\mathbf{z}_\alpha \in \mathcal{Z}$ the solution $\mathbf{x}(t, \mathbf{z}_\alpha)$ of (1.35) is T-periodic;*

(ii) *for each $\mathbf{z}_\alpha \in \mathcal{Z}$ there is a fundamental matrix $M_{\mathbf{z}_\alpha}(t)$ of (1.36) such that the matrix $M^{-1}_{\mathbf{z}_\alpha}(0) - M^{-1}_{\mathbf{z}_\alpha}(T)$ has in the right up corner the $k \times (n-k)$ zero matrix, and in the right lower corner a $(n-k) \times (n-k)$ matrix Δ_α with $\det(\Delta_\alpha) \neq 0$.*

We consider the function $\mathcal{F} \colon \operatorname{Cl}(V) \to \mathbb{R}^k$ defined as

$$\mathcal{F}(\alpha) = \xi\left(\int_0^T M^{-1}_{\mathbf{z}_\alpha}(t) F_1(t, \mathbf{x}(t, \mathbf{z}_\alpha))dt\right). \tag{1.37}$$

If there exists $a \in V$ with $\mathcal{F}(a) = 0$ and $\det\left((d\mathcal{F}/d\alpha)(a)\right) \neq 0$, then there is a T-periodic solution $\mathbf{x}(t, \varepsilon)$ of system (1.34) such that $\mathbf{x}(0, \varepsilon) \to \mathbf{z}_a$ as $\varepsilon \to 0$.

Theorem 1.2.9 is proved in Subsection 1.2.7. In the next subsection we provide some applications of this theorem.

We assume that there exists an open set V with $\mathrm{Cl}(V) \subset \Omega$ such that for each $\mathbf{z} \in \mathrm{Cl}(V)$, $\mathbf{x}(t, \mathbf{z}, 0)$ is T-periodic, where $\mathbf{x}(t, \mathbf{z}, 0)$ denotes the solution of the unperturbed system (1.35) with $\mathbf{x}(0, \mathbf{z}, 0) = \mathbf{z}$. The set $\mathrm{Cl}(V)$ is *isochronous* for the system (1.34), i.e., it is a set formed only by periodic orbits, all of them having the same period. Then, an answer to the problem of the bifurcation of T-periodic solutions from the periodic solutions $\mathbf{x}(t, \mathbf{z}, 0)$ contained in $\mathrm{Cl}(V)$ is given in the following result.

Corollary 1.2.10 (Perturbations of an isochronous set)**.** *We assume that there exists an open and bounded set V with $\mathrm{Cl}(V) \subset \Omega$ and such that, for each $\mathbf{z} \in \mathrm{Cl}(V)$, the solution $\mathbf{x}(t, \mathbf{z})$ is T-periodic; then we consider the function $\mathcal{F}\colon \mathrm{Cl}(V) \to \mathbb{R}^n$,*

$$\mathcal{F}(\mathbf{z}) = \int_0^T M_{\mathbf{z}}^{-1}(t, \mathbf{z}) F_1(t, \mathbf{x}(t, \mathbf{z}))dt. \tag{1.38}$$

If there exists $a \in V$ with $\mathcal{F}(a) = 0$ and $\det\left((d\mathcal{F}/d\mathbf{z})(a)\right) \neq 0$, then there exists a T-periodic solution $\mathbf{x}(t, \varepsilon)$ of system (1.34) such that $\mathbf{x}(0, \varepsilon) \to a$ as $\varepsilon \to 0$.

Proof. It follows immediately from Theorem 1.2.9 taking $k = n$. □

1.2.4 Three applications

In this subsection we shall develop three applications of Theorem 1.2.9 and of its Corollary 1.2.10.

The Hopf bifurcation of the Michelson system

The *Michelson system*

$$\dot{x} = y, \quad \dot{y} = z, \quad \dot{z} = c^2 - y - \frac{x^2}{2}, \tag{1.39}$$

with $(x, y, z) \in \mathbb{R}^3$ and the parameter $c \geq 0$, was introduced by Michelson [72] in the study of the travelling wave solutions of the Kuramoto–Sivashinsky equation. It is well known that system (1.39) is reversible with respect to the involution $R(x, y, z) = (-x, y, -z)$ and is volume-preserving under the flow of the system. It is easy to check that system (1.39) has two finite singularities $S_1 = (-\sqrt{2}c, 0, 0)$ and $S_2 = (\sqrt{2}c, 0, 0)$ for $c > 0$, which are both saddle-foci. The former has a two dimensional stable manifold and the latter has a two dimensional unstable manifold.

For $c > 0$ small numerical experiments (see for instance Kent–Elgin [49]) and asymptotic expansions in sinus series (see Michelson [72] in 1986 and Webster–Elgin [86] in 2003) revealed the existence of a zero-Hopf bifurcation at the origin for $c = 0$. But their results do not provide an analytic proof on the existence of

such zero-Hopf bifurcation. By a *zero-Hopf bifurcation* we mean that when $c = 0$ the Michelson system has the origin as a singularity having eigenvalues $0, \pm i$, and when $c > 0$ sufficiently small the Michelson system has a periodic orbit which tends to the origin when c tends to zero. The analytic proof of this zero-Hopf bifurcation has been provided by Llibre–Zang [59]. Now we state this result and reproduce its proof.

Theorem 1.2.11. *For $c \geq 0$ sufficiently small the Michelson system (1.39) has a zero-Hopf bifurcation at the origin for $c = 0$. Moreover, the bifurcated periodic orbit satisfies $x(t) = -2c\cos t + o(c)$, $y(t) = 2c\sin t + o(c)$ and $z(t) = 2c\cot t + o(c)$, for $c > 0$ sufficiently small.*

Proof. For any $\varepsilon \neq 0$ we apply the change of variables $x = \varepsilon\overline{x}$, $y = \varepsilon\overline{y}$, $z = \varepsilon\overline{z}$ and $c = \varepsilon d$, and Michelson system (1.39) becomes

$$\dot{x} = y, \quad \dot{y} = z, \quad \dot{z} = -y + \varepsilon d^2 - \varepsilon\frac{1}{2}x^2, \tag{1.40}$$

where we still use x, y, z instead of $\overline{x}, \overline{y}, \overline{z}$. Now doing the change of variables $x = x$, $y = r\sin\theta$ and $z = r\cos\theta$, system (1.40) goes over to

$$\dot{x} = r\sin\theta, \quad \dot{r} = \frac{\varepsilon}{2}(2d^2 - x^2)\cos\theta, \quad \dot{\theta} = 1 - \frac{\varepsilon}{2r}(2d^2 - x^2)\sin\theta. \tag{1.41}$$

This system can be written as

$$\begin{aligned} \frac{dx}{d\theta} &= r\sin\theta + \frac{\varepsilon}{2}(2d^2 - x^2)\sin^2\theta + \varepsilon^2 f_1(\theta, r, \varepsilon), \\ \frac{dr}{d\theta} &= \frac{\varepsilon}{2}(2d^2 - x^2)\cos\theta + \varepsilon^2 f_2(\theta, r, \varepsilon), \end{aligned} \tag{1.42}$$

where f_1 and f_2 are analytic functions in their variables.

For arbitrary $(x_0, r_0) \neq (0, 0)$, the system $(1.42)_{\varepsilon=0}$ has the 2π-periodic solution

$$x(\theta) = r_0 + x_0 - r_0\cos\theta, \quad r(\theta) = r_0, \tag{1.43}$$

such that $x(0) = x_0$ and $r(0) = r_0$. It is easy to see that the first variational equation of $(1.42)_{\varepsilon=0}$ along the solution (1.43) is

$$\begin{pmatrix} \dfrac{dy_1}{d\theta} \\ \dfrac{dy_2}{d\theta} \end{pmatrix} = \begin{pmatrix} 0 & \sin\theta \\ 0 & 0 \end{pmatrix} \begin{pmatrix} y_1 \\ y_2 \end{pmatrix}.$$

It has the fundamental solution matrix

$$M = \begin{pmatrix} 1 & 1 - \cos\theta \\ 0 & 1 \end{pmatrix}, \tag{1.44}$$

which is independent from the initial condition (x_0, r_0). Applying Corollary 1.2.10 to the differential system (1.42) we have that

$$\mathcal{F}(x_0, r_0) = \frac{1}{2} \int_0^{2\pi} M^{-1} \left(\begin{array}{c} (2d^2 - x^2)\sin^2\theta \\ (2d^2 - x^2)\cos\theta \end{array} \right) \Big|_{(1.43)} d\theta.$$

Then, $\mathcal{F}(x_0, r_0) = (g_1(x_0, r_0),\, g_2(x_0, r_0))$ with

$$g_1(x_0, r_0) = \frac{1}{4}\left(4d^2 - 5r_0^2 - 6r_0x_0 - 2x_0^2\right), \quad g_2(x_0, r_0) = \frac{1}{2} r_0(x_0 + r_0).$$

We can check that $\mathcal{F} = 0$ has a unique non-trivial solution $x_0 = -2d$ and $r_0 = 2d$, and that $\det D\mathcal{F}(x_0, r_0)|_{x_0=-2d,\, r_0=2d} = d^2$. Hence by Corollary 1.2.10 it follows that, for any given $d > 0$ and for $|\varepsilon| > 0$ sufficiently small, the system (1.42) has a periodic orbit $(x(\theta, \varepsilon),\, r(\theta, \varepsilon))$ of period 2π, such that $(x(0, \varepsilon), r(0, \varepsilon)) \to (-2d, 2d)$ as $\varepsilon \to 0$. We note that the eigenvalues of $D\mathcal{F}(x_0, r_0)|_{x_0=-2d,\, r_0=2d}$ are $\pm di$. This shows that the periodic orbit is linearly stable.

Going back to system (1.39) we get that, for $c > 0$ sufficiently small, the Michelson system has a periodic orbit of period close to 2π given by $x(t) = -2c\cos t + o(c)$, $y(t) = 2c\sin t + o(c)$ and $z(t) = 2c\cos t + o(c)$. We think that this periodic orbit is symmetric with respect to the involution R, but we do not have a proof of it. □

A third-order differential equation

Using Theorem 1.2.9 in the next result we present a third-order differential equation having as many limit cycles as we want.

Proposition 1.2.12. *Let us consider the third-order differential equation*

$$\dddot{x} - \ddot{x} + \dot{x} - x = \varepsilon \cos(x + t). \tag{1.45}$$

Then for all positive integer m there is $\varepsilon_m > 0$ such that if $\varepsilon \in [-\varepsilon_m, \varepsilon_m] \setminus \{0\}$ the differential equation (1.45) *has at least m limit cycles.*

Proof. If $y = \dot{x}$ and $z = \ddot{x}$, then (1.45) can be written as

$$\begin{aligned} \dot{x} &= y, \\ \dot{y} &= z, \\ \dot{z} &= x - y + z + \varepsilon\cos(x + t) = x - y + z + \varepsilon F(t, x, y, z). \end{aligned} \tag{1.46}$$

The origin $(0, 0, 0)$ is the unique singular point of (1.46) when $\varepsilon = 0$. The eigenvalues of the linearized system at this singular point are $\pm i$ and 1. By the linear invertible transformation $(X, Y, Z)^T = C(x, y, z)^T$, where

$$C = \begin{pmatrix} 1 & -1 & 0 \\ 0 & -1 & 1 \\ 1 & 0 & 1 \end{pmatrix},$$

we transform the differential system (1.46) into another such that its linear part is the real Jordan normal form of the linear part of system (1.46) with $\varepsilon = 0$, i.e.,

$$\begin{aligned} \dot{X} &= -Y, \\ \dot{Y} &= X + \varepsilon \tilde{F}(X, Y, Z, t), \\ \dot{Z} &= Z + \varepsilon \tilde{F}(X, Y, Z, t), \end{aligned} \tag{1.47}$$

where

$$\tilde{F}(X, Y, Z, t) = F\left(\frac{X - Y + Z}{2}, \frac{-X - Y + Z}{2}, \frac{-X + Y + Z}{2}, t\right).$$

Using the notation introduced in (1.34) we have that $\mathbf{x} = (X, Y, Z)$, $F_0(\mathbf{x}, t) = (-Y, X, Z)$, $F_1(\mathbf{x}, t) = (0, \tilde{F}, \tilde{F})$ and $F_2(\mathbf{x}, t) = 0$. Let $\mathbf{x}(t; X_0, Y_0, Z_0, \varepsilon)$ be the solution to system (1.47) with $\mathbf{x}(0; X_0, Y_0, Z_0, \varepsilon) = (X_0, Y_0, Z_0)$. Clearly the unperturbed system (1.47) with $\varepsilon = 0$ has a linear center at the origin in the (X, Y)-plane, which is an invariant plane under the flow of the unperturbed system, and the periodic solution $\mathbf{x}(t; X_0, Y_0, 0, 0) = (X(t), Y(t), Z(t))$ is

$$X(t) = X_0 \cos t - Y_0 \sin t, \quad Y(t) = Y_0 \cos t + X_0 \sin t, \quad Z(t) = 0. \tag{1.48}$$

Note that all these periodic orbits have period 2π.

For our system, V and α from Theorem 1.2.9 are $V = \{(X, Y, 0) : 0 < X^2 + Y^2 < \rho\}$, for some arbitrary $\rho > 0$ and $\alpha = (X_0, Y_0) \in V$.

The fundamental matrix solution $M(t)$ of the variational equation of the unperturbed system $(1.47)_{\varepsilon=0}$ with respect to the periodic orbits (1.48) satisfying that $M(0)$ is the identity matrix is

$$M(t) = \begin{pmatrix} \cos t & -\sin t & 0 \\ \sin t & \cos t & 0 \\ 0 & 0 & e^t \end{pmatrix}.$$

We remark that it is independent from the initial condition $(X_0, Y_0, 0)$. Moreover an easy computation shows that

$$M^{-1}(0) - M^{-1}(2\pi) = \begin{pmatrix} 0 & 0 & 0 \\ 0 & 0 & 0 \\ 0 & 0 & 1 - e^{-2\pi} \end{pmatrix}.$$

In short we have shown that all the assumptions of Theorem 1.2.9 hold. Hence we shall study the zeros $\alpha = (X_0, Y_0) \in V$ of the two components of the function $\mathcal{F}(\alpha)$ given in (1.37). More precisely we have $\mathcal{F}(\alpha) = (\mathcal{F}_1(\alpha), \mathcal{F}_2(\alpha))$ where

$$\begin{aligned}\mathcal{F}_1(\alpha) &= \int_0^{2\pi} \sin t \tilde{F}(\mathbf{x}(t; X_0, Y_0, 0, 0), t) dt \\ &= \int_0^{2\pi} \sin t F\left(\frac{X(t)-Y(t)}{2}, -\frac{X(t)+Y(t)}{2}, \frac{-X(t)+Y(t)}{2}, t\right) dt, \\ \mathcal{F}_2(\alpha) &= \int_0^{2\pi} \cos t \tilde{F}(\mathbf{x}(t; X_0, Y_0, 0, 0), t) dt \\ &= \int_0^{2\pi} \cos t F\left(\frac{X(t)-Y(t)}{2}, -\frac{X(t)+Y(t)}{2}, \frac{-X(t)+Y(t)}{2}, t\right) dt,\end{aligned}$$

where $X(t), Y(t)$ are given by (1.48).

First, we consider the third-order differential equation (1.45). For this equation we have that

$$\begin{aligned}f_1(X_0, Y_0) &= \int_0^{2\pi} \sin t \cos\left(t + \frac{(X_0 - Y_0)\cos t - (X_0 + Y_0)\sin t)}{2}\right) dt, \\ f_2(X_0, Y_0) &= \int_0^{2\pi} \cos t \cos\left(t + \frac{(X_0 - Y_0)\cos t - (X_0 + Y_0)\sin t)}{2}\right) dt.\end{aligned}$$

To simplify the computation of these two integrals we do the change of variables $(X_0, Y_0) \mapsto (r, s)$ given by

$$X_0 - Y_0 = 2r\cos s, \quad X_0 + Y_0 = -2r\sin s, \tag{1.49}$$

where $r > 0$ and $s \in [0, 2\pi)$. From now on and until the end of the paper, we write $f_1(r, s)$ instead of

$$f_1(X_0, Y_0) = f_1\big(r(\cos s - \sin s), -r(\cos s + \sin s)\big).$$

Similarly for $f_2(r, s)$.

We compute the two previous integrals and we get

$$\begin{aligned}f_1(r, s) &= -\pi J_2(r)\sin 2s, \\ f_2(r, s) &= 2\pi\left(\frac{1}{r}J_1(r) - J_2(r)\cos^2 s\right),\end{aligned} \tag{1.50}$$

where J_1 and J_2 are the *first* and *second Bessel functions of the first kind*. For more details on Bessel functions, see [2]. These computations become easier with the help of an algebraic manipulator such as Mathematica or Maple.

Using the asymptotic expressions of the Bessel functions of first kind it follows that Bessel functions $J_1(r)$ and $J_2(r)$ have different zeros. Hence, $f_i(r, s) = 0$ for $i = 1, 2$ imply that $s \in \{0, \pi/2, \pi, 3\pi/2\}$. Therefore, we have to study the zeros of

$$f_2(r, 0) = f_2(r, \pi) = 2\pi\left(\frac{1}{r}J_1(r) - J_2(r)\right), \tag{1.51}$$

$$f_2(r,\pi/2) = f_2(r,3\pi/2) = \frac{2\pi}{r} J_1(r). \tag{1.52}$$

We claim that function (1.51) has also infinite zeros for $r \in (0,\infty)$. Note that if ρ is sufficiently large, and we choose $r < \rho$ also sufficiently large, then

$$J_n(r) \approx \sqrt{\frac{2}{\pi r}} \cos\left(r - \frac{n\pi}{2} - \frac{\pi}{4}\right), \quad \text{for} \quad n = 1, 2,$$

are asymptotic estimations, see [2]. Considering (1.51) for r sufficiently large we obtain

$$\begin{aligned} f_2(r,0) &\approx \frac{2}{r}\sqrt{\frac{2\pi}{r}} \left(\cos\left(r - \frac{3\pi}{4}\right) + r\cos\left(r - \frac{\pi}{4}\right)\right) \\ &= \frac{2}{r}\sqrt{\frac{\pi}{r}}((r-1)\cos r + (r+1)\sin r). \end{aligned}$$

The above function has infinite zeros because the equation

$$\tan r = \frac{1-r}{r+1}$$

has infinitely many solutions.

For every zero $r_0 > 0$ of the function (1.51) we have two zeroes of system (1.50), namely $(r,s) = (r_0,0)$ and $(r,s) = (r_0,\pi)$.

We have from (1.50) that

$$\begin{aligned} \left|\frac{\partial(f_1,f_2)}{\partial(r,s)}\right|_{(r,s)=(r_0,0)} &= \frac{4\pi^2(J_0(r_0)r_0 - 2J_1(r_0))(J_0(r_0)r_0 + (r_0^2-2)J_1(r_0))}{r_0^3} \\ &= \frac{4\pi^2}{r_0} J_2(r_0)(J_1(r_0)r_0 - J_2(r_0)), \end{aligned} \tag{1.53}$$

where we have used several relations between the Bessel functions of the first kind, see [2]. Clearly, it is impossible that (1.51) and (1.53) are equal to zero at the same time. Therefore, by Theorem 1.2.1, there is a periodic orbit of the system (1.45) for each $(r_0,0)$, that is, for each value of $(X_0,Y_0) = (r_0,-r_0)$.

In an analogous way, there is a periodic orbit of the system (1.45) for each (r_0,π), that is, for each value of $(X_0,Y_0) = (-r_0,r_0)$. In fact, the periodic orbit with these initial conditions and the previous one with initial conditions $(X_0,Y_0) = (r_0,-r_0)$ are the same.

Similarly, since $J_1(r)$ has infinitely many zeroes (see [2]), the function (1.52) has infinitely many positive zeroes r_1. Every one of these zeroes provides two solutions to the system (1.50), namely $(r,s) = (r_1,\pi/2)$ and $(r,s) = (r_1,3\pi/2)$.

Moreover we have from (1.50) that

$$\left|\frac{\partial(f_1,f_2)}{\partial(r,s)}\right|_{(r,s)=(r_1,\pi/2)} = \frac{4\pi^2}{r_1} J_2^2(r_1) \neq 0. \tag{1.54}$$

Therefore, by Theorem 1.2.1, there is a periodic orbit of the system (1.45) for each $(r_1, \pi/2)$, that is, for each value of $(X_0, Y_0) = (-r_1, -r_1)$.

In an analogous way there is also a periodic orbit of the system (1.45) for each $(r_1, 3\pi/2)$, that is, for each value of $(X_0, Y_0) = (r_1, r_1)$. In fact, the periodic orbit with these initial conditions and the previous one with initial conditions $(X_0, Y_0) = (-r_1, -r_1)$ are the same.

Taking the radius ρ of the disc $V = \{(X_0, Y_0, 0) : 0 < X^2 + Y^2 < \rho\}$ in the proof of Theorem 1.2.9 conveniently large, we include in it as many zeros of the system $f_1(X_0, Y_0) = f_2(X_0, Y_0) = 0$ as we want, so from Theorem 1.2.9, Proposition 1.2.12 follows. □

The Vallis system (El Niño phenomenon)

The results of this subsubsection come from the paper Euzébio–Llibre [32].

The Vallis system, introduced by Vallis [84] in 1988, is a periodic non-autonomous three dimensional system modeling the atmosphere dynamics in the tropics over the Pacific Ocean, related to the yearly oscillations of precipitation, temperature and wind force. Denoting by x the wind force, by y the difference of near-surface water temperatures of the east and west parts of the Pacific Ocean, and by z the average near-surface water temperature, the Vallis system is

$$\begin{aligned} \frac{dx}{dt} &= -ax + by + au(t), \\ \frac{dy}{dt} &= -y + xz, \\ \frac{dz}{dt} &= -z - xy + 1, \end{aligned} \tag{1.55}$$

where $u(t)$ is some C^1 T-periodic function describing the wind force under seasonal motions of air masses, and the parameters a and b are positive.

Although this model neglects some effects like Earth's rotation, pressure field and wave phenomena, it provides a correct description of the observed processes and recovers many of the observed properties of El Niño. The properties of El Niño phenomena are studied analytically in [82, 84]. More precisely, in [84] it is shown that, taking $u \equiv 0$, it is possible to observe the presence of chaos by considering $a = 3$ and $b = 102$. Later on, in [82], it is proved that there exists a chaotic attractor for the system (1.55) after a Hopf bifurcation. This chaotic motion can be easily understood if we observe the strong similarity between the system (1.55) and the Lorenz system, which becomes more clear under the replacement of z by $z + 1$ in (1.55).

Now we shall provide sufficient conditions in order that system (1.55) has periodic orbits and, additionally, we shall characterize the stability of these periodic orbits. As far as we know, the study of the periodic orbits in the non-autonomous Vallis system has not been considered in the literature, with the exception of the Hopf bifurcation studied in [82].

We define

$$I = \int_0^T u(s)ds.$$

Now we state our main result.

Theorem 1.2.13. *For $I \neq 0$ and $a \neq b$ the Vallis system (1.55) has a T-periodic solution $(x(t), y(t), z(t))$ such that*

$$(x(t), y(t), z(t)) \approx \left(\frac{aI}{T(a-b)}, \frac{aI}{T(a-b)}, 1 \right).$$

Moreover this periodic orbit is stable if $a > b$, and unstable if $a < b$.

We do not know the reliability of the Vallis model approximating the Niño phenomenon but it seems that, for the moment, this is one of the best existing models. Accepting this reliability we can say the following.

The stable periodic solution provided by Theorem 1.2.13 says that the Niño phenomenon exhibits a periodic behavior if the T-periodic function $u(t)$ and the parameters a and b of the system satisfy $I \neq 0$ and $a > b$. Moreover, Theorem 1.2.13 states that this periodic solution lives near the point

$$(x, y, z) = \left(\frac{aI}{T(a-b)}, \frac{aI}{T(a-b)}, 1 \right).$$

Since the periodic solutions found in the following Theorems 1.2.15, 1.2.16 and 1.2.17 are also stable, we can provide a similar physical interpretation for them as we have done for the periodic solution from Theorem 1.2.13.

Theorem 1.2.14. *For $I \neq 0$ the Vallis system (1.55) has a T-periodic solution $(x(t), y(t), z(t))$ such that*

$$(x(t), y(t), z(t)) \approx \left(-\frac{aI}{Tb}, -\frac{aI}{Tb}, 1 \right).$$

Moreover this periodic orbit is always unstable.

Theorem 1.2.15. *For $I \neq 0$ the Vallis system (1.55) has a T-periodic solution $(x(t), y(t), z(t))$ such that*

$$(x(t), y(t), z(t)) \approx \left(\frac{I}{T}, \frac{I}{T}, 1 \right).$$

Moreover this periodic orbit is always stable.

Theorem 1.2.16. *For $I \neq 0$ the Vallis system (1.55) has a T-periodic solution $(x(t), y(t), z(t))$ such that*

$$(x(t), y(t), z(t)) \approx \left(\frac{I}{T}, 0, 1 \right).$$

Moreover this periodic orbit is always stable.

In what follows we consider the function

$$J(t) = \int_0^t u(s)ds,$$

and note that $J(T) = I$. So, we have the following result.

Theorem 1.2.17. *Consider $I = 0$ and $J(t) \neq 0$ if $0 < t < T$. Then, the Vallis system (1.55) has a T-periodic solution $(x(t), y(t), z(t))$ such that*

$$(x(t), y(t), z(t)) \approx \left(-\frac{a}{T} \int_0^T J(s)ds, 0, 1 \right).$$

Moreover this periodic orbit is always stable.

The tool for proving our results will be the averaging theory. This theory applies to periodic non-autonomous differential systems depending on a small parameter ε. Since the Vallis system already is a T-periodic non-autonomous differential system, in order to apply to it the averaging theory described in Section 1.4 we need to introduce in such system a small parameter. This is reached doing convenient rescalings in the variables (x, y, z), in the parameters (a, b), and in the function $u(t)$. Playing with different rescalings we shall obtain different results on the periodic solutions of the Vallis system. More precisely, in order to study the periodic solutions of the differential system (1.55), we start doing a rescaling of the variables (x, y, z), of the function $u(t)$, and of the parameters a and b, as follows:

$$\begin{array}{lll} x = \varepsilon^{m_1} X, & y = \varepsilon^{m_2} Y, & z = \varepsilon^{m_3} Z, \\ u(t) = \varepsilon^{n_1} U(t), & a = \varepsilon^{n_2} A, & b = \varepsilon^{n_3} B, \end{array} \tag{1.56}$$

where ε is always positive and sufficiently small, and where m_i and n_j are non-negative integers, for all $i, j = 1, 2, 3$. Then, in the new variables (X, Y, Z), the system (1.55) is written

$$\begin{aligned} \frac{dX}{dt} &= -\varepsilon^{n_2} AX + \varepsilon^{-m_1+m_2+n_3} BY + \varepsilon^{-m_1+n_1+n_2} AU(t), \\ \frac{dY}{dt} &= -Y + \varepsilon^{m_1-m_2+m_3} XZ, \\ \frac{dZ}{dt} &= -Z - \varepsilon^{m_1+m_2-m_3} XY + \varepsilon^{-m_3}. \end{aligned} \tag{1.57}$$

Consequently, in order to have non-negative powers of ε we must impose the conditions

$$m_3 = 0 \quad \text{and} \quad 0 \leq m_2 \leq m_1 \leq L, \tag{1.58}$$

where $L = \min\{m_2 + n_3, n_1 + n_2\}$. So, system (1.57) becomes

$$\begin{aligned} \frac{dX}{dt} &= -\varepsilon^{n_2} AX + \varepsilon^{-m_1+m_2+n_3} BY + \varepsilon^{-m_1+n_1+n_2} AU(t), \\ \frac{dY}{dt} &= -Y + \varepsilon^{m_1-m_2} XZ, \\ \frac{dZ}{dt} &= 1 - Z - \varepsilon^{m_1+m_2} XY. \end{aligned} \tag{1.59}$$

Our aim is to find periodic solutions of the system (1.59) for some special values of m_i, n_j, $i, j = 1, 2, 3$, and after we go back through the rescaling (1.56) to guarantee the existence of periodic solutions in system (1.55). In what follows we consider the case where n_2 and n_3 are positive and $m_2 = m_1 < n_1 + n_2$. These conditions lead to the proofs of Theorems 1.2.13, 1.2.14 and 1.2.15. For this reason we present these proofs together in order to avoid repetitive arguments. Moreover, in what follows we consider

$$K = \int_0^T U(s)ds.$$

Proofs of Theorems 1.2.13, 1.2.14 and 1.2.15. We start considering system (1.59) with n_2 and n_3 positive and $m_2 = m_1 < n_1 + n_2$. So we have

$$\begin{aligned} \frac{dX}{dt} &= -\varepsilon^{n_2} AX + \varepsilon^{n_3} BY + \varepsilon^{-m_1+n_1+n_2} AU(t), \\ \frac{dY}{dt} &= -Y + XZ, \\ \frac{dZ}{dt} &= 1 - Z - \varepsilon^{2m_1} XY. \end{aligned} \tag{1.60}$$

Now we apply the averaging method to the differential system (1.60). Using the notation of Subsection 1.2.5, we have $\mathbf{x} = (X, Y, Z)^T$ and

$$F_0(t, \mathbf{x}) = \begin{pmatrix} 0 \\ -Y + XZ \\ 1 - Z \end{pmatrix}. \tag{1.61}$$

We start considering the system

$$\dot{\mathbf{x}} = F_0(t, \mathbf{x}). \tag{1.62}$$

Its solution $\mathbf{x}(t, \mathbf{z}, 0) = (X(t), Y(t), Z(t))$ such that $\mathbf{x}(0, \mathbf{z}, 0) = \mathbf{z} = (X_0, Y_0, Z_0)$ is

$$\begin{aligned} X(t) &= X_0, \\ Y(t) &= (1 - e^{-t}(1 + t))X_0 + e^{-t}Y_0 + e^{-t}tX_0Z_0, \\ Z(t) &= 1 - e^{-t} + e^{-t}Z_0. \end{aligned}$$

In order that $\mathbf{x}(t,\mathbf{z},0)$ is a periodic solution we must choose $Y_0 = X_0$ and $Z_0 = 1$. This implies that, through every point of the straight line $X = Y$, $Z = 1$, there passes a periodic orbit lying in the phase space $(X, Y, Z, t) \in \mathbb{R}^3 \times \mathbb{S}^1$. Here and in what follows, $\mathbb{S}^1$ is the interval $[0, T]$ identifying T with 0.

Observe that, using the notation of Subsection 1.2.5, we have $n = 3$, $k = 1$, $\alpha = X_0$ and $\beta(X_0) = (X_0, 1)$ and, consequently, $\mathcal{M}$ is a one dimensional manifold given by $\mathcal{M} = \{(X_0, X_0, 1) \in \mathbb{R}^3 : X_0 \in \mathbb{R}\}$. The fundamental matrix $M_{\mathbf{z}}(t)$ of (1.62), satisfying that $M_{\mathbf{z}}(0)$ is the identity of $\mathbb{R}^3$, is

$$\begin{pmatrix} 1 & 0 & 0 \\ 1 - \cosh t + \sinh t & e^{-t} & e^{-t} t X_0 \\ 0 & 0 & e^{-t} \end{pmatrix},$$

and its inverse matrix $M_{\mathbf{z}}^{-1}(t)$ is

$$\begin{pmatrix} 1 & 0 & 0 \\ 1 - e^{t} & e^{t} & -e^{t} t X_0 \\ 0 & 0 & e^{t} \end{pmatrix}.$$

Since the matrix $M_{\mathbf{z}}^{-1}(0) - M_{\mathbf{z}}^{-1}(T)$ has an 1×2 zero matrix in the upper right corner, and a 2×2 lower right corner matrix

$$\Delta = \begin{pmatrix} 1 - e^{T} & e^{T} T X_0 \\ 0 & 1 - e^{T} \end{pmatrix},$$

with $\det(\Delta) = (1 - e^T)^2 \neq 0$ because $T \neq 0$, we can apply the averaging theory described in Subsection 1.2.5.

Let F be the vector field of system (1.60) minus F_0 given in (1.61). Then the components of the function $M_{\mathbf{z}}^{-1}(t) F(t, \mathbf{x}(t,\mathbf{z},0))$ are

$$\begin{aligned} g_1(X_0, t) &= -\varepsilon^{n_2} A X_0 + \varepsilon^{n_3} B X_0 + \varepsilon^{-m_1+n_1+n_2} A U(t), \\ g_2(X_0, t) &= \varepsilon^{2m_1} e^t t X_0^3 + (1 - e^t) g_1(X_0, t), \\ g_3(X_0, t) &= -\varepsilon^{2m_1} e^t X_0^2. \end{aligned}$$

In order to apply averaging theory of first order we need to consider only terms up to order ε. Analysing the expressions of g_1, g_2 and g_3 we note that these terms depend on the values of m_1 and n_j, for each $j = 1, 2, 3$. In fact, we just need to study the integral of g_1 because $k = 1$. Moreover, studying the function g_1 we observe that the only possibility to obtain an isolated zero of the function

$$f_1(X_0) = \int_0^T g_1(X_0, t) dt$$

is assuming that $n_1 + n_2 - m_1 = 1$. Otherwise, the only solution of $f_1(X_0) = 0$ is $X_0 = 0$, which corresponds to the equilibrium point $(X_0, Y_0, Z_0) = (0, 0, 1)$ of

system (1.62). The same occurs if n_2 and n_3 are greater than 1 simultaneously. This analysis reduces the existence of possible periodic solutions to the following cases:

(p_1) $n_2 = 1$ and $n_3 = 1$;

(p_2) $n_2 > 1$ and $n_3 = 1$;

(p_3) $n_2 = 1$ and $n_3 > 1$.

In the case (p_1) we have $M_{\mathbf{z}}^{-1}(t)F_1(t, \mathbf{x}(t, \mathbf{z}, 0)) = -AX_0 + BX_0 + AU(t)$, and then

$$f_1(X_0) = (-A + B)TX_0 + AK.$$

Consequently, if $A \neq B$, then $f_1(X_0) = 0$ implies $X_0 = AK/(T(A - B))$. So, by Theorem 1.2.9, system (1.60) has a periodic solution $(X(t, \varepsilon), Y(t, \varepsilon), Z(t, \varepsilon))$ such that

$$(X(0, \varepsilon), Y(0, \varepsilon), Z(0, \varepsilon)) \longrightarrow (X_0, Y_0, Z_0) = \left(\frac{AK}{T(A - B)}, \frac{AK}{T(A - B)}, 1 \right)$$

when $\varepsilon \to 0$. Note that the point (X_0, Y_0, Z_0) is an equilibrium point of the system (1.60). Then, taking $n_1 = n_2 = n_3 = 1$ and going back through the rescaling (1.56) of the variables and parameters, we obtain that the periodic solution of system (1.60) becomes the periodic solution $(x(t), y(t), z(t))$ of system (1.55) satisfying

$$(x(t), y(t), z(t)) \approx \left(\frac{aI}{T(a - b)}, \frac{aI}{T(a - b)}, 1 \right).$$

Indeed, we observe that

$$x_0 = \varepsilon X_0 = \varepsilon \frac{(a\varepsilon^{-1})(I\varepsilon^{-1})}{T\varepsilon^{-1}(a - b)} = \frac{aI}{T(a - b)}.$$

Moreover, we note that $f_1'(x_0) = \varepsilon f_1'(X_0) = -a + b \neq 0$ so, the periodic orbit corresponding to x_0 is stable if $a > b$, and unstable otherwise. This completes the proof of Theorem 1.2.13.

Analogously the function f_1 in the cases (p_2) and (p_3) is

$$f_1(X_0) = TBX_0 + AK \quad \text{and} \quad f_1(X_0) = -TAX_0 + AK,$$

respectively. In the first case the condition $f_1(X_0) = 0$ implies $X_0 = -(AK)/(TB)$. Now we observe that $n_2 > 1$ and $n_3 = 1$. So, going back through the rescaling, we obtain

$$x_0 = \varepsilon X_0 = \varepsilon \frac{(-a\varepsilon^{-n_2})(I\varepsilon^{-n_1})}{Tb\varepsilon^{-1}} = -\frac{aI}{Tb\varepsilon^{n_1+n_2-2}}$$

and consequently, choosing $n_1 = 0$ and $n_2 = 2$, we get $x_0 = -aI/(Tb)$. Note also that $f_1'(x_0) = Tb > 0$, then the periodic orbit corresponding to x_0 is always unstable. Thus, Theorem 1.2.14 is proved.

Finally, in the case (p_3), $f_1(X_0) = 0$ implies $X_0 = K/T$. So, taking $n_1 = 1$ and going back through the rescaling, we have $x_0 = \varepsilon X_0 = \varepsilon I/(T\varepsilon) = I/T$. Additionally, $f_1'(x_0) = -Ta < 0$. Therefore, the periodic solution coming from x_0 is always stable. This proves Theorem 1.2.15. □

Proof of Theorem 1.2.16. As in the proofs of Theorems 1.2.13, 1.2.14 and 1.2.15, we start by considering a more general case in the powers of ε in (1.59), taking $n_2 > 0$ and $m_2 < m_1 < L$. In this case the function $F_0(t, \mathbf{x})$ of system (1.34) is

$$F_0(t, \mathbf{x}) = \begin{pmatrix} 0 \\ Y \\ 1 - Z \end{pmatrix}. \tag{1.63}$$

Then the solution $\mathbf{x}(t, \mathbf{z}, 0)$ of system (1.35) satisfying $\mathbf{x}(0, \mathbf{z}, 0) = \mathbf{z}$ is

$$(X(t), Y(t), Z(t)) = (X_0, e^{-t}Y_0, 1 - e^{-t} + e^{-t}Z_0).$$

This solution is periodic if $Y_0 = 0$ and $Z_0 = 1$. Then, through every point in the straight line $Y = 0$, $Z = 1$ there passes a periodic orbit lying in the phase space $(X, Y, Z, t) \in \mathbb{R}^3 \times \mathbb{S}^1$. We observe that using the notation of Subsection 1.2.5 we have $n = 3$, $k = 1$, $\alpha = X_0$ and $\beta(\alpha) = (0, 1)$. Consequently, $\mathcal{M}$ is a one dimensional manifold given by $\mathcal{M} = \{(X_0, 0, 1) \in \mathbb{R}^3 : X_0 \in \mathbb{R}\}$.

The fundamental matrix $M_{\mathbf{z}}(t)$ from (1.36) and satisfying $M_{\mathbf{z}}(0) = Id_3$ (with F_0 given by (1.63)), and its inverse $M_{\mathbf{z}}^{-1}(t)$ are, respectively

$$M_{\mathbf{z}}(t) = \begin{pmatrix} 1 & 0 & 0 \\ 0 & e^{-t} & 0 \\ 0 & 0 & e^{-t} \end{pmatrix} \quad \text{and} \quad M_{\mathbf{z}}^{-1}(t) \begin{pmatrix} 1 & 0 & 0 \\ 0 & e^{t} & 0 \\ 0 & 0 & e^{t} \end{pmatrix}.$$

Since the matrix $M_{\mathbf{z}}^{-1}(0) - M_{\mathbf{z}}^{-1}T$ has an 1×2 zero matrix in the upper right corner, and a 2×2 lower right corner matrix

$$\Delta = \begin{pmatrix} 1 - e^T & 0 \\ 0 & 1 - e^T \end{pmatrix},$$

with $\det(\Delta) = (1 - e^T)^2 \neq 0$, we can apply the averaging theory described in Subsection 1.2.5. Again, using the notations introduced in the proofs of Theorems 1.2.13, 1.2.14 and 1.2.15, since $k = 1$ we will look only to the integral of the first coordinate of $\mathcal{F} = (f_1, f_2, f_3)$. In this case we have

$$g_1(X_0, Y_0, Z_0, t) = -\varepsilon^{n_2} A X_0 + \varepsilon^{-m_1+n_1+n_2} A U(t).$$

Comparing this function g_1 with the same function obtained in the proof of Theorems 1.2.13, 1.2.14 and 1.2.15, it is easy to see that this case corresponds to the case (p_3) of the mentioned theorems. Then, in order to have periodic solutions, we need to choose $n_2 = 1$ and $n_1 + n_2 - m_1 = 1$. So, following the steps of the proof of case (p_3) by choosing $n_1 = 1$ and coming back through the rescaling (1.56) to system (1.55), Theorem 1.2.16 is proved. □

Proof of Theorem 1.2.17. We start by considering the system (1.59) with $n_3 = 2$, $n_2 > 0$, $m_1 = n_1 + n_2$ and $m_2 < m_1 < m_2 + n_3$. With these conditions the system (1.59) becomes

$$\begin{aligned} \frac{dX}{dt} &= -\varepsilon^{n_2} AX + \varepsilon^{m_2 - n_1 - n_2 + n_3} BY + AU(t), \\ \frac{dY}{dt} &= -Y + \varepsilon^{-m_2 + n_1 + n_2} XZ, \\ \frac{dZ}{dt} &= 1 - Z - \varepsilon^{m_2 + n_1 + n_2} XY. \end{aligned} \tag{1.64}$$

Again, we will use the averaging theory described in Subsection 1.2.5. So, considering $\mathbf{x} = (X, Y, Z)^T$ we obtain

$$F_0(t, \mathbf{x}) = \begin{pmatrix} AU(t) \\ -Y \\ 1 - Z \end{pmatrix}. \tag{1.65}$$

Now we note that the solution $\mathbf{x}(t, \mathbf{z}, 0) = (X(t), Y(t), Z(t))$ such that $\mathbf{x}(0, \mathbf{z}, 0) = \mathbf{z} = (X_0, Y_0, Z_0)$ of the system

$$\dot{\mathbf{x}} = F_0(t, \mathbf{x}) \tag{1.66}$$

is

$$X(t) = X_0 + \int_0^t AU(s)ds, \quad Y(t) = e^{-t} Y_0, \quad Z(t) = 1 - e^{-t} + e^{-t} Z_0.$$

Since $I = 0$ and $J(t) \neq 0$ for $0 < t < T$, in order that $\mathbf{x}(t, \mathbf{z}, 0)$ is a periodic solution we need to fix $Y_0 = 0$ and $Z_0 = 1$. This implies that through every point in a neighbourhood of X_0 in the straight line $Y = 0$, $Z = 1$ there passes a periodic orbit lying in the phase space $(X, Y, Z, t) \in \mathbb{R}^3 \times \mathbb{S}^1$.

Following the notation of Subsection 1.2.5, we have $n = 3$, $k = 1$, $\alpha = X_0$ and $\beta(X_0) = (0, 1)$. Hence, $\mathcal{M}$ is a one dimensional manifold $\mathcal{M} = \{(X_0, 0, 1) \in \mathbb{R}^3 : X_0 \in \mathbb{R}\}$, and the fundamental matrix $M_{\mathbf{z}}(t)$ of (1.66) satisfying $M_{\mathbf{z}}(0) = Id_3$ is

$$\begin{pmatrix} 1 & 0 & 0 \\ 0 & e^{-t} & 0 \\ 0 & 0 & e^{-t} \end{pmatrix}.$$

It is easy to see that the matrix $M_{\mathbf{z}}^{-1}(0) - M_{\mathbf{z}}^{-1}(T)$ has a 1×2 zero matrix in the upper right corner, and a 2×2 lower right corner matrix

$$\Delta = \begin{pmatrix} 1 - e^T & 0 \\ 0 & 1 - e^T \end{pmatrix},$$

with $\det(\Delta) = (1-e^T)^2 \neq 0$. Then, the hypotheses of Theorem 1.2.9 are satisfied. Now the components of the function $M_{\mathbf{z}}^{-1}(t)F(t,\mathbf{x}(t,\mathbf{z},\mathbf{0}))$ are

$$g_1(X_0,t) = -\varepsilon^{n_2} A\left(X_0 + \int_0^t AU(s)ds\right) + AU(t),$$

$$g_2(X_0,t) = \varepsilon^{-m_2+n_1+n_2}\left(X_0 + \int_0^t AU(s)ds\right)e^t,$$

$$g_3(X_0,t) = 0.$$

Taking $n_1 = n_2 = 1$ and observing that $k = 1$ and $n = 3$, we are interested only in the first component of the function $F_1 = (F_{11}, F_{12}, F_{13})$ described in Subsection 1.2.5. Indeed, applying the averaging theory, we must study the zeros of the first component of the function

$$\mathcal{F}(X_0) = (f_1(X_0), f_2(X_0), f_3(X_0)) = \int_0^T M_{\mathbf{z}}^{-1}(t,\mathbf{z})F_{11}(t,\mathbf{x}(t,\mathbf{z}))dt.$$

Since

$$F_{11} = -A\left(X_0 + \int_0^t AU(s)ds\right),$$

we deduce

$$\begin{aligned} f_1(X_0) &= \int_0^T -A\left(X_0 + \int_0^t AU(s)ds\right)dt \\ &= -ATX_0 - A^2\int_0^T\left(\int_0^t U(s)ds\right)ds. \end{aligned}$$

Therefore, from $f_1(X_0) = 0$ we obtain

$$X_0 = -\frac{A}{T}\int_0^T\left(\int_0^t U(s)ds\right)ds \neq 0.$$

So, rescaling (1.56), we get

$$x_0 = \varepsilon^2 X_0 = -\varepsilon^2\frac{a\varepsilon^{-1}}{\varepsilon T}\int_0^T J(s)ds = -\frac{a}{T}\int_0^T J(s)ds.$$

Moreover, since $f_1'(x_0) = -a/T < 0$, because a and ε are positive, the T-periodic orbit detected by the averaging theory is always stable. This ends the proof. □

1.2.5 Another first order averaging method for periodic orbits

The next result proved in [56] extends the result of Theorem 1.2.9 to the case $n = 2m$ and when the matrix Δ_α is the zero matrix. Here, $\xi^\perp\colon \mathbb{R}^n = \mathbb{R}^m \times \mathbb{R}^m \to \mathbb{R}^m$ is the projection of $\mathbb{R}^n$ onto its second set of m coordinates, i.e., $\xi^\perp(x_1,\ldots,x_n) = (x_{m+1},\ldots,x_n)$.

Theorem 1.2.18. *Let $V \subset \mathbb{R}^m$ be open and bounded, let $\beta_0 \colon \mathrm{Cl}(V) \to \mathbb{R}^m$ be a $\mathcal{C}^k$ function and $\mathcal{Z} = \{\mathbf{z}_\alpha = (\alpha, \beta_0(\alpha)) \,|\, \alpha \in \mathrm{Cl}(V)\} \subset \Omega$ its graphic in $\mathbb{R}^{2m}$. Assume that for each $\mathbf{z}_\alpha \in \mathcal{Z}$ the solution $\mathbf{x}(t, \mathbf{z}_\alpha)$ of $(1.34)_{\varepsilon=0}$ is T-periodic and that there exists a fundamental matrix $M_{\mathbf{z}_\alpha}(t)$ of (1.3) such that the matrix $M^{-1}_{\mathbf{z}_\alpha}(0) - M^{-1}_{\mathbf{z}_\alpha}(T)$ has in the upper right corner the $m \times m$ matrix Ω_α with $\det(\Omega_\alpha) \neq 0$, and in the lower right corner the $m \times m$ zero matrix. Consider the function $\mathcal{G} \colon \mathrm{Cl}(V) \to \mathbb{R}^m$ defined by*

$$\mathcal{G}(\alpha) = \xi^\perp \left(\int_0^T M^{-1}_{\mathbf{z}_\alpha}(t) F_1(t, \mathbf{x}(t, \mathbf{z}_\alpha)) dt \right). \tag{1.67}$$

If there is $\alpha_0 \in V$ with $\mathcal{G}(\alpha_0) = 0$ and $\det((\partial \mathcal{G}/\partial \alpha)(\alpha_0)) \neq 0$ then, for $\varepsilon \neq 0$ sufficiently small, there is a unique T-periodic solution $\mathbf{x}(t, \varepsilon)$ of the system (1.34) such that $\mathbf{x}(t, \varepsilon) \to \mathbf{x}(t, \mathbf{z}_{\alpha_0})$ as $\varepsilon \to 0$.

Theorem 1.2.18 is proved in Subsection 1.2.8. In the next subsubsection we provide some applications.

A class of Duffing differential equations

Many different classes of Duffing differential equations have been studied by different authors. They are mainly interested in the existence of periodic solutions, in their multiplicity, stability, bifurcation, etc. See for instance the survey of J. Mawhin [70], and the articles [26, 73].

In this subsubsection we shall study the class of Duffing differential equations of the form

$$x'' + cx' + a(t)x + b(t)x^3 = h(t), \tag{1.68}$$

where $c > 0$ is a constant, and $a(t)$, $b(t)$ and $h(t)$ are continuous T-periodic functions. These differential equations were studied by Chen–Li in the papers [15, 16]. Their results were improved in [5] by Benterki–Llibre; we present a part of these improvements here, as an application of Theorem 1.2.18.

Instead of working with the Duffing differential equation (1.68) we shall work with the equivalent differential system

$$\begin{aligned} x' &= y, \\ y' &= -cy - a(t)x - b(t)x^3 + h(t). \end{aligned} \tag{1.69}$$

Theorem 1.2.19. *For every simple real root of the polynomial*

$$q(x_0) = -\left(\int_0^T b(s)\, ds \right) x_0^3 - \left(\int_0^T a(s)\, ds \right) x_0 + \int_0^T h(s)\, ds,$$

the differential system (1.69) has a periodic solution $(x(t), y(t))$ with $(x(0), y(0))$ close to $(x_0, 0)$.

Proof. We start by doing a rescaling of the variables (x, y), of the functions $a(t)$, $b(t)$ and $h(t)$, and of the parameter c as follows

$$\begin{array}{ll} x = \varepsilon X, & y = \varepsilon^2 Y, \\ c = \varepsilon C, & a(t) = \varepsilon A(t), \\ b(t) = \varepsilon^{-1} B(t), & h(t) = \varepsilon^2 H(t). \end{array} \tag{1.70}$$

Then the system (1.69) becomes

$$\begin{array}{l} \dot{X} = \varepsilon Y, \\ \dot{Y} = -\varepsilon C Y - A(t)X - B(t)X^3 + H(t). \end{array} \tag{1.71}$$

We shall apply the averaging Theorem 1.2.18 to system (1.71) and we shall obtain Theorem 1.2.19. In what follows, we shall use the notation from Theorem 1.2.18. Thus $\mathbf{x} = (X, Y)^T$ and

$$\begin{aligned} F_0(t, \mathbf{x}) &= \begin{pmatrix} 0 \\ -A(t)X - B(t)X^3 + H(t) \end{pmatrix}, \\ F_1(t, \mathbf{x}) &= \begin{pmatrix} Y \\ -CY \end{pmatrix}, \\ F_2(t, \mathbf{x}) &= \begin{pmatrix} 0 \\ 0 \end{pmatrix}. \end{aligned}$$

The differential system (1.71) with $\varepsilon = 0$ has $\mathbf{x}(t, \mathbf{z}, 0) = (X(t), Y(t))^T$ as a solution with $\mathbf{x}(0, \mathbf{z}, 0) = \mathbf{z} = (X_0, Y_0)^T$, and where

$$\begin{aligned} X(t) &= X_0, \\ Y(t) &= Y_0 + \int_0^t \left(-B(s)X_0^3 - A(s)X_0 + H(s)\right) ds. \end{aligned}$$

For $\mathbf{x}(t, \mathbf{z}, 0)$ to be a periodic solution, X_0 must satisfy

$$\int_0^T \left(-B(s)X_0^3 - A(s)X_0 + H(s)\right) ds = 0, \tag{1.72}$$

and Y_0 is arbitrary. Therefore we get

$$\mathbf{z}_\alpha = (\alpha, \beta_0(\alpha)) = \left(Y_0, \bar{X}_0\right),$$

where $\bar{X}_0$ is a real root of the cubic polynomial (1.72). In short, the unperturbed system (i.e., system (1.71) with $\varepsilon = 0$) has at most three families of periodic solutions because Y_0 is arbitrary and $\bar{X}_0$ is a real root of the cubic polynomial (1.72). Therefore, using the notation of Theorem 1.2.18, we have $n = 2$ and $m = 1$ for each one of these possible families of periodic solutions.

We compute the fundamental matrix $M_{\mathbf{z}_\alpha}(t)$ associated to the first variational system (1.36), associated to the vector field $(\dot{Y}, \dot{X})$ given by (1.71) with $\varepsilon = 0$ and such that $M_{\mathbf{z}_\alpha}(0) = Id_2$, and we obtain

$$M_{\mathbf{z}_\alpha}(t) = \begin{pmatrix} 1 & -\displaystyle\int_0^t \left(3B(s)X_0^2 + A(s)\right) ds \\ 0 & 1 \end{pmatrix}.$$

The matrix

$$M_{\mathbf{z}_\alpha}^{-1}(0) - M_{\mathbf{z}_\alpha}^{-1}(T) = \begin{pmatrix} 0 & -\displaystyle\int_0^T \left(3B(s)X_0^2 + A(s)\right) ds \\ 0 & 0 \end{pmatrix}$$

has a non-zero 1×1 matrix in the upper right corner if the real root $\bar{X}_0$ of the cubic polynomial (1.72) is simple, and a zero 1×1 matrix in its lower right corner. Therefore, the assumptions of Theorem 1.2.18 hold and, by applying this theorem, we study the periodic solutions which can be prolonged from the unperturbed differential system to the perturbed one. Since for our differential system we have $\xi^\perp(Y, X) = X$, we must compute the function $\mathcal{G}(\alpha) = \mathcal{G}(Y_0)$ given in (1.4), i.e.,

$$\mathcal{G}(Y_0) = \xi^\perp \left(\int_0^T M_{\mathbf{z}_\alpha}^{-1}(t) F_1(t, \mathbf{x}(t, \mathbf{z}_\alpha, 0)) dt \right) = -\int_0^T CY_0 = -CTY_0.$$

Theorem 1.2.18 says that, for every simple real root $Y_0 = 0$ of the polynomial $\mathcal{G}(Y_0)$, the differential system (1.71) with $\varepsilon \neq 0$ sufficiently small has a periodic solution $(X(t), Y(t))$ such that $(X(0), Y(0))$ tends to $(\bar{X}_0, 0)$ when $\varepsilon \to 0$, being $\bar{X}_0$ a simple real root of the cubic polynomial (1.72).

Now it is easy to check that the cubic polynomial (1.72) after the change of variables (1.70), i.e.,

$$X = \frac{x}{\varepsilon}, \quad Y = \frac{y}{\varepsilon^2}, \quad H(t) = \frac{h(t)}{\varepsilon^2}, \quad B(s) = \varepsilon b(s), \quad A(s) = \frac{a(s)}{\varepsilon},$$

becomes the polynomial $q(x_0)$. Hence the theorem is proved. □

1.2.6 Proof of Theorem 1.2.1

Proof of Theorem 1.2.1(i). The assumptions guarantee the existence and uniqueness of the solutions of the initial valued problems (1.3) and (1.4) on the time-scale $1/\varepsilon$. We introduce

$$u(t, \mathbf{x}) = \int_0^t [F(s, \mathbf{x}) - f^0(\mathbf{x})] ds. \tag{1.73}$$

Since we have subtracted the average of $f(s, \mathbf{x})$ in the integrand, the integral is bounded, i.e.,

$$||u(t, \mathbf{x})|| \leq 2MT, \quad t \geq 0, \quad \mathbf{x} \in D.$$

We now introduce a transformation near the identity

$$\mathbf{x}(t) = \mathbf{z}(t) + \varepsilon u(t, \mathbf{z}(t)). \tag{1.74}$$

This transformation will be used for simplifying equation (1.3). Differentiation of (1.74) and substitution in (1.3) yields

$$\dot{\mathbf{x}} = \dot{\mathbf{z}} + \varepsilon \frac{\partial}{\partial t} u(t, \mathbf{z}) + \varepsilon \frac{\partial}{\partial \mathbf{z}} u(t, \mathbf{z}) \dot{\mathbf{z}} = \varepsilon F(t, \mathbf{z} + \varepsilon u(t, \mathbf{z})) + \varepsilon^2 R(t, \mathbf{z} + \varepsilon u(t, \mathbf{z}), \varepsilon).$$

Using (1.73), we write this equation in the form

$$\left(I + \varepsilon \frac{\partial}{\partial \mathbf{z}} u(t, \mathbf{z}) \right) \dot{\mathbf{z}} = \varepsilon f^0(\mathbf{z}) + S,$$

with I the $n \times n$ identity matrix, and where

$$S = \varepsilon F(t, \mathbf{z} + \varepsilon u(t, \mathbf{z})) - \varepsilon F(t, \mathbf{z}) + \varepsilon^2 R(t, \mathbf{z} + \varepsilon u(t, \mathbf{z}), \varepsilon).$$

Since $\partial u / \partial \mathbf{z}$ is uniformly bounded (as u) we can invert to obtain

$$\left(I + \varepsilon \frac{\partial}{\partial \mathbf{z}} u(t, \mathbf{z}) \right)^{-1} = I - \varepsilon \frac{\partial}{\partial \mathbf{z}} u(t, \mathbf{z}) + O(\varepsilon^2), \quad t \geq 0, \quad \mathbf{z} \in D. \tag{1.75}$$

From the Lipschitz continuity of $F(t, \mathbf{z})$ we have

$$||F(t, \mathbf{z} + \varepsilon u(t, \mathbf{z})) - F(t, \mathbf{z})|| \leq L\varepsilon ||u(t, \mathbf{z})|| \leq L\varepsilon 2MT,$$

where L is the Lispchitz constant. Due to the boundedness of R it follows that, for some positive constant C independent from ε, we have

$$||S|| \leq \varepsilon^2 C, \quad t \geq 0, \quad \mathbf{z} \in D. \tag{1.76}$$

From (1.75) and (1.76) we get that

$$\dot{\mathbf{z}} = \varepsilon f^0(\mathbf{z}) + S - \varepsilon^2 \frac{\partial u}{\partial \mathbf{z}} f^0(\mathbf{z}) + O(\varepsilon^3), \quad \mathbf{z}(0) = \mathbf{x}(0). \tag{1.77}$$

As $S = O(\varepsilon^2)$ by introducing the time-like variable $\tau = \varepsilon t$, we obtain that the solution of

$$\frac{d\mathbf{y}}{d\tau} = f^0(\mathbf{y}), \quad \mathbf{y}(0) = \mathbf{z}(0)$$

approximates the solution of (1.77) with error $O(\varepsilon)$ on the time-scale 1 in τ, i.e., on the time-scale $1/\varepsilon$ in t. Due to the near identity transformation (1.74) we obtain that

$$\mathbf{x}(t) - \mathbf{y}(t) = O(\varepsilon) \tag{1.78}$$

in the time-scale $1/\varepsilon$.

Now we shall impose the periodicity condition after which we can apply the Implicit Function Theorem. We transform $\mathbf{x} \to \mathbf{z}$ with the near identity transformation (1.74), then the equation for $\mathbf{z}$ becomes

$$\dot{\mathbf{z}} = \varepsilon f^0(\mathbf{z}) + \varepsilon^2 S(t, \mathbf{z}, \varepsilon). \tag{1.79}$$

Due to the choice of $u(t, \mathbf{z}(t))$, a T-periodic solution $\mathbf{z}(t)$ produces a T-periodic solution $\mathbf{x}(t)$. For S we have the expression

$$S(t, \mathbf{z}, \varepsilon) = \frac{\partial F}{\partial \mathbf{z}}(t, \mathbf{z}) u(t, \mathbf{z}) - \frac{\partial u}{\partial \mathbf{z}}(t, \mathbf{z}) f^0(\mathbf{z}) + R(t, \mathbf{z}, 0) + O(\varepsilon).$$

This expression is T-periodic in t and continuously differentiable with respect to $\mathbf{z}$. Equation (1.79) is equivalent to the integral equation

$$\mathbf{z}(t) = \mathbf{z}(0) + \varepsilon \int_0^t f^0(\mathbf{z}(s)) ds + \varepsilon^2 \int_0^t S(s, \mathbf{z}(s), \varepsilon) ds.$$

The solution $\mathbf{z}(t)$ is T-periodic if $\mathbf{z}(t+T) = \mathbf{z}(t)$ for all $t \geq 0$, which leads to the equation

$$h(\mathbf{z}(0), \varepsilon) = \int_0^T f^0(\mathbf{z}(s)) ds + \varepsilon \int_0^T S(s, \mathbf{z}(s), \varepsilon) ds = 0. \tag{1.80}$$

Note that this is a short-hand notation. The right hand side of equation (1.80) does not depend on $\mathbf{z}(0)$ explicitly. But the solutions depend continuously on the initial values and so the dependence on $\mathbf{z}(0)$ is implicitly by the bijection $\mathbf{z}(0) \to \mathbf{z}(x)$.

It is clear that $h(p, 0) = 0$. If ε is in a neighborhood of $\varepsilon = 0$, then equation (1.80) has a unique solution $\mathbf{x}(t, \varepsilon) = \mathbf{z}(t, \varepsilon)$ because of the assumption on the Jacobian determinant (1.6). If $\varepsilon \to 0$ then $\mathbf{z}(0, \varepsilon) \to p$. This completes the proof of statement (i). □

For proving statement (ii) of Theorem 1.2.1 we need some preliminary results. The first result is Gronwall's inequality.

Lemma 1.2.20. *Let a be a positive constant. Assume that $t \in [t_0, t_0 + a]$ and*

$$\varphi(t) \leq \delta_1 \int_{t_0}^t \psi(s)\varphi(s) ds + \delta_2, \tag{1.81}$$

where $\psi(t) \leq 0$ and $\varphi(t) \leq 0$ are continuous functions, and $\delta_i > 0$ for $i = 1, 2$. Then,

$$\varphi(t) \leq \delta_2 e^{\delta_1 \int_{t_0}^t \psi(s) ds}.$$

Proof. From (1.81) we get

$$\frac{\varphi(t)}{\delta_1 \int_{t_0}^t \psi(s)\varphi(s) ds + \delta_2} \leq 1.$$

Multiplying by $\delta_1\psi(t)$ and integrating we obtain

$$\int_{t_0}^{t} \frac{\delta_1\psi(s)\varphi(s)}{\delta_1\int_{t_0}^{s}\psi(r)\varphi(r)dr+\delta_2}ds \le \delta_1\int_{t_0}^{t}\psi(s)ds,$$

therefore

$$\log\left(\delta_1\int_{t_0}^{t}\psi(s)\varphi(s)ds+\delta_2\right)-\log\delta_2 \le \delta_1\int_{t_0}^{t}\psi(s)ds.$$

Hence,

$$\delta_1\int_{t_0}^{t}\psi(s)\varphi(s)ds+\delta_2 \le \delta_2 e^{\delta_1\int_{t_0}^{t}\psi(s)ds}.$$

From (1.81) the lemma follows. □

We consider the linear differential system

$$\dot{\mathbf{x}} = A\mathbf{x}, \tag{1.82}$$

where A is a constant $n\times n$ matrix. The *eigenvalues* $\lambda_1,\dots,\lambda_n$ *of system* (1.82) are the zeros of the *characteristic polynomial* $\det(A-\lambda Id)$.

If these eigenvalues λ_k are different, with eigenvectors e_k for $k=1,\dots,n$, then $e_k e^{\lambda_k t}$, for $k=1,\dots,n$, are n independent solutions of the system (1.82).

Assume now that not all eigenvalues are different, thus suppose that the eigenvalue λ has multiplicity $m>1$. Then λ generates m independent solutions of the system (1.82) of the form

$$P_0e^{\lambda t}, P_1(t)e^{\lambda t},\dots,P_{m-1}(t)e^{\lambda t},$$

where $P_i(t)$ for $i=0,1,\dots,m-1$ are polynomial vectors of degree at most i.

With n independent solutions $x_1(t),\dots,x_n(t)$ of system (1.82) we form a matrix

$$\Phi(t)=(x_1(t),\dots,x_n(t)),$$

called a *fundamental matrix* of system (1.82). Every solution $\mathbf{x}(t)$ of system (1.82) can be written as $\mathbf{x}(t)=\Phi(t)\mathbf{c}$, where $\mathbf{c}$ is a constant vector. Moreover the solution $\mathbf{x}(t)$ with $\mathbf{x}(t_0)=\mathbf{x}_0$ is

$$\mathbf{x}(t)=\Phi(t)\Phi(t_0)^{-1}\mathbf{x}_0. \tag{1.83}$$

Usually, we choose the fundamental matrix $\Phi(t)$ in such a way that $\Phi(t_0)=Id$. From (1.83) and the explicit form of the independent solutions of system (1.82), the next result follows easily.

Proposition 1.2.21. *We consider the linear differential system* $\dot{\mathbf{x}}=A\mathbf{x}$*, where* A *is a constant* $n\times n$ *matrix with eigenvalues* $\lambda_1,\dots,\lambda_n$*. Then the following statements hold:*

(i) *if* $\mathrm{Re}\lambda_k < 0$ *for* $k = 1, \ldots, n$ *then, for each solution* $\mathbf{x}(t)$ *with* $\mathbf{x}(t_0) = \mathbf{x}_0$, *there exist two positive constants* C *and* μ *satisfying*

$$||\mathbf{x}(t)|| \leq C||\mathbf{x}_0||e^{-\mu t} \quad \textit{and} \quad \lim_{t\to\infty} \mathbf{x}(t) = 0;$$

(ii) *if* $\mathrm{Re}\lambda_k \leq 0$ *for* $k = 1, \ldots, n$ *and the eigenvalues with* $\mathrm{Re}\lambda_k = 0$ *are different, then the solution* $\mathbf{x}(t)$ *is bounded for* $t \geq t_0$*; more precisely,*

$$||\mathbf{x}(t)|| \leq C||\mathbf{x}_0|| \quad \textit{with } C > 0;$$

(iii) *if there exists an eigenvalue* λ_k *with* $\mathrm{Re}\lambda_k > 0$, *then in each neighborhood of* $\mathbf{x} = 0$ *there are solutions* $\mathbf{x}(t)$ *such that*

$$\lim_{t\to\infty} ||\mathbf{x}(t)|| = \infty.$$

Under the assumptions of statement (i) of Proposition 1.2.21, the solution $\mathbf{x} = 0$ is called *asymptotically stable*. Under the assumptions of statement (ii), the solution $\mathbf{x} = 0$ is called *Liapunov stable*. Finally, under the assumptions of statement (iii) the solution $\mathbf{x} = 0$ is called *unstable*.

The next result is also known as the Poincaré–Liapunov Theorem.

Theorem 1.2.22. *Consider the differential system*

$$\dot{\mathbf{x}} = A\mathbf{x} + B(t)\mathbf{x} + f(t, \mathbf{x}), \quad \mathbf{x}(t_0) = \mathbf{x}_0, \tag{1.84}$$

where $t \in \mathbb{R}$, A *is a constant* $n \times n$ *matrix having all its eigenvalues with negative real part, and* $B(t)$ *is a continuous* $n \times n$ *matrix such that* $\lim_{t\to\infty} ||B(t)|| = 0$. *The function* $f(t, \mathbf{x})$ *is continuous in* t *and* $\mathbf{x}$, *and Lipschitz in* $\mathbf{x}$ *in a neighborhood of* $\mathbf{x} = 0$. *If*

$$\lim_{||\mathbf{x}||\to 0} \frac{f(t, \mathbf{x})}{||\mathbf{x}||} = 0 \quad \textit{uniformly in } t,$$

then there exists positive constants C, t_0, δ *and* μ *such that* $||\mathbf{x}_0|| \leq \delta$ *implies*

$$||\mathbf{x}(t)|| \leq C||\mathbf{x}_0||e^{-\mu(t-t_0)} \quad \textit{for } t \geq t_0.$$

The solution $\mathbf{x} = 0$ *is asymptotically stable and the attraction is exponential in a* δ*-neighborhood of* $\mathbf{x} = 0$.

Proof. By Proposition 1.2.21 we have an estimate for the fundamental matrix of the differential system

$$\dot{\Phi} = A\Phi, \quad \Phi(t_0) = Id.$$

Since all the eigenvalues of the matrix A have negative real part, there exist positive constants C and μ_0 such that

$$||\Phi(t)|| \leq Ce^{-\mu_0(t-t_0)}, \quad \text{for } t \geq t_0.$$

From the assumptions on f and B, for $\delta_0 > 0$ sufficiently small there exist a constant $b(\delta_0)$ such that if $||\mathbf{x}|| \leq \delta_0$ then

$$||f(t,\mathbf{x})|| \leq b(\delta_0)||\mathbf{x}|| \quad \text{for } t \geq t_0,$$

and if t_0 is sufficiently large

$$||B(t)|| \leq b(\delta_0), \quad \text{for } t \geq t_0.$$

The existence and uniqueness Theorem states that in a neighborhood of $\mathbf{x} = 0$ the solution of the initial problem (1.84), exists for $t_0 \leq t \leq t_1$. It can be shown that this solution is defined for all $t \geq t_0$.

We claim that the initial problem (1.84) is equivalent to the integral equation

$$\mathbf{x}(t) = \Phi(t)\mathbf{x}_0 + \int_{t_0}^{t} \Phi(t-s+t_0)[B(s)\mathbf{x}(s) + f(s,\mathbf{x}(s))]ds. \tag{1.85}$$

Now we prove the claim. The fundamental matrix $\Phi(t)$ of the differential system $\dot{\mathbf{x}} = A\mathbf{x}$ can be written as $\Phi(t) = e^{A(t-t_0)}$. We substitute $\mathbf{x} = \Phi(t)\mathbf{z}$ into the differential system (1.84) and obtain

$$\frac{d\Phi(t)}{dt}\mathbf{z} + \Phi(t)\dot{\mathbf{z}} = A\Phi(t)\mathbf{z} + B(t)\Phi(t)\mathbf{z} + f(t,\Phi(t)\mathbf{z}).$$

Since $d\Phi(t)/dt = A\Phi(t)$, we get

$$\dot{\mathbf{z}} = \Phi(t)^{-1}B(t)\Phi(t)\mathbf{z} + \Phi(t)^{-1}f(t,\Phi(t)\mathbf{z}).$$

Integrating this expression between t_0 and t and multiplying by $\Phi(t)$ we get the integral equation (1.85). So the claim is proved.

Using the estimates for Φ, B and f we have

$$\begin{aligned}||\mathbf{x}(t)|| &\leq ||\Phi(t)||||\mathbf{x}_0|| + \int_{t_0}^{t} \left[||\Phi(t-s+t_0)||||B(s)||||\mathbf{x}(s)|| + ||f(s,\mathbf{x}(s))||\right] ds \\ &\leq Ce^{-\mu_0(t-t_0)}||\mathbf{x}_0|| + \int_{t_0}^{t} Ce^{-\mu_0(t-s)}2b||\mathbf{x}(s)||ds\end{aligned}$$

for $t_0 \leq t \leq t_2 \leq t_1$. Therefore

$$e^{\mu_0(t-t_0)}||\mathbf{x}(t)|| \leq C||\mathbf{x}_0|| + \int_{t_0}^{t} Ce^{-\mu_0(s-t_0)}2b||\mathbf{x}(s)||ds,$$

for $t_0 \leq t \leq t_2$, where t_2 is determined by the condition $||\mathbf{x}|| \leq \delta_0$. Using now Gronwall's inequality (Lemma 1.2.20 with $\phi(s) = 2Cb$) we obtain

$$e^{-\mu_0(s-t_0)}||\mathbf{x}(t)|| \leq C||\mathbf{x}_0||e^{2Cb(t-t_0)},$$

or

$$||\mathbf{x}(t)|| \leq C||\mathbf{x}_0||e^{(2Cb-\mu_0)(t-t_0)}.$$

If δ, and consequently b, are sufficiently small we have that $\mu = \mu_0 - 2Cb$ is positive, and the inequality of the statement in the theorem follows for $t \in [t_0, t_2]$.

Finally, if we choose $||\mathbf{x}_0||$ such that $||\mathbf{x}_0|| \leq \delta_0$, then $||\mathbf{x}(t)||$ decreases, consequently the solution $\mathbf{x} = 0$ is asymptotically stable and the attraction is exponential in a δ-neighborhood of $\mathbf{x} = 0$. □

Now we shall consider linear differential systems of the form

$$\dot{\mathbf{x}} = A(t)\mathbf{x}, \tag{1.86}$$

where $A(t)$ is a continuous T-periodic $n \times n$ matrix, i.e., $A(t+T) = A(t)$ for all $t \in \mathbb{R}$. For these systems we can define again a *fundamental matrix* putting in each column of this matrix an independent solution of the system (1.86).

The next result usually called the *Floquet Theorem* says that the fundamental matrix of system (1.86) can be written as a product of a T-periodic matrix and a non-periodic matrix in general.

Theorem 1.2.23. *Consider the linear differential system* (1.86) *with $A(t)$ a continuous T-periodic $n \times n$ matrix. Then each fundamental matrix $\Phi(t)$ of system* (1.86) *can be written as the product of two $n \times n$ matrices*

$$\Phi(t) = P(t)e^{Bt},$$

where $P(t)$ is T-periodic and B is a constant matrix.

Proof. Since $\Phi(t)$ is a fundamental matrix of system (1.86), $\Phi(t+T)$ is also a fundamental matrix. Indeed, define $\tau = t + T$, then

$$\frac{d\mathbf{x}}{d\tau} = A(\tau - T)\mathbf{x} = A(\tau)\mathbf{x}.$$

Therefore $\Phi(\tau)$ is also a fundamental matrix.

The fundamental matrices $\Phi(t)$ and $\Phi(t+T)$ are linearly dependent, i.e., there exists a non-singular matrix C such that $\Phi(t+T) = \Phi(t)C$. Let B be a constant matrix such that $C = e^{BT}$. We claim that the matrix $\Phi(t)e^{-Bt}$ is T-periodic. Write $\Phi(t)e^{-Bt} = P(t)$. Then,

$$P(t+T) = \Phi(t+T)e^{-B(t+T)} = \Phi(t)Ce^{-BT}e^{-Bt} = \Phi(t)e^{-Bt} = P(t).$$

This completes the proof of the theorem. □

Remark 1.2.24. The matrix C introduced in the proof of Theorem 1.2.23 is called the *monodromy matrix* of system (1.86). The eigenvalues ρ_k of the matrix C are called the *characteristic multipliers*. Each complex number λ_k such that $\rho_k = e^{\lambda_k T}$ is called a *characteristic exponent*. The characteristic multipliers are determined uniquely. We can choose the exponents λ_k so that they coincide with the eigenvalues of the matrix B.

Proposition 1.2.25. *Consider the differential system*

$$\dot{\mathbf{x}} = A(t)\mathbf{x} + f(t, \mathbf{x}), \tag{1.87}$$

in $\mathbb{R}^n$ *with* $A(t)$ *a* T*-periodic continuous matrix,* $f(t, \mathbf{x})$ *continuous in* $t \in \mathbb{R}$ *and in* $\mathbf{x}$ *in a neighborhood of* $\mathbf{x} = 0$*. Assume that*

$$\lim_{||\mathbf{x}||\to 0} \frac{f(t, \mathbf{x})}{||\mathbf{x}||} = 0 \quad \textit{uniformly in } t.$$

If the real parts of the characteristic exponents of the linear periodic differential system

$$\dot{\mathbf{y}} = A(t)\mathbf{y} \tag{1.88}$$

are negative, then the solution $\mathbf{x} = 0$ *of system* (1.87) *is asymptotically stable.*

Proof. By remark 1.2.24 and Theorem 1.2.23, we can use the change of variables $\mathbf{x} = M(t)\mathbf{z}$ being $M(t)$ the periodic fundamental matrix solution of the system (1.88). Then, the differential system (1.87) becomes

$$\dot{\mathbf{z}} = B\mathbf{z} + M(t)^{-1} f(t, M(t)\mathbf{z}).$$

The constant matrix B has all its eigenvalues with negative real part. The solution $\mathbf{z}$ of the previous system satisfies the assumptions of Theorem 1.2.22 from which the proposition follows. □

Proposition 1.2.26. *Consider the differential system*

$$\dot{\mathbf{x}} = A\mathbf{x} + B(t)\mathbf{x} + f(t, \mathbf{x}) \quad \textit{with } t \geq t_0, \tag{1.89}$$

in $\mathbb{R}^n$*, where* A *is a constant* $n \times n$ *matrix having at least one eigenvalue with positive real part, and* $B(t)$ *is a continuous* $n \times n$ *matrix such that* $\lim_{t\to\infty} ||B(t)|| = 0$*. The function* $f(t, \mathbf{x})$ *is continuous in* t *and* $\mathbf{x}$*, and Lipschitz in* $\mathbf{x}$ *in a neighborhood of* $\mathbf{x} = 0$*. If*

$$\lim_{||\mathbf{x}||\to 0} \frac{f(t, \mathbf{x})}{||\mathbf{x}||} = 0 \quad \textit{uniformly in } t,$$

then the solution $\mathbf{x} = 0$ *is unstable.*

Proof. Doing the change of variables $\mathbf{x} = S\mathbf{y}$, where S is a non-singular constant $n \times n$ matrix, the system (1.89) becomes

$$\dot{\mathbf{y}} = S^{-1}AS\mathbf{y} + S^{-1}B(t)S\mathbf{y} + S^{-1}f(t, S\mathbf{y}). \tag{1.90}$$

While the solution $\mathbf{x}(t)$ is real, in general, the solution $\mathbf{y}(t)$ will be complex. The instability for the solution $\mathbf{y} = 0$ of system (1.90) implies the instability for the solution $\mathbf{x} = 0$ of system (1.89). We assume that S can be taken in such a way that $S^{-1}AS$ is diagonal, otherwise the proof is similar, or see [21, Chapter 13.1].

Assume now that $\mathrm{Re}(\lambda_i) \geq \sigma > 0$ for $i = 1, \ldots, k$, and that $\mathrm{Re}(\lambda_i) \leq 0$ for $i = k+1, \ldots, n$. Let

$$R^2 = \sum_{i=1}^{k} |y_i|^2 \quad \text{and} \quad r^2 = \sum_{i=k+1}^{n} |y_i|^2.$$

From system (1.90) we shall compute the derivatives of R^2 and r^2 with respect to t. First, we have

$$\begin{aligned} \frac{d|y_i|^2}{dt} &= \frac{d(y_i\overline{y}_i)}{dt} = \dot{y}_i\overline{y}_i + y_i\dot{\overline{y}}_i \\ &= 2\mathrm{Re}\lambda_i|y_i|^2 + (S^{-1}B(t)S\mathbf{y})\overline{y}_i + y_i(S^{-1}B(t)S\mathbf{y})_i \\ &\quad + (S^{-1}f(t,S\mathbf{y})_i\overline{y}_i + y_i(S^{-1}f(t,S\mathbf{y})_i. \end{aligned}$$

We can choose $\varepsilon > 0$, δ_0 and δ such that, for $t \geq t_0$ and $||\mathbf{y}|| \leq \delta$, we have

$$|S^{-1}B(t)S\mathbf{y}|_i \leq \varepsilon|y_i|, \quad |(S^{-1}f(t,S\mathbf{y})_i| \leq \varepsilon|y_i|.$$

Therefore,

$$\frac{1}{2}\frac{d(R^2 - r^2)}{dt} \geq \sum_{i=1}^{k}(\mathrm{Re}\lambda_i - \varepsilon)|y_i|^2 - \sum_{i=k+1}^{n}(\mathrm{Re}\lambda_i + \varepsilon)|y_i|^2.$$

Taking $0 < \varepsilon \leq \sigma/2$, we obtain $\mathrm{Re}\lambda_i - \varepsilon \geq \sigma - \varepsilon \geq \varepsilon$ for $i = 1, \ldots, k$, and $\mathrm{Re}\lambda_i + \varepsilon \geq \varepsilon$ for $i = k+1, \ldots, n$. Then,

$$\frac{1}{2}\frac{d(R^2 - r^2)}{dt} \geq \varepsilon(R^2 - r^2) \quad \text{for } t \geq t_0 \text{ and } ||\mathbf{y}|| \leq \delta. \tag{1.91}$$

Taking the initial conditions in such a way that $(R^2 - r^2)_{t=t_0} = k > 0$, from (1.91) we get that

$$||\mathbf{y}||^2 \geq R^2 - r^2 \geq ke^{2\varepsilon(t-t_0)}.$$

Hence, this solution leaves the ball $||\mathbf{y}|| \leq \delta$. Consequently, $\mathbf{y} = 0$ is unstable. □

Proof of Theorem 1.2.1(ii). We linearize equation (1.3) in a neighborhood of the periodic solution $\mathbf{x}(t,\varepsilon)$. After translating $\mathbf{x} = \mathbf{z} + \mathbf{x}(t,\varepsilon)$, expanding with respect to $\mathbf{z}$, omitting the non-linear terms and renaming the dependent variable again by $\mathbf{x}$, we get the linear differential equation with T-periodic coefficients

$$\dot{\mathbf{x}} = \varepsilon A(t,\varepsilon)\mathbf{x}, \tag{1.92}$$

where

$$A(t,\varepsilon) = \frac{\partial}{\partial \mathbf{x}}[F(t,\mathbf{x}) + \varepsilon R(t,\mathbf{x},\varepsilon)]_{\mathbf{x}=\mathbf{x}_\varepsilon(t)}.$$

We define the T-periodic matrix

$$B(t) = \frac{\partial F}{\partial \mathbf{x}}(t, p),$$

and from statement (i) we have $\lim_{\varepsilon \to 0} A(t, \varepsilon) = B(t)$. We also define the matrices

$$B^0 = \frac{1}{T} \int_0^T B(t)dt \quad \text{and} \quad C(t) = \int_0^T [B(s) - B^0]ds.$$

Note that B^0 is the matrix of the linearized averaging system. The matrix $C(t)$ is T-periodic and its average is zero. The near-identity transformation $\mathbf{x} \to \mathbf{y}$ defined by $\mathbf{y} = (I - \varepsilon C(t))\mathbf{x}$ provides

$$\begin{aligned} \dot{\mathbf{y}} &= -\varepsilon \dot{C}(t)\mathbf{x} + (I - \varepsilon C(t))\dot{\mathbf{x}} \\ &= -\varepsilon B(t)\mathbf{x} + \varepsilon B^0 \mathbf{x} + (I - \varepsilon C(t))\varepsilon A(t, \varepsilon)\mathbf{x} \\ &= [\varepsilon B^0 + \varepsilon(A(t, \varepsilon) - B(t)) - \varepsilon^2 C(t)]A(t, \varepsilon)](I - \varepsilon C(t))^{-1}\mathbf{y} \\ &= \varepsilon B^0 \mathbf{y} + \varepsilon(A(t, \varepsilon) - B(t))\mathbf{y} + \varepsilon^2 S(t, \varepsilon)\mathbf{y}. \end{aligned} \tag{1.93}$$

The function $S(t, \varepsilon)$ is T-periodic and bounded. We note that $A(t, \varepsilon) - B(t) \to 0$ when $\varepsilon \to 0$, and also that the characteristic exponents of the differential system (1.93) depend continuously on the small parameter ε. Therefore, for ε sufficiently small, the sign of the real parts of the characteristic exponents is equal to the sign of the real parts of the eigenvalues of the matrix B^0. The same conclusion holds, using the near-identity transformation, for the characteristic exponents of the differential system (1.92).

Applying now Proposition 1.2.25 we obtain the stability of the periodic solution in the case of negative real parts. If at least one real part is positive, the Floquet transformation and the application of Proposition 1.2.26 provides the instability of the periodic solution. □

1.2.7 Proof of Theorem 1.2.9

Proof of Theorem 1.2.9. We consider the function $f\colon D \times (-\varepsilon_0, \varepsilon_0) \to \mathbb{R}^n$, given by

$$f(z, \varepsilon) = x(T, z, \varepsilon) - z. \tag{1.94}$$

Then, every $(z_\varepsilon, \varepsilon)$ such that

$$f(z_\varepsilon, \varepsilon) = 0 \tag{1.95}$$

provides the periodic solution $x(\cdot, z_\varepsilon, \varepsilon)$ of (1.34).

We need to study the zeros of the function (1.94), or, equivalently, of

$$g(z, \varepsilon) = Y^{-1}(T, z) f(z, \varepsilon).$$

We have that $g(z_\alpha, 0) = 0$, because $x(\cdot, z_\alpha, 0)$ is T-periodic, and we shall prove that

$$G_\alpha = \frac{dg}{dz}(z_\alpha, 0) = Y_\alpha^{-1}(0) - Y_\alpha^{-1}(T). \tag{1.96}$$

For this, we need to know $(\partial x/\partial z)(\cdot, z, 0)$. Since it is the matrix solution of (1.36) with $(\partial x/\partial z)(0, z, 0) = I_n$, we have that $(\partial x/\partial z)(t, z, 0) = Y(t, z)Y^{-1}(0, z)$. Moreover,

$$\frac{df}{dz}(z, 0) = \frac{\partial x}{\partial z}(T, z, 0) - I_n = Y(T, z)Y^{-1}(0, z) - I_n$$

and

$$\frac{dg}{dz}(z, 0) = Y^{-1}(0, z) - Y^{-1}(T, z) + \left(\frac{\partial Y^{-1}}{\partial z_1}(T, z)f(z, 0), \ldots, \frac{\partial Y^{-1}}{\partial z_n}(T, z)f(z, 0) \right),$$

which, for $z_\alpha \in \mathcal{Z}$, reduces to (1.96).

We have

$$\frac{\partial g}{\partial \varepsilon}(z, 0) = Y^{-1}(T, z)\frac{\partial x}{\partial \varepsilon}(T, z, 0).$$

The function $(\partial x/\partial \varepsilon)(\cdot, z, 0)$ is the unique solution of the initial value problem

$$y' = D_x F_0(t, x(t, z, 0))y + F_1(t, x(t, z, 0)), \quad y(0) = 0.$$

Hence,

$$\frac{\partial x}{\partial \varepsilon}(t, z, 0) = Y(t, z) \int_0^t Y^{-1}(s, z)F_1(s, x(s, z, 0))ds.$$

Now we have

$$\frac{\partial g}{\partial \varepsilon}(z, 0) = \int_0^T Y^{-1}(s, z)F_1(s, x(s, z, 0))ds,$$

and hence

$$\frac{\partial (\pi g)}{\partial \varepsilon}(z_\alpha, 0) = f_1(\alpha),$$

where f_1 is given by (1.37). Applying Theorem 2.1, there exists $\alpha_\varepsilon \in V$ such that $g(z_{\alpha_\varepsilon}, \varepsilon) = 0$ and, further, $f(z_{\alpha_\varepsilon}, \varepsilon) = 0$, which assures that $\varphi(\cdot, \varepsilon) = x(\cdot, z_{\alpha_\varepsilon}, \varepsilon)$ is a T-periodic solution of (1.34). □

1.2.8 Proof of Theorem 1.2.18

Since the result of Theorem 1.2.18 is analogous to the result of Theorem 1.2.9, their proofs are similar.

Proof of Theorem 1.2.18. Since $\mathcal{Z}$ is a compact set and $\mathbf{x}(t, \mathbf{z}_\alpha)$ is T-periodic for each $\mathbf{z}_\alpha \in \mathcal{Z}$, there is an open neighborhood D of $\mathcal{Z}$ in Ω, and $0 < \varepsilon_1 \leq \varepsilon_0$ such that any solution $\mathbf{x}(t, \mathbf{z}, \varepsilon)$ of (1.34) with initial conditions in $D \times (-\varepsilon_1, \varepsilon_1)$ is well defined in $[0, T]$. We consider the function $L\colon D \times (-\varepsilon_1, \varepsilon_1) \to \mathbb{R}^{2m}$, $(\mathbf{z}, \varepsilon) \mapsto \mathbf{x}(T, \mathbf{z}, \varepsilon) - \mathbf{z}$. If $(\bar{\mathbf{z}}, \bar{\varepsilon}) \in D \times (-\varepsilon_1, \varepsilon_1)$ is such that $L(\bar{\mathbf{z}}, \bar{\varepsilon}) = 0$, then $\mathbf{x}(t, \bar{\mathbf{z}}, \bar{\varepsilon})$ is a T-periodic

solution of $(1.34)_{\varepsilon=\bar{\varepsilon}}$. Clearly, the converse is also true. Hence, the problem of finding T-periodic orbits of (1.34) close to the periodic orbits with initial conditions in $\mathcal{Z}$ is reduced to finding the zeros of $L(\mathbf{x},\varepsilon)$.

The sets of zeros of $L(\mathbf{z},\varepsilon)$ and $\widetilde{L}(\mathbf{z},\varepsilon) = M_{\mathbf{z}}^{-1}(T)L(\mathbf{z},\varepsilon)$ coincide, since $M_{\mathbf{z}}(T)$ is a fundamental matrix. Moreover, following the proof of Theorem 1.2.9, we can compute that

$$D_{\mathbf{z}}\widetilde{L}(\mathbf{z},\varepsilon)=\big(M_{\mathbf{z}}^{-1}(0)-M_{\mathbf{z}}^{-1}(T)\big)+D_{\mathbf{z}}\left(\int_0^T M_{\mathbf{z}}^{-1}(t)F_1(t,\mathbf{x}(t,\mathbf{z},0))dt\right)\varepsilon+O(\varepsilon^2). \tag{1.97}$$

We note that $\widetilde{L}^{-1}(0) = (\xi^{\perp}\circ\widetilde{L})^{-1}(0)\cap(\xi\circ\widetilde{L})^{-1}(0)$. From (1.97) we obtain $D_{\mathbf{z}}\widetilde{L}(\mathbf{z}_\alpha,0) = M_{\mathbf{z}_\alpha}^{-1}(0)-M_{\mathbf{z}_\alpha}^{-1}(T)$. If we write $\mathbf{z}\in\mathbb{R}^{2m}$ as $\mathbf{z}=(u,v)$ with $u,v\in\mathbb{R}^m$, then $D_v(\xi\circ\widetilde{L})(\mathbf{z}_\alpha,0)$ is the upper right corner of $M_{\mathbf{z}}^{-1}(0)$–$M_{\mathbf{z}}^{-1}(T)$. Then, from (i), we can apply the Implicit Function Theorem, deducing the existence of an open neighborhood $U\times(-\varepsilon_2,\varepsilon_2)$ of $\mathrm{Cl}(V)$ in $\xi(D)\times(-\varepsilon_1,\varepsilon_1)$, an open neighborhood $\mathcal{O}$ of $\beta_0(\mathrm{Cl}(V))$ in $\mathbb{R}^m$ and a unique $\mathcal{C}^k$ function $\beta(\alpha,\varepsilon)\colon U\times(-\varepsilon_2,\varepsilon_2)\to\mathcal{O}$ such that $(\xi\circ\widetilde{L})^{-1}(0)\cap(U\times\mathcal{O}\times(-\varepsilon_2,\varepsilon_2))$ is exactly the graphic of $\beta(\alpha,\varepsilon)$. Now, if we define the function $\delta\colon U\times(-\varepsilon_2,\varepsilon_2)\to\mathbb{R}$ as $\delta(\alpha,\varepsilon)=(\xi^{\perp}\circ\widetilde{L})(\alpha,\beta(\alpha,\varepsilon),\varepsilon)$, then δ is a function of class $\mathcal{C}^k$ and $\widetilde{L}^{-1}(0)\cap(U\times\mathcal{O}\times(-\varepsilon_2,\varepsilon_2)) = \{(\alpha,\beta(\alpha,\varepsilon),\varepsilon)\,|\,(\alpha,\varepsilon)\in\delta^{-1}(0)\}$. Therefore, to describe the set $\widetilde{L}^{-1}(0)$ in an open neighborhood of $\mathcal{Z}$ in $\mathbb{R}^n\times(-\varepsilon_0,\varepsilon_0)$, it suffices to describe $\delta^{-1}(0)$ in an open neighborhood of $\mathrm{Cl}(V)$ in $\mathbb{R}\times(-\varepsilon_0,\varepsilon_0)$.

Since $M_{\mathbf{z}_\alpha}^{-1}(0)-M_{\mathbf{z}_\alpha}^{-1}(T)$ has in the lower right corner the $m\times m$ zero matrix and $\delta(\alpha,0)=0$ in $V\times(-\varepsilon_2,\varepsilon_2)$, the function $\delta(\alpha,\varepsilon)$ can be written as $\delta(\alpha,\varepsilon) = \varepsilon\mathcal{G}(\alpha)+\varepsilon^2\widetilde{\mathcal{G}}(\alpha,\varepsilon)$ in $V\times(-\varepsilon_2,\varepsilon_2)$, where $\mathcal{G}(\alpha)$ is the function given in (1.67), see [12]. In addition, if $\widetilde{\delta}(\alpha,\varepsilon)=\mathcal{G}(\alpha)+\varepsilon\widetilde{\mathcal{G}}(\alpha,\varepsilon)$ then $\delta^{-1}(0)=\widetilde{\delta}^{-1}(0)$.

If there is $\alpha_0\in V$ such that $\widetilde{\delta}(\alpha_0,0)=\mathcal{G}(\alpha_0)=0$ and $\det((\partial\mathcal{G}/\partial\alpha)(\alpha_0))\neq 0$ then, from the Implicit Function Theorem, there exist $\varepsilon_3>0$ small, an open neighborhood V_0 of α_0 in V and a unique function $\alpha(\varepsilon)\colon(-\varepsilon_3,\varepsilon_3)\to V_0$ of class $\mathcal{C}^k$ such that $\widetilde{\delta}^{-1}(0)\cap(V_0\times(-\varepsilon_3,\varepsilon_3))$ is the graphic of $\alpha(\varepsilon)$, which also represents the set $\delta^{-1}(0)\cap(V_0\times(-\varepsilon_3,\varepsilon_3))$. This completes the proof of the theorem. □

1.3 Averaging theory of arbitrary order and dimension for finding periodic solutions

In this section we shall study periodic solutions of systems of the form

$$x'(t)=\sum_{i=0}^{k}\varepsilon^i F_i(t,x)+\varepsilon^{k+1}R(t,x,\varepsilon), \tag{1.98}$$

where $F_i\colon\mathbb{R}\times D\to\mathbb{R}^n$ for $i=0,1,\dots,k$, and $R\colon\mathbb{R}\times D\times(-\varepsilon_0,\varepsilon_0)\to\mathbb{R}^n$ are locally Lipschitz functions, being T-periodic in the first variable, and where D is

an open subset of $\mathbb{R}^n$; eventually F_0 can be the zero constant function.

The classical works using the averaging theory for studying the periodic solutions of a differential system (1.98) usually only provide this theory up to first ($k = 1$) or second order ($k = 2$) in the small parameter ε. Moreover, these theories assume differentiability of the functions F_i and R up to class $\mathcal{C}^2$ or $\mathcal{C}^3$, respectively. Recently, in [14], this averaging theory for computing periodic solutions was developed up to second order in dimension n, and up to third order ($k = 3$) in dimension 1, only using that the functions F_i and R are locally Lipschitz. Also, in the recent work [37], the averaging theory for computing periodic solutions was developed to an arbitrary order k in ε for analytical differential equations in dimension 1.

In this section we shall develop the averaging theory for studying the periodic solutions of a differential system (1.98) up to arbitrary order k in dimension n, with zero or non-zero F_0, and where the functions F_i and R are only locally Lipschitz. In fact this section is based in the results of the paper Llibre–Novaes–Teixeira [55].

An example that qualitative new phenomena can be found only when considering higher order analysis is the following. Consider arbitrary polynomial perturbations

$$\begin{aligned} \dot{x} &= -y + \textstyle\sum_{j\geq 1} \varepsilon^j f_j(x,y), \\ \dot{y} &= x + \textstyle\sum_{j\geq 1} \varepsilon^j g_j(x,y), \end{aligned} \tag{1.99}$$

of the harmonic oscillator, where ε is a small parameter. In this differential system the polynomials f_j and g_j are of degree n in the variables x and y, and the system is analytic in the variables x, y and ε. Then in [37] (see also Iliev [45]) it is proved that system (1.99) for $\varepsilon \neq 0$ sufficiently small has no more than $[s(n-1)/2]$ periodic solutions bifurcating from the periodic solutions of the linear center $\dot{x} = -y$, $\dot{y} = x$, using the averaging theory up to order s, and this bound can be reached. Here, $[\cdot]$ denotes the integer part function. So, higher order averaging theory can improve the results on the periodic solutions, both qualitatively and quantitatively.

In short, the goal of this section is to extend the averaging theory for computing periodic solutions of the differential system in n variables (1.98) up to an arbitrary order k in ε for locally Lipschitz differential systems, using the Brouwer degree.

1.3.1 Statement of the main results

We are interested in studying the existence of periodic orbits of general differential systems expressed by

$$x'(t) = \sum_{i=0}^{k} \varepsilon^i F_i(t,x) + \varepsilon^{k+1} R(t,x,\varepsilon), \tag{1.100}$$

where $F_i \colon \mathbb{R} \times D \to \mathbb{R}^n$ for $i = 1, 2, \ldots, k$, and $R \colon \mathbb{R} \times D \times (-\varepsilon_0, \varepsilon_0) \to \mathbb{R}^n$ are continuous functions, being T-periodic in the first variable, and where D is an open subset of $\mathbb{R}^n$.

In order to state our main results we introduce some notation. Let L be a positive integer, let $x = (x_1, \dots, x_n) \in D$, $t \in \mathbb{R}$ and $y_j = (y_{j1}, \dots, y_{jn}) \in \mathbb{R}^n$ for $j = 1, \dots, L$. Given $F\colon \mathbb{R} \times D \to \mathbb{R}^n$ a sufficiently smooth function, for each $(t, x) \in \mathbb{R} \times D$ we denote by $\partial^L F(t, x)$ a symmetric L-multilinear map which is applied to a "product" of L vectors of $\mathbb{R}^n$, which we denote as $\bigodot_{j=1}^{L} y_j \in \mathbb{R}^{nL}$. The definition of this L-multilinear map is

$$\partial^L F(t,x) \bigodot_{j=1}^{L} y_j = \sum_{i_1,\dots,i_L=1}^{n} \frac{\partial^L F(t,x)}{\partial x_{i_1} \cdots \partial x_{i_L}} y_{1i_1} \cdots y_{Li_L}. \tag{1.101}$$

We define ∂^0 as the identity functional. Given a positive integer b and a vector $y \in \mathbb{R}^n$, we also write $y^b = \bigodot_{i=1}^{b} y \in \mathbb{R}^{nb}$.

Remark 1.3.1. The L-multilinear map defined in (1.101) is the L^{th} Fréchet derivative of the function $F(t, x)$ with respect to the variable x. Indeed, for every fixed $t \in \mathbb{R}$, if we consider the function $F_t\colon D \to \mathbb{R}^n$ such that $F_t(x) = F(t, x)$, then $\partial^L F(t, x) = F_t^{(L)}(x) = \partial^L / \partial x^L F(t, x)$.

Example 1.3.2. To illustrate the above notation (1.101), we consider a smooth function $F\colon \mathbb{R} \times \mathbb{R}^2 \to \mathbb{R}^2$. So, for $x = (x_1, x_2)$ and $y^1 = (y_1^1, y_2^1)$, we have

$$\partial F(t,x) y^1 = \frac{\partial F}{\partial x_1}(t,x) y_1^1 + \frac{\partial F}{\partial x_2}(t,x) y_2^1.$$

Now, for $y^1 = (y_1^1, y_2^1)$ and $y^2 = (y_1^2, y_2^2)$, we have

$$\begin{aligned}\partial^2 F(t,x)(y^1, y^2) =& \frac{\partial^2 F(t,x)}{\partial x_1 \partial x_1} y_1^1 y_1^2 + \frac{\partial^2 F(t,x)}{\partial x_1 \partial x_2} y_1^1 y_2^2 \\ &+ \frac{\partial^2 F(t,x)}{\partial x_2 \partial x_1} y_2^1 y_1^2 + \frac{\partial^2 F(t,x)}{\partial x_2 \partial x_2} y_2^1 y_2^2.\end{aligned}$$

Observe that, for each $(t, x) \in \mathbb{R} \times D$, $\partial F(t, x)$ is a linear map in $\mathbb{R}^2$ and $\partial^2 F(t, x)$ is a bilinear map in $\mathbb{R}^2 \times \mathbb{R}^2$.

Let $\varphi(\cdot, z)\colon [0, t_z] \to \mathbb{R}^n$ be the solution of the unperturbed system

$$x'(t) = F_0(t, x) \tag{1.102}$$

such that $\varphi(0, z) = z$. For $i = 1, 2, \dots, k$, we define the *averaged function of order* i, $f_i\colon D \to \mathbb{R}^n$, as

$$f_i(z) = \frac{y_i(T, z)}{i!}, \tag{1.103}$$

where $y_i\colon \mathbb{R} \times D \to \mathbb{R}^n$, for $i = 1, 2, \dots, k-1$, are defined recurrently by the

integral equation

$$y_i(t,z) = i! \int_0^t \Big(F_i\big(s,\varphi(s,z)\big) + \sum_{l=1}^{i} \sum_{S_l} \frac{1}{b_1!\, b_2! 2!^{b_2} \cdots b_l! l!^{b_l}} \partial^L F_{i-l}\big(s,\varphi(s,z)\big) \bigodot_{j=1}^{l} y_j(s,z)^{b_j} \Big) ds, \quad (1.104)$$

where S_l is the set of all l-tuples of non-negative integers $(b_1, b_2, \ldots, b_l)$ satisfying $b_1 + 2b_2 + \cdots + lb_l = l$, and $L = b_1 + b_2 + \cdots + b_l$.

In Subsection 1.3.3 we compute the sets S_l for $l = 1, 2, 3, 4, 5$. Furthermore, we make the functions $f_k(z)$ explicit, up to $k = 5$ when $F_0 = 0$, and up to $k = 4$ when $F_0 \neq 0$.

Related to the averaging functions (1.103) there exist two cases of (1.100), essentially different, that must be treated separately, namely, when $F_0 = 0$ and when $F_0 \neq 0$. It can be seen in the following remarks.

Remark 1.3.3. If $F_0 = 0$, then $\varphi(t,z) = z$ for each $t \in \mathbb{R}$. So,

$$y_1(t,z) = \int_0^t F_1(t,z)ds, \quad \text{and} \quad f_1(t,z) = \int_0^T F_1(t,z)dt,$$

as usual in averaging theory; see, for instance, [5].

Remark 1.3.4. If $F_0 \neq 0$, then

$$y_1(t,z) = \int_0^t F_1\left(s,\varphi(s,z)\right) + \partial F_0\left(s,\varphi(s,z)\right) y_1(s,z)ds. \quad (1.105)$$

The integral equation (1.105) is equivalent to the following *Cauchy problem*:

$$\dot{u}(t) = F_1\left(t,\varphi(t,z)\right) + \partial F_0\left(t,\varphi(t,z)\right) u \quad \text{and} \quad u(0) = 0, \quad (1.106)$$

i.e., $y_1(t,z) = u(t)$. If we write

$$\eta(t,z) = \int_0^t \partial F_0(s,\varphi(s,z))ds, \quad (1.107)$$

we have

$$y_1(t,z) = e^{\eta(t,z)} \int_0^t e^{-\eta(s,z)} F_1(s,\varphi(s,z))ds \quad (1.108)$$

and

$$f_1(z) = \int_0^T e^{-\eta(t,z)} F_1(t,\varphi(t,z))dt.$$

Moreover, each $y_i(t,z)$ is obtained similarly from a Cauchy problem. The formulae are given explicitly in Subsection 1.3.3.

In the following, we state our main results: Theorem 1.3.5 when $F_0 = 0$, and Theorem 1.3.6 when $F_0 \neq 0$. The Brouwer degree d_B, which is defined in Appendix 1.3.6, is used.

Theorem 1.3.5. *Suppose that $F_0 = 0$. In addition, for the functions of (1.100), we assume the following conditions:*

(i) *for each $t \in \mathbb{R}$, $F_i(t,\cdot) \in \mathcal{C}^{k-i}$ for $i = 1, 2, \ldots, k$; $\partial^{k-i} F_i$ is locally Lipschitz in the second variable for $i = 1, 2, \ldots, k$; and R is continuous and locally Lipschitz in the second variable;*

(ii) *$f_i = 0$ for $i = 1, 2, \ldots, r-1$ and $f_r \neq 0$, where $r \in \{1, 2, \ldots, k\}$ (here, we are taking $f_0 = 0$). Moreover, suppose that for some $a \in D$ with $f_r(a) = 0$, there exists a neighborhood $V \subset D$ of a such that $f_r(z) \neq 0$ for all $z \in \overline{V} \setminus \{a\}$, and that $d_B\left(f_r(z), V, a\right) \neq 0$.*

Then, for $|\varepsilon| > 0$ sufficiently small, there exists a T-periodic solution $x(\cdot, \varepsilon)$ of (1.100) such that $x(0, \varepsilon) \to a$ when $\varepsilon \to 0$.

Theorem 1.3.6. *Suppose that $F_0 \neq 0$. In addition, for the functions of (1.100), we assume the following conditions:*

(i) *there exists an open subset W of D such that, for any $z \in \overline{W}$, $\varphi(t, z)$ is T-periodic in the variable t;*

(ii) *for each $t \in \mathbb{R}$, $F_i(t,\cdot) \in \mathcal{C}^{k-i}$ for $i = 0, 1, 2, \ldots, k$; $\partial^{k-i} F_i$ is locally Lipschitz in the second variable for $i = 0, 1, 2, \ldots, k$; and R is continuous and locally Lipschitz in the second variable;*

(iii) *$f_i = 0$ for $i = 1, 2, \ldots, r-1$ and $f_r \neq 0$, where $r \in \{1, 2, \ldots, k\}$; moreover, suppose that for some $a \in W$ with $f_r(a) = 0$, there exists a neighborhood $V \subset W$ of a such that $f_r(z) \neq 0$ for all $z \in \overline{V} \setminus \{a\}$, and that $d_B\left(f_r(z), V, a\right) \neq 0$.*

Then, for $|\varepsilon| > 0$ sufficiently small, there exists a T-periodic solution $x(\cdot, \varepsilon)$ of (1.100) such that $x(0, \varepsilon) \to a$ when $\varepsilon \to 0$.

Theorems 1.3.5 and 1.3.6 are proved in Subsection 1.3.2.

Remark 1.3.7. When the functions f_i defined in (1.103), for $i = 1, 2, \ldots, k$, are $\mathcal{C}^1$, the hypotheses (ii) from Theorem 1.3.5 and (iii) from Theorem 1.3.6 become:

(iv) $f_i = 0$ for $i = 1, 2 \ldots, r-1$ and $f_r \neq 0$, where $r \in \{1, 2, \ldots, k\}$; moreover, suppose that for some $a \in W$ with $f_r(a) = 0$ we have that $f_r'(a) \neq 0$.

In this case, instead of Brouwer degree theory, the Implicit Function Theorem could be used to prove Theorems 1.3.5 and 1.3.6.

We emphasize that our main contribution to the advanced averaging theory is based on Theorems 1.3.5 and 1.3.6. In fact, we provide conditions on the regularity of the functions, weaker than those given in [37].

1.3.2 Proofs of Theorems 1.3.5 and 1.3.6

Let $g\colon (-\varepsilon_0,\varepsilon_0)\to\mathbb{R}^n$ be a function defined on a small interval $(-\varepsilon_0,\varepsilon_0)$. We say that $g(\varepsilon)=\mathcal{O}(\varepsilon^\ell)$ for some positive integer ℓ if there exists constants $\varepsilon_1>0$ and $M>0$ such that $||g(\varepsilon)||\le M|\varepsilon^\ell|$ for $-\varepsilon_1<\varepsilon<\varepsilon_1$. The symbol $\mathcal{O}$ is one of the *Landau's symbols* (see for instance [78]).

To prove Theorems 1.3.5 and 1.3.6 we need the following lemma.

Lemma 1.3.8 (Fundamental Lemma)**.** *Under the assumptions of Theorems* 1.3.5 *or* 1.3.6 *let* $x(\cdot,z,\varepsilon)\colon[0,t_z]\to\mathbb{R}^n$ *be the solution of* (1.100) *with* $x(0,z,\varepsilon)=z$*. If* $t_z=T$*, then*

$$x(t,z,\varepsilon)=\varphi(t,z)+\sum_{i=1}^{k}\varepsilon^i\frac{y_i(t,z)}{i!}+\varepsilon^{k+1}\mathcal{O}(1),$$

where $y_i(t,z)$ *are defined in* (1.104)*, for* $i=1,2,\dots,k$*.*

Proof. By continuity of the solution $x(t,z,\varepsilon)$ and by compactness of the set $[0,T]\times\overline{V}\times[-\varepsilon_1,\varepsilon_1]$, there exits a compact subset K of D such that $x(t,z,\varepsilon)\in K$ for all $t\in[0,T]$, $z\in\overline{V}$ and $\varepsilon\in[-\varepsilon_1,\varepsilon_1]$. Now, by continuity of the function R, $|R(s,x(s,z,\varepsilon),\varepsilon)|\le\max\{|R(t,x,\varepsilon)|,(t,x,\varepsilon)\in[0,T]\times K\times[-\varepsilon_1,\varepsilon_1]\}=N$. Then

$$\left|\int_0^t R(s,x(s,z,\varepsilon),\varepsilon)ds\right|\le\int_0^T|R(s,x(s,z,\varepsilon),\varepsilon)|\,ds=TN,$$

which implies that

$$\int_0^t R(s,x(s,z,\varepsilon),\varepsilon)ds=\mathcal{O}(1). \tag{1.109}$$

Related to the functions $x(t,z,\varepsilon)$ and $\varphi(t,z)$ we have the following two equalities:

$$\begin{aligned} x(t,z,\varepsilon)&=z+\sum_{i=0}^{k}\varepsilon^i\int_0^t F_i(s,x(s,z,\varepsilon))ds+\mathcal{O}(\varepsilon^{k+1}),\\ \varphi(t,z)&=z+\int_0^t F_0(s,\varphi(s,z))ds. \end{aligned} \tag{1.110}$$

Moreover, $x(t,z,\varepsilon)=\varphi(t,z)+\mathcal{O}(\varepsilon)$. Indeed, F_0 is locally Lipschitz in the second variable, so from the compactness of the set $[0,T]\times\overline{V}\times[-\varepsilon_0,\varepsilon_0]$ and from (1.110) it follows that

$$\begin{aligned} |x(t,z,\varepsilon)-\varphi(t,z)|&\le\int_0^t|F_0(s,x(s,z,\varepsilon))-F_0(s,\varphi(s,z))|ds\\ &\quad+|\varepsilon|\int_0^t|F_1(s,x(s,z,\varepsilon))|ds+\mathcal{O}(\varepsilon^2)\\ &\le|\varepsilon|M+\int_0^t L_0|x(s,z,\varepsilon)-\varphi(s,z)|ds<|\varepsilon|Me^{TL_0}. \end{aligned}$$

Here, L_0 is the Lipschitz constant of F_0 on the compact K. The first and second inequalities were obtained similarly to (1.109). The last inequality is a consequence of the Gronwall Lemma (see, for example, [78, Lemma 1.3.1]).

In order to prove the present lemma we need the following claim.

Claim. For some positive integer m, let $G\colon \mathbb{R}\times D\to\mathbb{R}^n$ be a $\mathcal{C}^m$ function. Then

$$\begin{aligned}
&G(t,x(t,z,\varepsilon))\\
&\quad=\int_0^1\lambda_1^{m-1}\int_0^1\lambda_2^{m-2}\cdots\int_0^1\lambda_{m-1}\int_0^1\Big[\partial^m G\big(t,\ell_m\circ\ell_{m-1}\circ\cdots\circ\ell_1(x(t,z,\varepsilon))\big)\\
&\qquad\qquad-\partial^m G(t,\varphi(t,z))\Big]d\lambda_m d\lambda_{m-1}\cdots d\lambda_1\cdot(x(t,z,\varepsilon)-\varphi(t,z))^m\\
&\qquad+\sum_{L=0}^{m}\partial^L G(t,\varphi(t,z))\frac{(x(t,z,\varepsilon)-\varphi(t,z))^L}{L!},
\end{aligned}$$

where $\ell_i(v)=\lambda_i v+(1-\lambda_i)\varphi(t,z)$ for $v\in\mathbb{R}^n$.

We shall prove this claim using induction on m. For $m=1$, $G\in\mathcal{C}^1$. Let $\updownarrow_1(\lambda_1)=G\big(t,\ell_1(x(t,z,\varepsilon))\big)$. So,

$$\begin{aligned}
G(t,x(t,z,\varepsilon))=&G(t,\varphi(t,z))+\updownarrow_1(1)-\updownarrow_1(0)=G(t,\varphi(t,z))+\int_0^1\updownarrow_1'(\lambda_1)d\lambda_1\\
=&G(t,\varphi(t,z))+\int_0^1\partial G(t,\ell_1(x(t,z,\varepsilon)))d\lambda_1\cdot(x(t,z,\varepsilon)-\varphi(t,z))\\
=&\int_0^1\Big[\partial G(t,\ell_1(x(t,z,\varepsilon)))-\partial G(t,\varphi(t,z))\Big]d\lambda_1\cdot(x(t,z,\varepsilon)-\varphi(t,z))\\
&G(t,\varphi(t,z))+\partial G(t,\varphi(t,z))(x(t,z,\varepsilon)-\varphi(t,z)).
\end{aligned}$$

Given an integer $\overline{k}>1$, we assume as the *inductive hypothesis* $(I1)$ that the claim is true for $m=\overline{k}-1$.

Now, for $m=\overline{k}$, $G\in\mathcal{C}^{\overline{k}}\subset\mathcal{C}^{\overline{k}-1}$. So, from inductive hypothesis $(I1)$,

$$\begin{aligned}
G(t,x(t,z,\varepsilon))=&\int_0^1\lambda_1^{\overline{k}-2}\int_0^1\lambda_2^{\overline{k}-3}\cdots\int_0^1\lambda_{\overline{k}-2}\int_0^1\Big[\partial^{\overline{k}-1}G\big(t,\ell_{\overline{k}-1}\circ\ell_{\overline{k}-2}\circ\cdots\\
&\circ\ell_1(x(t,z,\varepsilon))\big)-\partial^{\overline{k}-1}G(t,\varphi(t,z))\Big]d\lambda_{\overline{k}-1}d\lambda_{\overline{k}-2}\cdots d\lambda_1\\
&\cdot(x(t,z,\varepsilon)-\varphi(t,z))^{\overline{k}-1}\\
&+\sum_{L=0}^{\overline{k}-1}\partial^L G(t,\varphi(t,z))\frac{(x(t,z,\varepsilon)-\varphi(t,z))^L}{L!}.
\end{aligned}\tag{1.111}$$

Let $\updownarrow(\lambda_{\overline{k}})=\partial^{\overline{k}-1}G\big(t,\ell_{\overline{k}}\circ\ell_{\overline{k}-1}\circ\cdots\circ\ell_1(x(t,z,\varepsilon))\big)$. So,

$$\begin{aligned}
\int_0^1\updownarrow'(\lambda_{\overline{k}})d\lambda_{\overline{k}}&=\updownarrow(1)-\updownarrow(0)\\
&=\partial^{\overline{k}-1}G\big(t,\ell_{\overline{k}-1}\circ\ell_{\overline{k}-2}\circ\cdots\circ\ell_1(x(t,z,\varepsilon))\big)-\partial^m G(t,\varphi(t,z)).
\end{aligned}\tag{1.112}$$

The derivative of $\updownarrow(\lambda_{\overline{k}})$ can be easily obtained as

$$\updownarrow'(\lambda_{\overline{k}}) = \lambda_{\overline{k}-1}\lambda_{\overline{k}-2}\cdots\lambda_1\partial^{\overline{k}}G\big(t, \ell_{\overline{k}}\circ\ell_{\overline{k}-1}\circ\cdots\circ\ell_1(x(t,z,\varepsilon))\big)(x(t,z,\varepsilon)-\varphi(t,z)).$$

Hence,

$$\begin{aligned}\int_0^1 \updownarrow'(\lambda_{\overline{k}})d\lambda_{\overline{k}} = \lambda_{\overline{k}-1}\lambda_{\overline{k}-2}\cdots\lambda_1\int_0^1 \Big[&\partial^{\overline{k}}G\big(t, \ell_{\overline{k}}\circ\ell_{\overline{k}-1}\circ\cdots\circ\ell_1(x(t,z,\varepsilon))\big)\\ &-\partial^{\overline{k}}G(t,\varphi(t,z))\Big]d\lambda_{\overline{k}}\cdot(x(t,z,\varepsilon)-\varphi(t,z))\\ &+\lambda_{\overline{k}-1}\lambda_{\overline{k}-2}\cdots\lambda_1\partial^{\overline{k}}G(t,\varphi(t,z))(x(t,z,\varepsilon)-\varphi(t,z)).\end{aligned} \tag{1.113}$$

Therefore, from (1.111) and (1.113), we conclude that

$$\begin{aligned}&G(t,x(t,z,\varepsilon))\\ &=\int_0^1\lambda_1^{\overline{k}-1}\int_0^1\lambda_2^{\overline{k}-2}\cdots\int_0^1\lambda_{\overline{k}-1}\int_0^1\Big[\partial^{\overline{k}}G\big(t,\ell_{\overline{k}}\circ\ell_{\overline{k}-1}\circ\cdots\circ\ell_1(x(t,z,\varepsilon))\big)\\ &\quad-\partial^{\overline{k}}G(t,\varphi(t,z))\Big]d\lambda_{\overline{k}}d\lambda_{\overline{k}-1}\cdots d\lambda_1\cdot(x(t,z,\varepsilon)-\varphi(t,z))^{\overline{k}}\\ &\quad+\sum_{L=0}^{\overline{k}}\partial^L G(t,\varphi(t,z))\frac{(x(t,z,\varepsilon)-\varphi(t,z))^L}{L!}.\end{aligned}$$

This completes the proof of the claim.

Given a non-negative integer m, we note that for a $\mathcal{C}^m$ function G such that $\partial^m G$ is locally Lipschitz in the second variable, the claim implies the equality

$$G(t,x(t,z,\varepsilon)) = \textstyle\sum_{L=0}^m \partial^L G(t,\varphi(t,z))\dfrac{(x(t,z,\varepsilon)-\varphi(t,z))^L}{L!} + \mathcal{O}(\varepsilon^{m+1}). \tag{1.114}$$

Indeed, for $m=0$, G is a continuous function locally Lipschitz in the second variable so,

$$|G(t,x(t,z,\varepsilon))-G(t,\varphi(t,z))| \le L_G|x(t,z,\varepsilon)-\varphi(t,z)| < |\varepsilon|L_G M e^{TL_0}.$$

Here, L_G is the Lipschitz constant of the function G on the compact K. Thus,

$$G(t,x(t,z,\varepsilon)) = G(t,\varphi(t,z)) + \mathcal{O}(\varepsilon).$$

Moreover, for $m\ge 1$ the claim implies (1.114) in a similar way to (1.109).

Again, we shall use induction, now on k, to prove the present lemma. For $k=1$, $F_0\in\mathcal{C}^1$ and the functions ∂F_0 and F_1 are locally Lipschitz in the second variable. Thus, from (1.114) and taking $G=F_0$ and $G=F_1$, we obtain

$$\begin{aligned}F_0(t,x(t,z,\varepsilon)) &= F_0(t,\varphi(t,z)) + \partial F_0(t,\varphi(t,z))(x(t,z,\varepsilon)-\varphi(t,z)) + \mathcal{O}(\varepsilon^2),\\ F_1(t,x(t,z,\varepsilon)) &= F_1(t,\varphi(t,z)) + \mathcal{O}(\varepsilon),\end{aligned} \tag{1.115}$$

respectively. From (1.110) and (1.115) we compute

$$\frac{d}{dt}\left(x(t,z,\varepsilon)-\varphi(t,z)\right)=\partial F_0(t,\varphi(t,z))\left(x(t,z,\varepsilon)-\varphi(t,z)\right)+\varepsilon F_1(t,\varphi(t,z))+\mathcal{O}(\varepsilon^2). \tag{1.116}$$

Solving the linear differential equation (1.115) with respect to $x(t,z,\varepsilon)-\varphi(t,z)$ for the initial condition $x(0,z,\varepsilon)-\varphi(0,z,\varepsilon)=0$, and comparing the solution with (1.108), we conclude that

$$x(t,z,\varepsilon)=\varphi(t,z)+\varepsilon y_1(t,z)+\mathcal{O}(\varepsilon^2).$$

Given an integer $\overline{k}$ we assume as the *inductive hypothesis* $(I2)$ that the lemma is true for $k=\overline{k}-1$.

Now for $k=\overline{k}$, $F_i=\mathcal{C}^{\overline{k}-i}$ for $i=0,1,\ldots,\overline{k}$ and $\partial^{\overline{k}-i}F_i$ is locally Lipschitz in the second variable for $i=0,1,\ldots,\overline{k}$. So, from (1.114),

$$F_i(t,x(t,z,\varepsilon))=\sum_{L=0}^{\overline{k}-i}\partial^L F_i(t,\varphi(t,z))\frac{(x(t,z,\varepsilon)-\varphi(t,z))^L}{L!}+\mathcal{O}(\varepsilon^{\overline{k}-i+1}), \tag{1.117}$$

for $i=0,1,\ldots,\overline{k}$. Applying the inductive hypothesis $(I2)$ in (1.117) we get

$$\begin{aligned}F_i(t,x(t,z,\varepsilon))&=F_1(t,\varphi(t,z))\\&\quad+\sum_{L=1}^{\overline{k}-i}\partial^L F_i(t,\varphi(t,z))\left(\sum_{i=1}^{\overline{k}-i-L+1}\varepsilon^i\frac{y_i(t,z)}{i!}\right)^L+\mathcal{O}(\varepsilon^{\overline{k}-i+1}),\end{aligned} \tag{1.118}$$

for $i=1,2,\ldots,\overline{k}$. Now using the *Multinomial Theorem* in (1.118) (see, for instance, [43, pag. 186]), we obtain

$$\begin{aligned}F_i(t,x(t,z,\varepsilon))&=F_i\left(t,\varphi(t,z)\right)\\&\quad+\sum_{L=1}^{\overline{k}-i}\sum_{l=L}^{\overline{k}-i}\sum_{S_{l,L}^{\overline{k}-1}}\frac{\varepsilon^l}{b_1!\,b_2!2!^{b_2}\cdots b_{\overline{k}-1}!(\overline{k}-1)!^{b_{\overline{k}-1}}}\partial^L F_i\left(t,\varphi(t,z)\right)\bigodot_{j=1}^{\overline{k}-1}y_j(t,z)^{b_j}\\&\quad+\mathcal{O}(\varepsilon^{\overline{k}-i+1}),\end{aligned}$$

for $i=1,2,\ldots,\overline{k}$. Here, $S_{l,L}^n$ is the set of all n-tuples of non-negative integers $(b_1,b_2,\ldots,b_n)$ satisfying $b_1+2b_2+\cdots+nb_n=l$ and $b_1+b_2+\cdots+b_n=L$. We note that if $n>l$ then $b_{l+1}=b_{l+2}=\cdots=b_n=0$. Hence,

$$\begin{aligned}F_i(t,x(t,z,\varepsilon))&=F_i\left(t,\varphi(t,z)\right)\\&\quad+\sum_{L=1}^{\overline{k}-i}\sum_{l=L}^{\overline{k}-i}\sum_{S_{l,L}^{l}}\frac{\varepsilon^l}{b_1!\,b_2!2!^{b_2}\cdots b_l!l!^{b_l}}\partial^L F_i\left(t,\varphi(t,z)\right)\bigodot_{j=1}^{l}y_j(t,z)^{b_j}\\&\quad+\mathcal{O}(\varepsilon^{\overline{k}-i+1}),\end{aligned} \tag{1.119}$$

for $i = 1, 2, \dots, \overline{k}$, because $\overline{k} - i \geq l$.

Finally, doing a change of indexes in (1.119), and observing that $\cup_{L=1}^{l} S_{l,L}^{l} = S_l$, we may write

$$\begin{aligned} F_i(t, x(t,z,\varepsilon)) &= F_i\left(t, \varphi(t,z)\right) \\ &+ \sum_{l=1}^{\overline{k}-i} \varepsilon^l \sum_{S_l} \frac{1}{b_1!\, b_2! 2!^{b_2} \cdots b_l! l!^{b_l}} \partial^L F_i\left(t, \varphi(t,z)\right) \bigodot_{j=1}^{l} y_j(t,z)^{b_j} \\ &+ \mathcal{O}(\varepsilon^{\overline{k}-i+1}), \end{aligned} \tag{1.120}$$

for $i = 1, 2, \dots, \overline{k}$. Following the above steps we also obtain

$$\begin{aligned} F_0(t, x(t,z,\varepsilon)) &= F_0\left(t, \varphi(t,z)\right) + \partial F_0(t, \varphi(t,z))(x(t,z,\varepsilon) - \varphi(t,z)) \\ &+ \sum_{i=1}^{\overline{k}} \varepsilon^i \Bigg[\sum_{S_i} \frac{1}{b_1!\, b_2! 2!^{b_2} \cdots b_i! i!^{b_r}} \partial^L F_0\left(t, \varphi(t,z)\right) \bigodot_{j=1}^{i} y_j(t,z)^{b_j} \\ &- \partial F_0(t, \varphi(t,z)) \frac{y_i(t,z)}{i!} \Bigg] + \mathcal{O}(\varepsilon^{\overline{k}+1}). \end{aligned} \tag{1.121}$$

Now, from (1.110), we compute

$$\begin{aligned} \frac{d}{dt}\left(x(t,z,\varepsilon) - \varphi(t,z)\right) &= F_0(t, x(t,z,\varepsilon)) \\ &- F_0(t, \varphi(t,z)) + \sum_{i=1}^{\overline{k}} \varepsilon^i F_i(t, x(t,z,\varepsilon)) + \mathcal{O}(\varepsilon^{\overline{k}+1}). \end{aligned} \tag{1.122}$$

Proceeding with a change of index we obtain from (1.120) that

$$\begin{aligned} \sum_{i=1}^{\overline{k}} \varepsilon^i F_i(t, x(t,z,\varepsilon)) &= \sum_{i=1}^{\overline{k}} \varepsilon^i \sum_{l=0}^{i-1} \sum_{S_l} \frac{1}{b_1!\, b_2! 2!^{b_2} \cdots b_l! l!^{b_l}} \partial^L F_{i-l}\left(t, \varphi(t,z)\right) \\ &\bigodot_{j=1}^{l} y_j(t,z)^{b_j} + \mathcal{O}(\varepsilon^{\overline{k}+1}). \end{aligned} \tag{1.123}$$

Substituting (1.121) and (1.123) in (1.122), we conclude that

$$\begin{aligned} \frac{d}{dt}\left(x(t,z,\varepsilon) - \varphi(t,z)\right) &= \partial F_0(t, \varphi(t,z))\left(x(t,z,\varepsilon) - \varphi(t,z)\right) \\ &+ \sum_{i=1}^{\overline{k}} \varepsilon^i \Bigg[\sum_{l=0}^{i} \sum_{S_l} \frac{1}{b_1!\, b_2! 2!^{b_2} \cdots b_l! l!^{b_l}} \partial^L F_{i-l}\left(t, \varphi(t,z)\right) \\ &\bigodot_{j=1}^{l} y_j(s,z)^{b_j} - \partial F_0(t, \varphi(t,z)) \frac{y_i(t,z)}{i!} \Bigg] + \mathcal{O}(\varepsilon^{\overline{k}+1}). \end{aligned} \tag{1.124}$$

Solving the linear differential equation (1.124) with respect to $x(t,z,\varepsilon)-\varphi(t,z)$ for the initial condition $x(0,z,\varepsilon)-\varphi(0,z)=0$, we obtain

$$x(t,z,\varepsilon)=\varphi(t,z)+\sum_{i=1}^{\overline{k}}\varepsilon^i\frac{Y_i(t,z)}{i!}+\mathcal{O}(\varepsilon^{\overline{k}+1}),$$

where

$$Y_i(t,z)=e^{\eta(t,z)}\int_0^t e^{-\eta(s,z)}\left[\sum_{l=0}^{i}\sum_{S_l}\frac{i!}{b_1!\,b_2!2!^{b_2}\cdots b_l!l!^{b_l}}\partial^L F_{i-l}\left(s,\varphi(s,z)\right)\right.$$
$$\left.\bigodot_{j=1}^{l}y_j(s,z)^{b_j}-\partial F_0(s,\varphi(s,z))y_i(s,z)\right]ds.$$

The function $\eta(t,z)$ was defined in (1.107). Hence,

$$\begin{aligned}\frac{d}{dt}Y_i(t,z)&=\partial F_0(t,\varphi(t,z))Y_i(t,z)\\&\quad+\sum_{l=0}^{i}\sum_{S_l}\frac{i!}{b_1!\,b_2!2!^{b_2}\cdots b_l!l!^{b_l}}\partial^L F_{i-l}\left(t,\varphi(t,z)\right)\bigodot_{j=1}^{l}y_j(t,z)^{b_j}\\&\quad-\partial F_0(t,\varphi(t,z))y_i(t,z)ds.\end{aligned}$$

Computing the derivative of the function $y_i(t,z)$, we conclude that the functions $y_i(t,z)$ and $Y_i(t,z)$ are defined by the same differential equation. Since $Y_i(0,z)=y_i(0,z)=0$, it follows that $Y_r(t,z)\equiv y_r(t,z)$ for every $i=1,2,\ldots,\overline{k}$. So, we have concluded the induction which completes the proof of the lemma. □

In a few words, the proof of Theorem 1.3.5 is an application of the Brouwer degree (see Appendix 1.3.6) to the approximated solution given by Lemma 1.3.8.

Proof of Theorem 1.3.5. Let $x(\cdot,z,\varepsilon)$ be a solution of (1.100) such that $x(0,z,\varepsilon)=z$. For each $z\in\overline{V}$, there exists $\varepsilon_1>0$ such that if $\varepsilon\in[-\varepsilon_1,\varepsilon_1]$ then $x(\cdot,z,\varepsilon)$ is defined in $[0,T]$. Indeed, by the *Existence and Uniqueness Theorem* of solutions (see, for example, [78, Theorem 1.2.4]), $x(\cdot,z,\varepsilon)$ is defined for all $0\le t\le\inf\left(T,d/M(\varepsilon)\right)$, where

$$M(\varepsilon)\ge\left|\sum_{i=1}^{k}\varepsilon^i F_i(t,x)+\varepsilon^{k+1}R(t,x,\varepsilon)\right|$$

for all $t\in[0,T]$, for each x with $|x-z|<d$, and for every $z\in\overline{V}$. When ε is sufficiently small we can take $d/M(\varepsilon)$ sufficiently large in order that $\inf\left(T,d/M(\varepsilon)\right)=T$ for all $z\in\overline{V}$. We write $\varepsilon f(z,\varepsilon)=x(T,z,\varepsilon)-z$. From Lemma 1.3.8 and equation (1.109) we have that

$$f(z,\varepsilon)=f_1(z)+\varepsilon f_2(z)+\varepsilon^2 f_3(z)+\cdots+\varepsilon^{k-1}f_k(z)+\varepsilon^k\mathcal{O}(1),$$

where the function f_i is the one defined in (1.103) for $i = 1, 2, \dots, k$. From the assumption (ii) of the theorem we have that

$$f(z,\varepsilon) = \varepsilon^{r-1} f_r(z) + \cdots + \varepsilon^{k-1} f_k(z) + \varepsilon^k \mathcal{O}(1).$$

Clearly, $x(\cdot, z, \varepsilon)$ is a T-periodic solution if and only if $f(z,\varepsilon) = 0$, because $x(t, z, \varepsilon)$ is defined for all $t \in [0, T]$.

From the Brouwer degree theory (see Lemma 1.3.12 in Appendix 1.3.6) and hypothesis (ii) we have, for $|\varepsilon| > 0$ sufficiently small, that

$$d_B\left(f_r(z), V, a\right) = d_B\left(f(z,\varepsilon), V, a\right) \neq 0.$$

Hence, by Theorem 1.3.10(i) (see Appendix 1.3.6), $0 \in f(V,\varepsilon)$ for $|\varepsilon| > 0$ sufficiently small, i.e, there exists $a_\varepsilon \in V$ such that $f(a_\varepsilon, \varepsilon) = 0$.

Therefore, for $|\varepsilon| > 0$ sufficiently small, $x(t, a_\varepsilon, \varepsilon)$ is a periodic solution of (1.100). Clearly, we can choose a_ε such that $a_\varepsilon \to a$ when $\varepsilon \to 0$, because $f(z,\varepsilon) \neq 0$ in $V \setminus \{a\}$. This completes the proof of the theorem. □

For proving Theorem 1.3.6 we also need the following lemma.

Lemma 1.3.9. *Let $w(\cdot, z, \varepsilon)\colon [0, \check{t}_z] \to \mathbb{R}^n$ be the solution of the system*

$$w'(t) = \sum_{i=1}^{k} \varepsilon^i \left([D_2\varphi(t,w)]^{-1} F_i(t, \varphi(t,w)) \right) + \varepsilon^{k+1} [D_2\varphi(t,w)]^{-1} R(t, \varphi(t,w), \varepsilon), \tag{1.125}$$

such that $w(0, z, \varepsilon) = z$. Then, $\psi(\cdot, z, \varepsilon)\colon [0, \tilde{t}_z] \to \mathbb{R}^n$ defined as $\psi(t, z, \varepsilon) = \varphi\left(t, w(t, z, \varepsilon)\right)$ is the solution of (1.100) with $\psi(0, z, \varepsilon) = z$.

Proof. Given $z \in D$, let $M(t) = D_2\varphi(t, z)$. The result about differentiable dependence on initial conditions implies that the function $M(t)$ is given as the fundamental matrix of the differential equation $u' = \partial F_0(t, \varphi(t, z))u$. So the matrix $M(t)$ is invertible for each $t \in [0, T]$. Now the proof follows immediately from the derivative of $\psi(t, \xi, \varepsilon)$ with respect to t. □

Proof of Theorem 1.3.6. Let $x(\cdot, z, \varepsilon)$ be a solution of (1.100) with $x(0, z, \varepsilon) = z$. For each $z \in \overline{V}$, there exists $\varepsilon_1 > 0$ such that if $\varepsilon \in [-\varepsilon_1, \varepsilon_1]$ then $x(\cdot, z, \varepsilon)$ is defined in $[0, T]$. Indeed, from Lemma 1.3.9, $x(t, z, \varepsilon) = \varphi\left(t, w(t, z, \varepsilon)\right)$ for each $z \in \overline{V}$, where $w(\cdot, z, \varepsilon)$ is the solution of (1.125). Moreover, for $|\varepsilon_1| > 0$ sufficiently small, $w(t, z, \varepsilon) \in W$ for each $(t, z, \varepsilon) \in [0, T] \times \overline{V} \times [-\varepsilon_1, \varepsilon_1]$. Repeating the argument of the proof of Theorem 1.3.5, we can show that $\check{t}_z = T$ for every $z \in \overline{V}$. Since $\varphi(\cdot, z)$ is defined in [0,T] for every $z \in W$, it follows that $\tilde{t}_z = T$, i.e., $x(\cdot, z, \varepsilon)$ is also defined in $[0, T]$. Now, denoting $f(z,\varepsilon) = x(T, z, \varepsilon) - z$, the proof follows like that of Theorem 1.3.5. □

1.3.3 Computing formulae

Now we shall illustrate how to compute the formulae from Theorems 1.3.5 and 1.3.6 for some $k \in \mathbb{N}$. In Subsection 1.3.4 we compute the formulae when $F_0 = 0$ for Theorem 1.3.5 up to $k = 5$. And in Subsection 1.3.5 we compute the formulae when $F_0 \neq 0$ for Theorem 1.3.6 up to $k = 4$.

First of all, from (1.104) we should determine the sets S_l for $l = 1, 2, 3, 4, 5$:

$$
\begin{aligned}
&S_1 = \{1\},\\
&S_2 = \{(0,1),(2,0)\},\\
&S_3 = \{(0,0,1),(1,1,0),(3,0,0)\},\\
&S_4 = \{(0,0,0,1),(1,0,1,0),(2,1,0,0),(0,2,0,0),(4,0,0,0)\}.
\end{aligned}
$$

To compute S_l it is convenient to exhibit a table of possibilities with the value b_i in the column i. We start from the last column.

Clearly, the last column can be filled only by zeroes and ones because $5b_5 > 5$ for $b_5 > 1$; the same happens with the fourth and the third column, because $3b_3$, $4b_4 > 5$, for b_3, $b_4 > 1$. Taking $b_5 = 1$, the unique possibility is $b_1 = b_2 = b_3 = b_4 = 0$, thus any other solution satisfies $b_5 = 0$. Taking $b_5 = 0$ and $b_4 = 1$, the unique possibility is $b_1 = 1$ and $b_2 = b_3 = 0$, thus any other solution must have $b_4 = b_5 = 0$. Finally, taking $b_5 = b_4 = 0$ and $b_3 = 1$, we have two possibilities either $b_1 = 2$ and $b_2 = 0$, or $b_1 = 0$ and $b_2 = 1$. Thus any other solution satisfies $b_3 = b_4 = b_5 = 0$.

Now we observe that the second column can be filled only by 0, 1 or 2, since $2b_2 > 5$ for $b_2 > 2$; and taking $b_3 = b_4 = b_5 = 0$ and $b_2 = 1$ the unique possibility is $b_1 = 3$. Taking $b_3 = b_4 = b_5 = 0$ and $b_2 = 2$ the unique possibility is $b_1 = 1$, thus any other solution satisfies $b_2 = b_3 = b_4 = b_5 = 0$. Finally, taking $b_2 = b_3 = b_4 = b_5 = 0$ the unique possibility is $b_1 = 5$. Therefore the complete table of solutions is

$S_5 =$

b_1	b_2	b_3	b_4	b_5
0	0	0	0	1
1	0	0	1	0
0	1	1	0	0
2	0	1	0	0
3	1	0	0	0
1	2	0	0	0
5	0	0	0	0

Now we can use (1.104) and (1.103) to compute the expressions of the y_i's and f_i's in each case.

1.3.4 Fifth order averaging of Theorem 1.3.5

Let us assume that $F_0 \equiv 0$. From (1.104) we obtain the functions $y_i(t,z)$ for $k = 1,2,3,4,5$:

$$
\begin{aligned}
y_1(t,z) &= \int_0^t F_1(s,z)ds,\\
y_2(t,z) &= \int_0^t \left(2F_2(s,z) + 2\frac{\partial F_1}{\partial x}(s,z)y_1(s,z)\right)ds,\\
y_3(t,z) &= \int_0^t \Bigg(6F_3(s,z) + 6\frac{\partial F_2}{\partial x}(s,z)y_1(t,z)\\
&\quad + 3\frac{\partial^2 F_1}{\partial x^2}(s,z)y_1(s,z)^2 + 3\frac{\partial F_1}{\partial x}(s,z)\, y_2(s,z)\Bigg)ds,\\
y_4(t,z) &= \int_0^t \Bigg(24F_4(s,z) + 24\frac{\partial F_3}{\partial x}(s,z)y_1(s,z)\\
&\quad + 12\frac{\partial^2 F_2}{\partial x^2}(s,z)y_1(s,z)^2 + 12\frac{\partial F_2}{\partial x}(s,z)y_2(s,z)\\
&\quad + 12\frac{\partial^2 F_1}{\partial x^2}(s,z)y_1(s,z)\odot y_2(s,z)\\
&\quad + 4\frac{\partial^3 F_1}{\partial x^3}(s,z)y_1(s,z)^3 + 4\frac{\partial F_1}{\partial x}(s,z)y_3(s,z)\Bigg)ds,\\
y_5(t,z) &= \int_0^t \Bigg(120F_5(s,z) + 120\frac{\partial F_4}{\partial x}(s,z)y_1(s,z\\
&\quad + 60\frac{\partial^2 F_3}{\partial x^2}(s,z)y_1(s,z)^2\\
&\quad + 60\frac{\partial F_3}{\partial x}(s,z)y_2(s,z) + 60\frac{\partial^2 F_2}{\partial x^2}(s,z)y_1(s,z)\odot y_2(s,z)\\
&\quad + 20\frac{\partial^3 F_2}{\partial x^3}(s,z)y_1(s,z)^3 + 20\frac{\partial F_2}{\partial x}(s,z)y_3(s,z)\\
&\quad + 20\frac{\partial^2 F_1}{\partial x^2}(s,z)y_1(s,z)\odot y_3(s,z)\\
&\quad + 15\frac{\partial^2 F_1}{\partial x^2}(s,z)y_2(s,z)^2 + 30\frac{\partial^3 F_1}{\partial x^3}(s,z)y_1(s,z)^2\odot y_2(s,z)\\
&\quad + 5\frac{\partial^4 F_1}{\partial x^4}(s,z)y_1(s,z)^4 + 5\frac{\partial F_1}{\partial x}(s,z)y_4(s,z)\Bigg)ds.
\end{aligned}
$$

Therefore, from (1.103) we have that

$$
\begin{aligned}
f_0(z) =& 0,\\
f_1(z) =& \int_0^T F_1(t,z)dt,
\end{aligned}
$$

$$
\begin{aligned}
f_2(z) &= \int_0^T \left(F_2(t,z)ds + \frac{\partial F_1}{\partial x}(t,z)y_1(t,z) \right) dt,\\
f_3(z) &= \int_0^T \left(F_3(t,z) + \frac{\partial F_2}{\partial x}(t,z)y_1(t,z) \right.\\
&\quad \left. + \frac{1}{2}\frac{\partial^2 F_1}{\partial x^2}(t,z)y_1(t,z)^2 + \frac{1}{2}\frac{\partial F_1}{\partial x}(t,z)y_2(t,z) \right) dt,\\
f_4(z) &= \int_0^T \left(F_4(t,z) + \frac{\partial F_3}{\partial x}(t,z)y_1(t,z) \right.\\
&\quad + \frac{1}{2}\frac{\partial^2 F_2}{\partial x^2}(t,z)y_1(t,z)^2 + \frac{1}{2}\frac{\partial F_2}{\partial x}(t,z)y_2(t,z)\\
&\quad + \frac{1}{2}\frac{\partial^2 F_1}{\partial x^2}(t,z)y_1(t,z) \odot y_2(t,z)dt\\
&\quad \left. + \frac{1}{6}\frac{\partial^3 F_1}{\partial x^3}(t,z)y_1(t,z)^3 + \frac{1}{6}\frac{\partial F_1}{\partial x}(t,z)y_3(t,z) \right) dt,\\
f_5(z) &= \int_0^T \left(F_5(t,z) + \frac{\partial F_4}{\partial x}(t,z)y_1(t,z) \right.\\
&\quad + \frac{1}{2}\frac{\partial^2 F_3}{\partial x^2}(t,z)y_1(t,z)^2 + \frac{1}{2}\frac{\partial F_3}{\partial x}(t,z)y_2(t,z)\\
&\quad + \frac{1}{2}\frac{\partial^2 F_2}{\partial x^2}(t,z)y_1(t,z) \odot y_2(t,z)\\
&\quad + \frac{1}{6}\frac{\partial^3 F_2}{\partial x^3}(t,z)y_1(t,z)^3 + \frac{1}{6}\frac{\partial F_2}{\partial x}(t,z)y_3(t,z)\\
&\quad + \frac{1}{6}\frac{\partial^2 F_1}{\partial x^2}(t,z)y_1(t,z) \odot y_3(t,z)\\
&\quad + \frac{1}{8}\frac{\partial^2 F_1}{\partial x^2}(t,z)y_2(t,z)^2 + \frac{1}{4}\frac{\partial^3 F_1}{\partial x^3}(t,z)y_1(t,z)^2 \odot y_2(t,z)\\
&\quad \left. + \frac{1}{24}\frac{\partial^4 F_1}{\partial x^4}(t,z)y_1(t,z)^4 + \frac{1}{24}\frac{\partial F_1}{\partial x}(t,z)y_4(t,z) \right) dt.
\end{aligned}
$$

1.3.5 Fourth order averaging of Theorem 1.3.6

Now we assume that $F_0 \not\equiv 0$. First a Cauchy problem or, equivalently, an integral equation (see Remark 1.3.4) must be solved to compute the expressions $y_i(t,z)$ for $i = 1, 2, \ldots, k$. We give the integral equations and its solutions for $k = 1, 2, 3, 4$.

Let $\eta(t,z)$ be the function defined in (1.107), and let $M(z) = \eta(T,z)$. Hence, from (1.104) and (1.103) we obtain the functions $y_1(t,z)$ and $f_1(z)$:

$$
y_1(t,z) = \int_0^t \left(F_1(s,\varphi(s,z)) + \frac{\partial F_0}{\partial x}(s,\varphi(s,z))y_1(s,z) \right) ds,
$$

so

$$y_1(t,z) = e^{\eta(t,z)} \int_0^t e^{-\eta(s,z)} F_1(s,\varphi(s,z))ds,$$

and

$$f_1(z) = M(z) \int_0^T e^{-\eta(t,z)} F_1(t,\varphi(t,z))dt.$$

Similarly, the functions $y_2(t,z)$ and $f_2(z)$ are given by:

$$\begin{aligned} y_2(t,z) = \int_0^t \Bigg(& 2F_2(s,\varphi(s,z)) + 2\frac{\partial F_1}{\partial x}(s,\varphi(s,z))y_1(s,z) \\ & + \frac{\partial^2 F_0}{\partial x^2}(s,\varphi(s,z))y_1(s,z)^2 + \frac{\partial F_0}{\partial x}(s,\varphi(s,z))\, y_2(s,z) \Bigg) dt, \end{aligned}$$

so

$$\begin{aligned} y_2(t,z) = & e^{\eta(t,z)} \int_0^t e^{-\eta(s,z)} \Bigg(2F_2(s,\varphi(s,z)) + 2\frac{\partial F_1}{\partial x}(s,\varphi(s,z))y_1(s,z) \\ & \frac{\partial^2 F_0}{\partial x^2}(s,\varphi(s,z))y_1(s,z)^2 \Bigg) ds, \end{aligned}$$

and

$$\begin{aligned} f_2(z) = & M(z) \int_0^T e^{-\eta(t,z)} \Bigg(F_2(t,\varphi(t,z)) + \frac{\partial F_1}{\partial x}(t,\varphi(t,z))y_1(t,z) \\ & \frac{1}{2}\frac{\partial^2 F_0}{\partial x^2}(t,\varphi(t,z))y_1(t,z)^2 \Bigg) dt. \end{aligned}$$

The functions $y_3(t,z)$ and $f_3(z)$ are given by

$$\begin{aligned} y_3(t,z) = \int_0^t \Bigg(& 6F_3(s,\varphi(s,z)) + 6\frac{\partial F_2}{\partial x}(s,\varphi(s,z))y_1(s,z) \\ & + 3\frac{\partial^2 F_1}{\partial x^2}(s,\varphi(s,z))y_1(s,z)^2 + 3\frac{\partial F_1}{\partial x}(s,\varphi(s,z))\, y_2(s,z) \\ & + 3\frac{\partial^2 F_0}{\partial x^2}(s,\varphi(s,z))y_1(s,z) \odot y_2(s,z) \\ & + \frac{\partial^3 F_0}{\partial x^3}(s,\varphi(s,z))y_1(s,z)^3 + \frac{\partial F_0}{\partial x}(s,\varphi(s,z))y_3(s,z) \Bigg) ds, \end{aligned}$$

so

$$\begin{aligned} y_3(t,z) =& e^{\eta(t,z)} \int_0^t e^{-\eta(s,z)} \left(6F_3(s,\varphi(s,z)) + 6\frac{\partial F_2}{\partial x}(s,\varphi(s,z))y_1(s,z) \right. \\ & + 3\frac{\partial^2 F_1}{\partial x^2}(s,\varphi(s,z))y_1(s,z)^2 + 3\frac{\partial F_1}{\partial x}(s,\varphi(s,z))\, y_2(s,z) \\ & + 3\frac{\partial^2 F_0}{\partial x^2}(s,\varphi(s,z))y_1(s,z) \odot y_2(s,z) \\ & \left. + \frac{\partial^3 F_0}{\partial x^3}(s,\varphi(s,z))y_1(s,z)^3 \right) ds, \end{aligned}$$

and

$$\begin{aligned} f_3(z) =& M(z) \int_0^T e^{-\eta(t,z)} \left(F_3(t,\varphi(t,z)) + \frac{\partial F_2}{\partial x}(t,\varphi(t,z))y_1(t,z) \right. \\ & + \frac{1}{2}\frac{\partial^2 F_1}{\partial x^2}(t,\varphi(t,z))y_1(t,z)^2 + \frac{1}{2}\frac{\partial F_1}{\partial x}(t,\varphi(t,z))\, y_2(t,z) \\ & + \frac{1}{2}\frac{\partial^2 F_0}{\partial x^2}(t,\varphi(t,z))y_1(t,z) \odot y_2(t,z) \\ & \left. + \frac{1}{6}\frac{\partial^3 F_0}{\partial x^3}(t,\varphi(t,z))y_1(t,z)^3 \right) ds. \end{aligned}$$

Finally, the functions $y_4(t,z)$ and $f_4(z)$ are given by

$$\begin{aligned} y_4(t,z) = & \int_0^t \left(24F_4(s,\varphi(s,z)) + 24\frac{\partial F_3}{\partial x}(s,\varphi(s,z))y_1(s,z) \right. \\ & + 12\frac{\partial^2 F_2}{\partial x^2}(s,\varphi(s,z))y_1(s,z)^2 + 12\frac{\partial F_2}{\partial x}(s,\varphi(s,z))y_2(s,z) \\ & + 12\frac{\partial^2 F_1}{\partial x^2}(s,\varphi(s,z))y_1(s,z) \odot y_2(s,z) \\ & + 4\frac{\partial^3 F_1}{\partial x^3}(s,\varphi(s,z))y_1(s,z)^3 + 4\frac{\partial F_1}{\partial x}(s,\varphi(s,z))y_3(s,z) \\ & + 4\frac{\partial^2 F_0}{\partial x^2}(s,\varphi(s,z))y_1(s,z) \odot y_3(s,z) \\ & + 3\frac{\partial^2 F_0}{\partial x^2}(s,\varphi(s,z))y_2(s,z)^2 ds + 6\frac{\partial^3 F_0}{\partial x^3}(s,\varphi(s,z))y_1(s,z)^2 \odot y_2(s,z) \\ & \left. + \frac{\partial^4 F_0}{\partial x^4}(s,\varphi(s,z))y_1(s,z)^4 + \frac{\partial F_0}{\partial x}(s,\varphi(s,z))y_4(s,z) \right) ds, \end{aligned}$$

so

$$
\begin{aligned}
y_4(t,z) =& e^{\eta(t,z)} \int_0^t e^{-\eta(s,z)} \left(24F_4(s,\varphi(s,z)) + 24\frac{\partial F_3}{\partial x}(s,\varphi(s,z))y_1(s,z) \right. \\
&+ 12\frac{\partial^2 F_2}{\partial x^2}(s,\varphi(s,z))y_1(s,z)^2 + 12\frac{\partial F_2}{\partial x}(s,\varphi(s,z))y_2(s,z) \\
&+ 12\frac{\partial^2 F_1}{\partial x^2}(s,\varphi(s,z))y_1(s,z) \odot y_2(s,z) \\
&+ 4\frac{\partial^3 F_1}{\partial x^3}(s,\varphi(s,z))y_1(s,z)^3 + 4\frac{\partial F_1}{\partial x}(s,\varphi(s,z))y_3(s,z) \\
&+ 4\frac{\partial^2 F_0}{\partial x^2}(s,\varphi(s,z))y_1(s,z) \odot y_3(s,z) \\
&+ 3\frac{\partial^2 F_0}{\partial x^2}(s,\varphi(s,z))y_2(s,z)^2 ds + 6\frac{\partial^3 F_0}{\partial x^3}(s,\varphi(s,z))y_1(s,z)^2 \odot y_2(s,z) \\
&\left. + \frac{\partial^4 F_0}{\partial x^4}(s,\varphi(s,z))y_1(s,z)^4 \right) ds,
\end{aligned}
$$

and

$$
\begin{aligned}
f_4(z) =& M(z) \int_0^T e^{-\eta(t,z)} \left(F_4(t,\varphi(t,z)) + \frac{\partial F_3}{\partial x}(t,\varphi(t,z))y_1(t,z) \right. \\
&+ \frac{1}{2}\frac{\partial^2 F_2}{\partial x^2}(t,\varphi(t,z))y_1(t,z)^2 + \frac{1}{2}\frac{\partial F_2}{\partial x}(t,\varphi(t,z))y_2(t,z) \\
&+ \frac{1}{2}\frac{\partial^2 F_1}{\partial x^2}(t,\varphi(t,z))y_1(t,z) \odot y_2(t,z) \\
&+ \frac{1}{6}\frac{\partial^3 F_1}{\partial x^3}(t,\varphi(t,z))y_1(t,z)^3 + \frac{1}{6}\frac{\partial F_1}{\partial x}(t,\varphi(t,z))y_3(t,z) \\
&+ \frac{1}{6}\frac{\partial^2 F_0}{\partial x^2}(t,\varphi(t,z))y_1(t,z) \odot y_3(t,z) \\
&+ \frac{1}{8}\frac{\partial^2 F_0}{\partial x^2}(t,\varphi(t,z))y_2(t,z)^2 ds + \frac{1}{4}\frac{\partial^3 F_0}{\partial x^3}(t,\varphi(t,z))y_1(t,z)^2 \odot y_2(t,z) \\
&\left. + \frac{1}{24}\frac{\partial^4 F_0}{\partial x^4}(t,\varphi(t,z))y_1(t,z)^4 \right) ds.
\end{aligned}
$$

1.3.6 Appendix: basic results on the Brouwer degree

In this appendix we present the existence and uniqueness result from the degree theory in finite dimensional spaces. We follow Browder's paper [11], where the properties of the classical Brouwer degree are formalized. We also present some results we shall need for proving our main results.

Theorem 1.3.10. *Let $X = \mathbb{R}^n = Y$ for a given positive integer n. For bounded open subsets V of X, consider continuous mappings $f\colon \overline{V} \to Y$, and points y_0 in Y such that y_0 does not lie in $f(\partial V)$ (as usual, ∂V denotes the boundary of V).*

Then to each such triple (f, V, y_0), there corresponds an integer $d(f, V, y_0)$ having the following three properties:

(i) *If $d(f, V, y_0) \neq 0$ then $y_0 \in f(V)$. If f_0 is the identity map of X onto Y then, for every bounded open set V and $y_0 \in V$, we have $d\left(f_0|_V, V, y_0\right) = \pm 1$.*

(ii) *(Additivity) If $f\colon \overline{V} \to Y$ is a continuous map with V a bounded open set in X, and V_1 and V_2 are a pair of disjoint open subsets of V such that $y_0 \notin f(\overline{V} \backslash (V_1 \cup V_2))$ then, $d(f_0, V, y_0) = d(f_0, V_1, y_0) + d(f_0, V_1, y_0)$.*

(iii) *(Invariance under homotopy) Let V be a bounded open set in X, and consider a continuous homotopy $\{f_t : 0 \leq t \leq 1\}$ of maps of $\overline{V}$ into Y. Let $\{y_t : 0 \leq t \leq 1\}$ be a continuous curve in Y such that $y_t \notin f_t(\partial V)$ for any $t \in [0, 1]$. Then $d(f_t, V, y_t)$ is constant in t on $[0, 1]$.*

Theorem 1.3.11. *The degree function $d(f, V, y_0)$ is uniquely determined by the conditions of Theorem* 1.3.10.

For the proofs of Theorems 1.3.10 and 1.3.11, see [11].

Lemma 1.3.12. *We consider continuous functions $f_i\colon \overline{V} \to \mathbb{R}^n$, for $i = 0, 1, \ldots, k$, and $f, g, r\colon \overline{V} \times [\varepsilon_0, \varepsilon_0] \to \mathbb{R}^n$, given by*

$$g(\cdot, \varepsilon) = f_1(\cdot) + \varepsilon f_2(\cdot) + \varepsilon^2 f_3(\cdot) + \cdots + \varepsilon^{k-1} f_k(\cdot),$$

$$f(\cdot, \varepsilon) = g(\cdot, \varepsilon) + \varepsilon^k r(\cdot, \varepsilon).$$

Assume that $g(z, \varepsilon) \neq 0$ for all $z \in \partial V$ and $\varepsilon \in [-\varepsilon_0, \varepsilon_0]$. If for $|\varepsilon| > 0$ sufficiently small $d_B(f(\cdot, \varepsilon), V, y_0)$ is well defined, then $d_B(f(\cdot, \varepsilon), V, y_0) = d_B(g(\cdot, \varepsilon), V, y_0)$.

For a proof of Lemma 1.3.12, see [14, Lemma 2.1].

1.4 Three applications of Theorem 1.3.5

The first application studies the periodic solutions of the Hénon–Heiles Hamiltonian using the averaging theory of second order. The other two examples analyze the limit cycles of some classes of polynomial differential systems in the plane. These last two applications use the averaging theory of third order. More precisely, these three applications are based in Theorem 1.3.5.

In the next subsection we summarize the results of Theorem 1.3.5 up to third order, precisely the ones used in the applications here considered.

1.4.1 The averaging theory of first, second and third order

As far as we know, the averaging theory of third order for studying specifically periodic orbits was developed by first time in [14]. Now we summarize it here from Theorem 1.3.5 which is given at any order.

Consider the differential system

$$\dot{x}(t) = \varepsilon F_1(t,x) + \varepsilon^2 F_2(t,x) + \varepsilon^3 F_3(t,x) + \varepsilon^4 R(t,x,\varepsilon), \tag{1.126}$$

where $F_1, F_2, F_3 \colon \mathbb{R} \times D \to \mathbb{R}$ and $R \colon \mathbb{R} \times D \times (-\varepsilon_f, \varepsilon_f) \to \mathbb{R}$ are continuous functions, T-periodic in the first variable, and D is an open subset of $\mathbb{R}^n$. Assume that the following hypotheses (i) and (ii) hold:

(i) $F_1(t,\cdot) \in \mathcal{C}^2(D)$, $F_2(t,\cdot) \in \mathcal{C}^1(D)$ for all $t \in \mathbb{R}$, F_1, F_2, F_3, R, $D_x^2 F_1$,$D_x F_2$ are locally Lipschitz with respect to x, and R is twice differentiable with respect to ε. We define $F_{k0} \colon D \to \mathbb{R}$ for $k = 1, 2, 3$ as

$$\begin{aligned}
F_{10}(z) =& \frac{1}{T} \int_0^T F_1(s,z) ds, \\
F_{20}(z) =& \frac{1}{T} \int_0^T \left[D_z F_1(s,z) \cdot y_1(s,z) + F_2(s,z) \right] ds, \\
F_{30}(z) =& \frac{1}{T} \int_0^T \Big[\frac{1}{2} y_1(s,z)^T \frac{\partial^2 F_1}{\partial z^2}(s,z) y_1(s,z) + \frac{1}{2} \frac{\partial F_1}{\partial z}(s,z) y_2(s,z) \\
& + \frac{\partial F_2}{\partial z}(s,z)(y_1(s,z)) + F_3(s,z) \Big] ds,
\end{aligned}$$

where

$$\begin{aligned}
y_1(s,z) &= \int_0^s F_1(t,z) dt, \\
y_2(s,z) &= \int_0^s \left[\frac{\partial F_1}{\partial z}(t,z) \int_0^t F_1(r,z) dr + F_2(t,z) \right] dt.
\end{aligned}$$

(ii) For $V \subset D$ an open and bounded set, and for each $\varepsilon \in (-\varepsilon_f, \varepsilon_f) \setminus \{0\}$ there exists $a_\varepsilon \in V$ such that $F_{10}(a_\varepsilon) + \varepsilon F_{20}(a_\varepsilon) + \varepsilon^2 F_{30}(a_\varepsilon) = 0$ and $d_B(F_{10} + \varepsilon F_{20} + \varepsilon^2 F_{30}, V, a_\varepsilon) \neq 0$.

Then for $|\varepsilon| > 0$ sufficiently small there exists a T-periodic solution $\varphi(\cdot,\varepsilon)$ of the system such that $\varphi(0,\varepsilon) = a_\varepsilon$.

The expression $d_B(F_{10} + \varepsilon F_{20} + \varepsilon^2 F_{30}, V, a_\varepsilon) \neq 0$ means that the Brouwer degree of the function $F_{10} + \varepsilon F_{20} + \varepsilon^2 F_{30} \colon V \to \mathbb{R}^n$ at the fixed point a_ε is not zero. A sufficient condition for the inequality to be true is that the Jacobian of the function $F_{10} + \varepsilon F_{20} + \varepsilon^2 F_{30}$ at a_ε is not zero.

If F_{10} is not identically zero, then the zeros of $F_{10} + \varepsilon F_{20} + \varepsilon^2 F_{30}$ are mainly the zeros of F_{10} for ε sufficiently small. In this case, the previous result provides the *averaging theory of first order*.

If F_{10} is identically zero and F_{20} is not identically zero, then the zeros of $F_{10} + \varepsilon F_{20} + \varepsilon^2 F_{30}$ are mainly the zeros of F_{20} for ε sufficiently small. In this case, the previous result provides the *averaging theory of second order*.

If F_{10} and F_{20} are both identically zero and F_{30} is not identically zero, then the zeros of $F_{10}+\varepsilon F_{20}+\varepsilon^2 F_{30}$ are mainly the zeros of F_{30} for ε sufficiently small. In this case, the previous result provides the *averaging theory of third order*.

1.4.2 The Hénon–Heiles Hamiltonian

The results presented in this subsection have been proved by Jiménez–Llibre [50].

The classical Hénon–Heiles potential consists of a two dimensional harmonic potential plus two cubic terms. It was introduced in 1964, as a model for studying the existence of a third integral of motion of a star in a rotating meridian plane of a galaxy in the neighborhood of a circular orbit [40]. The classical *Hénon–Heiles* potential has been generalized by introducing two parameters to each cubic term,

$$\frac{1}{2}(p_x^2+p_y^2+x^2+y^2)+Bxy^2+\frac{1}{3}Ax^3, \tag{1.127}$$

such that $B\neq 0$, with $x,y,p_x,p_y\in\mathbb{R}$. Then the classical Hénon–Heiles Hamiltonian system corresponds to $A=-1$, $B=1$. It is given by

$$\begin{aligned}\dot{x}&=p_x,\\ \dot{p}_x&=-x-(Ax^2+By^2),\\ \dot{y}&=p_y,\\ \dot{p}_y&=-y-2Bxy.\end{aligned} \tag{1.128}$$

As usual, the dot denotes derivative with respect to the independent variable $t\in\mathbb{R}$, the time. We name (1.128) the *Hénon–Heiles Hamiltonian systems with two parameters*, or simply the *Hénon–Heiles systems*.

The periodic orbits in the Hénon–Heiles potential have been numerically studied and classified by Churchill–Pecelli–Rod [20], Davies–Huston–Baranger [24] and others [10, 31, 74]. Maciejewski–Radzki–Rybicki [68] did an analytical study of a more general Hénon–Heiles Hamiltonians including a third cubic term of the form Cx^2y, which can be removed by a proper rotation, and two more parameters associated with the quadratic part of the potential. They proved the existence of connected branches of non-stationary periodic orbits in the neighborhood of a given degenerate stationary point.

Theorem 1.4.1. *At every positive energy level the Hénon–Heiles Hamiltonian system* (1.128) *has at least*

(i) *one periodic orbit if* $(2B-5A)(2B-A)<0$ (*see Figure* 1.1),

(ii) *two periodic orbits if* $A+B=0$ *and* $A\neq 0$ (*this case contains the classical Hénon–Heiles system*), *and*

(iii) *three periodic orbits if* $B(2B-5A)>0$ *and* $A+B\neq 0$ (*see Figure* 1.2).

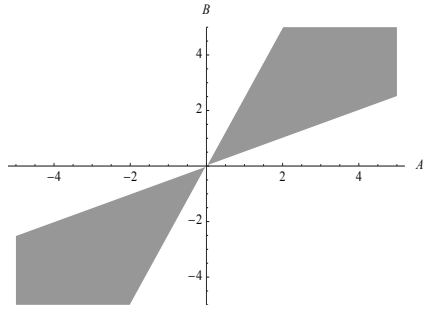

Figure 1.1: Open region $(2B - 5A)(2B - A) < 0$ in the parameter space (A, B), where there is at least one periodic orbit with multipliers different from 1.

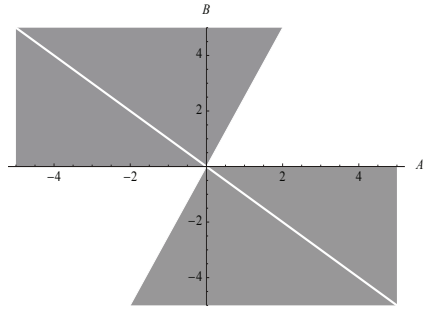

Figure 1.2: Open region $B(2B - 5A) > 0$ and $A + B \neq 0$ in the parameter space (A, B), where there are at least three periodic orbits with multipliers different from 1. When $A + B = 0$, there are at least two periodic orbits with multipliers different from 1.

Proof. For proving this theorem we shall apply Theorem 1.3.5 to the Hamiltonian system (1.128). Generically, the periodic orbits of a Hamiltonian system with more than one degree of freedom are on cylinders fulfilled by periodic orbits. Therefore we cannot apply directly Theorem 1.3.5 to a Hamiltonian system, since the Jacobian of the function f at the fixed point a will always be zero. Then we must apply Theorem 1.3.5 to every Hamiltonian fixed level, where the periodic orbits generically are isolated.

On the other hand, in order to apply Theorem 1.3.5 we need a small parameter ε. So in the Hamiltonian system (1.128) we change the variables (x, y, p_x, p_y) to (X, Y, p_X, p_Y) where $x = \varepsilon X$, $y = \varepsilon Y$, $p_x = \varepsilon p_X$ and $p_y = \varepsilon p_Y$. In the new

variables, the system (1.128) becomes

$$\begin{aligned} \dot{X} &= p_X, \\ \dot{p}_X &= -X - \varepsilon(AX^2 + BY^2), \\ \dot{Y} &= p_Y, \\ \dot{p}_Y &= -Y - 2\varepsilon BXY. \end{aligned} \tag{1.129}$$

This system again is Hamiltonian with Hamiltonian

$$\frac{1}{2}(p_X^2 + p_Y^2 + X^2 + Y^2) + \varepsilon \left(BXY^2 + \frac{1}{3}AX^3 \right). \tag{1.130}$$

As the change of variables is only a scale transformation, for all ε different from zero, the original and the transformed systems (1.128) and (1.129) have essentially the same phase portrait and, additionally, the system (1.129) for ε sufficiently small is close to an integrable one.

First we change the Hamiltonian (1.130) and the equations of motion (1.129) to polar coordinates for $\varepsilon = 0$, which is an harmonic oscillator. Thus we have

$$X = r\cos\theta, \quad p_X = r\sin\theta, \quad Y = \rho\cos(\theta + \alpha), \quad p_Y = \rho\sin(\theta + \alpha).$$

Recall that this is a change of variables when $r > 0$ and $\rho > 0$. Moreover, doing this change of variables, the angular variables θ and α appear in the system. Later on, the variable θ will be used for obtaining the periodicity necessary for applying the averaging theory.

The fixed value of the energy in polar coordinates is

$$h = \frac{1}{2}(r^2 + \rho^2) + \varepsilon \left(\frac{1}{3}Ar^3\cos^3\theta + Br\rho^2\cos\theta\cos^2(\theta + \alpha) \right), \tag{1.131}$$

and the equations of motion are given by

$$\begin{aligned} \dot{r} &= -\varepsilon\sin\theta \left(A\, r^2\cos^2\theta + B\, \rho^2\cos^2(\theta + \alpha) \right), \\ \dot{\theta} &= -1 - \varepsilon\cos\theta \left(A\, r\cos^2\theta + \frac{\rho^2}{r} B\, \cos^2(\theta + \alpha) \right), \\ \dot{\rho} &= -\varepsilon B\, r\rho\cos\theta\sin(2(\theta + \alpha)), \\ \dot{\alpha} &= \varepsilon\frac{\cos\theta}{r} \left(A\, r^2\cos^2\theta + B(\rho^2 - 2r^2)\cos^2(\theta + \alpha) \right). \end{aligned} \tag{1.132}$$

However, the derivatives of the left hand side of these equations are with respect to the time variable t, which is not periodic. We change to the θ variable as the independent one, and we denote by a prime the derivative with respect to θ. The angular variable α cannot be used as the independent variable since the new

differential system would not have the form (1.98) for applying Theorem 1.3.5. The system (1.132) goes over to

$$
\begin{aligned}
r' &= \frac{\varepsilon\, r \sin\theta \left(A\, r^2 \cos^2\theta + B\rho^2 \cos^2(\theta+\alpha)\right)}{r + \varepsilon(A\, r^2 \cos^3\theta + B\rho^2 \cos\theta \cos^2(\theta+\alpha))},\\
\rho' &= \frac{\varepsilon\, B r^2 \rho \cos\theta \sin(2(\theta+\alpha))}{r + \varepsilon(A\, r^2 \cos^3\theta + B\rho^2 \cos\theta \cos^2(\theta+\alpha))},\\
\mathcal{A}' &= -\frac{\varepsilon \cos\theta \left(B\left(\rho^2 - 2r^2\right)\cos^2(\theta+\alpha) + A\, r^2 \cos^2\theta\right)}{r + \varepsilon(B\rho^2 \cos\theta \cos^2(\theta+\alpha) + A\, r^2 \cos^3\theta)}.
\end{aligned}
$$

Of course this system has now only three equations because we do not need the θ equation. If we write the previous system as a Taylor series in powers of ε, we have

$$
\begin{aligned}
r' &= \varepsilon \sin\theta(A\, r^2 \cos^2\theta + B\rho^2 \cos^2(\theta+\alpha))\\
&\quad - \varepsilon^2 \frac{\sin 2\theta}{8r} \left(A\, r^2(1+\cos(2\theta)) + B\rho^2(1+\cos(2(\theta+\alpha)))\right)^2 + O(\varepsilon^3),\\
\rho' &= \varepsilon B r \rho \cos\theta \sin(2(\theta+\alpha))\\
&\quad - \varepsilon^2 B\rho \cos^2\theta \sin(2(\theta+\alpha))(Ar^2 \cos^2\theta + B\rho^2 \cos^2(2(\theta+\alpha))) + O(\varepsilon^3),
\end{aligned}
\tag{1.133}
$$

$$
\begin{aligned}
\mathcal{A}' &= -\varepsilon \frac{\cos\theta}{r}(A\, r^2 \cos^2\theta + B(\rho^2 - 2r^2)\cos^2(\theta+\alpha))\\
&\quad + \varepsilon^2 \frac{\cos^2\theta}{r^2}(Ar^2 \cos^2\theta + B\rho^2 \cos^2(\theta+\alpha))\\
&\qquad \cdot (A\, r^2 \cos^2\theta + B(\rho^2 - 2r^2)\cos^2(\theta+\alpha)) + O(\varepsilon^3).
\end{aligned}
$$

Now system (1.133) is 2π-periodic in the variable θ. In order to apply Theorem 1.3.5 we must fix the value of the first integral at $h > 0$ and, by solving equation (1.131) for ρ, we obtain

$$
\rho = \sqrt{\frac{h - r^2/2 - \varepsilon A\, r^3 \cos^3\theta/3}{1/2 + \varepsilon\, B\, r \cos\theta \cos^2(\theta+\alpha)}}. \tag{1.134}
$$

Then, substituting ρ in equations (1.133), we obtain the two differential equations

$$
\begin{aligned}
r' &= \varepsilon \sin\theta(A\, r^2 \cos^2\theta + B(2h - r^2)\cos^2(\theta+\alpha))\\
&\quad - \varepsilon^2 \Big(\frac{\sin 2\theta}{8r} \big(A\, r^2(1+\cos(2\theta)) + B\left(2h - r^2\right)(1+\cos(2(\theta+\alpha)))\big)^2\\
&\quad + \frac{2}{3} AB\, r^3 \sin\theta \cos^3\theta \cos^2(\theta+\alpha)\\
&\quad + 2B^2 hr \sin(2\theta)\cos^4(\theta+\alpha) - B^2 r^3 \sin(2\theta)\cos^4(\theta+\alpha)\Big) + O(\varepsilon^3),
\end{aligned}
\tag{1.135}
$$

and

$$\begin{aligned}\alpha' = \varepsilon &\left(\frac{B}{r}(3r^2-2h)\cos\theta\cos^2(\theta+\alpha) - Ar\cos^3\theta\right)\\ &+\varepsilon^2(A^2r^2\cos^6\theta + \frac{2}{3}AB(6h-5r^2)\cos^4\theta\cos^2(\theta+\alpha)\\ &+\frac{B^2}{r^2}(r^2-2h)^2\cos^2\theta\cos^4(\theta+\alpha)\ ) + O(\varepsilon^3).\end{aligned} \tag{1.136}$$

Clearly, equations (1.135) and (1.136) satisfy the assumptions of Theorem 1.3.5, and it has the form of (1.98) with $F_1 = (F_{11}, F_{12})$ and $F_2 = (F_{21}, F_{22})$, where

$$\begin{aligned}F_{11} &= \sin\theta\big(A\,r^2\cos^2\theta + B(2h-r^2)\cos^2(\theta+\alpha)\big),\\ F_{12} &= \frac{B}{r}(3r^2-2h)\cos\theta\cos^2(\theta+\alpha) - Ar\cos^3\theta,\end{aligned}$$

and

$$\begin{aligned}F_{21} = &-\frac{\sin 2\theta}{8r}\left(A\,r^2(1+\cos(2\theta)) + B\left(2h-r^2\right)(1+\cos(2(\theta+\alpha)))\ \right)^2\\ &-\frac{2}{3}AB\,r^3\sin\theta\cos^3\theta\cos^2(\theta+\alpha) - 2B^2hr\sin(2\theta)\cos^4(\theta+\alpha)\\ &+B^2r^3\sin(2\theta)\cos^4(\theta+\alpha),\\ F_{22} = &\,A^2r^2\cos^6\theta + \frac{2}{3}AB(6h-5r^2)\cos^4\theta\cos^2(\theta+\alpha)\\ &+\frac{B^2}{r^2}(r^2-2h)^2\cos^2\theta\cos^4(\theta+\alpha).\end{aligned}$$

As $r \neq 0$ the functions F_1 and F_2 are analytical. Furthermore, they are 2π-periodic in the variable θ, the independent variable of the system (1.135)-(1.136). However, the averaging theory of first order does not apply because the average functions of F_1 and F_2 in the period vanish,

$$f_1(r,\mathcal{A}) = \int_0^{2\pi}(F_{11}, F_{12})\,d\theta = (0,0)\,.$$

As the function f_1 from Theorem 1.3.5 is zero, we procede to calculate the function f_2 by applying the second order averaging theory. We have that f_2 is defined by

$$f_2(r,\mathcal{A}) = \int_0^{2\pi}[D_{r\mathcal{A}}F_1(\theta,r,\mathcal{A}).y_1(\theta,r,\mathcal{A}) + F_2(\theta,r,\mathcal{A})]\,d\theta, \tag{1.137}$$

where

$$y_1(\theta,r,\mathcal{A}) = \int_0^{\theta}F_1(t,r,\mathcal{A})\,dt\,.$$

The two components of the vector y_1 are

$$\begin{aligned} y_{11} &= \int_0^\theta F_{11}(t,r,\mathcal{A})\,dt \\ &= \frac{1}{3}\left(B(2h-r^2)\sin^2(\theta/2)\left(\cos(2(\theta+\alpha))+2\cos(2\alpha+\theta)+3\right)-Ar^2(\cos^3\theta-1)\right), \end{aligned}$$

and

$$\begin{aligned} y_{12} &= \int_0^\theta F_{12}(t,r,\mathcal{A})\,dt \\ &= -\frac{Ar}{12}(9\sin\theta+\sin 3\theta)-\frac{Bh}{6r}(3\sin(2\alpha+\theta)+\sin(2\alpha+3\theta)-4\sin 2\alpha+6\sin\theta) \\ &\quad+\frac{Br}{4}(3\sin(2\alpha+\theta)+\sin(2\alpha+3\theta)-4\sin(2\alpha)+6\sin\theta). \end{aligned}$$

For the Jacobian matrix

$$D_{r\mathcal{A}}F_1(\theta,r,\mathcal{A}) = \begin{pmatrix} \dfrac{\partial F_{11}}{\partial r} & \dfrac{\partial F_{11}}{\partial \mathcal{A}} \\ \dfrac{\partial F_{12}}{\partial r} & \dfrac{\partial F_{12}}{\partial \mathcal{A}} \end{pmatrix},$$

we obtain

$$\begin{pmatrix} \big(2Ar\cos^2\theta-2Br\cos^2(\theta+\alpha)\big)\sin\theta & -2B(2h-r^2)\cos(\theta+\alpha)\sin\theta\sin(\theta+\alpha) \\ -A\cos^3\theta+6B\cos^2(\theta+\alpha)\cos\theta & -\dfrac{2B}{r}(3r^2-2h)\cos\theta\cos(\theta+\alpha)\sin(\theta+\alpha) \\ -\dfrac{B}{r^2}\left(3r^2-2h\right)\cos^2(\theta+\alpha)\cos\theta & \end{pmatrix}.$$

We can now calculate the function (1.137) from Theorem 1.3.5, and we obtain

$$\begin{aligned} f_2 = \Big(&-\frac{Br}{12}(6B-A)(r^2-2h)\sin 2\mathcal{A}, \\ &\frac{1}{12}\big(r^2(5A^2-12AB-3B^2)-2B(A-6B)(h-r^2)\cos(2\alpha)+2Bh(6A-B)\big)\Big). \end{aligned}$$

We have to find the zeros $(r^*,\mathcal{A}^*)$ of $f_2(r,\mathcal{A})$, and to check that the Jacobian determinant

$$|D_{r,\mathcal{A}}f_2(r^*,\mathcal{A}^*)| \neq 0. \tag{1.138}$$

Solving the equation $f_2(r,\mathcal{A})=0$, we obtain five solutions $(r^*,\mathcal{A}^*)$ with $r^*>0$, namely

$$\left(\sqrt{2}h, \pm\operatorname{arcsec}\frac{B(A-6B)}{4B^2+6AB-5A^2}\right), \left(\sqrt{\frac{2Bh}{3B-A}},0\right), \left(\sqrt{\frac{14Bh}{9B-5A}},\pm\pi/2\right). \tag{1.139}$$

The first two solutions are not good, because for them we would get from (1.134) that $\rho = 0$ when $\varepsilon = 0$, and ρ must be positive. The third solution exists if $B(3B - A) > 0$. The last two solutions exist if $B(9B - 5A) > 0$. The Jacobian (1.138) of the third solution is

$$-\frac{5B^2h^2(A-6B)(A-2B)(A+B)}{9(A-3B)} \tag{1.140}$$

and, for the last two solutions, the Jacobian coincides and is equal to

$$\frac{7B^2h^2(A-6B)(5A-2B)(A-B)}{9(5A-9B)}. \tag{1.141}$$

Summarizing, from Theorem 1.3.5 the third solution of $f_2(r, \mathcal{A}) = 0$ provides a periodic orbit for the system (1.135)-(1.136) (and consequently of the Hamiltonian system (1.129) on the Hamiltonian level $h > 0$) if $B(3B-A) > 0$, $(A-6B)(A-2B)(A+B) \neq 0$, and from (1.134) we get $\rho = \sqrt{2(A-2B)h/(A-3B)}$; we also need $(2B-A)(3B-A) > 0$. The conditions $B(3B-A) > 0$ and $(2B-A)(3B-A) > 0$ can be reduced to $B(2B - A) > 0$, where $(A - 6B)(A - 2B) \neq 0$ is included, but $A + B \neq 0$ is not. Then the third solution provides a periodic orbit when $B(2B - A) > 0$ and $A + B \neq 0$.

In a similar way the last two solutions of $f_2(r, \mathcal{A}) = 0$ provide two periodic orbits for the system (1.135)-(1.136) if $B(9B - 5A) > 0$, $(A - 6B)(5A - 2B)(A - B) \neq 0$, and from (1.134) we get $\rho = \sqrt{2(5A-2B)h/(5A-9B)}$; we also need $(2B-5A)(9B-5A) > 0$. The conditions $B(9B-5A) > 0$ and $(2B-5A)(9B-5A) > 0$ can be reduced to $B(2B-5A) > 0$, where the condition $(A-6B)(5A-2B)(A-B) \neq 0$ is included. Then the fourth and fifth solutions provide two periodic orbits whenever $B(2B - 5A) > 0$.

There is one periodic orbit if the third solution exists, and the last two solutions do not. There are two periodic orbits if the two last solutions exist, and not the third one, i.e., when $A + B = 0$. Finally, there are three periodic orbits if the third, fourth and fifth solutions exist. Now the statements of Theorem 1.3.5 follow easily.

The regions in the parameter space where periodic orbits exist are summarized in Figures 1.1 and 1.2. □

1.4.3 Limit cycles of polynomial differential systems

The results presented in this subsection come from Llibre–Swirszcz [57].

After the definition of limit cycle due to Poincaré [75], the statement of the 16-th Hilbert's problem [41], and the discovery by Liénard [52] that limit cycles are important in nature, the study of limit cycles of planar differential systems has been one of the main problems of the qualitative theory of differential equations.

One of the best ways of producing limit cycles is by perturbing the periodic orbits of a center. This has been studied intensively perturbing the periodic orbits

of the centers of the quadratic polynomial differential systems, see the book of Christopher–Li [18] and the references quoted there.

It is well known that if a quadratic polynomial differential system has a limit cycle, this must surround a focus. Up to now, the maximum number of known limit cycles surrounding a focus of a quadratic polynomial differential system is 3, which coincides with the maximum number of small limit cycles which can bifurcate by Hopf from a singular point of a quadratic polynomial differential system, see Bautin [4]. But, as far as we know, up to now there are few quadratic centers for which it is proved that the perturbation of their periodic orbits inside the class of all quadratic polynomial differential systems can produce 3 limit cycles. These are the center whose exterior boundary is formed by three invariant straight lines (see Żołądek [88]), three different families of reversible quadratic centers (see Świrszcz [83]), and the center $\dot{x} = -y(1+x)$, $\dot{y} = x(1+x)$ (see Buică–Gasull–Yang [13]). The study of the perturbation of this last center has been made through the Melnikov function of third order, computed using the algorithm developed by Françoise [35] and Iliev [44]. Here, we can provide a new and shorter proof of this second result by using the averaging theory, see Theorem 1.4.2.

We study the limit cycles of the following two differential systems: the *quadratic systems*

$$\begin{aligned} \dot{x} &= -y(1+x) + \varepsilon(\lambda x + \bar{A}x^2 + \bar{B}xy + \bar{C}y^2),\\ \dot{y} &= \quad x(1+x) + \varepsilon(\lambda y + \bar{D}x^2 + \bar{E}xy + \bar{F}y^2), \end{aligned} \tag{1.142}$$

such that, for $\varepsilon = 0$, have a straight line consisting of singular points, and the *cubic systems* of the form

$$\begin{aligned} \dot{x} &= -y(1-x^2-y^2) + \varepsilon^3\lambda x + \sum_{s=1}^{3}\varepsilon^s \sum_{i=0}^{3} a_{i,s}x^i y^{3-i},\\ \dot{y} &= \quad x(1-x^2-y^2) + \varepsilon^3\lambda y + \sum_{s=1}^{3}\varepsilon^s \sum_{i=0}^{3} b_{i,s}x^i y^{3-i}, \end{aligned} \tag{1.143}$$

such that, for $\varepsilon = 0$, have a unit circle consisting of singular points. Note that the perturbation of these cubic systems is inside the class of all polynomial differential system with linear and cubic homogeneous non-linearities.

We study for $\varepsilon \neq 0$ sufficiently small the number of limit cycles of the systems (1.142) and (1.143) bifurcating from the periodic orbits of the centres of (1.142) and (1.143) for $\varepsilon = 0$, respectively. Our main results are the following.

Theorem 1.4.2. *For convenient λ, $\bar{A}$, $\bar{B}$, $\bar{C}$, $\bar{D}$, $\bar{E}$ and $\bar{F}$, the system* (1.142) *has* 3 *limit cycles bifurcating from the periodic orbits of the center for $\varepsilon = 0$.*

Theorem 1.4.3. *The following statements hold for system* (1.143)*:*

(i) *using the averaging theory of third order for $\varepsilon \neq 0$ sufficiently small, we can obtain at most* 5 *limit cycles of the system* (1.143) *bifurcating from the periodic orbits of the center located at the origin of system* (1.143) *with $\varepsilon = 0$;*

(ii) *for convenient* λ, $a_{i,s}$, $b_{i,s}$, $i = 0, 1, 2, 3$, $s = 1, 2, 3$, *the system* (1.143) *has* 0, 1, 2, 3, 4 *or* 5 *limit cycles bifurcating from the periodic orbits of the center for* $\varepsilon = 0$.

It is known that systems of the form $\dot{x} = -y + P_3(x, y)$, $\dot{y} = x + Q_3(x, y)$, with P_3 and Q_3 homogeneous polynomials of degree 3 can have 5 small limit cycles bifurcating by Hopf from the origin, see [62, 81]. We are going to use the following result due to Cherkas [17].

Lemma 1.4.4. *The differential equation*

$$\frac{dr}{d\varphi} = \frac{\lambda r + a(\varphi) r^k}{1 + b(\varphi) r^{k-1}}$$

after the change of variable

$$\rho(\varphi) = \frac{r(\varphi)^{k-1}}{1 + b(\varphi) r(\varphi)^{k-1}}$$

becomes the Abel equation

$$\begin{aligned}\frac{d\rho}{d\varphi} &= (k-1)b(\varphi)(\lambda b(\varphi) - a(\varphi))\rho^3 \\ &\quad + \left[(k-1)(a(\varphi) - 2\lambda b(\varphi)) - b'(\varphi)\right]\rho^2 + (k-1)\lambda\rho.\end{aligned}$$

Combining Lemma 1.4.4 with polar coordinates transformation we immediately get the next result.

Corollary 1.4.5. *Let* $P(x, y)$ *and* $Q(x, y)$ *be homogenous polynomials of degree* n. *Then the differential system*

$$\begin{aligned}\dot{x} &= -y + \lambda x + P_n(x, y) \\ \dot{y} &= x + \lambda y + Q_n(x, y)\end{aligned} \tag{1.144}$$

can be transformed into the Abel equation

$$\begin{aligned}\frac{d\rho}{d\varphi} &= (k-1)B(\varphi)(\lambda B(\varphi) - A(\varphi))\rho^3 \\ &\quad + \left[(k-1)(A(\varphi) - 2\lambda B(\varphi)) - B'(\varphi)\right]\rho^2 + (k-1)\lambda\rho,\end{aligned}$$

where

$$A(\varphi) = \cos\varphi P_n(\cos\varphi, \sin\varphi) + \sin\varphi Q_n(\sin\varphi, \cos\varphi),$$

and

$$B(\varphi) = \cos\varphi Q_n(\cos\varphi, \sin\varphi) - \sin\varphi P_n(\sin\varphi, \cos\varphi).$$

Proof. The system (1.144) expressed in polar coordinates becomes

$$\begin{aligned}\dot{r} &= \lambda r + A(\varphi)r^n,\\ \dot{y} &= 1 + B(\varphi)r^n.\end{aligned}$$

Dividing $\dot{r}$ by $\dot{\varphi}$ and using Lemma 1.4.4 the proof of the corollary follows. □

Proof of Theorem 1.4.2. From Corollary 1.4.5 applied to the system (1.142), it follows that finding limit cycles of (1.142) is equivalent to finding periodic solutions of

$$\begin{aligned}\frac{d\rho}{d\varphi} = (\sin\varphi)\rho^2 + \epsilon\Big[&-\frac{1}{4}\cos\varphi((3\bar{A}+\bar{C}+\bar{E}-4\lambda)\cos\varphi\\ &+ (\bar{A}-\bar{C}-\bar{E})\cos 3\varphi\\ &+ 2(\bar{B}+\bar{D}+\bar{F}+(\bar{B}+\bar{D}-\bar{F})\cos 2\varphi)\sin\varphi)\rho^3\\ &+ ((\bar{A}+\bar{C}-2\lambda)\cos\varphi + (\bar{A}-\bar{C}-\bar{E})\cos 3\varphi\\ &+ (\bar{D}+\bar{F})\sin\varphi + (\bar{B}+\bar{D}-\bar{F})\sin 3\varphi)\rho^2 + \lambda\rho\Big].\end{aligned} \tag{1.145}$$

We are going to apply Theorem 1.3.5 to system (1.145). We first solve the differential equation

$$\frac{d\rho}{d\varphi} = (\sin\varphi)\rho^2,$$

with initial condition $\rho(0) = R/(1+R)$, and we get $\rho(\varphi, R) = R/(1+R\cos\varphi)$. Thus $M_R(\varphi)$ in (1.37) will be a solution of the differential equation $M_R'(\varphi) = (2R\sin\varphi)/(1+R\cos\varphi)$, namely, $M_R(\varphi) = 1+2\ln(1+R)-2\ln(1+r\cos\varphi)$. Thus, formula (1.37) yields

$$\begin{aligned}\mathcal{F}(R) = \int_0^{2\pi}\Big(&\lambda\frac{R}{\Xi(\varphi,R)}\\ &+ \bar{A}\frac{\cos\varphi(R\cos\varphi + 8\cos(2\varphi) + 3R\cos(3\varphi))R^2}{4\Xi(\varphi,R)}\\ &+ \bar{B}\frac{(2R\sin 2\varphi + 8\sin 3\varphi + 3R\sin 4\varphi)R^2}{8\Xi(\varphi,R)}\\ &- \bar{C}\frac{\cos\varphi(3R\cos\varphi+4)\sin^2\varphi R^2}{\Xi(\varphi,R)}\\ &+ \bar{D}\frac{\cos^2\varphi(3R\cos\varphi+4)\sin\varphi R^2}{\Xi(\varphi,R)}\\ &- \bar{E}\frac{\cos\varphi(R\cos\varphi + 8\cos 2\varphi + 3R\cos 3\varphi - 4)R^2}{4\Xi(\varphi,R)}\\ &+ \bar{F}\frac{(5R\cos\varphi + 8\cos 2\varphi + 3R\cos 3\varphi)\sin\varphi R^2}{4\Xi(\varphi,R)}\Big)\,d\varphi,\end{aligned} \tag{1.146}$$

where $\Xi(\varphi,R)=(R\cos\varphi+1)^3(2\log(R+1)-2\log(R\cos\varphi+1)+1)$. Now, observe that the terms in front of $\bar{B}$, $\bar{D}$ and $\bar{F}$ are odd π-periodic functions of φ, thus their integrals from 0 to 2π are equal to zero. Therefore,

$$\begin{aligned}\mathcal{F}(R)=\int_0^{2\pi}\Bigg(&\lambda\frac{R}{\Xi(\varphi,R)}\\&+\bar{A}\frac{\cos\varphi(R\cos\varphi+8\cos(2\varphi)+3R\cos(3\varphi))R^2}{4\Xi(\varphi,R)}\\&+\bar{C}\frac{\cos\varphi(3R\cos\varphi+4)\sin^2\varphi R^2}{\Xi(\varphi,R)}\\&+\bar{E}\frac{\cos\varphi(R\cos\varphi+8\cos 2\varphi+3R\cos 3\varphi-4)R^2}{4\Xi(\varphi,R)}\Bigg)d\varphi\\=\lambda f_1(R)+\bar{A}f_2(R)+\bar{C}f_3(R)-\bar{E}f_4(R).&\end{aligned}\tag{1.147}$$

We claim that the four functions f_1, f_2, f_3 and f_4 are linearly independent. Now we prove the claim. By straightforward calculation we obtain the following Taylor expansions:

$$\begin{aligned}f_1(R)=&\ \frac{1}{24}\pi R\left(2615R^4-800R^3+312R^2-96R+48\right)+\mathcal{O}(R^6),\\f_2(R)=&\ \frac{1}{24}\pi R^3\left(313R^2-60,R-18\right)+\mathcal{O}(R^6),\\f_3(R)=&\ \frac{1}{24}\pi R^3\left(401R^2-84R-6\right)+\mathcal{O}(R^6),\\f_4(R)=&-\frac{1}{24}\pi R^3\left(43R^2-12R+6\right)+\mathcal{O}(R^6).\end{aligned}$$

The determinant of the coefficient matrix of terms $R^2,\dots,R^5$ is $\pi^4/3$ and the claim follows.

A well-known classical result states that if a family of n functions is linearly independent, then there exists a linear combination of them with at least $n-1$ zeroes. Thus, Theorem 1.4.2 follows. □

Proof of Theorem 1.4.3. First we prove statement (ii). We shall use third order averaging to show that the system

$$\begin{aligned}\dot{x}=&-y(1-x^2-y^2)+\varepsilon^3\lambda x\\&-\frac{1}{1200}(75\mathcal{B}\varepsilon+108\mathcal{E}+19840)\varepsilon x^3+(j+24)\varepsilon x^2y\\&+\left(4\varepsilon^3(\mathcal{A}-4\lambda)+\varepsilon^2\left(\frac{27\mathcal{B}}{128}-\mathcal{C}\right)+\frac{(81\mathcal{E}+16480)\varepsilon}{300}\right)xy^2\\&+\frac{1}{2}\varepsilon(2j+\mathcal{D}\varepsilon)y^3,\end{aligned}\tag{1.148}$$

$$\begin{aligned}\dot{y} = \quad & x(1-x^2-y^2)+\varepsilon^3\lambda y \\ & + \frac{1}{2}(\mathcal{D}\varepsilon - 2j)\varepsilon x^3 + \left(\varepsilon^2\left(\mathcal{C} - \frac{3\mathcal{B}}{128}\right) + \frac{(81\mathcal{E}+18080)\varepsilon}{300}\right)x^2 y \\ & - (j+40)\varepsilon x y^2 - \frac{1}{300}(27\mathcal{E}+6560)\varepsilon y^3,\end{aligned} \tag{1.149}$$

can have 0, 1, 2, 3, 4 or 5 limit cycles for an appropriate choice of the parameters λ, $\mathcal{A}$, $\mathcal{B}$, $\mathcal{C}$, $\mathcal{D}$ and $\mathcal{E}$. The system (1.148)-(1.149) is, clearly, a special case of (1.143); thus this will prove statement (ii).

Using Cherkas Transformation (see Lemma 1.4.4) we transform the system (1.148)-(1.149) into the Abel equation

$$\frac{d\rho}{d\varphi} = \varepsilon F_1 + \varepsilon^2 F_2 + \varepsilon^3 F_3, \tag{1.150}$$

where

$$\begin{aligned}F_1 = {} & \rho^3\left(\frac{3}{50}(3\mathcal{E}+640)\cos(4\varphi) + 8(\sin(2\varphi) - 2\sin(4\varphi)) - \frac{16}{3}\cos(2\varphi)\right) \\ & + \rho^2\left(-\frac{9}{50}(3\mathcal{E}+640)\cos(4\varphi) - 8\sin(2\varphi) + 48\sin(4\varphi) + \frac{16}{3}\cos(2\varphi)\right), \\ F_2 = {} & \frac{\rho^3}{30000}\Big[25(6400j + 75\mathcal{B} + 432\mathcal{E} + 117760)\cos(2\varphi) \\ & - 75\cos(4\varphi)(72(j+8)\mathcal{E} + 15360(j+8) - 25\mathcal{B}) \\ & - 600\sin(2\varphi)(400j + 25\mathcal{D} + 12\mathcal{E} + 7360) \\ & + 480000(j+8)\sin(4\varphi) - 7200(\mathcal{E}+80)\sin(6\varphi) \\ & + 3(9\mathcal{E}+1120)(9\mathcal{E}+2720)\sin(8\varphi) \\ & - 400(27\mathcal{E}+7360)\cos(6\varphi) + 14400(3\mathcal{E}+640)\cos(8\varphi)\Big] \\ & + \rho^2\left(\left(\frac{3\mathcal{B}}{128} - \mathcal{C}\right)\cos(2\varphi) - \frac{3}{16}\mathcal{B}\cos(4\varphi) + 3\mathcal{D}\sin(\varphi)\cos(\varphi)\right), \\ F_3 = {} & -2\lambda\rho \\ & + \rho^2\Big((\mathcal{A}-4\lambda)(2\cos(2\varphi) - 3\cos(4\varphi)) + \mathcal{A}\Big) \\ & + \rho^3\Big\{\mathcal{A}\cos 4\varphi - \mathcal{A} - \frac{11\mathcal{B}}{64} + 2\mathcal{C} - \frac{4\mathcal{D}}{3} + 2\lambda \\ & + \frac{1}{76800}\Big[\sin(2\varphi)(384(100(j+4)\mathcal{D} - 3\mathcal{C}(3\mathcal{E}+640)) + \mathcal{B}(513\mathcal{E}+103040)) \\ & - 96\cos(2\varphi)(25(2j-7)\mathcal{B} + 3200\mathcal{C} - 6\mathcal{D}(3\mathcal{E}+640)) \\ & - 400\cos(4\varphi)(3(4j+21)\mathcal{B} + 128(3\mathcal{C} + 2\mathcal{D} + 6\lambda)) \\ & + \sin(6\varphi)(1152(3\mathcal{C}\mathcal{E} + 640\mathcal{C} - 400\mathcal{D}) - \mathcal{B}(81\mathcal{E}+23680))\end{aligned}$$

$$
\begin{aligned}
&- 96\cos(6\varphi)(175\mathcal{B} - 640(5\mathcal{C} + 18\mathcal{D}) - 54\mathcal{D}\mathcal{E}) \\
&+ 800\sin(4\varphi)(11\mathcal{B} + 64(3\mathcal{D} - 2\mathcal{C})) + 144\mathcal{B}(3\mathcal{E} + 640)\sin(8\varphi) \\
&+ 38400\mathcal{B}\cos(8\varphi)\Big]\Big\}.
\end{aligned}
$$

By straightforward calculations, we verify that $F_{10} = 0$,

$$
\begin{aligned}
y_1(\rho,\varphi) = {} & \frac{\rho^3}{300}\sin\varphi((27\mathcal{E} + 4160)\cos\varphi + 3(3(3\mathcal{E} + 640)\cos 3\varphi - 800\sin 3\varphi)) \\
& - \frac{\rho^2}{600}\left(2\sin(2\varphi)(27(3\mathcal{E} + 640)\cos 2\varphi - 800(9\sin 2\varphi + 1)) + 4800\sin^2\varphi\right),
\end{aligned}
$$

and $F_{20} = 0$. Next,

$$
\begin{aligned}
y_2(\rho,\varphi) = {} & \frac{1}{128}\rho^2(9\mathcal{B}\cos\varphi + 12\mathcal{B}\cos(3\varphi) + 128\mathcal{C}\cos\varphi - 192\mathcal{D}\sin\varphi)\sin\varphi \\
& + \rho^3\left[\left(\frac{8j}{3} + \frac{\mathcal{B}}{32} - \frac{9\mathcal{E}}{25} + \frac{128}{15}\right)\sin(2\varphi)\right. \\
& - \frac{1}{50}(400j + 25\mathcal{D} - 24\mathcal{E} + 1280)\sin^2\varphi \\
& - \frac{9}{200}j\mathcal{E}\sin(4\varphi) + \frac{8}{9}(9j + 494)\sin^2(2\varphi) - \frac{48}{5}j\sin(4\varphi) \\
& + \frac{1}{64}\mathcal{B}\sin(4\varphi) + \frac{81\mathcal{E}^2\sin^2(4\varphi)}{4000} - \frac{4}{5}\mathcal{E}\sin^2(3\varphi) + \frac{216}{25}\mathcal{E}\sin^2(4\varphi) \\
& - \frac{63}{25}\mathcal{E}\sin(4\varphi) - \frac{3}{5}\mathcal{E}\sin(6\varphi) + \frac{9}{5}\mathcal{E}\sin(8\varphi) - 64\sin^2(3\varphi) \\
& \left. + \frac{3808}{5}\sin^2(4\varphi) - \frac{7904}{15}\sin(4\varphi) - \frac{1472}{9}\sin(6\varphi) + 384\sin(8\varphi)\right] \\
& + \rho^4\left[-\frac{243\mathcal{E}^2\sin^2(4\varphi)}{16000} - \frac{1}{25}(21\mathcal{E} + 2480)\sin^2\varphi + \frac{29}{25}\mathcal{E}\sin^2(3\varphi)\right. \\
& - \frac{162}{25}\mathcal{E}\sin^2(4\varphi) + \frac{1}{300}(189\mathcal{E} + 9920)\sin(2\varphi) + \frac{27}{25}\mathcal{E}\sin(4\varphi) \\
& + \frac{87}{100}\mathcal{E}\sin(6\varphi) - \frac{27}{20}\mathcal{E}\sin(8\varphi) - \frac{1528}{9}\sin^2(2\varphi) + \frac{464}{5}\sin^2(3\varphi) \\
& \left. - \frac{2856}{5}\sin^2(4\varphi) + \frac{3056}{15}\sin(4\varphi) + \frac{10672}{45}\sin(6\varphi) - 288\sin(8\varphi)\right] \\
& + \rho^5\frac{((27\mathcal{E} + 4160)\cos\varphi + 3(3(3\mathcal{E} + 640)\cos(3\varphi) - 800\sin(3\varphi)))^2\sin^2\varphi}{60000}
\end{aligned}
$$

and

$$
\begin{aligned}
F_{30}(\rho) = {} & -2\lambda\rho + \mathcal{A}\rho^2 - \left(\mathcal{A} - \mathcal{B} - \frac{2\mathcal{D}}{3} - 2\lambda\right)\rho^3 \\
& - \left(\frac{91\mathcal{B}}{128} - \mathcal{C} + \frac{7\mathcal{D}}{3} - \frac{4\mathcal{E}}{5}\right)\rho^4 + \left(\mathcal{D} - \frac{9\mathcal{E}}{5}\right)\rho^5 + \mathcal{E}\rho^6.
\end{aligned}
$$

The coefficients of F_{30} are linearly independent (linear) functions of λ, $\mathcal{A}$, $\mathcal{B}$, $\mathcal{C}$, $\mathcal{D}$ and $\mathcal{E}$. Therefore, for any $\rho_1, \rho_2, \rho_3, \rho_4, \rho_5 \in \mathbb{R}$ there exist λ, $\mathcal{A}$, $\mathcal{B}$, $\mathcal{C}$, $\mathcal{D}$, $\mathcal{E}$ such that $F_{30}(\rho_i) = 0$ for $i = 1, 2, 3, 4, 5$. This ends the proof of (ii).

Now we sketch the proof of statement (i). If, instead of doing the computations of the proof of statement (ii) for the system (1.148)-(1.149), we did them for the general system (1.143) we would obtain a function $F_{30}(\rho)$ which again is a polynomial of degree 6 in ρ without independent term. Thus the averaging theory of third order can only produce for $\varepsilon \neq 0$ sufficiently small at most 5 limit cycles for system (1.143), bifurcating from the periodic orbits at the origin of system (1.143) with $\varepsilon = 0$. □

1.4.4 The generalized polynomial differential Liénard equation

The results in this subsection have been proved by Llibre–Mereu–Teixeira [54].

The second part of the Hilbert's problem is related with the least upper bound on the number of limit cycles of polynomial vector fields having a fixed degree. The *generalized polynomial Liénard differential equations*

$$\ddot{x} + f(x)\dot{x} + g(x) = 0, \tag{1.151}$$

was introduced in [52]. Here, the dot denotes differentiation with respect to the time t, and $f(x)$ and $g(x)$ are polynomials in the variable x of degrees n and m, respectively. For this subclass of polynomial vector fields we have a simplified version of Hilbert's problem, see [53, 80].

In 1977 Lins–de Melo–Pugh [53] studied the classical polynomial Liénard differential equations (1.151) obtained when $g(x) = x$, and stated the following conjecture: *"if $f(x)$ has degree $n \geq 1$ and $g(x) = x$, then* (1.151) *has at most* $[n/2]$ *limit cycles"*. They also proved the conjecture for $n = 1, 2$. The conjecture for $n \in \{3, 4, 5\}$ is still open. For $n \geq 5$ this conjecture is not true as it has been proved recently by Dumortier–Panazzolo–Roussarie [29], and De Maesschalck–Dumortier [25]. Recently, this conjecture has been proved for $n = 3$, see Chengzhi–Llibre [61]. So, at this moment, it only remains to know if the conjecture holds or not for $n = 4$.

We note that a classical polynomial Liénard differential equation has a unique singular point. However, it is possible for generalized polynomial Liénard differential equations to have more than one singular point.

Many of the results on the limit cycles of polynomial differential systems have been obtained by considering limit cycles which bifurcate from a single degenerate singular point; these are the so called *small amplitud limit cycles*, see [60]. We denote by $\hat{H}(m, n)$ the maximum number of small amplitude limit cycles for systems of the form (1.151). The values of $\hat{H}(m, n)$ give a lower bound for the maximum number $H(m, n)$ (i.e., the *Hilbert number*) of limit cycles that the differential equation (1.151) with m and n fixed can have. The finiteness of

$H(m,n)$ for every positive integers m and n is unknown. For more information about Hilbert's 16-th problem and related topics, see [46, 50].

		n																
		1	2	3	4	5	6	7	8	9	10	11	12	13	...	48	49	50
	1	0	1*	1	2	2	3	3	4	4	5	5	6	6	$\cdots$	24	24	$\rightarrow$
	2	1*	1*	2	3	3	4	5	5	6	7	7	8	9	$\cdots$	32	33	$\rightarrow$
	3	1*	2	2	4	4	6	6	6	8	8	8	10	10	$\cdots$	36	38	38
	4	2	3	4	4	6	7	8	9	9	10	11	12	13				
	5	2	3	4	6	6	8	9	10	11								
	6	3	4	6	7	8	8	9										
	7	3	5	6	8	9	9	9										
m	8	4	5	6	9	10												
	9	4	6	8	9	11												
	10	5	7	8	10													
	11	5	7	8	11													
	12	6	8	10	12													
	13	6	9	10	13													
	$\vdots$	$\vdots$	$\vdots$	$\vdots$														
	20	10	13	14	17													
	$\vdots$	$\vdots$	$\vdots$	$\vdots$														
	48	24	32	36														
	49	24	33	38														
	50	$\downarrow$	$\downarrow$	38														

Table 1.1: The values of $H(m,n)$ or $\hat{H}(m,n)$ for Liénard systems.

Now we shall describe, briefly, the main results about the limit cicles on Liénard differential systems:

(i) in 1928 Liénard [52] proved that, if $m = 1$ and $F(x) = \int_0^x f(s)ds$ is a continuous odd function having a unique root at $x = a$ and being monotone increasing for $x \geq a$, then equation (1.151) has a unique limit cycle;

(ii) in 1973 Rychkov [77] proved that, if $m = 1$ and $F(x) = \int_0^x f(s)ds$ is an odd polynomial of degree five, then equation (1.151) has at most two limit cycles;

(iii) in 1977 Lins–de Melo–Pugh [53] proved that $H(1,1) = 0$ and $H(1,2) = 1$;

(iv) in 1998 Coppel [22] proved that $H(2,1) = 1$;

(v) Dumortier, Li and Rousseau in [27] and [30] proved that $H(3,1) = 1$:

(vi) in 1997 Dumortier–Li [28] proved that $H(2,2)=1$.

Up to now and as far as we know, the four cases (iii) to (vi) (marked with asterisks in Table 1.1) are the only ones for which Hilbert numbers $H(m,n)$ are determined.

Blows, Lloyd and Lynch, in the papers [6], [61] and [64] have used inductive arguments in order to prove the following results:

(vii) if g is odd then $\hat{H}(m,n)=[n/2]$;

(viii) if f is even then $\hat{H}(m,n)=n$, whatever g is;

(ix) if f is odd then $\hat{H}(m,2n+1)=[(m-2)/2]+n$;

(x) if $g(x)=x+g_e(x)$, where g_e is even, then $\hat{H}(2m,2)=m$.

Christopher–Lynch [19, 67] and Lynch [65, 66] have developed a new algebraic method for determining the Liapunov quantities of system (1.151) and proved the following:

(xi) $\hat{H}(m,2)=[(2m+1)/3]$;

(xii) $\hat{H}(2,n)=[(2n+1)/3]$;

(xiii) $\hat{H}(m,3)=2[(3m+2)/8]$ for all $1<m\leq 50$;

(xiv) $\hat{H}(3,n)=2[(3n+2)/8]$ for all $1<m\leq 50$;

(xv) the values in Table 1.1 for $\hat{H}(4,k)=\hat{H}(k,4)$, $k=6,7,8,9$ and $\hat{H}(5,6)=\hat{H}(6,5)$.

In 1998 Gasull–Torregrosa [36] obtained upper bounds for $\hat{H}(7,6)$, $\hat{H}(6,7)$, $\hat{H}(7,7)$ and $\hat{H}(4,20)$.

In 2006 the values in Table 1.1 for $\hat{H}(m,n)=\hat{H}(n,m)$, for $n=4$, $m=10,11,12,13$; $n=5$, $m=6,7,8,9$; and $n=6$, $m=5,6$ were given by Yu–Han in [87].

By using the averaging theory, we shall study the maximum number of limit cycles $\tilde{H}(m,n)$ which can bifurcate from the periodic orbits of a linear center perturbed inside the class of all generalized polynomial Liénard differential equations of degrees m and n as follows:

$$\begin{aligned}\dot{x}&=y,\\ \dot{y}&=-x-\sum_{k\geq 1}\varepsilon^k(f_n^k(x)y+g_m^k(x)),\end{aligned}\tag{1.152}$$

where for every k the polynomials $g_m^k(x)$ and $f_n^k(x)$ have degree m and n respectively, and ε is a small parameter; i.e., the maximal number of *medium amplitude limit cycles* which can bifurcate from the periodic orbits of the linear center $\dot{x}=y$, $\dot{y}=-x$, perturbed as in (1.152).

In fact, we shall mainly compute lower estimations of $\tilde{H}(m,n)$. More precisely, we compute the maximum number of limit cycles $\tilde{H}_k(m,n)$ which bifurcate

from the periodic orbits of the linear center $\dot{x} = y$, $\dot{y} = -x$, using the averaging theory of order k, for $k = 1, 2, 3$. Of course, $\tilde{H}_k(m, n) \leq \tilde{H}(m, n) \leq H(m, n)$. Note that, up to now, there were no known lowers estimations for $H(m, n)$ when

(i) $m = 4$ and $n > 13$, or $m > 20$ and $n = 4$,

(ii) $m = 5$ and $n > 9$, or $m > 9$ and $n = 5$,

(iii) $m = 6$ and $n > 7$, or $m > 7$ and $n = 6$,

(iv) $m, n > 7$.

After our results we will have lowers estimations of $H(m, n)$ for all $m, n \geq 1$. From these estimations we obtain that $\tilde{H}_k(m, n) \leq \hat{H}(m, n)$ for $k = 1, 2, 3$ for the values which $\hat{H}(m, n)$ is known.

Theorem 1.4.6. *If for every $k = 1, 2, 3$, the polynomials $f_n^k(x)$ and $g_m^k(x)$ have degree n and m respectively, with $m, n \geq 1$, then for $|\varepsilon|$ sufficiently small, the maximum number of medium limit cycles of the polynomial Liénard differential systems* (1.152) *bifurcating from the periodic orbits of the linear center $\dot{x} = y$, $\dot{y} = -x$, using the averaging theory*

(i) *of first order is* $\tilde{H}_1(m, n) = \left[\frac{n}{2}\right]$;

(ii) *of second order is* $\tilde{H}_2(m, n) = \max\left\{\left[\frac{n-1}{2}\right] + \left[\frac{m}{2}\right], \left[\frac{n}{2}\right]\right\}$; *and*

(iii) *of third order is* $\tilde{H}_3(m, n) = \left[\frac{n+m-1}{2}\right]$.

From Theorem 1.4.6, Table 1.2 follows immediately.

It seems that the numbers $\hat{H}(m, n)$ can be symmetric with respect to m and n. Some studies is this direction are made in [63]. We remark that in general $\tilde{H}_k(m, n) \neq \tilde{H}_k(n, m)$ for $k = 1, 2$, but $\tilde{H}_3(m, n) = \tilde{H}_3(n, m)$.

Proof of Theorem 1.4.6(i). We shall need the first order averaging theory. In order to apply the first order averaging method we write (1.152) with $k = 1$ in polar coordinates, (r, θ), where $x = r\cos\theta$, $y = r\sin\theta, r > 0$. In this way, (1.152) is written in the standard form for applying the averaging theory. If we write $f(x) = \sum_{i=0}^{n} a_i x^i$ and $g(x) = \sum_{i=0}^{m} b_i x^i$, then the system (1.152) becomes

$$\dot{r} = -\varepsilon \left(\sum_{i=0}^{n} a_i r^{i+1} \cos^i\theta \sin^2\theta + \sum_{i=0}^{m} b_i r^i \cos^i\theta \sin\theta \right), \tag{1.153}$$

		n																
		1	2	3	4	5	6	7	8	9	10	11	12	13	...	48	49	50
m	1	0	1	1	2	2	3	3	4	4	5	5	6	6	⋯	24	24	→
	2	1	1	2	*2*	*3*	*3*	*4*	*4*	*5*	*5*	*6*	*6*	*7*	⋯	*24*	*25*	→
	3	1	2	2	*3*	*3*	*4*	*4*	*5*	*5*	*6*	*6*	*7*	*7*	⋯	*25*	*25*	→
	4	2	*2*	*3*	*3*	*4*	*4*	*5*	*5*	*6*	*6*	*7*	*7*	*8*	⋯	**25**	**26**	→
	5	2	*3*	*3*	*4*	*4*	*5*	*5*	*6*	*6*	**7**	**7**	**8**	**8**	⋯	**26**	**26**	→
	6	3	*3*	*4*	*4*	*5*	*5*	*6*	**6**	**7**	**7**	**8**	**8**	**9**	⋯	**26**	**27**	→
	7	3	*4*	*4*	*5*	*5*	*6*	*6*	**7**	**7**	**8**	**8**	**9**	**9**	⋯	**27**	**27**	→
	8	4	*4*	*5*	*5*	*6*	*6*	**7**	**7**	**8**	**8**	**9**	**9**	**10**	⋯	**27**	**28**	→
	9	4	*5*	*5*	*6*	*6*	*7*	**7**	**8**	**8**	**9**	**9**	**10**	**10**	⋯	**28**	**28**	→
	10	5	*5*	*6*	*6*	*7*	**7**	**8**	**8**	**9**	**9**	**10**	**10**	**11**	⋯	**28**	**29**	→
	11	5	*6*	*6*	*7*	*7*	**8**	**8**	**9**	**9**	**10**	**10**	**11**	**11**	⋯	**29**	**29**	→
	12	6	*6*	*7*	*7*	*8*	**8**	**9**	**9**	**10**	**10**	**11**	**11**	**12**	⋯	**29**	**30**	→
	13	6	*7*	*7*	*8*	*8*	**9**	**9**	**10**	**10**	**11**	**11**	**12**	**12**	⋯	**30**	**30**	→
	⋮	⋮	⋮	⋮	⋮	⋮	⋮	⋮	⋮	⋮	⋮	⋮	⋮	⋮	⋮	⋮	⋮	⋮
	20	10	*10*	*11*	*11*	**12**	**12**	**13**	**13**	**14**	**14**	**15**	**15**	**16**	⋯	**33**	**34**	→
	⋮	⋮	⋮	⋮	⋮	⋮	⋮	⋮	⋮	⋮	⋮	⋮	⋮	⋮	⋮	⋮	⋮	⋮
	48	24	*24*	*25*	*25*	**26**	**26**	**27**	**27**	**28**	**28**	**29**	**29**	**30**	⋯	**47**	**48**	→
	49	24	*25*	*25*	*26*	**26**	**27**	**27**	**28**	**28**	**29**	**29**	**30**	**30**	⋯	**48**	**48**	→
	50	↓	↓	↓	↓	↓	↓	↓	↓	↓	↓	↓	↓	↓	↓	↓	↓	

Table 1.2: Values of $\tilde{H}_3(m,n)$. The numbers written in roman style (like "6") coincide with the ones of Table 1.1. The numbers written in italic (like "*6*") are smaller than the corresponding of Table 1.1. Finally, the numbers written in boldface (like "**6**") are unknown in Table 1.1.

$$\dot{\theta} = -1 - \frac{\varepsilon}{r}\left(\sum_{i=0}^{n} a_i r^{i+1}\cos^{i+1}\theta\sin\theta + \sum_{i=0}^{m} b_i r^i \cos^{i+1}\theta\right). \tag{1.154}$$

Taking θ as the new independent variable, system (1.153)-(1.154) becomes

$$\frac{dr}{d\theta} = \varepsilon\left(\sum_{i=0}^{n} a_i r^{i+1}\cos^i\theta\sin^2\theta + \sum_{i=0}^{m} b_i r^i\cos^i\theta\sin\theta\right) + O(\varepsilon^2),$$

and

$$F_{10}(r) = \frac{1}{2\pi}\int_0^{2\pi}\left(\sum_{i=0}^{n} a_i r^{i+1}\cos^i\theta\sin^2\theta + \sum_{i=0}^{m} b_i r^i\cos^i\theta\sin\theta\right)d\theta.$$

In order to calculate the exact expression of F_{10} we use the following formulas

$$\int_0^{2\pi} \cos^{2k+1}\theta \sin^2\theta d\theta = 0, \qquad k = 0, 1, \dots$$

$$\int_0^{2\pi} \cos^{2k}\theta \sin^2\theta d\theta = \alpha_{2k} \neq 0, \qquad k = 0, 1, \dots$$

$$\int_0^{2\pi} \cos^{k}\theta \sin\theta d\theta = 0, \qquad k = 0, 1, \dots$$

Hence,

$$F_{10}(r) = \frac{1}{2} \sum_{\substack{i=0 \\ i \text{ even}}}^{n} a_i \alpha_i r^{i+1}. \tag{1.155}$$

Then the polynomial $F_{10}(r)$ has at most $[n/2]$ positive roots, and we can choose the coefficients a_i with i even in such a way that $F_{10}(r)$ has exactly $[n/2]$ simple positive roots. Hence, statement (i) of Theorem 1.4.6 is proved. □

Proof of Theorem 1.4.6(ii). We shall now use the second order averaging theory.

If we write $f_1(x) = \sum_{i=0}^{n} a_i x^i$, $f_2(x) = \sum_{i=0}^{n} c_i x^i$, $g_1(x) = \sum_{i=0}^{m} b_i x^i$ and $g_2(x) = \sum_{i=0}^{m} d_i x^i$, then system (1.152) with $k = 2$ in polar coordinates (r, θ), $r > 0$ becomes

$$\begin{aligned}
\dot{r} =& -\varepsilon \left(\sum_{i=0}^{n} a_i r^{i+1} \cos^i\theta \sin^2\theta + \sum_{i=0}^{m} b_i r^i \cos^i\theta \sin\theta \right) \\
& - \varepsilon^2 \left(\sum_{i=0}^{n} c_i r^{i+1} \cos^i\theta \sin^2\theta + \sum_{i=0}^{m} d_i r^i \cos^i\theta \sin\theta \right), \\
\dot{\theta} =& -1 - \frac{\varepsilon}{r} \left(\sum_{i=0}^{n} a_i r^{i+1} \cos^{i+1}\theta \sin\theta + \sum_{i=0}^{m} b_i r^i \cos^{i+1}\theta \right) \\
& - \frac{\varepsilon^2}{r} \left(\sum_{i=0}^{n} c_i r^{i+1} \cos^{i+1}\theta \sin\theta + \sum_{i=0}^{m} d_i r^i \cos^{i+1}\theta \right).
\end{aligned} \tag{1.156}$$

Taking θ as the new independent variable system, (1.156) is written

$$\frac{dr}{d\theta} = \varepsilon F_1(\theta, r) + \varepsilon^2 F_2(\theta, r) + O(\varepsilon^3),$$

where

$$F_1(\theta,r) = \sum_{i=0}^{n} a_i r^{i+1} \cos^i\theta \sin^2\theta + \sum_{i=0}^{m} b_i r^i \cos^i\theta \sin\theta,$$

$$F_2(\theta,r) = \left(\sum_{i=0}^{n} c_i r^{i+1} \cos^i\theta \sin^2\theta + \sum_{i=0}^{m} d_i r^i \cos^i\theta \sin\theta\right) - r\sin\theta\cos\theta\left(\sum_{i=0}^{n} a_i r^i \cos^i\theta \sin\theta + \sum_{i=0}^{m} b_i r^{i-1}\cos^i\theta\right)^2.$$

Now we determine the corresponding function F_{20}. For this we compute

$$\frac{d}{dr}F_1(\theta,r) = \sum_{i=0}^{n}(i+1)a_i r^i \cos^i\theta\sin^2\theta + \sum_{i=1}^{m} i b_i r^{i-1}\cos^i\theta\sin\theta,$$

and $\int_0^\theta F_1(\phi,r)d\phi$ which is equal to

$$\begin{aligned} &a_1 r^2\left(\alpha_{11}\sin\theta + \alpha_{21}\sin(3\theta)\right) + \cdots \\ &\quad + a_l r^{l+1}\left(\alpha_{1l}\sin\theta + \alpha_{2l}\sin(3\theta) + \cdots + \alpha_{(\frac{l+3}{2})l}\sin((l+2)\theta\right) \\ &\quad + a_0 r\left(\alpha_{10}\theta + \alpha_{20}\sin(2\theta)\right) + \cdots \\ &\quad + a_b r^{b+1}\left(\alpha_{1b}\theta + \alpha_{2b}\sin(2\theta) + \cdots + \alpha_{(\frac{b+4}{2})b}\sin(b+2)\theta\right) \\ &b_0(1-\cos\theta) + \cdots + b_m r^m\left(\frac{1}{m+1}(1-\cos^{m+1}\theta)\right), \end{aligned} \tag{1.157}$$

where l is the greatest odd number less than or equal to n, b is the greatest even number less than or equal to n, and α_{ij} are real constants exhibited during the computation of $\int_0^\theta \cos^i\phi\sin^2\phi\ d\phi$ for all i. We know from (1.155) that F_{10} is identically zero if and only if $a_i = 0$ for all i even. Moreover,

$$\int_0^{2\pi} \cos^i\theta\sin^3\theta d\theta = 0, \qquad i = 0,1,\ldots$$

$$\int_0^{2\pi} \cos^i\theta\sin^2\theta\sin((2k+1)\theta)d\theta = 0, \qquad i,k = 0,1,\ldots$$

$$\int_0^{2\pi} \cos^{2i+1}\theta\sin^2\theta d\theta = 0, \qquad i = 0,1,\ldots$$

$$\int_0^{2\pi} \cos^{2i}\theta\sin^2\theta d\theta = A_{2i} \neq 0, \qquad i = 0,1,\ldots$$

$$\int_0^{2\pi} \cos^i\theta \sin\theta d\theta = 0, \qquad i = 0, 1, \dots$$

$$\int_0^{2\pi} \cos^{2i}\theta \sin\theta \sin((2k+1)\theta) d\theta = B_{2i}^{2k+1} \neq 0, \qquad i, k = 0, 1, \dots$$

$$\int_0^{2\pi} \cos^{2i+1}\theta \sin\theta \sin((2k+1)\theta) d\theta = 0, \qquad i, k = 0, 1, \dots$$

So

$$\begin{aligned}
&\int_0^{2\pi} \frac{d}{dr} F_1(\theta, r) y_1(\theta, r) d\theta \\
&= \sum_{\substack{j=2 \\ j \text{ even}}}^{k} \sum_{\substack{i=1 \\ i \text{ odd}}}^{l} -\frac{i+1}{j+1} a_i b_j r^{i+j} \int_0^{2\pi} \cos^{i+j+1}\theta \sin^2\theta d\theta \\
&\quad + \sum_{\substack{j=2 \\ j \text{ even}}}^{k} \sum_{\substack{i=1 \\ i \text{ odd}}}^{l} j a_i b_j r^{i+j} \int_0^{2\pi} \cos^j\theta \sin\theta \left(\alpha_{1i} \sin\theta + \cdots + \alpha_{\frac{i+3}{2} i} \sin((i+2)\theta) \right) d\theta \\
&= r\Big(\tilde{\alpha}_{10} a_1 b_0 + (\tilde{\alpha}_{12} a_1 b_2 + \tilde{\alpha}_{30} a_3 b_0) r^2 + \cdots + \sum_{i+j=l+k} \tilde{\alpha}_{ij} a_i b_j r^{l+k-1} \Big),
\end{aligned}$$

where $\tilde{\alpha}_{ij} = -\dfrac{1+i}{j+i} A_{i+j+1} + j \left(\alpha_{1i} B_j^1 + \alpha_{2i} B_j^2 + \cdots + \alpha_{\frac{i+3}{2} i} B_j^{i+2} \right)$, for all i, j and k being the greatest even number less than or equal to m. Moreover,

$$\begin{aligned}
\int_0^{2\pi} F_2(\theta, r) d\theta &= \sum_{\substack{i=0 \\ i \text{ even}}}^{b} c_i r^{i+1} \int_0^{2\pi} \cos^i\theta \sin^2\theta d\theta \\
&\quad + \sum_{\substack{j=0 \\ j \text{ even}}}^{k} \sum_{\substack{i=1 \\ i \text{ odd}}}^{l} 2 r^{i+j} a_i b_j \int_0^{2\pi} \cos^{i+j+1}\theta \sin^2\theta d\theta \\
&= A_0 c_0 r + \cdots + A_b c_b r^{b+1} \\
&\quad + 2\Big(A_2 a_1 b_0 r + A_4 (a_3 b_0 + a_1 b_2) r^3 + \cdots + A_{l+k+1} r^{l+k} \sum_{i+j=l+k} a_i b_j \Big).
\end{aligned}$$

Then $F_{20}(r)$ is the polynomial

$$\begin{aligned}
&r\Big(\rho_{10} a_1 b_0 + (\rho_{12} a_1 b_2 + \rho_{30} a_3 b_0) r^2 + (\rho_{14} a_1 b_4 + \rho_{32} a_3 b_2 + \rho_{50} a_5 b_0) r^4 \\
&+ \cdots + \rho_{lk} a_l b_k r^{l+k-1} + A_0 c_0 + A_2 c_2 r^2 + \cdots + A_b c_b r^b \Big),
\end{aligned} \tag{1.158}$$

where $\rho_{ij} = \tilde{\alpha}_{ij} + 2A_{i+j+1}$ for all i, j. Note that, in order to find the positive roots of F_{20}, we must find the zeros of a polynomial in r^2 of degree equal to

$\max\{(l+k-1)/2, b/2\}$. We have that $b/2 = [n/2]$ and $(l+k-1)/2 = [(n-1)/2] + [m/2]$; see Table 1.3:

n	m	l	k	$(l+k-1)/2$	$[(n-1)/2]+[m/2]$
odd	even	n	m	$(n+m-1)/2$	$(n-1)/2+m/2$
even	even	n-1	m	$(n-1+m-1)/2$	$((n-1)-1)/2+m/2$
odd	odd	n	m-1	$(n+m-1-1)/2$	$(n-1)/2+(m-1)/2$
even	odd	n-1	m-1	$(n-1+m-1-1)/2$	$((n-1)-1)/2+(m-1)/2$

Table 1.3: Values of $(l+k-1)/2$ written using the integer part function.

We conclude that F_{20} has at most $\max\{[(n-1)/2]+[m/2], [n/2]\}$ positive roots. Moreover, we can choose the coefficients a_i, b_j, c_k in such a way that (1.158) has exactly $\max\{[(n-1)/2]+[m/2], [n/2]\}$ simple positive roots. Hence, the statement (ii) of Theorem 1.4.6 follows. □

Proof of Theorem 1.4.6(iii). We shall now use the third order averaging theory.

If we write $f_1(x) = \sum_{i=0}^{n} a_i x^i$, $f_2(x) = \sum_{i=0}^{n} c_i x^i$, $f_3(x) = \sum_{i=0}^{n} p_i x^i$, $g_1(x) = \sum_{i=0}^{m} b_i x^i$, $g_2(x) = \sum_{i=0}^{m} d_i x^i$ and $g_3(x) = \sum_{i=0}^{m} q_i x^i$, then an equivalent system to (1.152) with $k=3$ will be found by considering polar coordinates (r,θ). So,

$$\begin{aligned} \dot{r} &= -\sin\theta\left(\varepsilon A + \varepsilon^2 B + \varepsilon^3 C\right), \\ \dot{\theta} &= -1 - \frac{\cos\theta}{r}\left(\varepsilon A + \varepsilon^2 B + \varepsilon^3 C\right), \end{aligned} \tag{1.159}$$

where

$$\begin{aligned} A &= \sum_{i=0}^{n} a_i r^{i+1}\cos^i\theta\sin\theta + \sum_{i=0}^{m} b_i r^i \cos^i\theta, \\ B &= \sum_{i=0}^{n} c_i r^{i+1}\cos^i\theta\sin\theta + \sum_{i=0}^{m} d_i r^i \cos^i\theta, \\ C &= \sum_{i=0}^{n} p_i r^{i+1}\cos^i\theta\sin\theta + \sum_{i=0}^{m} q_i r^i \cos^i\theta. \end{aligned}$$

Taking θ as the new independent variable system, (1.159) becomes

$$\begin{aligned} \frac{dr}{d\theta} =& \varepsilon A\sin\theta + \varepsilon^2\left(B\sin\theta - \frac{A^2\cos\theta\sin\theta}{r}\right) \\ &+ \varepsilon^3\left(\frac{A^3\cos^2\theta\sin\theta}{r^2} - \frac{2AB\cos\theta\sin\theta}{r} + C\sin\theta\right). \end{aligned} \tag{1.160}$$

By (1.155), we know that F_{10} is identically zero if and only if $a_i = 0$ for all i even; and by (1.158) we obtain that F_{20} is identically zero if and only if the coefficients a_i, b_j and c_k satisfy

$$c_\mu = \frac{1}{A_\mu} \sum_{\substack{i+j=\mu+1 \\ i \text{ odd},\ j \text{ even}}} \rho_{i,j} a_i b_j, \tag{1.161}$$

where μ is even, and A_μ and $\rho_{i,j}$ are given in Subsection 1.3.2.

In order to apply the third order averaging method we need to compute the corresponding function F_{30}. So, the proof of statement (iii) of Theorem 1.4.6 will be a direct consequence of the next auxiliary lemmas.

The proof of the next lemma is straightforward and follows from some tedious computations; it will be omitted.

Lemma 1.4.7. *The corresponding functions $y_1(\theta, r)$ and $y_2(\theta, r)$ of the third order averaging method are expressed by* (1.157) *and*

$$y_2(\theta, r) = \quad C_0 + C_1 r + C_2 r^2 + \cdots + C_\lambda r^\lambda,$$

respectively, where $\lambda = \max\{2n+1, 2m-1\}$ and

$$\begin{aligned}
C_{2k+1} = & \sum_{i+j+=2k} c_{ij}^0 a_i a_j + \sum_{i+j=2k+2} d_{ij}^0 b_i b_j + \sum_{i+j=2k+1} e_{ij}^0 a_i b_j \theta \\
& + \sum_{i+j=2k} f_{ij}^0 a_i a_j \theta^2 + d_{2k+1} + c_{2k}\theta + \sum_{i+j=2k+2} b_i b_j \Big(\sum_{i=0}^{k+1} a_{2i+1}^0 \cos(2i+1)\theta \Big) \\
& + \Big(\sum_{i+j+=2k} a_i a_j + \sum_{i+j=2k+2} b_i b_j + \sum_{i+j=2k+1} a_i b_j \theta + d_{2k+1} \Big) \Big(\sum_{i=0}^{k+1} a_{2i+2}^0 \cos(2i+2)\theta \Big) \\
& + \sum_{i+j=2k+1} a_i b_j \Big(\sum_{i=0}^{k+1} a_{2i+1}^1 \sin(2i+1)\theta \Big) \\
& + \Big(\sum_{i+j+=2k+1} a_i b_j + \sum_{i+j=2k} a_i a_j \theta + c_{2k} \Big) \Big(\sum_{i=0}^{k+1} a_{2i+2}^1 \sin(2i+2)\theta) \Big),
\end{aligned}$$

$$\begin{aligned}
C_{2k} = & \sum_{i+j+=2k-1} c_{ij}^1 a_i a_j + \sum_{i+j=2k+1} d_{ij}^1 b_i b_j + \sum_{i+j=2k} e_{ij}^1 a_i b_j \theta \\
& + \Big(\sum_{i+j=2k-1} a_i a_j + \sum_{i+j=2k+1} b_i b_j + \sum_{i+j=2k} a_i b_j \theta \Big) \Big(\sum_{i=0}^{k+1} b_{2i+1}^0 \cos(2i+1)\theta \Big) \\
& + \Big(\sum_{i+j+=2k+1} b_i b_j \Big) \Big(\sum_{i=0}^{k+1} b_{2i+2}^0 \cos(2i+2)\theta \Big)
\end{aligned}$$

$$+\left(\sum_{i+j=2k} a_i b_j + c_{2k-1} + \sum_{i+j=2k} a_i b_j \theta\right)\left(\sum_{i=0}^{k+1} b^1_{2i+1}\sin(2i+1)\theta\right)$$
$$+\left(\sum_{i+j+=2k} a_i b_j\right)\left(\sum_{i=0}^{k+1} b^1_{2i+2}\sin(2i+2)\theta)\right),$$

where a^l_{2i+1}, a^l_{2i+2}, b^l_{2i+1}, a^l_{2i+2}, c^l_{ij}, d^l_{ij}, e^l_{ij}, f^l_{ij} *are real constants for* $l = 1, 2$ *and* $k = 0, 1, \ldots, \lambda/2$.

Lemma 1.4.8. *The integral* $\int_0^{2\pi} \frac{1}{2}\frac{\partial^2 F_1}{\partial r^2}(s,r)(y_1(s,r))^2 ds$ *equals the polynomial*

$$\pi(D_0 + D_1 r + D_2 r^2 + \cdots + D_\kappa r^\kappa), \tag{1.162}$$

where

$$\kappa = \begin{cases} n+2m-1 & \text{if } m > n+1 \text{ and either } m \text{ or } n \text{ is even,} \\ n+2m-2 & \text{if } m > n+1 \text{ and both } m \text{ and } n \text{ are odd,} \\ 3n+1 & \text{if } m \le n+1 \text{ and } n \text{ is even,} \\ 3n & \text{if } m \le n+1 \text{ and } n \text{ is odd,} \end{cases}$$

and

$$D_\chi = \sum_{i+j+k=\chi-1} \beta^1_{ijk} a_i a_j a_k + \sum_{i+j+k=\chi+1} \gamma^1_{ijk} a_i b_j b_k + \sum_{i+j+k=\chi} \delta^1_{ijk} a_i a_j b_k,$$

for $\chi = 0, 1, \ldots, \kappa$, *where* β^1_{ijk}, γ^1_{ijk}, δ^1_{ijk} *are real constants.*

Proof. Let us write

$$\frac{\partial^2 F_1}{\partial r^2}(s,r) = h_1(r) + h_2(r),$$

where

$$h_1(r) = \sum_{i=1}^{n} i(i+1) a_i r^{i-1} \cos^i\theta \sin^2\theta,$$
$$h_2(r) = \sum_{i=2}^{m} i(i-2) b_i r^{i-2} \cos^i\theta \sin\theta,$$

and

$$(y_1(s,r))^2 = g_1^2(r) + 2g_1(r)g_2(r) + g_2^2(r),$$

with

$$g_1(r) = s_1(r) + s_2(r),$$

where

$$s_1(r) = a_1 r^2 (\alpha_{11}\sin\theta + \alpha_{21}\sin(3\theta)) + \cdots$$
$$+ a_l r^{l+1}\left(\alpha_{1l}\sin\theta + \alpha_{2l}\sin(3\theta) + \cdots + \alpha_{(\frac{l+3}{2})l}\sin((l+2)\theta\right),$$
$$s_2(r) = a_0 r (\alpha_{10}\theta + \alpha_{20}\sin(2\theta)) + \cdots$$
$$+ a_b r^{b+1}\left(\alpha_{1b}\theta + \alpha_{2b}\sin(2\theta) + \cdots + \alpha_{(\frac{b+4}{2})b}\sin(b+2)\theta\right),$$

and

$$g_2(r) = \quad b_0(1-\cos\theta) + \cdots + b_m r^m \left(\frac{1}{m+1}(1-\cos^{m+1}\theta) \right).$$

Then,

$$\begin{aligned}\frac{\partial^2 F_1}{\partial r^2}(s,r)\left(y_1(s,r)\right)^2 =& h_1(r)\left(g_1^2(r)+2g_1(r)g_2(r)+g_2^2(r)\right)\\ &+ h_2(r)\left(g_1^2(r)+2g_1(r)g_2(r)+g_2^2(r)\right).\end{aligned}$$

From

$$\int_0^{2\pi} \cos^{2i}\theta \sin^2\theta \sin(\rho_1\theta)\sin(\rho_2\theta)d\theta = M_1(2i,\rho_1,\rho_2) \neq 0, \qquad \rho_1,\rho_2 \text{ odd},$$

$$\int_0^{2\pi} \cos^{2i+1}\theta \sin^2\theta \sin(\rho_1\theta)\sin(\rho_2\theta)d\theta = 0, \qquad \rho_1,\rho_2 \text{ odd},$$

for $i = 1, 2, \ldots$, we have that

$$\int_0^{2\pi} h_1(r)s_1(r)^2 d\theta = \sum_{\substack{k=1\\ k \text{ odd}}}^{l} \sum_{\substack{j=1\\ j \text{ odd}}}^{l} \sum_{\substack{i=2\\ i \text{ even}}}^{b} \zeta_{ijk}^1 a_i a_j a_k r^{i-1} r^{j+1} r^{k+1},$$

where

$$\zeta_{ijk}^1 = \sum_{\substack{\rho_1=1\\ \rho \text{ odd}}}^{k+2} \sum_{\substack{\rho'=1\\ \rho_1 \text{ odd}}}^{j+2} \delta_{\rho_1\rho_2}^{jk} i(i+1)\alpha_{\frac{\rho_1+1}{2}j}\alpha_{\frac{\rho_2+1}{2}k} M_1(i,\rho_1,\rho_2),$$

and

$$\delta_{\rho_1\rho_2}^{jk} = \begin{cases} 1 & \text{if } \rho_1 = \rho_2 \text{ and } j = k, \\ 2 & \text{if } \rho_1 \neq \rho_2 \text{ or } j \neq k. \end{cases}$$

Thus, $H_1(r) = \int_0^{2\pi} h_1(r)s_1(r)^2 d\theta$ is a polynomial in r of degree $3n-1$ if n even, and $3n$ if n odd. Knowing that

$$\int_0^{2\pi} \cos^{i}\theta \sin^2\theta \sin(\rho_1\theta)\theta d\theta = M_2(i,\rho_1,0) \neq 0, \qquad \rho_1 \text{ odd},$$

$$\int_0^{2\pi} \cos^{2i}\theta \sin^2\theta \sin(\rho_1\theta)\sin(\rho_2\theta)d\theta = 0, \qquad \rho_1 \text{ odd}, \rho_2 \text{ even},$$

$$\int_0^{2\pi} \cos^{2i+1}\theta \sin^2\theta \sin(\rho_1\theta)\sin(\rho_2\theta)d\theta = M_3(2i,\rho_1,\rho_2) \neq 0, \quad \rho_1 \text{ odd}, \rho_2 \text{ even},$$

for $i = 1, 2, \ldots$, we have that

$$\int_0^{2\pi} 2h_1(r)s_1(r)s_2(r)d\theta = \sum_{\substack{k=0\\ k \text{ even}}}^{b} \sum_{\substack{j=1\\ j \text{ odd}}}^{l} \sum_{i=1}^{n} \zeta_{ijk}^2 a_i a_j a_k r^{i-1} r^{j+1} r^{k+1} + \sum_{\substack{k=0\\ k \text{ even}}}^{b} \sum_{\substack{j=1\\ j \text{ odd}}}^{l} \sum_{\substack{i=1\\ i \text{ odd}}}^{l} \zeta_{ijk}^3 a_i a_j a_k r^{i-1} r^{j+1} r^{k+1},$$

where

$$\zeta_{ijk}^{\lambda} = \sum_{\substack{\rho_1=1\\ \rho_1 \text{ odd}}}^{k+2} \sum_{\substack{\rho_2=0\\ \rho_2 \text{ even}}}^{j+2} 2i(i+1)\alpha_{\frac{\rho_1+1}{2}j}\alpha_{\frac{\rho_2+2}{2}k} M_{\lambda}(i, \rho_1, \rho_2),\ \lambda = 2, 3.$$

Thus, the degree of the polynomial $H_2(r) = \int_0^{2\pi} 2h_1(r)s_1(r)s_2(r)d\theta$ in r is $3n$. From

$$\int_0^{2\pi} \cos^i\theta(\sin^2\theta)\theta^2 d\theta = M_4(i, 0, 0) \neq 0,$$

$$\int_0^{2\pi} \cos^{2i}\theta \sin^2\theta \sin(\rho_1\theta)\sin(\rho_2\theta)d\theta = M_5(2i, \rho_1, \rho_2) \neq 0, \quad \rho_1,\ \rho_2 \text{ even},$$

$$\int_0^{2\pi} \cos^{2i+1}\theta \sin^2\theta \sin(\rho_1\theta)\sin(\rho_2\theta)d\theta = 0, \quad \rho_1,\ \rho_2 \text{ even},$$

$$\int_0^{2\pi} \cos^i\theta \sin^2\theta \sin(\rho_1\theta)\theta d\theta = M_6(i, \rho_1, 0) \neq 0, \quad \rho_1 \text{ even},$$

for $i = 1, 2, \ldots$, we have that

$$\int_0^{2\pi} h_1(r)s_2^2(r)d\theta = \sum_{\substack{k=0\\ k \text{ even}}}^{b} \sum_{\substack{j=0\\ j \text{ even}}}^{b} \sum_{i=1}^{n} \zeta_{ijk}^4 a_i a_j a_k r^{i-1} r^{j+1} r^{k+1} + \sum_{\substack{k=0\\ k \text{ even}}}^{b} \sum_{\substack{j=1\\ j \text{ even}}}^{b} \sum_{\substack{i=2\\ i \text{ even}}}^{n} \zeta_{ijk}^5 a_i a_j a_k r^{i-1} r^{j+1} r^{k+1} + \sum_{\substack{k=0\\ k \text{ even}}}^{b} \sum_{\substack{j=0\\ j \text{ even}}}^{b} \sum_{i=1}^{n} \zeta_{ijk}^6 a_i a_j a_k r^{i-1} r^{j+1} r^{k+1},$$

where

$$\zeta_{ijk}^{\lambda} = \sum_{\substack{\rho_1=0\\ \rho_1 \text{ even}}}^{k+2} \sum_{\substack{\rho_2=0\\ \rho_2 \text{ even}}}^{j+2} \delta_{\rho_1\rho_2}^{jk} i(i+1)\alpha_{\frac{\rho_1+2}{2}j}\alpha_{\frac{\rho_2+2}{2}k} M_{\lambda}(i, \rho_1, \rho_2), \quad \lambda = 4, 5, 6,$$

with $\delta^{jk}_{\rho_1\rho_2}$ as above. Thus, $H_3(r) = \int_0^{2\pi} h_1(r)s_2^2(r)d\theta$ is a polynomial in r of degree $3n+1$ if n even, and $3n-1$ if n odd. Knowing that

$$\int_0^{2\pi} \cos^i\theta \sin^2\theta \sin(\rho_1\theta)d\theta = 0, \qquad \rho_1 = 1, 2, \ldots$$
$$\int_0^{2\pi} \cos^{2i}\theta(\sin^2\theta)\theta d\theta = M_7(i,0,0) \neq 0,$$
$$\int_0^{2\pi} \cos^{2i+1}\theta(\sin^2\theta)\theta d\theta = 0,$$

for $i = 1, 2, \ldots$, we have that

$$\int_0^{2\pi} h_1(r)(s_1(r) + s_2(r))g_2(r)d\theta = \sum_{k=0}^{m} \sum_{\substack{j=0 \\ j \text{ even}}}^{b} \sum_{i=1}^{n} \zeta^7_{ijk} a_i a_j b_k r^{i-1} r^{j+1} r^k,$$

where $k+i$ is odd, and $\zeta^7_{ijk} = i(i+1)\alpha_{1j}M_7(i,0,0)$. Thus, $H_4(r) = \int_0^{2\pi} h_1(r)(s_1(r) + s_2(r))g_2(r)d\theta$ is a polynomial in r of degree $2n+m-1$ if m is even, $2n+m$ if n is even and m is odd, and $2n+m-2$ if both n and m are odd.

The equalities

$$\int_0^{2\pi} \cos^{2i}\theta \sin^2\theta d\theta = M_8(i,0,0) \neq 0,$$
$$\int_0^{2\pi} \cos^{2i+1}\theta \sin^2\theta d\theta = 0,$$

for $i = 1, 2, \ldots$ imply

$$\int_0^{2\pi} h_1(r)g_2^2(r)d\theta = \sum_{k=0}^{m} \sum_{j=0}^{m} \sum_{i=1}^{n} \zeta^8_{ijk} a_i b_j b_k r^{i-1} r^j r^k,$$

where $\zeta^8_{ijk} = \delta_{jk} i(i+1)M_8(i,0,0)$ with

$$\delta_{jk} = \begin{cases} 1 & \text{if } j = k, \\ 2 & \text{if } j \neq k. \end{cases}$$

Thus, $H_5(r) = \int_0^{2\pi} h_1(r)g_2^2(r)d\theta$ is a polynomial in r of degree $2m+n-1$ if n or m is even, and $2m+n-2$ if n and m are both odd. From

$$\int_0^{2\pi} \cos^i\theta \sin\theta \sin(\rho_1\theta)\sin(\rho_2\theta)d\theta = 0, \qquad \rho_1,\ \rho_2 \text{ odd}$$

for $i = 1, 2, \ldots$, we have that $H_6(r) = \int_0^{2\pi} h_2(r)s_1^2(r)d\theta = 0$.

From the values of the integrals

$$\int_0^{2\pi} \cos^{2i}\theta(\sin\theta)\theta\sin(\rho_1\theta)d\theta = M_9(i,\rho_1,0) \neq 0, \qquad \rho_1 \text{ odd},$$
$$\int_0^{2\pi} \cos^{2i+1}\theta(\sin\theta)\theta\sin(\rho_1\theta)d\theta = 0, \qquad \rho_1 \text{ odd},$$
$$\int_0^{2\pi} \cos^{i}\theta\sin\theta\sin(\rho_1\theta)\sin(\rho_2\theta)d\theta = 0, \qquad \rho_1 \text{ even}, \rho_2 \text{ odd},$$

for $i = 1, 2, \ldots$, we have that

$$\int_0^{2\pi} h_2(r)s_1(r)s_2(r)d\theta = \sum_{\substack{k=1\\ k \text{ odd}}}^{l} \sum_{\substack{j=0\\ j \text{ even}}}^{b} \sum_{\substack{i=2\\ i \text{ even}}}^{m} \zeta_{ijk}^9 b_i a_j a_k r^{i-2} r^{j+1} r^{k+1},$$

where

$$\zeta_{ijk}^9 = \sum_{\substack{\rho_1=1\\ \rho_1 \text{ odd}}}^{l+2} i(i-1)\alpha_{1j}\alpha_{\frac{\rho_1+1}{2}k} M_9(i,\rho_1,0).$$

Thus, $H_7(r) = \int_0^{2\pi} h_2(r)s_1(r)s_2(r)d\theta$ is a polynomial in r of degree $2n+m-1$ if m even, and $2m+n-2$ if m odd. The formulas

$$\int_0^{2\pi} \cos^{i}\theta(\sin\theta)\theta^2 d\theta = M_{10}(i,0,0) \neq 0,$$
$$\int_0^{2\pi} \cos^{2i}\theta(\sin\theta)\theta\sin(\rho_1\theta)d\theta = 0, \qquad \rho_1 \text{ even},$$
$$\int_0^{2\pi} \cos^{2i+1}\theta(\sin\theta)\theta\sin(\rho_1\theta)d\theta = M_{11}(i,\rho_1,0) \neq 0, \qquad \rho_1 \text{ even},$$
$$\int_0^{2\pi} \cos^{i}\theta\sin\theta\sin(\rho_1\theta)\sin(\rho_2\theta)d\theta = 0, \qquad \rho_1, \rho_2 \text{ odd},$$

for $i = 1, 2, \ldots$ imply

$$\int_0^{2\pi} h_2(r)s_2^2(r)d\theta = \sum_{\substack{k=0\\ k \text{ even}}}^{b} \sum_{\substack{j=0\\ j \text{ even}}}^{b} \sum_{i=1}^{m} \zeta_{ijk}^{10} b_i a_j a_k r^{i-2} r^{j+1} r^{k+1}$$
$$+ \sum_{\substack{k=0\\ k \text{ even}}}^{b} \sum_{\substack{j=0\\ j \text{ even}}}^{b} \sum_{\substack{i=1\\ i \text{ odd}}}^{m} \zeta_{ijk}^{11} b_i a_j a_k r^{i-2} r^{j+1} r^{k+1},$$

where

$$\zeta_{ijk}^{10} = \delta_{jk}^{1} i(i-1)\alpha_{1j}\alpha_{1k} M_{10}(i,\rho_1,0),$$

$$\zeta_{ijk}^{11} = \sum_{\substack{\rho_1=1 \\ \rho_1 \text{ even}}}^{b+2} \delta_{jk\rho_1}^{2} i(i-1)\alpha_{1j}\alpha_{\frac{\rho_1+2}{2}k} M_{11}(i,\rho_1,0),$$

with

$$\delta_{jk}^{1} = \begin{cases} 1 & \text{if } j=k, \\ 2 & \text{if } j\neq k, \end{cases} \quad \text{and} \quad \delta_{jk\rho_1}^{2} = \begin{cases} 1 & \text{if } j=k,\ \rho_1=0, \\ 2 & \text{if } j\neq k,\ \rho_1\neq 0. \end{cases}$$

Thus, $H_8(r) = \int_0^{2\pi} h_2(r) s_2^2(r) d\theta$ is a polynomial in r of degree $m+2n$ if n even, and $m+2n-2$ if n odd. From

$$\int_0^{2\pi} \cos^{2i}\theta \sin\theta \sin(\rho_1\theta) d\theta = M_{12}(i,\rho_1,0) \neq 0, \qquad \rho_1 \text{ odd},$$

$$\int_0^{2\pi} \cos^{2i+1}\theta \sin\theta \sin(\rho_1\theta) d\theta = 0, \qquad \rho_1 \text{ odd},$$

$$\int_0^{2\pi} \cos^{i}\theta (\sin\theta)\theta d\theta = M_{13}(i,0,0) \neq 0,$$

$$\int_0^{2\pi} \cos^{2i}\theta \sin\theta \sin(\rho_1\theta) d\theta = M_{14}(i,\rho_1,0) \neq 0, \qquad \rho_1 \text{ even},$$

$$\int_0^{2\pi} \cos^{2i+1}\theta \sin\theta \sin(\rho_1\theta) d\theta = 0, \qquad \rho_1 \text{ even},$$

for $i = 1, 2, \ldots$, we have that

$$\begin{aligned} \int_0^{2\pi} h_2(r)(s_1(r)+s_2(r)) g_2(r) d\theta = & \sum_{k=0}^{m} \sum_{\substack{j=1 \\ j \text{ odd}}}^{l} \sum_{i=1}^{m} \zeta_{ijk}^{12} b_i a_j b_k r^{i-2} r^{j+1} r^k \\ & + \sum_{k=0}^{m} \sum_{\substack{j=0 \\ j \text{ even}}}^{b} \sum_{i=1}^{m} \zeta_{ijk}^{13} b_i a_j b_k r^{i-2} r^{j+1} r^k \\ & + \sum_{k=0}^{m} \sum_{\substack{j=1 \\ j \text{ even}}}^{l} \sum_{i=1}^{m} \zeta_{ijk}^{14} b_i a_j b_k r^{i-2} r^{j+1} r^k, \end{aligned}$$

where

$$\zeta_{ijk}^{12} = \begin{cases} \sum\limits_{\substack{\rho_1=1 \\ \rho_1 \text{ odd}}}^{j+2} \frac{i(i-1)}{k+2} \alpha_{\frac{\rho+1}{2} j} M_{12}(i, \rho_1, 0) & \text{for } k+i \text{ even}, \\ 0 & \text{for } k+i \text{ odd}, \end{cases}$$

$$\zeta_{ijk}^{13} = \frac{i(i-1)}{k+1} \alpha_{1j} M_{13}(i, 0, 0),$$

$$\zeta_{ijk}^{14} = \begin{cases} \sum\limits_{\substack{\rho_1=0 \\ \rho_1 \text{ even}}}^{j+2} \frac{i(i-1)}{k+2} \alpha_{\frac{\rho_1+2}{2} j} M_{14}(i, \rho_1, 0) & \text{for } k+i \text{ even}, \\ 0 & \text{for } k+i \text{ odd}. \end{cases}$$

Thus, $H_9(r) = \int_0^{2\pi} h_2(r)(s_1(r) + s_2(r))g_2(r)d\theta$ is a polynomial in r of degree $2m+n-1$ if n even, and $2m+n-2$ if n odd.

From the value of the integral

$$\int_0^{2\pi} \cos^i \theta \sin \theta d\theta = 0,$$

for $i = 1, 2, \ldots$, we have that $H_{10}(r) = \int_0^{2\pi} h_2(r) g_2^2(r) d\theta = 0$.

We conclude that

$$\int_0^{2\pi} \frac{1}{2} \frac{\partial^2 F_1}{\partial r^2}(s, r)(y_1(s, r))^2 ds = \sum_{i=1}^{10} H_i,$$

whose degree is the greatest of the degrees of H_i. Hence, the proof of the lemma follows. □

The proofs of the next three lemmas follow in a similar way to the previous one; they will be omitted.

Lemma 1.4.9. *The integral* $\int_0^{2\pi} \frac{1}{2} \frac{\partial F_1}{\partial r}(s, r)(y_2(s, r))ds$ *equals the polynomial*

$$\frac{\pi}{r}(E_0 + E_1 r + E_2 r^2 + \cdots + E_\vartheta r^\vartheta), \tag{1.163}$$

where

$$\vartheta = \begin{cases} n+2m & \text{if } m > n+1 \text{ and } n \text{ is even}, \\ n+2m-1 & \text{if } m > n+1 \text{ and } n \text{ is odd}, \\ 3n+2 & \text{if } m \leq n+1 \text{ and } n \text{ is even}, \\ 3n+1 & \text{if } m \leq n+1 \text{ and } n \text{ is odd}, \end{cases}$$

and

$$E_{2l+1} = \sum_{i+j+k=2l-1} \beta^2_{ijk} a_i a_j a_k + \sum_{i+j+k=2l+1} \gamma^2_{ijk} a_i b_j b_k + \sum_{i+j=2l} \delta^2_{ij} b_i c_j + \sum_{i+j=2l} \eta^2_{ij} a_i d_j + \sum_{\substack{i+j+k=2l \\ i \text{ even}}} \upsilon^2_{ijk} a_i a_j b_k \pi,$$

$$E_{2l} = \sum_{i+j+k=2l-2} \beta^2_{ijk} a_i a_j a_k + \sum_{i+j+k=2l} \gamma^2_{ijk} a_i b_j b_k + \sum_{i+j=2l-1} \delta^2_{ij} b_i c_j + \sum_{i+j=2l-1} \eta^2_{ij} a_i d_j + \sum_{\substack{i+j+k=2l-1 \\ i \text{ even}}} \upsilon^2_{ijk} a_i a_j b_k \pi + \sum_{\substack{i+j=2l-2 \\ i \text{ even}}} \varsigma^2_{ij} a_i c_j \pi,$$

for $l = 0, 1, \ldots, \vartheta/2$, *where* β^2_{ijk}, γ^2_{ijk}, δ^2_{ij}, η^2_{ij}, υ^2_{ijk}, ς^2_{ij} *are real constants.*

Lemma 1.4.10. *The integral* $\int_0^{2\pi} \frac{1}{2} \frac{\partial F_2}{\partial r}(s, r)(y_1(s, r))ds$ *equals the polynomial*

$$\frac{\pi}{r}(F_0 + F_1 r + F_2 r^2 + \cdots + F_\nu r^\nu), \tag{1.164}$$

where

$$\nu = \begin{cases} n + 2m & \text{if } m > n + 1 \text{ and } n \text{ is even}, \\ n + 2m - 1 & \text{if } m > n + 1 \text{ and } n \text{ is odd}, \\ 3n + 2 & \text{if } m \leq n + 1 \text{ and } n \text{ is even}, \\ 3n + 1 & \text{if } m \leq n + 1 \text{ and } n \text{ is odd}, \end{cases}$$

and

$$F_{2l+1} = \sum_{i+j+k=2l-1} \beta^3_{ijk} a_i a_j a_k + \sum_{i+j+k=2l+1} \gamma^3_{ijk} a_i b_j b_k + \sum_{i+j=2l} \delta^3_{ij} b_i c_j + \sum_{i+j=2l} \eta^3_{ij} a_i d_j,$$

$$F_{2l} = \sum_{i+j+k=2l-2} \beta^3_{ijk} a_i a_j a_k + \sum_{i+j+k=2l} \gamma^3_{ijk} a_i b_j b_k + \sum_{i+j=2l-1} \delta^3_{ij} b_i c_j + \sum_{i+j=2l-1} \eta^3_{ij} a_i d_j + \sum_{\substack{i+j+k=2l-1 \\ i \text{ even}}} \upsilon^3_{ijk} a_i a_j b_k \pi + \sum_{\substack{i+j+=2l-2 \\ i \text{ even}}} \varsigma^3_{ij} a_i c_j \pi,$$

for $l = 0, 1, \ldots, \nu/2$, *where* β^3_{ijk}, γ^3_{ijk}, δ^3_{ij}, η^3_{ij}, υ^3_{ijk}, ς^3_{ij} *are real constants.*

Lemma 1.4.11. *The integral* $\int_0^{2\pi} F_3(s, r)ds$ *equals the polynomial*

$$\frac{\pi}{r}(G_0 + G_2 r^2 + \cdots + G_\psi r^\psi), \tag{1.165}$$

where

$$\psi = \begin{cases} n+2m & \text{if } m > n+1 \text{ and } n \text{ is even,} \\ n+2m-1 & \text{if } m > n+1 \text{ and } n \text{ is odd,} \\ 3n+2 & \text{if } m \leq n+1 \text{ and } n \text{ is even,} \\ 3n+1 & \text{if } m \leq n+1 \text{ and } n \text{ is odd,} \end{cases}$$

and

$$\begin{aligned} G_{2l} = & \sum_{i+j+k=2l-2} \beta^4_{ijk} a_i a_j a_k + \sum_{i+j+k=2l} \gamma^4_{ijk} a_i b_j b_k + \sum_{i+j=2l-1} \delta^4_{ij} b_i c_j \\ & + \sum_{i+j=2l-1} \eta^4_{ij} a_i d_j + p_{2l-2}, \end{aligned}$$

for $l = 0, 1, \ldots, \psi/2$, *where* β^4_{ijk}, γ^4_{ijk}, δ^4_{ij}, η^2_{ij}, υ^4_{ijk} *are real constants.*

By Lemmas 1.4.8, 1.4.9, 1.4.10 and 1.4.11 we obtain

$$F_{30}(r) = \frac{\alpha}{r} \left(M_0 + M_1 r + M_2 r^2 + M_3 r^3 + M_4 r^4 + \cdots + M_{\varrho-1} r^{\varrho-1} + M_\varrho r^\varrho \right),$$

where

$$\begin{aligned} M_{2l+1} = & \sum_{i+j+k=2l-1} \beta_{ijk} a_i a_j a_k + \sum_{i+j+k=2l+1} \gamma_{ijk} a_i b_j b_k + \sum_{i+j=2l} \delta_{ij} b_i c_j \\ & + \sum_{i+j=2l} \eta_{ij} a_i d_j + \sum_{\substack{i+j=2l \\ i \text{ even}}} \nu_{ij} a_i a_j b_k \pi, \end{aligned}$$

$$\begin{aligned} M_{2l} = & \sum_{i+j+k=2l} \beta_{ijk} a_i b_j b_k + \sum_{i+j+k=2l-2} \gamma_{ijk} a_i a_j a_k + \sum_{i+j=2l-1} \delta_{ij} b_i c_j \\ & + \sum_{i+j=2l-1} \eta_{ij} a_i d_j + \sum_{i+j+k=2l-2} \mu_{ijk} a_i a_j a_k + \varpi_{2l-2} p_{2l-2} \\ & + \left(\sum_{\substack{i+j+k=2l-1 \\ i \text{ even}}} \nu_{ijk} a_i a_j b_k + \sum_{\substack{i+j=2l-2 \\ i \text{ even}}} \rho_{ijk} a_i c_j \right) \pi \\ & + \sum_{\substack{i+j+k=2l-2 \\ i \text{ even}}} \tau_{ijk} a_i a_j a_k \pi^2, \end{aligned}$$

for $l = 0, 1, 2, \ldots, \varrho/2$ and

$$\varrho = \begin{cases} n + 2m & \text{if } m > n+1 \text{ and } n \text{ is even,} \\ n + 2m - 1 & \text{if } m > n+1 \text{ and } n \text{ is odd,} \\ 3n + 2 & \text{if } m \leq n+1 \text{ and } n \text{ is even,} \\ 3n + 1 & \text{if } m \leq n+1 \text{ and } n \text{ is odd.} \end{cases}$$

Applying the equalities $a_i = 0$, for all i even and (1.161), we obtain that $M_0 = 0$ and $M_\kappa = 0$ for κ odd. Moreover, from (1.161) we obtain

$$c_k = \sum_{\substack{i+j=k+1 \\ i \text{ odd} \\ j \text{ even}}} a_i b_j = 0$$

for $k > b$. Then $M_k = 0$ for k greater than

$$\lambda = \begin{cases} n + m - 2 & \text{if } n \text{ and } m \text{ are odd,} \\ n + m - 1 & \text{if } n \text{ is odd and } m \text{ is even,} \\ n + m - 2 & \text{if } n \text{ and } m \text{ are even,} \\ n + m - 1 & \text{if } n \text{ is even and } m \text{ is odd.} \end{cases}$$

Thus

$$F_{30}(r) = \alpha r \left(M_2 + M_4 r^2 + M_6 r^4 + \cdots + M_{\lambda-4} r^{\lambda-2} + M_{\lambda-2} r^\lambda \right),$$

where

$$M_\omega = \sum_{\substack{i+j+k=\omega \\ i \text{ odd} \\ j \text{ even} \\ k \text{ odd}}} \beta'_{ijk} a_i b_j b_k + \sum_{\substack{i+j=\omega-1 \\ i \text{ even} \\ j \text{ odd}}} \delta'_{ij} b_i c_j + \sum_{\substack{i+j=\omega-1 \\ i \text{ odd} \\ j \text{ even}}} \eta'_{ij} a_i d_j \; + \; \varpi_\omega p_{\omega-2}.$$

Consequently, $F_3(z)$ is a polynomial of degree λ in the variable r^2. Then $F_3(z)$ has at most $[(n+m-1)/2]$ positive roots and, from the third order averaging method, we conclude that this is the maximum number of limit cycles of the polynomial Liénard differential systems (1.152) with $k = 3$ bifurcating from the periodic orbits of the linear center $\dot{x} = y$, $\dot{y} = -x$. This completes the proof of statement (iii) of Theorem 1.4.6. □

Bibliography

[1] R. Abraham, J.E. Marsden and T. Ratiu. *"Manifolds, tensor analysis and applications"* (second edition). Applied Mathematical Sciences **75**, Springer-Verlag, New York, 1988.

[2] M. Abramowitz and I.A. Stegun. *"Bessel Functions J and Y"*, §9.1 in "Handbook of Mathematical Functions with Formulas, Graphs, and Mathematical Tables", (9-th printing), New York, Dover (1972), 358–364.

[3] Y. Alhassid, E.A. Hinds, and D. Meschede. "Dynamical symmetries of the perturbed hydrogen atom: the van der Waals interaction". *Physical Review Letters* **59** (1987), 1545–1548.

[4] N.N. Bautin. "On the number of limit cycles which appear with the variation of the coefficients from an equilibrium position of focus or center type". *Math. USSR Sb.* **100** (1954), 397–413.

[5] R. Benterki and J. Llibre. "Periodic solutions of a class of Duffing differential equations". *Preprint.*

[6] T.R. Blows and N.G. Lloyd. "The number of small-amplitude limit cycles of Liénard equations". *Math. Proc. Camb. Phil. Soc.* **95** (1984), 359–366.

[7] N.N. Bogoliubov. "On some statistical methods in mathematical physics". Izv. vo Akad. Nauk Ukr. SSR. Kiev, 1945.

[8] N.N. Bogoliubov and N. Krylov. "The application of methods of non-linear mechanics in the theory of stationary oscillations", Publ. 8 of the Ukrainian Acad. Sci. Kiev, 1934.

[9] N.N. Bogoliubov and Yu.A. Mitropolsky. "Asymtotic mehtods in the theory of non-linear oscillations". Gordon and Breach, New York, 1961.

[10] M. Brack. "Orbits with analytical Scaling Constants in Hénon–Heiles type potentials". *Fundations of Phys.* **31** (2001), 209–232.

[11] F. Browder. "Fixed point theory and non-linear problems". *Bull. Amer. Math. Soc.* **9** (1983), 1–39.

[12] A. Buică, J.P. Françoise and J. Llibre. "Periodic solutions of non-linear periodic differential systems with a small parameter". To appear in *Communication on Pure and Applied Analysis* (2006).

[13] A. Buică, A. Gasull and Z. Yang, "The third order Melnikov function of a quadratic center under quadratic perturbations". *J. Math. Anal. Appl.* **331** (2007), 443–454.

[14] A. Buică and J. Llibre. "Averaging methods for finding periodic orbits via Brouwer degree". *Bulletin des Sciences Mathemàtiques* **128** (2004), 7–22.

[15] H.B. Chen and Y. Li. "Stability and exact multiplicity of periodic solutions of Duffing equations with cubic non-linearities". *Proc. Amer. Math. Soc.* **135** (2007), 3925–3932.

[16] H.B. Chen and Y. Li". "Bifurcation and stability of periodic solutions of Duffing equations". *Nonlinearity* **21** (2008), 2485–2503.

[17] L.A. Cherkas. "Number of limit cycles of an autonomous second-order system". *Differential Equations* **5** (1976), 666–668.

[18] C. Christopher and C. Li. "Limit cycles in differential equations". Birkhauser, Boston, 2007.

[19] C.J. Christopher and S. Lynch. "Small-amplitude limti cycle bifurcations for Liénard systems with quadratic or cubic dapimg or restoring forces". *Nonlinearity* **12** (1999), 1099–1112.

[20] R. Churchill, G. Pecelli and D. Rod. "A survey of the Hénon–Heiles Hamiltonian with applications to related examples". In "Stochastic Behaviour in Classical and Quantum Hamiltonian Systems", G. Casati and J. Ford eds., Springer NY (1979), 76–136.

[21] E.A. Coddington and N. Levinson. "Theory of ordinary differential equations". Mc-Graw-Hill Book Co., New York, 1955.

[22] W.A. Coppel. "Some quadratic systems with at most one limit cycles". *Dynamics Reported* **2**, Wiley, New York, 1998, 61–68.

[23] B. Cordani, "The Kepler problem". *Progress in Mathematical Physics* **29**, Springer–Verlag, 2003.

[24] K. Davies, T. Huston and M. Baranger. "Calculations of periodic trajectories for the Hénon–Heiles Hamiltonian using the monodromy method". *Chaos* **2** (1992), 215–224.

[25] P. De Maesschalck and F. Dumortier. "Classical Liénard equation of degree $n \geq 6$ can have $[(n-1)/2] + 2$ limit cycles". *Preprint* (2010).

[26] G. Duffing. "Erzwungen Schwingungen bei vernäderlicher Eigenfrequenz undihre technisch Bedeutung". *Sammlung Viewg Heft*, Viewg, Braunschweig **41/42** (1918).

[27] F. Dumortier and C. Li. "On the uniqueness of limit cycles surrounding one or more singularities for Liénard equations". *Nonlinearity* **9** (1996), 1489–1500.

[28] F. Dumortier and C. Li. "Quadratic Liénard equations with quadratic damping". *J. Diff. Eqs.* **139** (1997), 41–59.

[29] F. Dumortier, D. Panazzolo and R. Roussarie. "More limit cycles than expected in Liénard systems". *Proc. Amer. Math. Soc.* **135** (2007), 1895–1904.

[30] F. Dumortier and C. Rousseau. "Cubic Liénard equations with linear damping". *Nonlinearity* **3** (1990), 1015–1039.

[31] F. ElSabaa and H. Sherief. "Periodic orbits of galactic motions". *Astrophys. and Space Sci.* **167** (1990), 305–315.

[32] R.D. Euzébio and J. Llibre. "Periodic Solutions of *El Niño* Model through the Vallis Differential System". To appear in *Discrete and Continuous Dynamical System*, Series A.

[33] D. Farrelly and T. Uzer. "Normalization and Detection of the Integrability: The Generalized van der Waals Potential". *Celestial Mechanics and Dynamical Astronomy* **61** (1995), 71–95.

[34] P. Fatou. "Sur le mouvement d'un systàme soumis à des forces à courte période". *Bull. Soc. Math. France* **56** (1928), 98–139.

[35] J.P. Françoise. "Successive derivatives of a first return map, application to the study of quadratic vector fields". *Ergodic Theory Dynam. Systems* **16** (1996), 87–96.

[36] A. Gasull and J. Torregrosa. "Small amplitude limit cycles in Liénard systems via multiplicity". *J. Diff. Eqs.* **159** (1998), 1015–1039.

[37] J. Giné, M. Grau and J. Llibre. "Averaging theory at any order for computing periodic orbits". *Physica D* **250** (2013), 58–65.

[38] J.L.G. Guirao, J. Llibre and J.A. Vera. "Generalized van der Waals Hamiltonian: Periodic orbits and C^1 non-integrability". *Physical Review E* **85** (2012), 036603.

[39] J.L.G. Guirao, J. Llibre and J.A. Vera. "Periodic orbits of Hamiltonian systems: Applications to perturbed Kepler problems". *Chaos, Solitons and Fractals* **57** (2013), 105–111.

[40] M. Hénon and C. Heiles. "The applicability of the third integral of motion: some numerical experiments". *Astron. J.* **69** (1964), 73–84.

[41] D. Hilbert. "Mathematische Probleme". Lecture, Second Internat. Congr. Math. (Paris, 1900), *Nachr. Ges. Wiss. Göttingen Math. Phys. KL.* (1900), 253–297; English transl., *Bull. Amer. Math. Soc.* **8** (1902), 437–479.

[42] R.C. Howison and K.R. Meyer. "Doubly-symmetric periodic solutions of the spatial restricted three-body problem". *J. Differential Equations* **163** (2000), 174–197.

[43] W.L. Hosch. "The Britannica Guide to Algebra and Trigonometry". Britannica Educational Publishing, New York, 2010.

[44] I.D. Iliev. "On second order bifurcations of limit cycles". *J. London Math. Soc.* **58** (1998), 353–366.

[45] I. Iliev. "The number of limit cycles due to polynomial perturbations of the harmonic oscillator". *Math. Proc. Cambridge Philos. Soc.* **127** (1999), 317–322.

[46] Y. Ilyashenko. "Centennial history of Hilbert's 16-th problem". *Bull. Amer. Math. Soc.* **39** (2002), 301–354.

[47] M. Iñarrea, V. Lanchares, J. Palacián, A.I. Pascual, J.P. Salas and P. Yanguas". "Symplectic coordinates on $S^2 \times S^2$ for perturbed Keplerian problems: application to the dynamics of a generalised Stormer problem". *J. Differential Equations* **250** (2011), 1386–1407.

[48] L. Jiménez and J. Llibre. "Periodic orbits and non-integrability of Henon–Heiles systems". *J. of Physics A: Math. Theor.* **44** (2011), 205103.

[49] P. Kent and J. Elgin. "Noose bifurcation of periodic orbits". *Nonlinearity* **4** (1991), 1045–1061.

[50] J. Li. "Hilbert's 16-th problem and bifurcations of planar polynomial vector fields". *Internat. J. Bifur. Chaos Appl. Sci. Engrg.* **13** (2003), 47–106.

[51] C. Li and J. Llibre. "Uniqueness of limit cycle for Liénard equations of degree four". *J. Differential Equations* **252** (2012), 3142–3162.

[52] A. Liénard. "'Etude des oscillations entrenues". *Revue Génerale de l'Électricité* **23** (1928), 946–954.

[53] A. Lins, W. de Melo and C.C. Pugh. "On Liénard's Equation". Lecture Notes in Math. **597**, Springer, Berlin, 1977, pp 335–357.

[54] J. Llibre, A.C. Mereu and M.A. Teixeira. "Limit cycles of the generalized polynomial Liénard differential equations". *Math. Proceed. Camb. Phyl. Soc.* **148** (2009), 363–383.

[55] J. Llibre, D.D. Novaes and M.A. Teixeira. "Higher order averaging theory for finding periodic solutions via Brouwer degree". To appear in *Nonlinearity*.

[56] J. Llibre, S. Rebollo-Perdomo and J. Torregrosa. "Limit cycles bifurcating from isochronous surfaces of revolution in R^3". *J. Math. Anal. and Appl.* **381** (2011), 414–426.

[57] J. Llibre and G. Swirszcz. "On the limit cycles of polynomial vector fields". *Dyn. Contin. Discrete Impuls. Syst.* **18** (2011), 203–214.

[58] J. Llibre and X. Zhang. "Hopf bifurcation in higher dimensional differential systems via the averaging method". *Pacific J. of Math.* **240** (2009), 321–341.

[59] J. Llibre and X. Zhang. "On the zero-Hopf bifurcation of the Michelson system". *Nonlinear Analysis, Real World Applications* **12** (2011), 1650–1653.

[60] N.G. Lloyd. "Limit cycles of polynomial systems, some recent developments". *London Math. Soc. Lecture Note Ser.* 127, Cambridge University Press (1988), 192–234.

[61] N.G. Lloyd and S. Lynch. "Small amplitude limit cycles of certain Liénard systems". *Proc. Royal Soc. London Ser. A* **418** (1988), 199–208.

[62] N. Lloyd and J.M. Pearson. "Bifurcation of limit cycles and integrability of planar dynamical systems in complex form". *J. Phys. A: Math. Gen.* **32** (1999), 1973–1984.

[63] N. Lloyd and J.M. Pearson. "Symmetric in planar dynamical systems". *J. Symb. Comput.* **33** (2002), 357–366.

[64] S. Lynch. "Limit cycles if generalized Liénard equations". *Applied Math. Letters* **8** (1995), 15–17.

[65] S. Lynch. "Generalized quadratic Liénard equations". *Applied Math. Letters* **11** (1998), 7–10.

[66] S. Lynch. "Generalized cubic Liénard equations". *Applied Math. Letters* **12** (1999), 1–6.

[67] S. Lynch and C.J. Christopher. "Limit cycles in highly non-linear differential equations". *J. Sound Vib.* **224** (1999), 505–517.

[68] A. Maciejewski, W. Radzki and S. Rybicki. "Periodic trajectories near degenerate equilibria in the Hénon–Heiles and Yang–Mills Hamiltonian systems". *J. Dyn. and Diff. Eq.* **17** (2005), 475–488.

[69] I.G. Malkin. "Some problems of the theory of non-linear oscillations". (Russian) Gosudarstv. Izdat. Tehn.-Teor. Lit., Moscow, 1956.

[70] J. Mawhin. "Seventy-five years of global analysis around the forced pendulum equation". In *Equadiff* **9** (Brno Proceedings, Masaryk University) (1997), 115–145.

[71] K.R. Meyer, G.R. Hall and D. Offin. "Introduction to Hamiltonian dynamical systems and the N-body problem". *Applied Mathematical Sciences* **90**, Springer New York, 2009.

[72] D. Michelson. "Steady solutions for the Kuramoto–Sivashinsky equation". *Physica D* **19** (1986), 89–111.

[73] R. Ortega. "Stability and index of periodic solutions of an equation of Duffing type". *Boo. Uni. Mat. Ital B* **3** (1989), 533–546.

[74] J. Ozaki and S. Kurosaki. "Periodic orbits of Hénon–Heiles Hamiltonian". *Prog. in Theo. Phys.* **95** (1996), 519–529.

[75] H. Poincaré. "Mémoire sur les courbes définies par les équations différentielles". Oeuvreus de Henri Poincaré, Vol. I, Gauthiers–Villars, Paris (1951), 95–114.

[76] M. Roseau. "Vibrations non-linéaires et théorie de la stabilité". *Springer Tracts in Natural Philosophy* **8**, Springer–Verlag, Berlin–New York, 1966.

[77] G.S. Rychkov. "The maximum number of limit cycle of the system $\dot{x} = y - a_1x^3 - a_2x^5$, $\dot{y} = -x$ is two". *Differential'nye Uravneniya* **11** (1975), 380–391.

[78] J.A. Sanders F. Verhulst and J. Murdock. "Averaging Methods in Nonlinear Dynamical Systems" (second edition). *Applied Mathematical Sciences* **59**, Springer, New York, 2007.

[79] M. Santoprete. "Block regularization of the Kepler problem on surfaces of revolution with positive constant curvature". *J. Differential Equations* **247** (2009), 1043–1063.

[80] I.R. Shafarevich. "Basic Algebraic Geometry". Springer, 1974.

[81] K.S. Sibirskii. "On the number of limit cycles in the neighborhood of a singular point". *Differential Equations* **1** (1965), 36–47.

[82] D. Strozzi. "On the origin of interannual and irregular behaviour in the El Niño properties". Report of the Department of Physics, Princeton University (1999).

[83] G. Świrszcz. "Cyclicity of infinite contour around certain reversible quadratic center". *J. Differential Equations* **154** (1999), 239–266.

[84] G.K. Vallis. "Conceptual models of El Niño and the southern oscillation". *J. Geophys. Res.* **93** (1988), 13979–13991.

[85] F. Verhulst. "Nonlinear dierential equations and dynamical systems". Universitext, Springer, 1991.

[86] K.N. Webster and J. Elgin. "Asymptotic analysis of the Michelson system". *Nonlinearity* **16** (2003), 2149–2162.

[87] P. Yu and M. Han. "Limit cycles in generalized Liénard systems". *Chaos, Solitons and Fractals* **30** (2006), 1048–1068.

[88] H. Zołądek. "The cyclicity of triangles and segments in quadratic systems". *J. Differential Equations* **122** (1995), 137–159.

Chapter 2

Central Configurations

Richard Moeckel

The topic of the present chapter is one of my favorites: central configurations of the n-body problem. I gave a course on the same subject in Trieste in 1994 and wrote up some notes (by hand) which can be found on my website [23]. For the new course, I tried to focus on some new ideas and techniques which have been developed in the intervening twenty years. In particular, I consider space dimensions bigger than three. There are still a lot of open problems and it remains an attractive area for mathematical research.

2.1 The n-body problem

The Newtonian n-body problem is the study of the dynamics of n point particles with masses $m_i > 0$ and positions $x_i \in \mathbb{R}^d$, moving according to Newton's laws of motion:

$$m_j \ddot{x}_j = \sum_{i \neq j} \frac{m_i m_j (x_i - x_j)}{r_{ij}^3}, \quad 1 \leq j \leq n, \tag{2.1}$$

where $r_{ij} = |x_i - x_j|$ is the Euclidean distance between x_i and x_j. Although we are mainly interested in dimensions $d \leq 3$, it is illuminating and entertaining to consider higher dimensions as well.

Let $x = (x_1, \ldots, x_n) \in \mathbb{R}^{dn}$ be the *configuration vector* and let

$$U(x) = \sum_{i<j} \frac{m_i m_j}{r_{ij}} \tag{2.2}$$

be the *Newtonian potential*. Then we have

$$m_j \ddot{x}_j = \nabla_j U(x), \quad 1 \leq j \leq n, \tag{2.3}$$

© Springer Basel 2015

J. Llibre et al., *Central Configurations, Periodic Orbits, and Hamiltonian Systems*,
Advanced Courses in Mathematics - CRM Barcelona, DOI 10.1007/978-3-0348-0933-7_2

where ∇_j denotes the d-dimensional partial gradient with respect to x_j or

$$M\ddot{x} = \nabla U(x), \tag{2.4}$$

where ∇ is the dn-dimensional gradient and $M = \mathrm{diag}(m_1, \ldots, m_n)$ is the matrix with d copies of each mass along the diagonal. (Later there will be an $n \times n$ mass matrix, also called M.)

Let $v_j = \dot{x}_j \in \mathbb{R}^d$ be the velocity vectors and $v = (v_1, \ldots, v_n) \in \mathbb{R}^{dn}$. Then there is an equivalent first-order system

$$\begin{aligned} \dot{x} &= v, \\ \dot{v} &= M^{-1}\nabla U(x). \end{aligned}$$

Since Newtonian potential is singular at collisions, we have to restrict x to the *configuration space* $\mathbb{R}^{nd} \setminus \Delta$, where

$$\Delta = \{x : x_i = x_j \text{ for some } i \neq j\} \tag{2.5}$$

is the *singular set*.

The phase space for the first-order system is $(\mathbb{R}^{nd} \setminus \Delta) \times \mathbb{R}^{nd}$. Newton's equations are conservative. The *total energy*

$$H = K(v) - U(x), \quad K = \sum_{j=1}^{n} m_j |v_j|^2$$

is constant along solutions in phase space.

Even though we are considering the n-body problem in $\mathbb{R}^d$, it may happen that the motion that takes place in a subspace $\mathcal{W}$. In fact, let $\mathcal{W} \subset \mathbb{R}^d$ be any subspace. If all of the positions and velocities satisfy $x_j, v_j \in \mathcal{W}$, equation (2.1) shows that the acceleration vectors are also in $\mathcal{W}$. It follows that $\mathcal{W}^n \setminus \Delta \times \mathcal{W}^n$ is an invariant set for the flow in phase space. In particular we can consider the smallest subspace containing all of the positions and velocities,

$$\mathcal{S}(x, v) = \mathrm{span}\{x_j, v_j : j = 1, \ldots, n\} \subset \mathbb{R}^d.$$

If $(x(t), v(t))$ is any solution, then $\mathcal{S}(x(t), v(t))$ is independent of t. It will be called the *motion space* of the solution.

2.2 Symmetries and integrals

Newton's equations are invariant under simultaneous translations and rotations of all of the positions and velocities $x_j, v_j \in \mathbb{R}^d$. Symmetry under translations gives rise, via Nöther's Theorem [5], to conservation of the *total momentum* vector

$$p = m_1 v_1 + \cdots + m_n v_n.$$

Let

$$c = \frac{1}{m_0}\left(m_1 x_1 + \cdots + m_n x_n\right), \quad m_0 = m_1 + \cdots + m_n \tag{2.6}$$

be the *center of mass*, where m_0 is the *total mass*. Then

$$\begin{aligned} \dot{c} &= p/m_0, \\ \dot{p} &= 0 \end{aligned}$$

so $c(t)$ moves in a straight line with constant velocity. It follows that the positions relative to the center of mass, $y_j(t) = x_j(t) - c(t)$, are also solutions of Newton's equations. These have center of mass at the origin and total momentum zero. A solution with this property will be called *centered*. We will use the notation

$$x - c = (x_1 - c, \ldots, x_n - c) \in \mathbb{R}^{dn}$$

for the configuration relative to the center of mass.

For any configuration x, the vectors $x_j - c$, $j = 1, \ldots, n$, span a subspace of $\mathbb{R}^d$ which we will call the *centered position space* and denote by $\mathcal{C}(x)$. It is natural to define the *dimension of a configuration* to be $\dim(x) = \dim \mathcal{C}(x)$. The maximum possible dimension of a configuration of the n-body problem is $n-1$. For example, every configuration of the three-body problem has dimension 1 (collinear) or 2 (planar).

The rotation group $\mathrm{SO}(d)$ in $\mathbb{R}^d$ has dimension $\binom{d}{2} = \frac{d(d-1)}{2}$. The Lie algebra $\mathrm{so}(d)$ consists of all anti-symmetric $d \times d$ matrices. If $Q(t)$ is a one parameter subgroup, it can be written as a matrix exponential

$$Q(t) = e^{t\alpha}, \quad \alpha \in \mathrm{so}(d).$$

From linear algebra we know that there is a rotation $S \in \mathrm{SO}(d)$ putting α into the normal form:

$$S^{-1}\alpha S = \mathrm{diag}(a_1 j, \ldots, a_k j, 0 \ldots, 0), \quad j = \begin{bmatrix} 0 & -1 \\ 1 & 0 \end{bmatrix},$$

where $a_i \in \mathbb{R}$. Then α has even rank, say $2k$. The one-parameter group satisfies

$$S^{-1}Q(t)S = \mathrm{diag}(\rho(a_1 t), \ldots, \rho(a_k t), 1, \ldots, 1), \quad \rho(\theta) = \begin{bmatrix} \cos(\theta) & -\sin(\theta) \\ \sin(\theta) & \cos(\theta) \end{bmatrix}.$$

Thus $Q(t)$ acts by rotation at different rates in k orthogonal planes while fixing the part of $\mathbb{R}^d$ orthogonal to these planes.

For example, in $\mathbb{R}^3$, an angular velocity matrix can be written

$$\alpha = \begin{bmatrix} 0 & -c & b \\ c & 0 & -a \\ -b & a & 0 \end{bmatrix}$$

and the block-diagonal normal form is

$$S^{-1}\alpha S = \begin{bmatrix} 0 & -a_1 & 0 \\ a_1 & 0 & 0 \\ 0 & 0 & 0 \end{bmatrix}, \quad a_1 = \pm\sqrt{a^2+b^2+c^2}.$$

The corresponding one-parameter group is a rotation around the angular velocity vector (a, b, c) with constant angular speed $|a_1|$.

Symmetry under rotations implies that the *angular momentum* is preserved. The angular momentum (with respect to the origin) can be represented by an anti-symmetric $d \times d$ matrix $\omega(x, v)$ with entries

$$\omega_{kl} = \sum_{j=1}^{n} m_j(x_{jk}v_{jl} - x_{jl}v_{jk}), \tag{2.7}$$

where x_{jk}, v_{jk} denote the k-th components of the vectors $x_j, y_j \in \mathbb{R}^d$. In case $d = 2$, the angular momentum reduces to a scalar ω_{12}, while if $d = 3$ it can be viewed as a vector

$$\omega = (\omega_{23}, \omega_{31}, \omega_{12}) = \sum_{j=1}^{n} m_j x_j \times v_j,$$

where $\times$ denotes the cross product in $\mathbb{R}^3$.

The Newtonian potential is homogeneous of degree -1 and its gradient is homogeneous of degree -2. It follows that if $x(t)$ is any solutions of (2.1) and if $\lambda > 0$ is constant, then $\tilde{x}(t) = \lambda^2 x(\lambda^{-3}t)$ is also a solution. This will be called the *scaling symmetry* of the n-body problem.

For any configuration x, the *moment of inertia with respect to the center of mass* is

$$I(x) = (x-c)^T M(x-c) = \sum_j m_j|x_j - c|^2, \tag{2.8}$$

where y is the corresponding centered configuration. $I(x)$ is homogeneous of degree 2 with respect to the scaling symmetry. The following alternative formula in terms of mutual distances is also useful:

$$I(x) = \frac{1}{m_0}\sum_{i<j} m_i m_j r_{ij}^2. \tag{2.9}$$

2.3 Central configurations and self-similar solutions

At this point we can define the concept which will be the main focus of the present notes.

Definition 2.3.1. *A* central configuration (CC) *for masses $m_1, \dots, m_n$ is an arrangement of the n point masses whose configuration vector satisfies*

$$\nabla U(x) + \lambda M(x - c) = 0 \tag{2.10}$$

for some real constant λ.

Multiplying (2.10) on the left by $(x-c)^T$ and using the translation invariance and homogeneity of $U(x)$ shows that

$$\lambda = \frac{U(x)}{I(x)} > 0,$$

where $I(x)$ is the moment of inertia with respect to c from (2.8). If x is a central configuration then the gravitational acceleration on the j-th body due to the other bodies is

$$\ddot{x}_j = \tfrac{1}{m_j} \nabla_j U(x) = -\lambda(x_j - c).$$

In other words, all of the accelerations are pointing towards the center of mass, c, and are proportional to the distance from c. We will see that this delicate balancing of the gravitational forces gives rise to some remarkably simple solutions of the n-body problem. Before describing some of these, we will briefly consider the question of existence of central configurations.

For given masses $m_1, \dots, m_n$, it is far from clear that (2.10) has any solutions at all. We will consider this question in due course. For now we just note the existence of symmetrical examples for equal masses. If all n masses are equal we can arrange the bodies at the vertices of a regular polygon, polyhedron or polytope. Then it follows from symmetry that the acceleration vectors of each mass must point toward the barycenter of the configuration. This is the condition for a central configuration, i.e., there will be some λ for which the CC equations hold.

In $\mathbb{R}^2$ we can put three equal masses at the vertices of an equilateral triangle or n equal masses at the vertices of a regular n-gon to get simple examples. One can also put an arbitrary mass at the center of a regular n-gon of equal masses as in Figure 2.1 (left). In $\mathbb{R}^3$ we have the five regular Platonic solids, the tetrahedron, cube, octahedron, dodecahedron and icosahedron. It is not clear what to do if $n \neq 4, 6, 8, 12, 20$, however. It turns out that there are six kinds of regular, convex four-dimensional polytopes but in higher dimensions there are only three, namely the obvious generalization of the tetrahedron, cube and octahedron [9, 16].

The regular d-simplex provides an example of a central configuration of $d+1$ equal masses in $\mathbb{R}^d$ generalizing the equilateral triangle and tetrahedron. Remarkably, these turn out to be central configurations even when the masses are not equal (see Proposition 2.8.6) so we do indeed have at least one CC for any choice of masses, provided we are willing to work in high-dimensional spaces. As a special case, note that for the two-body problem, every configuration is a regular simplex, i.e., a line segment. So every configuration of $n = 2$ bodies is a central configuration.

Less obvious examples can be found by numerically solving (2.10), for example the asymmetrical CC of 8 equal masses shown in Figure 2.1 (right).

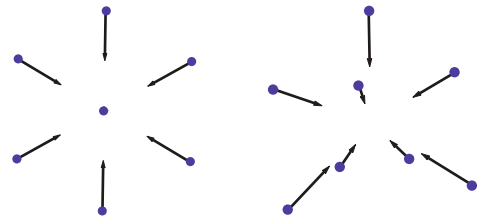

Figure 2.1: Central configurations.

Central configurations can be used to construct simple, special solutions of the n-body problem where the shape of the figure formed by the bodies remains constant. The configuration changes only by simultaneous translation, rotation and scaling. In other words, the configurations $x(t)$ at different times are all *similar*. In this case the configuration relative to the center of mass will change only by scaling and rotation.

Definition 2.3.2. *A solution of the n-body problem is* self-similar *or* homographic *if it satisfies*

$$x(t) - c(t) = r(t)Q(t)(x_0 - c_0), \tag{2.11}$$

where x_0 is a constant configuration, $r(t) > 0$ is a real scaling factor, and $Q(t) \in \mathrm{SO}(d)$ is a rotation. Here $c(t), c_0$ are the centers of mass of $x(t), x_0$.

Two special cases are the homothetic *solutions, where*

$$x(t) - c(t) = r(t)(x_0 - c_0), \tag{2.12}$$

and the rigid motions *or* relative equilibrium *solutions, where*

$$x(t) - c(t) = Q(t)(x_0 - c_0). \tag{2.13}$$

The simplest of these are the *homothetic* solutions. For example, if put three equal masses at the vertices of an equilateral triangle and release them with initial velocities all zero, it seems clear that the triangle will just collapse to the center of mass with each particle just moving on a line towards the center. It turns out that such a solution is possible only when x_0 is a central configuration.

Proposition 2.3.3. *If x_0 is a central configuration with constant λ and if $r(t)$ is any solution of the one-dimensional Kepler problem*

$$\ddot{r}(t) = -\frac{\lambda}{r(t)^2}, \tag{2.14}$$

then $x(t)$ as in (2.12) is a homothetic solution of the n-body problem, and every homothetic solution is of this form.

Proof. Substituting $x(t)$ from (2.12) into Newton's equation (2.4) gives

$$\ddot{r}(t)M(x_0 - c_0) = \nabla U(x(t)) = r(t)^{-2}\nabla U(x_0).$$

Now $\nabla U(x_0) \neq 0$ for all x_0, so this equation is satisfied if and only if there is some constant, call it $-\lambda$, such that

$$\ddot{r}(t)r(t)^2 = -\lambda, \quad -\lambda M(x_0 - c_0) = \nabla U(x_0). \qquad \square$$

The one-dimensional Kepler problem (2.14) describes the motion of a point on a line gravitationally attracted to a mass λ at the origin. It is easy to see qualitatively what will happen even without solving it. For example, the solution $r(t)$ with initial velocity $\dot{r}(0) = 0$ collapses to the origin in both forward and backward time. The corresponding homothetic solutions maintain the shape of the underlying central configuration x_0 while collapsing to a total collision at the center of mass in both forward and backward time (see Figure 2.2 for the forward-time half). Each body moves along a straight line towards the collision. From the examples of central configurations mentioned above we see that we can have homothetically collapsing solutions in the shape of an equilateral triangle, regular n-gon or regular polytope.

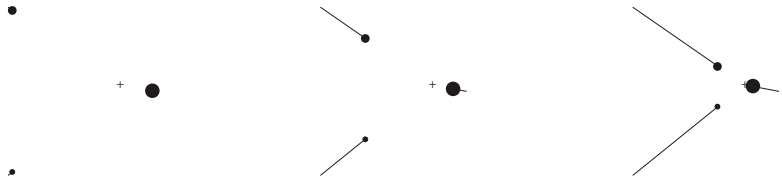

Figure 2.2: The forward-time half of a homothetic solution based on Lagrange's equilateral triangle with masses 10, 2, and 1. Released with zero velocity, the masses collapse to the center of mass (indicated by the + symbol) along straight lines, maintaining the equilateral shape.

It turns out that central configurations also lead to rigid motions and more general homographic solutions. We will postpone a general discussion of homographic solutions in $\mathbb{R}^d$ to later sections. For now we will consider the case of planar motions. Let $d = 2$ and suppose $x_0 \in \mathbb{R}^{2n}$ is a central configuration. Let

$$Q(\theta) = \begin{bmatrix} \cos(\theta) & -\sin(\theta) \\ \sin(\theta) & \cos(\theta) \end{bmatrix} \in \mathrm{SO}(2).$$

The most general planar homographic motion would be of the form

$$x(t) - c(t) = r(t)Q(\theta(t))(x_0 - c_0) \tag{2.15}$$

for some functions $r(t) > 0, \theta(t)$. Substituting this into Newton's equation leads, after some simplifications, to

$$(\ddot{r} - r\,\dot{\theta}^2)M(x_0 - c_0) + (r\,\ddot{\theta} + 2\,\dot{r}\,\dot{\theta})JM(x_0 - c_0) = r^{-2}\nabla U(x_0),$$

where J is the $2n \times 2n$ matrix

$$J = \mathrm{diag}(j, \ldots, j), \quad j = Q(\theta)^{-1}Q'(\theta) = \begin{bmatrix} 0 & -1 \\ 1 & 0 \end{bmatrix}.$$

Now $(x_0 - c_0)$ and $J(x_0 - c_0)$ are nonzero, orthogonal vectors in $\mathbb{R}^{2n}$ and the latter is also orthogonal to $\nabla U(x_0)$. Therefore, there must be some constant $-\lambda$ such that

$$\begin{aligned} \ddot{r}(t) - r(t)\dot{\theta}(t)^2 &= -\frac{\lambda}{r(t)^2}, \\ r(t)\ddot{\theta}(t) + 2\dot{r}(t)\dot{\theta}(t) &= 0, \end{aligned} \tag{2.16}$$

and

$$-\lambda M(x_0 - c_0) = \nabla U(x_0).$$

The differential equation is just the two-dimensional Kepler problem in polar coordinates whose solutions are of the familiar elliptical, parabolic or hyperbolic types and the last equation is the CC equation.

Proposition 2.3.4. *If x_0 is a planar central configuration with constant λ and if $r(t), \theta(t)$ is any solution of the two-dimensional Kepler problem* (2.16)*, then* (2.15) *is a planar homographic solution and every such solution is of this form.*

As a special case, we could take a circular solution of the Kepler problem with $r(t) = 1$. Then we get a rigid motion or relative equilibrium solution where the planar central configuration just rotates at constant angular speed around the center of mass. This is the most general relative equilibrium solution in the plane. In particular, nonuniform rotations are not possible.

In higher dimensions, the situation regarding rigid solutions and nonhomothetic homographic solutions is more complicated, mainly due to the increased complexity of the rotation group $\mathrm{SO}(d)$. The next few sections describe an approach to the general case developed by Albouy and Chenciner.

2.4 Matrix equations of motion

We will now describe an interesting reformulation of the n-body problem due to Albouy and Chenciner [2, 3, 7] which is very convenient for studying symmetric solutions. Let

$$X = \begin{bmatrix} x_1 | \cdots | x_n \end{bmatrix}, \quad V = \begin{bmatrix} v_1 | \cdots | v_n \end{bmatrix},$$

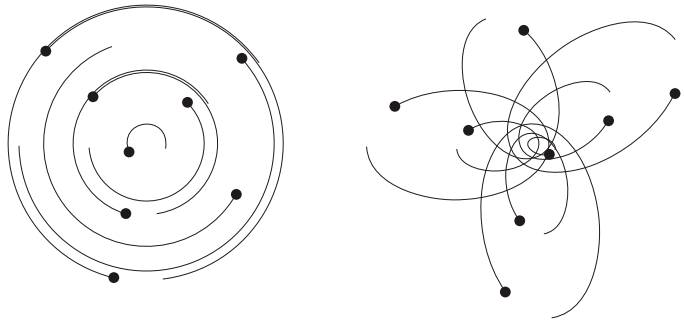

Figure 2.3: Planar homographic motions based on a central configuration of eight equal masses from Figure 2.1. On the left is a relative equilibrium solution while the solution on the right features elliptical orbits of eccentricity 0.8.

be the $d \times n$ matrix whose columns are the positions and velocities of the n bodies. For example, the matrix

$$X = \begin{bmatrix} 1 & -\frac{1}{2} & -\frac{1}{2} \\ 0 & \frac{\sqrt{3}}{2} & -\frac{\sqrt{3}}{2} \\ 0 & 0 & 0 \\ 0 & 0 & 0 \end{bmatrix} \tag{2.17}$$

represents a configuration of $n = 3$ bodies in $d = 4$ dimensions arranged at the vertices of an equilateral triangle.

We will view X, V as linear maps $X, V \colon \mathbb{R}^n \to \mathbb{R}^d$. The domain of these maps has no particular physical meaning; it is just a space of $n \times 1$ column vectors ξ with one coordinate for each of the n-bodies. We can think of the standard basis vectors $e_1, \ldots, e_n$ as representing the different bodies.

While the columns of X, V have an immediate dynamical meaning, it is not clear what to think about the rows. These are $1 \times n$ vectors which we will view as elements of the dual space $\mathbb{R}^{n*}$, another nonphysical space. For example, the first row $\begin{bmatrix} 1 & -\frac{1}{2} & -\frac{1}{2} \end{bmatrix}$ of the matrix above gives the coefficients of a linear function whose values on the basis vectors e_1, e_2, e_3 of $\mathbb{R}^3$ are the first coordinates of the three bodies in $\mathbb{R}^4$.

To get the matrix version of the laws of motion, write the j-th acceleration vector from Newton's equations (2.1) as a linear combination of the position vectors:

$$\ddot{x}_j = \frac{1}{m_j} \nabla_j U(x) = \sum_{i \neq j} \frac{m_i (x_i - x_j)}{r_{ij}^3} = \sum_{i \neq j} x_i \frac{m_i}{r_{ij}^3} - x_j \left(\sum_{i \neq j} \frac{m_i}{r_{ij}^3} \right).$$

So we get the matrix equation:

$$\ddot{X} = XA(X), \tag{2.18}$$

where $A(X)$ is the $n \times n$ matrix

$$A(X) = \begin{bmatrix} A_{11} & \frac{m_1}{r_{12}^3} & \cdots & \frac{m_1}{r_{1n}^3} \\ \frac{m_2}{r_{12}^3} & A_{22} & \cdots & \frac{m_2}{r_{2n}^3} \\ \vdots & & & \vdots \\ \frac{m_n}{r_{1n}^3} & \frac{m_n}{r_{2n}^3} & \cdots & A_{nn} \end{bmatrix}, \quad A_{jj} = -\sum_{i \neq j} A_{ij} = -\sum_{i \neq j} \frac{m_i}{r_{ij}^3}. \tag{2.19}$$

Note that $A(X)$ is invariant under translations and rotations, since it involves only the mutual distances. It is independent of the space dimension d. For example, consider the three-body problem in $\mathbb{R}^d$ where we have the 3×3 matrix

$$A = \begin{bmatrix} -\frac{m_2}{r_{12}^3} - \frac{m_3}{r_{13}^3} & \frac{m_1}{r_{12}^3} & \frac{m_1}{r_{13}^3} \\ \frac{m_2}{r_{12}^3} & -\frac{m_1}{r_{12}^3} - \frac{m_3}{r_{23}^3} & \frac{m_2}{r_{23}^3} \\ \frac{m_3}{r_{13}^3} & \frac{m_3}{r_{23}^3} & -\frac{m_1}{r_{13}^3} - \frac{m_2}{r_{23}^3} \end{bmatrix}.$$

$A(X)$ has some other useful properties. Let $M = \operatorname{diag}(m_1, \ldots, m_n)$ be an $n \times n$ version of the mass matrix. Then we have

$$XA(X)M = \begin{bmatrix} \nabla_1 U(X) & \cdots & \nabla_n U(X) \end{bmatrix}.$$

In addition, $A(X)M$ is symmetric:

$$AM = (AM)^T = MA^T.$$

Finally, $A(X)M$ is negative semi-definite. Indeed, for any $\xi \in \mathbb{R}^n$ one can check that

$$\xi^T AM \xi = -\sum_{i<j} \frac{m_i m_j}{r_{ij}^3} (\xi_i - \xi_j)^2.$$

We will also need a matrix version of the first-order differential equations of the n-body problem:

$$\begin{aligned} \dot{X} &= V, \\ \dot{V} &= XA(X). \end{aligned} \tag{2.20}$$

The $d \times 2n$ matrix $Z = \begin{bmatrix} X & V \end{bmatrix}$ will be called the *state matrix*.

It is interesting to look at the symmetries and integrals of the n-body problem from the matrix point of view. Let $k \in \mathbb{R}^d$ be a $d \times 1$ column vector. The translation $x_j \mapsto x_j + k$ has the effect of adding $k_i L$ to the i-th row of X, where

$$L = \begin{bmatrix} 1 & \cdots & 1 \end{bmatrix} \in \mathbb{R}^{n*}$$

is the $1 \times n$ row vector of 1's. In other words the configuration matrix transforms by addition of the $d \times n$ matrix kL,

$$X \mapsto X + kL. \tag{2.21}$$

We call two $d \times n$ matrices X, Y *translation equivalent* if $Y = X + kL$ for some $k \in \mathbb{R}^d$. If X, Y are translation equivalent then the corresponding linear maps $X, Y \colon \mathbb{R}^n \to \mathbb{R}^d$ take the same values when restricted to the hyperplane

$$\mathcal{D}^* = L^\perp = \{\xi \in \mathbb{R}^n : L\xi = \xi_1 + \cdots + \xi_n = 0\}.$$

The converse also holds so translation equivalence amounts to saying that

$$X|_{\mathcal{D}^*} = Y|_{\mathcal{D}^*}.$$

The notation $\mathcal{D}^*$, due to Albouy–Chenciner [3], is explained as follows. The quotient vector space $\mathbb{R}^{n^*}/L$ is called the *disposition space* and denoted by $\mathcal{D}$. Then $L^\perp$ can be identified with its dual vector space.

With this notation, the total mass and center of mass can be written

$$m_0 = Lm, \quad c = \frac{1}{m_0} Xm, \tag{2.22}$$

where m is the $n \times 1$ column vector

$$m = \begin{bmatrix} m_1 & \cdots & m_n \end{bmatrix}^T.$$

A state will have center of mass at the origin and total momentum zero if

$$Xm = Vm = 0.$$

We will call a $d \times n$ matrix X *centered* if $Xm = 0$.

Proposition 2.4.1. *Given a $d \times n$ matrix X, there is a unique centered matrix Y translation equivalent to X, namely*

$$Y = X - C, \quad C = cL,$$

where c is the center of mass (2.22)*. Moreover,*

$$Y = XP, \quad P = I - \frac{1}{m_0} mL.$$

The $n \times n$ matrix P represents the orthogonal projection of $\mathbb{R}^n$ onto the hyperplane $\mathcal{D}^*$ with respect to the inverse mass inner product *on $\mathbb{R}^n$.*

Proof. Let $Y = X - cL$. Then Y is translation equivalent to X and is centered if and only if c is given by (2.22). In this case it is easy to check that $Y = XP$ where P is as claimed. We have

$$P^2 = P, \quad LP = 0.$$

Hence, the linear map $P\colon \mathbb{R}^n \to \mathbb{R}^n$ is a projection map of $\mathbb{R}^n$ onto $\mathcal{D}^*$. One can also check that P is an M^{-1}-symmetric matrix:

$$P^T M^{-1} = M^{-1} P,$$

where M is the mass matrix. It follows that P represents the orthogonal projection onto $\mathcal{D}^*$ with respect to the inner product $\langle \xi, \eta \rangle = \xi^T M^{-1} \eta$. □

If the matrices $X(t), V(t)$ solve Newton's equations (2.20) so do the centered matrices

$$Y(t) = X(t) - C(t) = X(t)P, \quad W(t) = V(t)P$$

which describe the dynamics relative to the center of mass. This was shown already in Section 2.2 but it can also be verified directly from (2.20) with the help of the following easily verified formula:

$$A(X) = A(XP) = A(X - C) = A(X)P = PA(X). \tag{2.23}$$

The following facts about the right-hand side of Newton's equation are also useful

$$CA(X) = 0, \quad XA(X) = (X - C)A(X - C). \tag{2.24}$$

We will use the matrix formulation to study central configurations and homographic solutions in $\mathbb{R}^d$. The factorization (2.18) of the equations of motion is very useful for understanding symmetrical solutions. The CC equation (2.10) for configuration vectors gives the following equation for configuration matrices:

$$XA(X) + \lambda(X - C) = 0. \tag{2.25}$$

2.5 Homographic motions of central configurations in $\mathbb{R}^d$

We have already defined homographic, homothetic and rigid solutions. The configuration matrix of a homographic solution will satisfy

$$X(t) - C(t) = r(t)Q(t)(X_0 - C_0). \tag{2.26}$$

Homothetic and rigid solutions are of the same form but with $Q(t) = I$ and $r(t) = 1$, respectively.

We have seen in Proposition 2.3.3 that every homothetic motion comes from a CC, x_0, with $r(t)$ a solution of the one-dimensional Kepler problem. Also, Proposition 2.3.4 shows that planar CC's can execute Keplerian homographic motions. The next result treats *Keplerian homographic motions* of central configurations in $\mathbb{R}^d$.

Proposition 2.5.1. *Let X_0 be the configuration matrix of a central configuration with constant λ and let $\mathcal{C}(x_0) = \mathrm{im}(X_0 - C_0)$ be its centered position subspace. Suppose there is an antisymmetric $d \times d$ matrix J such that $J^2|_{\mathcal{C}} = -I|_{\mathcal{C}}$. Then for any solution $r(t), \theta(t)$ of the planar Kepler problem* (2.16) *there is a homographic solution of the form* (2.26) *with*

$$Q(t) = \exp(\theta(t)J).$$

Proof. Since X_0 is a CC, the right-hand side of (2.18) is

$$rQ(X_0 - C_0)A(rQ(X_0 - C_0)) = r^{-2}QX_0A(X_0) = -\frac{\lambda}{r^2}Q(X_0 - C_0),$$

where we have used the homogeneity and the translation and rotation invariance of A. The left-hand side is

$$\ddot{X} = \ddot{r}Q(X_0 - C_0) + 2\dot{r}\dot{Q}(X_0 - C_0) + r\ddot{Q}(X_0 - C_0).$$

We have

$$\dot{Q} = \dot{\theta}(t)JQ, \quad \ddot{Q}(t) = \ddot{\theta}(t)JQ + (\dot{\theta}(t))^2J^2Q.$$

Since J and Q commute and $J^2(X_0 - C_0) = -(X_0 - C_0)$, we get

$$\ddot{X} = (\ddot{r} - r(\dot{\theta})^2)Q(X_0 - C_0) + (r\ddot{\theta} + 2\dot{r}\dot{\theta})QJ(X_0 - C_0).$$

Since $r(t), \theta(t)$ are solutions of the Kepler problem, this reduces to

$$\ddot{X} = -\frac{\lambda}{r^2}Q(X_0 - C_0)$$

as required. □

Recall that a *complex structure* on a vector space $\mathcal{S}$ is given by a linear map $J\colon \mathcal{S} \to \mathcal{S}$ with $J^2 = -I$. If there is an inner product with respect to which J is antisymmetric then we have a *Hermitian structure*. An antisymmetric matrix J as above with $J^2|_{\mathcal{C}} = -I_{\mathcal{C}}$ determines a Hermitian structure on the larger space

$$\mathcal{S} = \mathcal{C} + J\mathcal{C}.$$

To see this, note that $\mathcal{S}$ is J-invariant. If $\eta \in J\mathcal{C}$ then $\eta = J\xi$ for some $\xi \in \mathcal{C}$ and we get

$$J^2\eta = J^3\xi = J(-\xi) = -\eta.$$

Thus, we actually have

$$J^2|_{\mathcal{S}} = -I\,|_{\mathcal{S}}.$$

Since J is antisymmetric, it has even rank and so $\dim \mathcal{S}$ must be even. In the proposition, $\mathcal{S}$ is the motion space of the Keplerian homographic motion.

Thus a necessary condition that a CC x_0 admits a matrix J as above is that $\mathcal{C}(x_0)$ be contained in an even dimensional subspace of $\mathbb{R}^d$. Since any even-dimensional subspace of the Euclidean space $\mathbb{R}^d$ has a natural Hermitian structure where J is rotation by $\pi/2$ in k mutually orthogonal planes, this condition is also sufficient. This will always be possible if either d is even or $\dim \mathcal{C} < d$. The only bad case is when $d = \dim \mathcal{C}$ is odd. For example, if we have a collinear central configuration in $\mathbb{R}^1$ or a nonplanar configuration in $\mathbb{R}^3$, we will not be able to find such an even-dimensional subspace.

Example 2.5.2. Consider the equilateral triangle in $\mathbb{R}^4$ whose configuration matrix X is given by (2.17). Then $\dim \mathcal{C} = \operatorname{rank} X = 2$. We could choose J to be a rotation by $\pi/2$ in the plane $\mathcal{C}$ which fixes the orthogonal complement. Then the motion space is also $\mathcal{S} = \mathcal{C}$ and the triangle rotates rigidly in its own plane.

On the other hand we could choose

$$J = \begin{bmatrix} 0 & 0 & -1 & 0 \\ 1 & 0 & 0 & 0 \\ 0 & 0 & 0 & -1 \\ 0 & 1 & 0 & 0 \end{bmatrix}.$$

Now the motion space will be $\mathcal{S} = \mathbb{R}^4$. Each body moves in a planar Keplerian orbit, but the orbits are in different planes. Indeed, we have

$$X(t) = r(t)\cos\theta(t) \begin{bmatrix} 1 & -\frac{1}{2} & -\frac{1}{2} \\ 0 & \frac{\sqrt{3}}{2} & -\frac{\sqrt{3}}{2} \\ 0 & 0 & 0 \\ 0 & 0 & 0 \end{bmatrix} + r(t)\sin\theta(t) \begin{bmatrix} 0 & 0 & 0 \\ 0 & 0 & 0 \\ 1 & -\frac{1}{2} & -\frac{1}{2} \\ 0 & \frac{\sqrt{3}}{2} & -\frac{\sqrt{3}}{2} \end{bmatrix}.$$

The i-th body moves in the plane spanned by the i-th columns in the two matrices.

On the other hand a regular tetrahedron in $\mathbb{R}^3$ is not contained in any even-dimensional subspace. But if we put it in $\mathbb{R}^4$ we can choose any 4×4 matrix J with $J^2 = -I$, such as the one in the last paragraph, and proceed to construct Keplerian homographic motions. Figure 2.4 shows a projection of such a motion onto the first three coordinate axes. Each body moves on a circular orbit at constant speed, but the circles are in different planes. In this projection the circles look like ellipses on a vertical cylinder. Initially, the projected shape is a regular tetrahedron as in the figure but later the projected bodies will form a square in the horizontal plane. Of course it is still a regular tetrahedron in $\mathbb{R}^4$.

Note that, on the centered position space $\mathcal{C}(X_0)$, the matrix exponential in Proposition 2.5.1 can be written

$$Q(t) = \exp(\theta(t)J) = \cos\theta(t)I + \sin\theta(t)J.$$

It follows that, for a Keplerian homographic solution as in the proposition, the j-th body moves in the two-dimensional plane spanned by the vectors x_{j_0}, Jx_{j_0}. All of

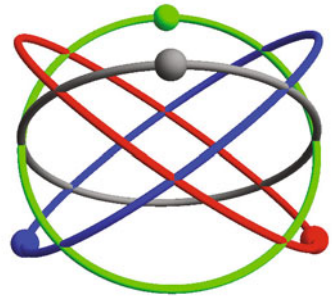

Figure 2.4: Three-dimensional projection of a rigid motion of a central configuration in $\mathbb{R}^4$. Four equal masses are at the vertices of a regular tetrahedron. Each body moves on a circle in $\mathbb{R}^4$ but the circles are in different planes. In the projection, the circles become ellipses.

the bodies describe similar Keplerian orbits and the overall configuration remains similar to the CC X_0 throughout the motion. In particular, for each admissible choice of J we get a family of periodic solutions with elliptical orbits of different eccentricities. Eccentricity zero gives the uniform rigid motions and eccentricity one gives the homothetic solutions.

2.6 Albouy–Chenciner reduction and relative equilibria in $\mathbb{R}^d$

The matrix formulation of Newton's equations leads to an elegant way to reduce by the rotational symmetry. The reduced equations lead to a deeper understanding of the most general rigid and homographic motions. This section is based on the works Albouy–Chenciner [3] and Chenciner [7]. The Albouy–Chenciner method of reducing the equations of motion is a far-reaching generalization of Lagrange's reduction method for the three-body problem [15].

Starting from the matrix equations of motion (2.20), we can eliminate the rotational symmetry of the n-body problem by passing to Gram matrices.

$$B(X) = X^T X, \quad C(X,V) = X^T V, \quad D(V) = V^T V.$$

The entries of these matrices are the dot products of the position and velocity vectors:

$$B_{ij} = x_i \cdot x_j, \quad C_{ij} = x_i \cdot v_j, \quad D_{ij} = v_i \cdot v_j.$$

It follows that the matrices are invariant under simultaneous rotation of all positions and velocities in $\mathbb{R}^d$. In other words, if $Q \in \mathrm{SO}(d)$ is any rotation matrix

then

$$B(QX) = B(X), \quad C(QX, QV) = C(X, V), \quad D(QV) = D(V).$$

Note also that $B(X), D(V)$ are symmetric and positive semi-definite.

To eliminate the translational symmetry we can work with the centered matrices $Y = X - C = XP$ and $W = VP$.

Definition 2.6.1. *Given configuration and velocity matrices X and V, $B(XP) = B(X - C)$ is the* relative configuration *matrix and $B(XP)$, $C(XP, VP)$, $D(VP)$ are the* relative state *matrices. If $X(t), V(t)$ is a solution, we will write $B(t)$, $C(t)$ and $D(t)$ for the corresponding relative state matrices.*

An alternative approach to eliminating the center of mass is just to view all of these matrices as representations of bilinear forms on the hyperplane $\mathcal{D}^*$. In other words, only the values $\xi^T B \eta$ for $\xi, \eta \in \mathcal{D}^*$ are significant. Let's call two $n \times n$ matrices *translation equivalent* if they define the same bilinear form on $\mathcal{D}^*$. Then, for example, $B(X) = X^T X$ and $B(X - C) = (X - C)^T (X - C)$ are translation equivalent. In fact any matrix obtained from B by adding multiples of L to the rows and multiples of L^T to the columns will be translation equivalent. Starting from $B(X)$ we get a particularly simple representative by adding subtracting $\frac{1}{2}|x_i|^2 L$ from the i-th row and $\frac{1}{2}|x_j|^2 L$ column. The diagonal entries of the new matrix are 0 and the off diagonals are

$$x_i^T x_j - \frac{1}{2}|x_i|^2 - \frac{1}{2}|x_j|^2 = -\frac{1}{2}|x_i - x_j|^2 = -\frac{1}{2} r_{ij}^2.$$

Thus the following matrix is translation equivalent to $B(X)$ and $B(X - C)$:

$$\hat{B}(X) = -\frac{1}{2} \begin{bmatrix} 0 & r_{12}^2 & \cdots & r_{1n}^2 \\ r_{21}^2 & 0 & \cdots & r_{2n}^2 \\ \vdots & & & \vdots \\ r_{n1}^2 & \cdots & r_{n(n-1)}^2 & 0 \end{bmatrix}. \tag{2.27}$$

Using (2.20) it is easy to derive differential equations for the matrices B, C, D. One finds

$$\begin{aligned} \dot{B} &= C + C^T, \\ \dot{C} &= D + BA, \\ \dot{D} &= C^T A + A^T C. \end{aligned} \tag{2.28}$$

These apply equally to the original Gram matrices $B(X), C(X, V), D(V)$ and to the translation reduced versions.

Recall that $A(X) = A(X - C)$ depends only on the mutual distances r_{ij}. The mutual distances can be expressed in terms of the Gram matrix B, since

$$r_{ij}^2 = |x_i - x_j|^2 = |x_i|^2 + |x_j|^2 - 2x_i \cdot x_j = B_{ii} + B_{jj} - 2B_{ij}.$$

Hence we can view A as a function $A(B)$. Then the system (2.28) could be used to find the time evolution of the relative state matrices B, C, D without reference to the actual state variables X, V.

The angular momentum is equivariant with respect to rotations

$$\omega(QX, QV) = Q\omega(X, V)Q^T = Q\omega(X, V)Q^{-1},$$

for $Q \in \mathrm{SO}(d)$. The eigenvalues of $\omega(X, V)$ are rotation invariant and provide constants of motion for the relative equations.

At this point we can write down the reduced version of the CC equation.

Proposition 2.6.2. *Let X be a $d \times n$ configuration matrix. Then X is a CC with constant λ if and only if the relative configuration matrix $B(X - C)$ satisfies*

$$BA(B) + \lambda B = 0. \tag{2.29}$$

Proof. By hypothesis, we have $XA(X) + \lambda(X - C) = 0$. Multiplying by $(X - C)^T$ and using the translation and rotation invariance of A, we get (2.29). Conversely, if (2.29) holds we get

$$(X - C)^T \left(XA(X) + \lambda(X - C)\right) = 0.$$

To eliminate $(X - C)^T$ note that the matrix in parentheses has range contained in $\mathrm{im}(X - C)$. Since $\mathrm{im}(X - C) \cap \ker(X - C)^T = \{0\}$, it must vanish. □

Next we will use the reduced equations to study general rigid motions of the n-body problem. For a rigid motion we have

$$X(t) - C(t) = Q(t)(X_0 - C_0) \tag{2.30}$$

for some $Q(t) \in \mathrm{SO}(d)$, and the relative configuration matrix

$$B(t) = B(X - C)$$

is constant. Conversely, if $B(t)$ is constant then all of the mutual distances are constant and (2.30) holds for some $Q(t) \in \mathrm{SO}(d)$. Thus rigid motions are characterized by the constancy of $B(t)$. It turns out that the other relative state matrices are also constant, so we have an equilibrium point of (2.28).

Proposition 2.6.3. *$X(t), V(t)$ are the state matrices of a rigid motion solution of the n-body problem in $\mathbb{R}^d$ if and only if the relative state matrices $B(t), C(t), D(t)$ are constant.*

Proof. We have seen that $X(t), V(t)$ is a rigid motion if and only if $B(t)$ is constant. It remains to show that the constancy of B implies that of C and D. Assuming $\dot{B} = 0$ we also get $\dot{A} = A(\dot{B}) = 0$. Now use (2.28) to calculate the derivatives of $B(t)$:

$$\begin{aligned}
\dot{B} &= C + C^T = 0,\\
\ddot{B} &= \dot{C} + \dot{C}^T = 2D + BA + A^T B = 0,\\
\dddot{B} &= 2\dot{D} = 2(C^T A + A^T C) = 0.
\end{aligned}$$

So we have $\dot{D} = 0$ and also find that $2D = -(BA + A^T B)$ which implies

$$\dot{C} = \frac{1}{2}(A^T B - BA).$$

We need to show that this vanishes. Computing one more derivative gives

$$\dddot{B} = 2(\dot{C}^T A + A^T \dot{C}) = (A^T B - BA)A - A^T(A^T B - BA) = 0.$$

It turns out that this equation can hold only when the quantity in parentheses is already zero.

To see this we use the fact that AM is a symmetric matrix so $AM = MA^T$. We have

$$M(A^T B - BA) = MA^T B - MBA = A^T MB - MBA = -[MB, A],$$

the commutator of MB and A. Similarly,

$$M\left((A^T B - BA)A - A^T(A^T B - BA)\right) = -[[MB, A], A].$$

Now the symmetry of AM also gives $A^T M^{-1} = M^{-1}A$, i.e., A is M^{-1}-symmetric. This implies that A is diagonalizable with respect to some M^{-1} orthogonal basis. Choose such a basis and let the matrix representing A be $\mathrm{diag}(a_1, \ldots, a_n)$ and that representing MB have entries b'_{ij}. Then the entries of $[MB, A]$ and $[[MB, A], A]$ are

$$b'_{ij}(a_i - a_j), \quad b'_{ij}(a_i - a_j)^2,$$

respectively. Thus $[[MB, A], A] = 0$ if and only if $[MB, A] = 0$ as claimed. Hence, $\dddot{B} = 0$ implies $\dot{C} = 0$ completing the proof. □

This result justifies the terminology *relative equilibrium solution (RE)* applied to rigid motion solutions. We really do have an equilibrium of the relative equations of motion (2.28). We have seen how to construct a uniformly rotating relative equilibrium solution based on a central configuration. But it is not at all clear that this is the only kind and, indeed, we will see that rotations of certain noncentral configurations are possible. However, it is true that every rigid motion is a uniform rotation.

Proposition 2.6.4. *Let $X(t), V(t)$ be any rigid motion (RE) solution. Then there is a configuration matrix X_0 (not necessarily central) and a constant antisymmetric $d \times d$ matrix α such that*

$$X(t) - C(t) = Q(t)(X_0 - C_0),$$

where $Q(t) = \exp(t\alpha)$.

We will call α the *angular velocity matrix*. The proof uses the following fact from linear algebra.

Lemma 2.6.5. *Let L_1, L_2 be $d \times k$ matrices such that $\ker L_1 \subset \ker L_2$. Then there is a $d \times d$ matrix J such that*

$$L_2 = JL_1.$$

Moreover, if $\operatorname{im} L_2 \subset \operatorname{im} L_1$ and if the $k \times k$ matrix $L_1^T L_2$ is symmetric (antisymmetric), then J can be chosen to be symmetric (antisymmetric).

Proof. The hypothesis about the kernels implies that we get a well-defined linear map $\operatorname{im} L_1 \to \mathbb{R}^d$ by setting $J\xi = L_2 u$ when $L_1 u = \xi$. We can extend it to $J\colon \mathbb{R}^d \to \mathbb{R}^d$ by making it vanish on the Euclidean orthogonal complement $(\operatorname{im} L_1)^\perp$ and this choice makes the extension unique.

If $\operatorname{im} L_2 \subset \operatorname{im} L_1$ then $J(\operatorname{im} L_1) \subset \operatorname{im} L_1$. Let ξ, η be two vectors in $\operatorname{im} L_1$ and write $\xi = L_1 u, \eta = L_1 v$. Then, by definition of J,

$$\xi^T J \eta = u^T L_1^T L_2 v.$$

If $L_1^T L_2$ is symmetric (antisymmetric), this shows that the restriction of J to $\operatorname{im} L_1$ is also symmetric (antisymmetric). Since we extended trivially on the orthogonal complement, it is easy to see that the extension has the same symmetry. □

Proof of Proposition 2.6.4. Let $Z(t) = \begin{bmatrix} X(t)P & V(t)P \end{bmatrix} = \begin{bmatrix} Y(t) & W(t) \end{bmatrix}$ be the $d \times 2n$ centered state matrix and note that the $2n \times 2n$ Gram matrix

$$Z^T Z = \begin{bmatrix} B & C^T \\ C & D \end{bmatrix}$$

encodes the relative state matrices B, C, D. For a RE solution this matrix is constant so

$$Z^T \dot{Z} + \dot{Z}^T Z = 0.$$

In other words, the $2n \times 2n$ matrix

$$Z(t)^T \dot{Z}(t)$$

is antisymmetric. Now apply Lemma 2.6.5 with $L_1 = Z(t)$ and $L_2 = \dot{Z}(t)$ to get an antisymmetric $d \times d$ matrix $\alpha(t)$ such that $\dot{Z}(t) = \alpha(t) Z(t)$, i.e.,

$$\dot{Y}(t) = \alpha(t) Y(t), \quad \dot{W}(t) = \alpha(t) W(t).$$

In particular, at $t = 0$, we have

$$\dot{Y}(0) = W_0 = \alpha_0 Y_0, \quad \dot{W}(0) = Y_0 A(Y_0) = \alpha_0 W_0 = \alpha_0^2 Y_0. \tag{2.31}$$

To complete the proof, we will show

$$Y(t) = Q(t) Y_0, \quad Q(t) = \exp(t\alpha_0).$$

Since this function has the right initial conditions, we need only to show that it is a solution of Newton's equations. We have

$$\ddot{Y}(t) = \alpha_0^2 Y(t),$$

so we need to show that

$$\alpha_0^2 Y(t) = Y(t)A(Y(t)). \tag{2.32}$$

From (2.31) we have

$$\alpha_0^2 Y_0 = Y_0 A(Y_0) \tag{2.33}$$

so (2.36) holds when $t = 0$. It follows for other times by multiplying by $Q(t)$ and using the rotation invariance of A. □

It follows from this result that if X_0 is a CC, then the most general possible rigid motions with shape X_0 are the circular Keplerian ones from Proposition 2.5.1. Comparing the antisymmetric matrices which appear in the two propositions, we should have $t\alpha = \theta(t)J$. Now for the circular Kepler orbit of radius $r = 1$ we have $\dot{\theta}^2 = \lambda$. With

$$\alpha = \pm\sqrt{\lambda}\, J \tag{2.34}$$

then one can check that, for the solution of Proposition 2.5.1, $\dot{Z} = \alpha Z$ holds.

The formulas in the last proof suggest a way to construct rigid motions whose configurations are not central. The condition (2.33) is enough to guarantee that a corresponding rigid solution exists.

Definition 2.6.6. *A configuration x is* balanced in $\mathbb{R}^d$ *or* d-balanced *if there is a $d \times d$ antisymmetric matrix α such that*

$$XA(X) - \alpha^2(X - C) = 0 \tag{2.35}$$

or, equivalently, if

$$\nabla_j U(x) - \alpha^2 M(x_j - c) = 0. \tag{2.36}$$

It is called balanced *if it is d-balanced for d sufficiently large.*

The definition of balanced configurations in [3] is equivalent to the one given here. The proof of Proposition 2.6.4 shows that every balanced configuration gives rise to a uniformly rotating relative equilibrium solution (2.30), with $Q(t) = \exp(t\alpha)$ in the appropriate ambient space $\mathbb{R}^d$. From (2.34) we see that every central configuration is balanced provided it is contained in an even-dimensional subspace hence, certainly, in $\mathbb{R}^d$ or in $\mathbb{R}^{d+1}$. However, there exist balanced configurations which are not central.

Before presenting an example we will derive a couple of equivalent versions of the concept of balance. Note that if X is balanced then the matrix $S = -\alpha^2$ is symmetric and positive semi-definite.

Proposition 2.6.7. *A configuration is balanced if and only if its configuration matrix satisfies*

$$XA(X) + S(X - C) = 0 \tag{2.37}$$

for some positive semi-definite matrix S. Equivalently, the relative configuration matrix $B(X - C)$ should satisfy

$$BA = (BA)^T. \tag{2.38}$$

Proof. If X is balanced in $\mathbb{R}^d$ then (2.37) holds with $S = -\alpha^2$. Conversely suppose (2.37) holds for a configuration in $\mathbb{R}^d$. If we double the dimension of the space, padding X with rows of zeros and replace S by the $2d \times 2d$ matrix $\hat{S} = \operatorname{diag}(S, S)$, then we can solve the equation $\hat{S} = -\alpha^2$ for the antisymmetric matrix α. To see this, assume without loss of generality that $\hat{S} = \operatorname{diag}(\sigma_1^2, \ldots, \sigma_d^2, \sigma_1^2, \ldots, \sigma_d^2)$. Then we can use the block matrix

$$\alpha = \begin{bmatrix} 0 & -\sigma \\ \sigma & 0 \end{bmatrix} \qquad \sigma = \operatorname{diag}(\sigma_1, \ldots, \sigma_d).$$

Thus, if X satisfies (2.37), it will give rise to a rigid motion in $\mathbb{R}^{2d}$, i.e., it will be $2d$-balanced.

Multiplying (2.37) by $(X-C)^T$ and using (2.24) shows that BA is symmetric. Conversely, suppose $BA = (X - C)^T(X - C)A(X)$ is symmetric. Using Lemma 2.6.5 with $L_1 = X - C$ and $L_2 = (X - C)A(X)$ gives a symmetric $d \times d$ matrix $-S$ with

$$(X - C)A(X) = -S(X - C),$$

as required. □

In the following example we will use (2.38) to check for balance. Moreover, we can avoid explicitly shifting the center of mass by just requiring $BA = (BA)^T$ on $\mathcal{D}^*$.

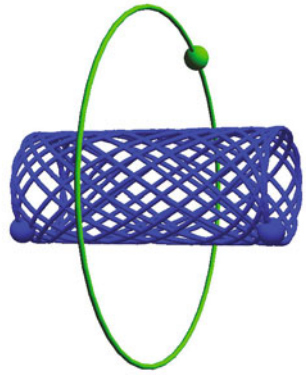

Figure 2.5: Three-dimensional projection of a rigid motion of a balanced configuration in $\mathbb{R}^4$. An isosceles triangle with edges $1, \sqrt{3}/2, \sqrt{3}/2$ and masses $1, 1, (\sqrt{5} - 1)/2$ is rotating with different frequencies in two orthogonal planes in $\mathbb{R}^4$. The mass on the symmetry axis is in one of the planes and moves on a circle while the other two masses move on a torus.

Example 2.6.8. Consider a triangle with sides $r_{12} = r$, $r_{13} = s$, $r_{23} = t$. We will investigate the *inverse problem*: given a configuration, find which masses make it balanced or central. We have

$$A(X) = \begin{bmatrix} -\frac{m_2}{r^3} - \frac{m_3}{s^3} & \frac{m_1}{r^3} & \frac{m_1}{s^3} \\ \frac{m_2}{r^3} & -\frac{m_1}{r^3} - \frac{m_3}{t^3} & \frac{m_2}{t^3} \\ \frac{m_3}{s^3} & \frac{m_3}{t^3} & -\frac{m_1}{s^3} - \frac{m_2}{t^3} \end{bmatrix}$$

and

$$\hat{B}(X) = -\frac{1}{2}\begin{bmatrix} 0 & r^2 & s^2 \\ r^2 & 0 & t^2 \\ s^2 & t^2 & 0 \end{bmatrix}.$$

The condition for a balanced triangle is that the restriction of BA to $\mathcal{D}^*$ be symmetric. To avoid explicitly shifting the center of mass, we calculate the commutator $\hat{B}A - A^T\hat{B}$ and require that $e_i^T(BA - AB)e_j = 0$ for some basis e_1, e_2 of the plane $\mathcal{D}^*$; for example, we could use $e_1 = (1, -1, 0), e_2 = (1, 0, -1)$. The result is a 2×2 antisymmetric matrix so there is only one equation which turns out to be

$$\begin{aligned} m_1(s^{-3} - r^{-3})(t^2 - r^2 - s^2) + m_2(r^{-3} - t^{-3})(s^2 - r^2 - t^2) \\ + m_3(t^{-3} - s^{-3})(r^2 - s^2 - t^2) = 0. \end{aligned} \tag{2.39}$$

For the equilateral triangle $r = s = t$ the equation is trivial, so the triangle is balanced for all choices of the masses. Of course we already knew this since it is a CC for all masses (and is even-dimensional). For any nonequilateral triangle (2.39) gives a two-dimensional plane of masses. This plane always intersects the positive octant, so every triangle is balanced for some two-dimensional cone of masses. For example, the isosceles triangle with $(r, s, t) = (r, s, s)$ is balanced for all mass vectors with $m_1 = m_2$ and arbitrary m_3. On the other hand, the right triangle with $(r, s, t) = (3, 4, 5)$ is balanced for $183m_2 = 392m_3$ with m_1 (the mass at the right angle) arbitrary. Since the only non-collinear CC is the equilateral triangle, there are plenty of triangles which are balanced but not central.

To investigate the possible rigid motions of such triangles we need to work with configuration matrices X and find the corresponding antisymmetric angular velocity matrices, α. For the isosceles case in $\mathbb{R}^2$ we can take

$$X = \begin{bmatrix} 0 & 0 & x \\ y & -y & 0 \end{bmatrix}$$

and in $\mathbb{R}^d$ we can just add rows of zeros. With masses $m_1 = m_2 = 1$ we find that

$$XA(X) + S(X - C) = 0, \quad S = \operatorname{diag}\left(\frac{2 + m_3}{s^3}, \frac{1}{4y^3} + \frac{m_3}{s^3}\right), \quad s = \sqrt{x^2 + y^2}.$$

We need a $d \times d$ antisymmetric matrix with $\alpha^2 = -S$. This is only possible in $\mathbb{R}^2$ when $S = \lambda I$, that is, only for the equilateral CC case. In the nonequilateral

case with $d = 4$ the only valid angular velocity matrices are the block-diagonal matrices

$$J = \begin{bmatrix} 0 & -\sigma \\ \sigma & 0 \end{bmatrix}, \quad \sigma = \operatorname{diag}(\sigma_1, \sigma_2), \quad \sigma_1^2 = \frac{2 + m_3}{s^3}, \quad \sigma_2^2 = \frac{1}{4y^3} + \frac{m_3}{s^3}.$$

The isosceles triangle rotates around its symmetry axis and simultaneously around an orthogonal axis with two different frequencies, the two planes of rotation being orthogonal. The motion of the mass on the symmetry axis is planar and periodic but the other two masses move on a torus which spans $\mathbb{R}^4$ (see Figure 2.5). For fixed $m_3 > 0$ one can check that the eigenvalue ratio σ_2^2/σ_1^2 of S varies over $((1 + 4m_3)/(8 + 4m_3), \infty)$ as the angle at m_3 of the isosceles shape decreases from π to 0.

2.7 Homographic motions in $\mathbb{R}^d$

Next we will show that the orbits described in Proposition 2.5.1 are actually the most general, *nonrigid* homographic motions. In particular, only central configurations give rise to such motions.

Proposition 2.7.1. *Every nonrigid homographic solution of the n-body problem in $\mathbb{R}^d$ is of the form*

$$X(t) - C(t) = r(t)Q(t)(X_0 - C_0), \quad Q(t) = \exp(\theta(t)J),$$

where X_0 is a central configuration with constant λ, $(r(t), \theta(t))$ is a solution of the Kepler problem (2.16)*, and J is an antisymmetric $d \times d$ matrix with $J^2|_{\mathcal{C}(X_0)} = -I|_{\mathcal{C}(X_0)}$.*

Proof following [7]. Since the motion is homographic, the right-hand side of equation (2.18) is

$$X(t)A(X(t)) = r(t)^{-3}X(t)A(X_0).$$

The fact that the $n \times n$ matrix $A(X_0)$ is M^{-1}-symmetric implies that it is diagonalizable. One of the eigenvalues is zero since the mass vector m is in the kernel, and the others are nonpositive because of the negative semi-definiteness of AM. Let R be an invertible $n \times n$ matrix with

$$R^{-1}A(X_0)R = \operatorname{diag}(-\lambda_1, -\lambda_2, \ldots, -\lambda_n).$$

If $W(t) = (X(t) - C(t))R$ then Newton's equations give

$$\ddot{W} = r(t)^{-3}X(t)A(X_0)R = r(t)^{-3}W(t)R^{-1}A(X_0)R$$

and so the columns $w_j(t)$ of $W(t)$ satisfy

$$\ddot{w}_j(t) = -\frac{\lambda_j w_j(t)}{r(t)^3}.$$

Since the solution is homographic, we have $W(t) = r(t)Q(t)W_0$ where $W_0 = (X_0 - C_0)R$. It follows that the columns of W, W_0 satisfy

$$|w_j(t)| = r(t)|w_{0j}|, \quad j = 1, \ldots, n.$$

For each column such that $|w_{0j}| \neq 0$, define $u_j(t) = w_j(t)/|w_{0j}|$. Then $|u_j(t)| = r(t)$ for $j = 1, \ldots, n$ and

$$\ddot{u}_j(t) = -\frac{\lambda_j u_j(t)}{|u_j(t)|^3},$$

i.e., the normalized nonzero columns solve Kepler's equations with constant λ_j. Moreover, they all have the same norm $r(t)$. It follows that each of these $u_j(t)$ moves in a plane and can be represented with respect to polar coordinates in that plane by functions $r(t), \theta(t)$ satisfying (2.16) with $\lambda = \lambda_j$.

Lemma 2.7.2. *If $r(t), \theta(t)$ solves (2.16) and $r(t)$ is not constant, then λ and $\dot{\theta}(t)$ are uniquely determined by $r(t)$.*

Proof. Exercise. □

Continuing with the proof of the proposition, we now see that all of the λ_j corresponding to nonzero columns of $W(t)$ are equal. Then we have

$$X_0 A(X_0) = W_0 \operatorname{diag}(-\lambda_1, \ldots, -\lambda_n) S^{-1} = -\lambda W_0 S^{-1} = -\lambda(X_0 - C_0),$$

where the second equation holds because changing λ_j to λ for a column $w_j = 0$ does no harm. This shows that X_0 is a central configuration.

To get the rest we will use the reduced equations of motion (2.28). Since we are assuming that $X(t)$ is homographic, the relative state matrices have a particularly simple form. Let $Y(t) = X(t) - C(t) = X(t)P$ and $W(t) = V(t)P$ be the centered position and velocity matrices. Then $Y(t) = r(t)Q(t)Y_0$ and $W(t) = \dot{r}(t)Q(t)Y_0 + r(t)\dot{Q}(t)Y_0$. The relative state matrices are

$$B(t) = r(t)^2 B_0, \quad C(t) = r(t)\dot{r}(t)B_0, \quad D(t) = \dot{r}(t)^2 B_0 - r(t)^2 Y_0^T \Omega(t)^2 Y_0,$$

where $\Omega(t) = Q(t)^T \dot{Q}(t) \in \mathrm{so}(d)$. The antisymmetry of this matrix implies that terms involving $Y_0^T \Omega(t) Y_0$ in the calculation of these matrices vanish. Now calculating $\dot{C}(t)$ and comparing with (2.28) gives

$$(r\ddot{r} + \dot{r}^2)B_0 = D + BA = D - \lambda r^2 B_0, \tag{2.40}$$

where we used (2.29).

Now we already found that $r(t), \theta(t)$ are solutions of Kepler's equation. By rescaling X_0 and choosing the origin of time, we may assume that $r(0) = 1$ and $\dot{r}(0) = 0$. The second assumption certainly holds at the perihelion of the Kepler orbit. At this point the velocities and positions are orthogonal. Evaluating (2.40) at $t = 0$ and using Kepler's equation (2.16) we get

$$D_0 = \dot{\theta}_0^2 B_0. \tag{2.41}$$

We also have $C_0 = 0$.

Let $Z_0 = \begin{bmatrix} Y_0 & W_0 \end{bmatrix}$ be the initial state matrix and consider the matrices

$$L_1 = Z_0, \quad L_2 = \begin{bmatrix} \dot\theta_0^{-1} W_0 & -\dot\theta_0 Y_0 \end{bmatrix}.$$

We have

$$L_1^T L_2 = \begin{bmatrix} \dot\theta_0^{-1} C_0 & -\dot\theta_0 B_0 \\ \dot\theta_0^{-1} D_0 & -\dot\theta_0 C_0 \end{bmatrix} = \begin{bmatrix} 0 & -\dot\theta_0 B_0 \\ \dot\theta_0^{-1} D_0 & 0 \end{bmatrix}.$$

This $2n \times 2n$ matrix is antisymmetric by (2.41) so, by Lemma 2.6.5, there is an antisymmetric $d \times d$ matrix J such that

$$W_0 = \dot\theta_0 J y_0, \quad Y_0 = -\dot\theta_0^{-1} W_0 = -J^2 Y_0.$$

By Proposition 2.5.1, $\tilde Y(t) = \exp(\theta(t)J) Y_0$ is a homographic solution and its initial conditions

$$\tilde Y(0) = Y_0, \quad \tilde W(0) = \dot\theta_0 J Y_0 = W_0$$

are the same as those of the given homographic solution, $Y(t)$. Therefore, $Y(t) = \exp(\theta(t)J) Y_0$ as claimed. □

Although we have made a point of studying the special solutions of the n-body problem in $\mathbb{R}^d$, we will summarize the results for the physical case $d = 3$. The homographic solutions in $\mathbb{R}^3$ are of the following types. For any central configuration and any solution of the one-dimensional Kepler problem there is a homothetic solution. For any central configuration which is contained in some two-dimensional subspace and any solution of the two-dimensional Kepler problem, there is a homographic solution for which the bodies remain in the same plane. This is a uniform planar rigid motion if we take the circular solution of the Kepler problem. There are no other homographic motions. In particular, a nonplanar CC does not lead to any rigid or homographic, nonhomothetic solutions. A configuration which is balanced but not central is not balanced in $\mathbb{R}^3$ so does not give rise to a RE solution in $\mathbb{R}^3$.

2.8 Central configurations as critical points

Now that we have some motivation for studying central configurations, lots of interesting questions arise. Fixing the masses m_i we can ask whether central configurations exist and if so, how many there are up to symmetry. Working with configuration vectors $x \in \mathbb{R}^{dn}$ we need to study solutions of the CC equation

$$\nabla U(x) + \lambda M(x - c) = 0. \tag{2.42}$$

If x is a CC then so is any configuration y obtained from x by translations and rotations. In particular, the centered configuration $x - c$ is also a CC. If $k > 0$

then kx is also a central configuration but with a different λ. Recall that $\lambda(x) = U(x)/I(x)$, where $I(x)$ is the moment of inertia around the center of mass. So

$$\lambda(kx) = \lambda(x)/k^3.$$

We will view such CC's as equivalent and refer to similarity classes of CC's.

The key idea in this section is to interpret CC's as constrained critical points of the Newtonian potential. The constraint is just to fix the moment of inertia. Since $\nabla I(x) = 2M(x - c)$, the CC equation can be written

$$\nabla U(x) + \tfrac{1}{2}\lambda \nabla I(x) = 0.$$

Interpreting $\lambda/2$ as Lagrange multiplier, we get:

Proposition 2.8.1. *A configuration vector x_0 is a central configuration if and only if it is a critical point of $U(x)$ subject to the constraint $I(x) = k$, where $k = I(x_0)$.*

It is useful for existence proofs to have a compact constraint set. We can use the scaling symmetry to normalize the moment of inertia to be $I(x) = 1$ but, because of the translation invariance, $\{x : I(x) = 1\}$ is not compact. We can eliminate the translation symmetry by fixing the center of mass.

Just as in the matrix formulation of the problem, we can view the passage from x to $x - c$ as an orthogonal projection. In fact

$$x - c = \hat{P}x,$$

where $\hat{P}\colon \mathbb{R}^{dn} \to \mathbb{R}^{dn}$ is the orthogonal projection onto the subspace where $m_1x_1 + \cdots + m_nx_n = 0 \in \mathbb{R}^d$ with respect to the mass inner product $v^T Mw$. The matrix of $\hat{P}$ is

$$\hat{P} = I - \frac{1}{m_0}\hat{L}^T\hat{L}M, \quad \hat{L} = \begin{bmatrix} I & I & \cdots & I \end{bmatrix}, \tag{2.43}$$

where $\hat{L}$ is $d \times dn$ with blocks of $d \times d$ identity matrices. One can check that $\hat{P}$ is an M-symmetric projection matrix.

Define the *normalized configuration space* as

$$\mathcal{N} = \{x : c = \hat{L}Mx = 0, I(x) = 1\}.$$

Any configuration x determines a unique *normalized* configuration with $c = 0$ and $I = 1$. Note that the center of mass condition defines a subspace of $\mathbb{R}^{dn}$ of dimension $d(n-1)$ and then $I = 1$ gives an ellipsoid in this subspace. Hence $\mathcal{N}$ is a smooth compact manifold diffeomorphic to a sphere, $\mathcal{N} \simeq \mathbf{S}^{d(n-1)-1}$.

Proposition 2.8.2. *A configuration vector x is a central configuration if and only if the corresponding normalized configuration is a critical point of the Newtonian potential $U(x)$ restricted to $\mathcal{N}$.*

Proof. If x is a CC, so is the corresponding normalized configuration. Proposition 2.8.1 shows that this normalized configuration is a critical point of $U(x)$ with the constraint $I(x) = 1$, so it is still a critical point if we add the center of mass constraint defining $\mathcal{N}$.

Conversely, suppose x is a critical point of $U(x)$ restricted to $\mathcal{N}$. We need to show that it is still a critical point if we remove the center of mass constraint. This can be checked using the orthogonal projection $\hat{P}$. Note that $\mathcal{N}$ is a smooth codimension one submanifold of the subspace $\ker \hat{L}M \subset \mathbb{R}^{dn}$. Therefore $x \in \mathcal{N}$ is a critical point of $U|_{\mathcal{N}}$ if and only if

$$(DU(x) + kDI_S(x))\, v = 0$$

for all $v \in \ker \hat{L}M$, where $k \in \mathbb{R}$ is a Lagrange multiplier. Equivalently we need

$$(DU(x) + kDI_S(x))\, \hat{P} = 0,$$

where $\hat{P}$ is the orthogonal projection onto $\ker \hat{L}M$ from (2.43). By translation invariance $U(\hat{P}x) = U(x)$, and differentiation gives $DU(x)\hat{P} = DU(x)$ for $x \in \mathcal{N}$. Similarly, $DI(x)\hat{P} = DI(x)$. So we can drop $\hat{P}$ from the last equation and take transposes to get

$$\nabla U(x) + k\, \nabla I(x) = 0,$$

which is the CC equation. □

An alternative approach is based on the moment of inertia with respect to the origin,

$$I_0(x) = x^T M x = \sum_{j=1}^{n} m_j |x_j|^2.$$

For configurations with $c = 0$, $I(x) = I_0(x)$ and the CC equation becomes

$$\nabla U(x) + \lambda M x = 0. \tag{2.44}$$

This is the critical point equation with fixed $I_0(x)$. It turns out that (2.44) forces $c = 0$ and we have:

Proposition 2.8.3. *The point x is a critical point of $U(x)$ on $\{x : I_0(x) = 1\}$ if and only if x is a normalized central configuration.*

Proof. If $x \in \mathcal{N}$ then $c = 0$ and $I(x) = I_0(x) = 1$. If it is also a central configuration then (2.44) holds, so it is a critical point of $U(x)$ on $\{I_0 = 1\}$. Conversely, suppose x is a critical point of $U(x)$ on $\{I_0 = 1\}$. Then (2.44) holds. We will show that this implies $c = 0$ and it follows that $x \in \mathcal{N}$ and that the CC equation (2.42) holds.

Equation (2.44) gives

$$\lambda m_j x_j = -\nabla_j U(x) = \sum_{i \neq j} F_{ji},$$

where $F_{ji} = (m_i m_j (x_i - x_j))/r_{ij}^3$ is the force on body j due to body i. Summing over j and dividing by the total mass gives

$$\lambda c = \frac{1}{m_0} \sum_{i<j} F_{ij}.$$

The terms in this sum cancel out in pairs because $F_{ij} = -F_{ji}$. Since $\lambda > 0$ we get $c = 0$ as required. □

The manifold $\{x : I_0(x) = 1\}$ is diffeomorphic to the sphere $\mathbf{S}^{dn-1}$ so this approach gives compactness without explicitly imposing the center of mass constraint. The critical points will automatically lie in our previous constraint manifold $\mathcal{N}$.

It is also possible to treat balanced configurations as critical points. Modify the vector version of the balance equation (2.37) by introducing a constant λ to get

$$\nabla U(x) + \lambda \hat{S} M(x - c) = 0. \tag{2.45}$$

Here $\lambda \in \mathbb{R}$ and $\hat{S} = \operatorname{diag}(S, \ldots, S)$ is a $dn \times dn$ block-diagonal matrix with identical $d \times d$ blocks S, the positive semi-definite, symmetric matrix from Proposition 2.6.7. We will call x an *S-balanced configuration (SBC)* if (2.45) holds for some λ. CC's are a special case with $S = I$. By putting a λ into (2.45) we can say that x and kx are both S-balanced. The equation is also invariant under translations but generally not invariant under rotations. In fact, the matrix S transforms under rotations and scalings via

$$S(kQx) = k^{-3} Q S Q^T.$$

In the CC case we have $S = I$ and we get rotation invariance. The other extreme would be that S has d distinct eigenvalues and then it is not stabilized by any rotation. By choosing an appropriate rotation Q we can get

$$Q S Q^T = \operatorname{diag}(\sigma_1^2, \sigma_2^2, \ldots, \sigma_d^2).$$

It is no loss of generality to assume S positive definite since it is definite on $\mathcal{C}(x)$ and we could extend it arbitrarily on $\mathcal{C}(x)^\perp$.

To handle SBC's in a similar way to CC's, we will define an S-weighted moment of inertia. Assuming that S is positive definite, we can use it to define a new inner product and norm on $\mathbb{R}^d$,

$$\langle \xi, \eta \rangle_S = \xi^T S \eta, \quad |\xi|_S^2 = \xi^T S \xi.$$

Then set

$$I_S(x) = (x - c)^T \hat{S} M (x - c) = \sum_{j=1}^{n} m_j |x_j - c|_S^2.$$

As in the CC case, the constant λ in (2.45) is $\lambda = U(x)/I_S(x)$. Define the *S-normalized configuration space*

$$\mathcal{N}(S) = \{x : c = \hat{L}Mx = 0, I_S(x) = 1\}.$$

Then, as for CC's, we have:

Proposition 2.8.4. *A configuration vector x is a S-balanced configuration if and only if the corresponding normalized configuration is a critical point of $U(x)$ restricted to $\mathcal{N}(S)$.*

One of the main applications of the characterization of CC's and SBC's as critical points are the existence proofs. For example:

Corollary 2.8.5. *For every choice of masses $m_i > 0$ in the n-body problem in $\mathbb{R}^d$, there is at least one central configuration. For every choice of masses and every $d \times d$ positive definite symmetric matrix S, there exists at least one S-balanced configuration.*

Proof. It suffices to consider SBC's, since CC's are a special case. Note that $\mathcal{N}(S)$ is a compact submanifold of $\mathbb{R}^{dn}$. The Newtonian potential defines a smooth function $U : \mathcal{N}(S) \setminus \Delta \to \mathbb{R}$. The singular set $\mathcal{N}(S) \cap \Delta$ is compact and $U(x) \to \infty$ as $x \to \Delta$. It follows that U attains a minimum at some point $x \in \mathcal{N}(S) \setminus \Delta$ and this point will be an S-balanced configuration. □

Although restricting to the compact space $\mathcal{N}$ or $\mathcal{N}(S)$ is useful, there are a couple of alternative variational characterizations of CC's and SBC's as unconstrained critical points. The first version is obtained by normalizing the constant λ instead of the moment of inertia. For every solution of (2.42) or (2.45), there is a rescaled solution with $\lambda = k$, where $k > 0$ is any positive constant. If we choose $k = 2$ then this rescaled configuration will be a critical point of the function

$$F(x) = U(x) + I_S(x)$$

on $\mathbb{R}^{dn}$, i.e., with no constraint on x. Or, we can impose the linear constraint $c = 0$. Another variational approach is to avoid normalization altogether and look for critical points of the homogeneous function

$$G(x) = \sqrt{I_S(x)}\, U(x) \quad \text{or} \quad I_S(x) U(x)^2.$$

One can check that if x is a solution of (2.45) we get a ray of critical points kx, $k > 0$, for these functions.

In the CC case, the Newtonian potential determines a function on the quotient space

$$\mathcal{M} = (\mathcal{N} \setminus \Delta)/\operatorname{SO}(d).$$

However, for $d > 2$ the action of the rotation group is not free and the quotient space is not a manifold. We can get a manifold by restricting to the configurations of a given dimension.

An amusing application of the variational approach on a reduced space is the study of central configurations of maximal dimension. For any configuration of n-bodies, the centered position space has $\dim C(x) \leq n-1$. We will look for CC's with $\dim C(x) = n-1$.

Proposition 2.8.6. *The only central configuration of n-bodies with $\dim C(x) = n-1$ is the regular n-simplex and it is a central configuration for all choices of the masses.*

Proof. Without loss of generality we can consider the n-body problem in $\mathbb{R}^{n-1}$. The configuration space is $\mathbb{R}^{n(n-1)} \setminus \Delta$ and the centered configurations form a subspace of dimension $n(n-1)-(n-1) = (n-1)^2$. The subset of configurations with $\dim C(x) = n-1$ is an open subset. The rotation group $\mathrm{SO}(n-1)$ acts freely on this open set and we can look for critical points on the quotient space which will be a smooth manifold of dimension

$$(n-1)^2 - \frac{(n-1)(n-2)}{2} = \frac{n(n-1)}{2}.$$

The dimension suggests using the mutual distances $r_{ij}, 1 \leq i < j \leq n$, as local coordinates. We will look for unconstrained critical points of $U(x) + I(x)$, where we express both terms as functions of the r_{ij} using (2.2) and (2.9). We get

$$\frac{\partial U}{\partial r_{ij}} + \frac{\partial I}{\partial r_{ij}} = -\frac{m_i m_j}{r_{ij}^2} + \frac{2 m_i m_j r_{ij}}{m_0} = 0.$$

The masses cancel out and the mutual distances are equal to $r_{ij}^3 = m_0/2$. □

The variational characterization suggests using the gradient flow of the Newtonian potential to understand central or balanced configurations. Generically, a smooth function on a smooth manifold is a Morse function, i.e., it has isolated critical points which are nondegenerate. Due to the rotational symmetry, critical points of $U|_{\mathcal{N}}$ will never be isolated for $d \geq 2$. One can try to eliminate the rotational symmetry or just work with the similarity classes of critical points. We can still hope for these classes to be isolated from one another or nondegenerate in some sense.

First we deal with another problematic aspect of the gradient flow, the lack of compactness. The manifold $\mathcal{N}(S)$ is compact, but the flow is only defined on the open subset $\mathcal{N}(S) \setminus \Delta$. The next result, known as Shub's lemma [32], shows that CC's and SBC's are bounded away from Δ.

Proposition 2.8.7. *For fixed masses $m_1, \ldots, m_n$ and a fixed positive definite symmetric matrix S, there is a neighborhood of Δ in $\mathcal{N}(S)$ which contains no S-balanced configurations.*

Proof. Otherwise, there would be some $\bar{x} \in \mathcal{N}(S) \cap \Delta$ and a sequence of SBC's $x^k \in \mathcal{N}(S)$ with $x^k \to \bar{x}$ as $k \to \infty$. The collision configuration $\bar{x}$ defines a partition of the bodies into *clusters*, where m_i, m_j are in the same cluster if $\bar{x}_i = \bar{x}_j$. For k

large, the bodies in each cluster will be close to each other but the clusters will be bounded away from one another.

Let $F_i(x^k) = \nabla_i U(x^k)$ be the force on the i-th body. Since x^k is a normalized SBC, we have

$$F_i = -\lambda_k m_i S x_i^k, \quad \lambda_k = U(x^k).$$

Let $\gamma \subset \{1, \ldots, n\}$ be the set of subscripts of one of the clusters. Then,

$$\sum_{i\in\gamma} F_i = -\lambda_k S \sum_{i\in\gamma} m_i x_i^k. \tag{2.46}$$

As $k \to \infty$, we have $\lambda_k = U(x^k) \to \infty$ since $\bar{x} \in \Delta$. On the other hand

$$S \sum_{i\in\gamma} m_i x_i^k \to S m_\gamma \bar{x}_\gamma,$$

where m_γ is the total mass of the cluster and $\bar{x}_\gamma$ is the common value of the limiting positions $\bar{x}_i, i \in \gamma$. We will show below that the left-hand side of (2.46) is bounded. It follows that we must have $\bar{x}_\gamma = 0$ for all of the clusters. In other words, there could be only one cluster and it would have to be at the origin. But this is impossible since $I_S(\bar{x}) = 1$.

To see that the left-hand side of (2.46) is bounded, we can split the sum as

$$\sum_{i\in\gamma} F_i = \sum_{\substack{i,j\in\gamma \\ i\neq j}} F_{ij} + \sum_{\substack{i\in\gamma \\ l\notin\gamma}} F_{il},$$

where $F_{ij} = (m_i m_j (x_j - x_i))/r_{ij}^3$ is the force on body i due to body j. The first sum is identically zero since $F_{ij} = -F_{ji}$, and the second is bounded by definition of cluster. □

It follows from Shub's lemma that if the similarity classes of CC's or SBC's are isolated then there are only finitely many of them. To see this, let U denote a neighborhood of Δ in $\mathcal{N}(S)$ which contains no SBC's. Since the complement $\mathcal{N}(S) \setminus U$ is compact, a hypothetical infinite sequence of distinct, similarity classes would have normalized representatives with a convergent subsequence. The limiting configuration would be a nonisolated SBC.

If we allow the masses to vary, it is possible to find a sequence of CC's, say $\bar{x}_k$, converging to Δ. This idea was used by Xia in [36], and further explored in [21]. The masses in each nontrivial cluster all tend to zero. The limiting shapes of the clusters are governed by equations similar to the CC equation.

It is interesting to classify CC's and SBC's by their Morse index. Recall that if x is a critical point of a smooth function V on a manifold $\mathcal{N}$, there is a *Hessian* quadratic form on the tangent space $T_x\mathcal{N}$ which is given in local coordinates by the symmetric matrix of second partial derivatives,

$$H(x)(v) = v^T D^2 V(x) v.$$

Alternatively, if $\gamma(t)$ is any smooth curve in $\mathcal{N}$ with $\gamma(0) = x$ and $\gamma'(0) = v$ then

$$H(x)(v) = \frac{1}{2}\frac{d^2}{dt^2}V(\gamma(t))|_{t=0}.$$

The *Morse index* $\mathrm{ind}(x)$ is the maximum dimension of a subspace of $T_x\mathcal{N}$ on which $H(x)$ is negative definite. The *nullity* is the dimension of

$$\ker H(x) = \{v : H(q)(v, w) = 0 \text{ for all } w \in T_x\mathcal{N}\},$$

where $H(x)(v, w) = v^T D^2V(x)w$ is the symmetric bilinear form associated to $H(x)$. We are interested in the function $V = U|_{\mathcal{N}(S)}$ given by restricting the Newtonian potential to the normalized configuration space.

Instead of working in local coordinates, we want to represent the Hessian by a $dn \times dn$ matrix, also called $H(x)$, whose restriction to $T_x\mathcal{N}(S)$ gives the correct values.

Proposition 2.8.8. *The Hessian of $V : \mathcal{N}(S) \to \mathbb{R}$ at a critical point x is given by $H(x)(v) = v^T H(x)v$, where $H(x)$ is the $dn \times dn$ matrix*

$$H(x) = D^2U(x) + U(x)\hat{S}M. \tag{2.47}$$

Proof. A critical point of V is also an unconstrained critical point of $G(x) = \sqrt{I_S(x)}U(x)$ in $\mathbb{R}^{dn}$. Since $G|_{\mathcal{N}(S)} = U|_{\mathcal{N}(S)} = V$, their Hessians on $T_x\mathcal{N}(S)$ agree.

To calculate D^2G first recall that $I_S(x) = x^T\hat{P}^T\hat{S}M\hat{P}x$. For any vector $w \in \mathbb{R}^{dn}$, we have

$$DI_S(x)w = 2x^T\hat{P}^T\hat{S}M\hat{P}w.$$

Hence,

$$DG(x)w = I_S(x)^{\frac{1}{2}}\, DU(x)w + I_S(x)^{-\frac{1}{2}}U(x)x^T\hat{P}^T\hat{S}M\hat{P}w.$$

We are only interested in computing $D^2G(x)(v, w)$ where $v, w \in T_x\mathcal{N}(S)$. In that case we have

$$I_S(x) = 1, \quad \hat{P}v = v, \quad x^T\hat{P}^T\hat{S}M\hat{P}v = 0,$$

and analogous equations for w. Differentiating G again and using these equations we get

$$D^2G(x)(v, w) = D^2U(x)(v, w) + U(x)v^T\hat{S}Mw,$$

as claimed. □

It is straightforward to calculate the $dn \times dn$ matrix $D^2U(x)$ with the result

$$D^2U(x) = \begin{bmatrix} D_{11} & D_{12} & \cdots & D_{1n} \\ D_{21} & D_{12} & \cdots & D_{2n} \\ \vdots & & & \vdots \end{bmatrix}, \tag{2.48}$$

where the $d \times d$ blocks are

$$D_{ij} = \frac{m_i m_j}{r_{ij}^3} \left(I - 3u_{ij} u_{ij}^T \right), \quad u_{ij} = \frac{x_i - x_j}{r_{ij}}, \quad \text{for } i \neq j,$$

and

$$D_{ii} = -\sum_{j \neq i} D_{ij}.$$

The following formula for the value of the Hessian quadratic form on a vector $v \in \mathbb{R}^{dn}$ is sometimes useful:

$$H(x)(v,v) = \sum_{i<j} \frac{m_i m_j}{r_{ij}^3} \left(-|v_{ij}|^2 + 3(u_{ij} \cdot v_{ij})^2 \right) + U(q) v^T M v, \tag{2.49}$$

where $v_{ij} = v_i - v_j \in \mathbb{R}^d$.

As noted above, the rotational symmetry implies that CC's are always degenerate as critical points for $d \geq 2$. The following result describes the minimal degeneracy.

Proposition 2.8.9. *Let $x \in \mathcal{N}$ be a CC in $\mathbb{R}^d$. Then the nullity of x as a critical point $U|_{\mathcal{N}}$ satisfies*

$$\text{null}(x) \geq \frac{d(d-1)}{2} - \frac{k(k-1)}{2}, \quad k = d - \dim(x) = d - \dim \mathcal{C}(x). \tag{2.50}$$

Proof. The formula just gives the dimension of the subspace of $T_x\mathcal{N}$ consisting of tangent vectors to the action of the rotation group, i.e., the subspace

$$\{v = \alpha x : \alpha \in \text{so}(d)\}.$$

To see this, first note that the manifold $\mathcal{N}$ is rotation invariant. For any curve of rotations $Q(t) \in \text{SO}(d)$ with $Q(0) = I$, we have

$$\dot{Q}(t)x|_{t=0} = \alpha x \in T_x\mathcal{N}.$$

But x is stabilized by rotations which fix the subspace $\mathcal{C}(x)$. This stabilizer is isomorphic to the rotation group of the orthogonal complement $\mathcal{C}(x)^\perp$ which has dimension k. □

For SBC's the corresponding minimal nullity will depend on how the rotation group acts on the symmetric matrix S. If S has distinct eigenvalues, it is possible for SBC's to be nondegenerate. For example, recall that for masses $m_1 = m_2 = 1$ and $m_3 > 0$ any isosceles triangle is balanced with the eigenvalues of S varying with the shape. One can check using a computer that generic choices of isosceles shape lead to nondegenerate SBC's.

In all cases, it is natural to call a critical point nondegenerate if its nullity is as small as possible given the rotational symmetry.

Definition 2.8.10. *A CC or SBC in* $\mathbb{R}^d$ *is* nondegenerate *if the nullity of the corresponding critical point is as small as possible consistent with the rotational symmetry. For CC's this means that equality should hold in* (2.50).

For example in $\mathbb{R}^3$ a nondegenerate collinear CC has nullity 2, while nondegenerate planar and spatial CC's have nullity 3.

2.9 Collinear central configurations

The first central configurations were discover by Euler in 1767, see [11]. He studied the collinear three-body problem where he found collinear central configurations and the corresponding homothetic motions. Moulton investigated the central configurations of the collinear n-body problem in 1910, see [25]. The results are definitive in contrast to the state of the theory for $d \geq 2$. This section is devoted to proving Moulton's theorem:

Proposition 2.9.1 (Moulton's Theorem)**.** *Given masses* $m_i > 0$*, there is a unique normalized collinear central configuration for each ordering of the masses along the line.*

Note that when $d = 1$ there is no difference between CC's and SBC's due to the lack of variety in 1×1 symmetric matrices.

It is instructive to start with Euler's case $n = 3$. The normalized configuration space

$$\mathcal{N} = \{x \in \mathbb{R}^3 : m_1x_1 + m_2x_2 + m_3x_3 = 0, \;\; m_1x_1^2 + m_2x_2^2 + m_3x_3^2 = m_0\}$$

is the curve of intersection of a plane and an ellipsoid. The collision set consists of three planes:

$$\Delta = \{x_1 = x_2\} \cup \{x_1 = x_3\} \cup \{x_2 = x_3\}$$

which divide the curve into six arcs corresponding to the different orderings of the three masses along the line (see Figure 2.6). Since $U \to \infty$ at these points, there must be at least one critical point in each of the arcs. To see that there is only one requires more work.

The three mutual distances provide convenient coordinates, but we need to subject them to a collinearity constraint. If we fix the ordering of the bodies to be $x_1 < x_2 < x_3$ then the constraint is $r_{12} + r_{23} - r_{13} = 0$. Looking for critical points of the homogeneous function $F = U(r_{ij})^2 I(r_{ij})$ with this constraint, and then normalizing by setting $r_{12} = r, r_{13} = 1, r_{23} = 1 - r$ gives a degree five polynomial equation for r:

$$\begin{aligned}(m_2 + m_3)r^5 + (2m_2 + 3m_3)r^4 + (m_2 + 3m_3)r^3 \\ - (3m_1 + m_2)r^2 - (3m_1 + 2m_2)r - (m_1 + m_2) = 0.\end{aligned} \tag{2.51}$$

Fortunately there is a single sign change so Descartes' rule of signs implies there is a unique positive real root. Of course, there is no simple formula for how this

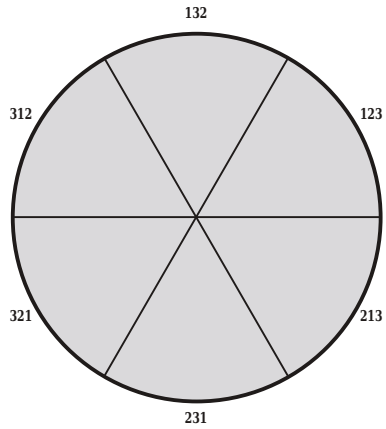

Figure 2.6: $\mathcal{N}$ for the collinear three-body problem is the boundary circle of the shaded disk which represents the set $I \leq 1$ in the plane of centered configurations. Δ intersects this plane in three lines which divide the circle into six arcs, one for each ordering of the bodies along the line.

root changes as a function of the masses. Euler's example is a shot over the bow about the CC equation. Even in the simplest nontrivial case, finding CC's for given masses involves solving complicated polynomial equations. Figure 2.7 shows a surface defined by Euler's quintic when one of the masses is normalized to 1. The surface lies over the mass plane in a complicated way making the uniqueness result for fixed positive masses all the more remarkable.

Before moving on to the proof of Moulton's theorem we will have a look at the geometry of the next case, $n = 4$. This time $\mathcal{N}$ is the intersection of a hyperplane and an ellipsoid in $\mathbb{R}^4$. So it is a two-dimensional surface diffeomorphic to $\mathbf{S}^2$. There are six collision planes which divide the sphere into $4! = 24$ triangles. Figure 2.8 shows how the collision planes divide the sphere.

Proof of Moulton's Theorem. The collision set Δ divides the ellipsoid $\mathcal{N}$ of normalized centered configurations into $n!$ components, one for each ordering of the bodies along the line. Let $\mathcal{V}$ denote any one of these components, an open set whose boundary is contained in Δ. The Newtonian potential gives a smooth function $U|_{\mathcal{V}} \colon \mathcal{V} \to \mathbb{R}$, and $U(x) \to \infty$ as $x \to \partial\mathcal{V}$. Hence $U|_{\mathcal{V}}$ attains its minimum at some $x_0 \in \mathcal{V}$ and x_0 is a CC with the given ordering of the bodies along the line.

Instead of working on the normalized space where $I(x) = 1$ we can study the function $F(x) = U(x) + I(x)$ on the cone $\tilde{\mathcal{V}}$ of all rays through the origin passing through $\mathcal{V}$ (in Figure 2.6 this would be an infinite triangular wedge based on one of the six arcs). Let $x, y \in \tilde{\mathcal{V}}$ and consider a line segment $p(t) = (1-t)x + ty$, $0 \leq t \leq 1$. Note that since the ordering is fixed, the sign of $p_i(t) - p_j(t) = (1-t)(x_i - x_j) + t(y_i - y_j)$ is equal to the common sign of $x_i - x_j$ and $y_i - y_j$. It

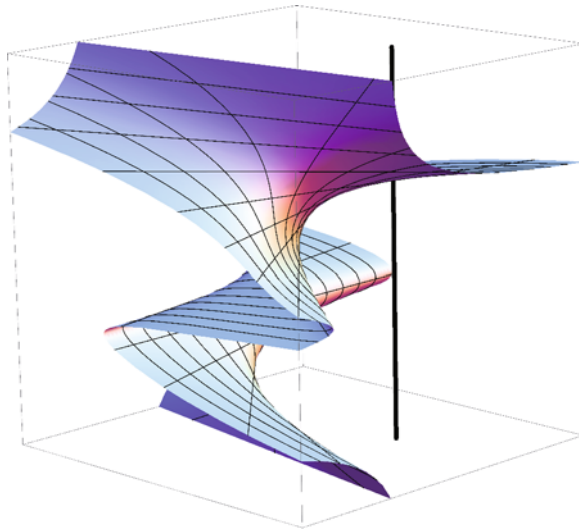

Figure 2.7: Surface defined by Euler's quintic equations in the product space of masses and configurations. Two mass parameters (horizontal) and one configuration variable r (vertical). Fixing the masses means looking for intersections of the surface with a vertical fiber, here a line segment. For positive masses, the segment cuts the surface just once.

follows that $p(t) \in \tilde{\mathcal{V}}$ for all t and so $\tilde{\mathcal{V}}$ is a convex set. We will show that if $x \neq y$ then $F(p(t))$ has a strictly positive second derivative. It follows that x, y cannot both be critical points of $F(x)$.

First consider $F(r_{ij})$ as a function of the mutual distances r_{ij} on $(\mathbb{R}^+)^{\frac{n(n-1)}{2}}$. We have

$$\frac{\partial^2 F}{\partial r_{ij}^2} = \frac{2m_i m_j}{r_{ij}^3} + \frac{2m_i m_j}{m_0} > 0.$$

Now since the configurations x, y are collinear, the mutual distances reduce to $r_{ij}(t) = |p_i(t) - p_j(t)|$ and, as the ordering is constant along the segment, this is a linear function of t. It follows that $F(p(t))''$ is a sum of terms

$$\frac{\partial^2 F}{\partial r_{ij}^2}(p(t)) \left(r'_{ij}(t)\right)^2.$$

These terms are all nonnegative and at least one is positive if $x \neq y$. □

Next we will take a look at the Hessian $H(x)$ of a collinear CC. Using the rotation invariance of U we get

$$H(Qx) = Q^T H(x) Q,$$

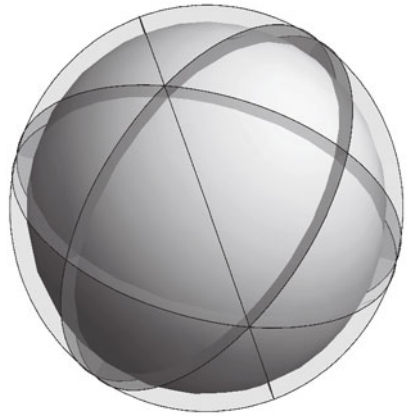

Figure 2.8: $\mathcal{N}$ for the collinear four-body problem. The collision planes divide the sphere into triangles representing the possible orderings of the bodies.

where $H(x)$ is given by (2.47) and $Q \in \mathrm{SO}(d)$ is any rotation. It follows that the index and nullity are unchanged by such rotations. If x is collinear, we can therefore assume that all of the bodies have positions $x_j \in \mathbb{R}^1 \times \{0\}^{d-1} \subset \mathbb{R}^d$. Then the unit vectors u_{ij} appearing in the formula (2.48) are all multiples of $e_1 = (1, 0, \ldots, 0)$. It follows that if we permute the components of configuration vectors into groups of n with all of the e_1 components first, the e_2 components next, etc., then $D^2U(x)$ will have a block-diagonal form

$$D^2U(x) = \mathrm{diag}(-2\tilde{A}, \tilde{A}, \ldots, \tilde{A}),$$

where

$$\tilde{A} = \begin{bmatrix} \tilde{A}_{11} & \frac{m_1 m_2}{r_{12}^3} & \cdots & \frac{m_1 m_n}{r_{1n}^3} \\ \frac{m_1 m_2}{r_{12}^3} & \tilde{A}_{22} & \cdots & \frac{m_2 m_n}{r_{2n}^3} \\ \vdots & & & \vdots \\ \frac{m_1 m_n}{r_{1n}^3} & \frac{m_2 m_n}{r_{2n}^3} & \cdots & \tilde{A}_{nn} \end{bmatrix}, \quad \tilde{A}_{jj} = -\sum_{i \neq j} \tilde{A}_{ij} = -\sum_{i \neq j} \frac{m_i}{r_{ij}^3}.$$

Note that $\tilde{A}$ is just the symmetric matrix $A(X)M$ from Section 2.4.

Let $v = (\xi_1, \xi_2, \ldots, \xi_d)^T$ denote a vector in $\mathbb{R}^{dn}$ with its coordinates permuted into groups of n as described above. Vectors of the form $v = (\xi_1, 0, \ldots, 0)^T$ will be called collinear vectors and those of the form $v = (0, \xi_2, \ldots, \xi_n)^T$ normal vectors. We are interested in the tangent space $T_x\mathcal{N}$ to the normalized configuration space. With these coordinates the center of mass subspace, $\ker \hat{L}M$, is given by

$$m \cdot \xi_i = 0, \quad i = 1, \ldots, d,$$

where $m \in \mathbb{R}^n$ is the mass vector. Since x is collinear, the equation $DI(x)v = 0$ affects only the first vector ξ_1:

$$m_1 x_{11}\xi_{11} + \cdots + m_n x_{n1}\xi_{1n} = 0.$$

Finally, the action of the rotation group leads to a $(d-1)$-dimensional subspace of vectors in the kernel of the Hessian. A basis is $\omega_2(x), \ldots, \omega_d(x)$, where $\omega_i(x)$ is the vector whose i-th group of n coordinates is the vector of first coordinates of the configuration, $(x_{11}, x_{21}, \ldots, x_{n1})$. For example, $\omega_2(x)$ is the tangent vector at x in the direction of a rotation in the $(1,2)$-coordinate plane.

Proposition 2.9.2. *Every collinear central configuration in* $\mathbb{R}^d$ *is nondegenerate with* $\operatorname{null}(x) = d-1$ *and* $\operatorname{ind}(x) = (d-1)(n-2)$. *In the collinear tangent directions,* $H(x)$ *is positive definite while in the normal directions it is negative semi-definite.*

Proof. We will analyze the Hessian block-by-block. The first block of the Hessian corresponds to the collinear directions and we have

$$\xi^T H(x)\xi = -2\xi^T \tilde{A}\xi + U(x)\xi^T M\xi,$$

where M is the $n \times n$ version of the mass matrix. We showed in Section 2.4 that the matrix $\tilde{A} = AM$ is negative semi-definite, so both terms here are nonnegative and the second is strictly positive for nonzero vectors. Therefore the collinear part of the Hessian is positive definite.

For each of the other blocks we have

$$\xi^T H(x)\xi = \xi^T \tilde{A}\xi + U(x)\xi^T M\xi.$$

The terms are of different signs and it is a subtle problem to see which is dominant. The following proof, due to Conley, appears in [27].

Instead of finding the index and nullity of $H(x)$ we will find the number of negative and zero eigenvalues of the linear map with matrix

$$M^{-1}H(x) = M^{-1}\tilde{A} + U(X)I.$$

It is possible to guess two eigenvalues and eigenvectors. Let $u_1 = \begin{bmatrix} 1 & \cdots & 1 \end{bmatrix}^T$. Since the row sums of $\tilde{A}$ are zero we have

$$M^{-1}Hu_1 = \lambda_1 u_1, \quad \lambda_1 = U(x) > 0.$$

However, this vector is orthogonal to the zero center of mass subspace so is not relevant for our index and nullity computation. Next we have $u_2 = x = \begin{bmatrix} x_1 & \cdots & x_n \end{bmatrix}^T$, where we have simplified the notation so $x_i \in \mathbb{R}$ denotes the position of the i-th body along the line. Then a short computation gives

$$M^{-1}\tilde{A}u_2 = M^{-1}\nabla U(x),$$

where ∇ is the gradient in $\mathbb{R}^n$. Since x is a normalized CC we have $M^{-1}\nabla U(x) = -U(x)x = -U(x)u_2$ and so

$$M^{-1}Hu_2 = (M^{-1}\tilde{A} + U(x)I)u_2 = -U(x)u_2 + U(x)u_2 = 0.$$

In other words u_2 is an eigenvector with eigenvalue $\lambda_2 = 0$. We have one such null vector for each of the last $d-1$ blocks. Note that u_2 is the vector $\omega_i(x)$ tangent to the rotation group action. If we can show that the other $n-2$ eigenvalues of $M^{-1}H$ are strictly negative, the proposition will be proved.

Conley's proof uses the dynamics of the linear flow of the differential equation

$$\dot{\xi} = M^{-1}\tilde{A}\xi.$$

Every linear flow determines a flow on the space of lines through the origin, and the eigenvector lines are exactly the equilibrium points. Moreover the equilibrium corresponding to the largest eigenvector is an attractor for this projectivized flow. If we can show that the line of the eigenvector $u_2 = x$ is an attractor, then it follows that all of the other eigenvalues of $M^{-1}\tilde{A}$ are strictly less than $-U(x)$ and so all of the other eigenvalues of $M^{-1}H(x)$ are negative.

Suppose that the ordering of the bodies along the line is $x_1 < x_2 < \cdots < x_n$. Define a cone in the zero center of mass subspace by

$$K = \{\xi : m \cdot \xi = 0, \xi_1 \le \xi_2 \le \cdots \le \xi_n\}.$$

This cone contains the line spanned by the eigenvector u_2 in its interior and does not contain any two-dimensional subspaces. We will show that the flow carries K strictly inside itself. It follows that for the projectivized flow, u_2 is an attractor.

Now the boundary of K is the set where one or more of the inequalities in the definition is an equality. Consider a boundary point where, for some $i < j$, we have

$$u_{i-1} \le u_i = \cdots = u_j \le u_{j+1}.$$

The differential equation gives

$$\dot{u}_i = \sum_{k \ne i} \frac{m_k}{r_{ik}^3}(u_k - u_i), \quad \dot{u}_j = \sum_{k \ne j} \frac{m_k}{r_{jk}^3}(u_k - u_j).$$

Since $u_i = u_j$ the difference of these can be written:

$$\dot{u}_j - \dot{u}_i = \sum_{k \ne i,j} m_k(u_k - u_i)\left[\frac{1}{r_{jk}^3} - \frac{1}{r_{ik}^3}\right].$$

Every term in this sum is nonnegative:

$$\text{if } k < i, \quad u_k - u_i \le 0 \text{ and } \tfrac{1}{r_{jk}^3} - \tfrac{1}{r_{ik}^3} < 0;$$

$$\text{if } i < k < j, \quad u_k - u_i = 0;$$

$$\text{if } j < k, \quad u_k - u_i \ge 0 \text{ and } \tfrac{1}{r_{jk}^3} - \tfrac{1}{r_{ik}^3} > 0.$$

Moreover, not all of the terms can vanish since otherwise u would be a multiple of $\begin{bmatrix}1 & \cdots & 1\end{bmatrix}^T$, which is not in the zero center of mass space. It follows that at this boundary point $\dot{u}_j - \dot{u}_i > 0$ so the point moves strictly inside the cone under the linear flow. It follows that the line determined by u_2 is an attractor, as required. □

2.10 Morse indices of non-collinear central configurations

Unfortunately, much less is known about the Morse indices of non-collinear CC's. The following result gives a weak lower bound on the index which, at least, shows that a minimum must have the maximum possible dimension.

Proposition 2.10.1. *Suppose x is a central configuration of the n-body problem in $\mathbb{R}^d$ with $\dim(x) < \min(d, n-1)$. Then the Morse index of the corresponding critical point satisfies $\mathrm{ind}(x) \geq d - \dim(x)$. In particular, the critical point is not a local minimum of $U|_{\mathcal{N}}$.*

As a corollary we get the existence of CC's of the n-body problem of all possible dimensions.

Corollary 2.10.2. *For the n-body problem in $\mathbb{R}^d$ and for any k with $1 \leq k \leq \min(d, n-1)$ there exists at least one central configuration with $\dim(x) = k$.*

Proof. We have seen that $U|_{\mathcal{N}}$ achieves a minimum at some CC x, and it follows from the proposition that $\dim(x) = \min(d, n-1)$. If $1 \leq k < \min(d, n-1)$ then we can further restrict U to a subspace of $\mathbb{R}^d$ of dimension k and get a CC of dimension $\min(k, n-1) = k$. □

Proof of Proposition 2.10.1. If $\dim(x) = k < \min(d, n-1)$ we can assume that all of the bodies have position vectors $x_j \in \mathcal{W} = \mathbb{R}^k \times \{0\}^{d-k}$. As in the last section we get a block decomposition of the Hessian $D^2U(x) = \mathrm{diag}(D^2(U|_{\mathcal{W}}), \tilde{A}, \ldots, \tilde{A})$, where $D^2(U|_{\mathcal{W}})$ is the $nk \times nk$ tangential part, and where there are $d-k$ copies of the familiar $n \times n$ block $\tilde{A}$. We will show that the matrix $M^{-1}\tilde{A} + U(x)I$ has at least one negative eigenvalue whose eigenvector has zero center of mass. Since the eigenvalue in the u_1-direction normal to the center of mass subspace is $\lambda_1 = U(x)$, it suffices to show that $\mathrm{tr}(M^{-1}\tilde{A} + U(x)I) < -U(x)$ or, equivalently,

$$\tau = -\operatorname{tr} M^{-1}\tilde{A} > (n-1)U(x).$$

Now

$$\tau = \sum_i \sum_{j \neq i} \frac{m_j}{r_{ij}^3} = \sum_{\substack{(i,j) \\ i<j}} \frac{m_i + m_j}{r_{ij}^3}.$$

The problem, of course, is that we do not have much control over the mutual distances. All we know is that we are at some CC. The following approach is due to Albouy [1].

We will use the reduced version of the CC equation (2.29). Viewing B as a bilinear form on the hyperplane $\mathcal{D}^*$, we can use the matrix representative $\hat{B}$ from (2.27). For each pair of standard basis vectors in $\mathbb{R}^n$, e_i, e_j, $i < j$, we have $e_i - e_j \in \mathcal{D}^*$. From (2.29),

$$(e_i - e_j)^T(\hat{B}A + \lambda\hat{B})(e_i - e_j) = 0, \quad i < j.$$

We have $(e_i - e_j)^T\hat{B}(e_i - e_j) = r_{ij}^2$. The other term is more complicated but with some effort we arrive at

$$2\lambda = \frac{2(m_i + m_j)}{r_{ij}^3} + \sum_{k\neq i,j} m_k\left(\frac{1}{r_{ik}^3} + \frac{1}{r_{jk}^3}\right) + \sum_{k\neq i,j} m_k(r_{ik}^2 - r_{jk}^2)\left(\frac{1}{r_{ik}^3} - \frac{1}{r_{jk}^3}\right).$$

Note that the two parentheses in the last sum always have opposite signs unless they are both zero. So the sum is strictly negative unless all of the mutual distances are equal. However, this would mean that the configuration was the regular simplex with $\dim(x) = n - 1$. By hypothesis, this is not the case, so we can drop the last sum to get a strict inequality. Summing this inequality over all pairs $i < j$ gives

$$n(n-1)\lambda < n\tau.$$

Since x is a normalized CC, we have $\lambda = U(x)$ and this is exactly the inequality we need. □

Upper bounds on the index are also of interest. For planar central configurations we have the following result of Palmore which shows that the collinear CC's have the maximum possible index.

Proposition 2.10.3. *If x is a central configuration of the n-body problem in $\mathbb{R}^2$, then* $\mathrm{ind}(x) \leq n - 2$.

Proof. For the planar problem, the dimension of the normalized configuration space is $\dim\mathcal{N} = 2n - 3$. The tangent space $T_x\mathcal{N}$ is given by

$$x^TMv = 0, \quad \hat{L}Mv = 0,$$

where $\hat{L}$ is the $2 \times 2n$ matrix consisting of n copies of the 2×2 identity matrix.

Let j be the rotation of the plane by $\pi/2$ and let it act on vectors $v = (v_1, \ldots, v_n) \in \mathbb{R}^{2n}$ by $jv = (jv_1, \ldots, jv_n)$, as usual. The vector $v_0 = jx$ is in the tangent space and is tangent to the action of the rotation group $\mathrm{SO}(2)$ so $v_0 \in \ker H(x)$. The orthogonal complement $v_0^\perp$ is a $(2n-4)$-dimensional subspace of $T_x\mathcal{N}$ and is invariant under the action of j.

For $v \in T_x\mathcal{N}$, it turns out that $H(x)(v, v) + H(x)(jv, jv) > 0$. To see this we will use formula (2.49). The inner product terms are

$$3(u_{ij} \cdot v_{ij})^2 + 3(u_{ij} \cdot jv_{ij})^2 = 3|v_{ij}|^2$$

since the vectors u_{ij} and ju_{ij} form an orthonormal basis for $\mathbb{R}^2$. Then (2.49) gives

$$H(x)(v,v) + H(x)(jv,jv) = \sum_{i<j} \frac{m_i m_j}{r_{ij}^3} \left(|v_{ij}|^2\right) + 2U(q)v^T Mv > 0.$$

Suppose $S \subset T_x\mathcal{N}$ is a maximal subspace on which $H(x)$ is negative semi-definite. We may as well assume that $S \subset v_0^\perp$. From the positivity of $H(x)(v,v) + H(x)(jv,jv)$ it follows that we must have $S \cap jS = \{0\}$ and hence $\mathrm{ind}(x) = \dim S \leq n-2$. □

For $d = 3$ it is known, at least, that $U|_{\mathcal{N}}$ does not have any local maxima. See [20, 23] for these results. I don't know if this is still true for $d > 3$.

2.11 Morse theory for CC's and SBC's

In this section we will describe how to use Morse theory to prove existence of CC's. This approach was initiated by Smale [34] and developed by Palmore [28] for the planar n-body problem, and then extended to three dimensions using equivariant Morse theory by Pacella [27]. An alternative approach to the three-dimensional case is due to Merkel [19].

Recall that central configurations in $\mathbb{R}^d$, $d \geq 2$, correspond to degenerate critical points of $U|_{\mathcal{N}}$ due to the action of the symmetry group $\mathrm{SO}(d)$. In the planar case, $\mathrm{SO}(2) \simeq \mathbf{S}^1$ acts freely on $\mathcal{N} \setminus \Delta$ and we can think of U as a smooth function on the quotient manifold

$$\mathcal{M} = (\mathcal{N} \setminus \Delta)/\,\mathrm{SO}(2).$$

We can still define such a quotient space when $d > 2$ but, due to the non-free action of $\mathrm{SO}(d)$, it will not be a manifold. In Section 2.8, we defined the concept of non-degeneracy for CC's with the symmetry group in mind so, using this terminology, a nondegenerate CC of the planar n-body problem determines a nondegenerate critical point in the manifold $\mathcal{M}$.

A generic smooth function on a manifold is a *Morse function*, that is, all of its critical points are nondegenerate. But it is difficult to actually verify this for particular functions like the Newtonian potential. From Proposition 2.9.2 we know that the collinear CC's are nondegenerate.

When $n = 3$ the only non-collinear CC's are the equilateral triangles and these are nondegenerate. The same holds for the regular simplex in the n-body problem.

Proposition 2.11.1. *For every choice of n positive masses, the regular simplex is a nondegenerate central configuration. It is a nondegenerate minimum of the potential in the quotient space $\mathcal{M}$.*

Proof. Suppose $d = n-1$. As noted above, $\mathrm{SO}(d)$ acts freely on the open subset of $\mathbb{R}^{n(n-1)} \setminus \Delta$ consisting of configurations with $\dim(x) = n-1$, and we can use the mutual distances r_{ij} as local coordinates in the corresponding open subset of the quotient space under rotations and translations. In these coordinates, the matrix of second derivatives of $F = I + U$ is diagonal and the partial derivatives $\partial^2 F/\partial r_{ij}^2$ are all positive.

Now suppose we have a curve $\gamma(t)$ of normalized configurations passing through the regular simplex when $t = 0$, and whose tangent vector $\gamma'(0)$ is not in the direction of the rotational symmetry. We would like to show that $U(\gamma(0))'' > 0$. The corresponding curve of mutual distances $r_{ij}(t)$ passes through the equal-distance point corresponding to the normalized regular simplex and we have $F(r_{ij}(t)) = 1 + U(\gamma(t))$. From the discussion in the previous paragraph we have $U(\gamma(0))'' = F(r_{ij}(0))'' > 0$, as required. □

It follows that for the planar three-body problem and for all choices of the three masses, the Newtonian potential determines a Morse function on $\mathcal{M}$. The space of normalized triangles is a three-dimensional ellipsoid. The quotient space under the rotation group is diffeomorphic to $\mathbf{S}^2$ and is called the *shape sphere* since it represents all possible shapes of triangles in the plane up to translation, rotation and scaling. $\mathcal{M}$ is the shape sphere with three collision shapes deleted. Figure 2.9 shows the level curves of the potential for two choices of the masses. The poles represent the equilateral triangles which are minima. On the equator, which represents the collinear shapes, there are the three collinear central configurations found by Euler, which are saddle points.

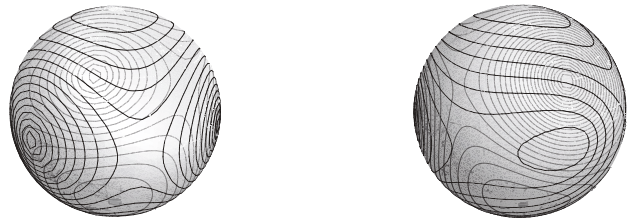

Figure 2.9: $\mathcal{M}$ for the planar three-body problem is the shape sphere. The Newtonian potential determines a Morse function with five critical points, shown here for the case of equal masses (left) and masses 1, 2, and 10 (right).

For $n > 3$, $d \geq 2$, it is much harder to check whether the critical points are nondegenerate. For the planar four-body problem Palmore showed that degenerate central configurations can occur for some choices of the masses and this is related to bifurcations in the number of central configurations as the masses are varied. Simó investigated the bifurcations numerically [33]. In Section 2.14 we will show

that for generic choices of the masses in the planar four-body problem the potential determines a Morse function.

Now we will see what Morse theory tells us about the number of central configurations in the plane, taking the nondegeneracy of the critical points as an assumption. Morse theory is based on the gradient flow induced by a function on a Riemannian manifold. In our case the manifold is the quotient manifold $\mathcal{M}$, where we can use the restriction of the mass inner product as the Riemannian metric. First consider the gradient flow on $\mathcal{N} \setminus \Delta$. If the masses are fixed, Shub's lemma allows us to restrict to a compact set of the form $K = \{x \in \mathcal{N} : U(x) \leq U_0\}$ for some sufficiently large U_0. By definition, the gradient vector field of $U|_{\mathcal{N}}$ with respect to an inner product is the unique tangent vector field $\tilde{\nabla} U(x)$ with the property

$$\langle \tilde{\nabla} U(x), W \rangle = DU(x)W, \quad W \in T_x \mathcal{N}.$$

Using the mass inner product $\langle \xi, \eta \rangle = \xi^T M \eta$, one can check that the gradient vector field is the restriction of

$$\tilde{\nabla} U(x) = M^{-1} \nabla U(x) + U(x)x$$

to $\mathcal{N}$. By rotation invariance, this vector field determines a gradient flow on the quotient space $\mathcal{M}$. Orbits of the gradient flow cross the level sets of U orthogonally in the direction of increasing U. Orbits starting in the compact set K will continue to exist at least until they reach the exit level $U = U_0$.

The Morse inequalities relate the indices of the critical points of a Morse function on a manifold $\mathcal{M}$ to the topology of the manifold. They are most easily expressed in terms of polynomial generating functions. Define the *Morse polynomial* as

$$M(t) = \sum_k \gamma_k t^k,$$

where γ_k is the number of critical points of index k, and the *Poincaré polynomial* as

$$P(t) = \sum_k \beta_k t^k,$$

where β_k is the k-th Betti number of the manifold, i.e., the rank of the homology group $H_k(\mathcal{M}, \mathbb{R})$ with real (or rational) coefficients. Then the Morse inequalities can be written

$$M(t) = P(t) + (1 + t)R(t), \tag{2.52}$$

where $R(t)$ is some polynomial with nonnegative integer coefficients. In particular, the Betti number β_k is a lower bound on the number of critical points of index k.

It turns out that the manifold $\mathcal{M}$ has a complicated topology so the Morse inequalities give interesting results. Recall that, for the n-body problem in $\mathbb{R}^d$, the space $\mathcal{N}$ of normalized configurations is an ellipsoid of dimension $d(n-1)-1$. It is the deletion of collision set Δ which produces the topological complexity.

Proposition 2.11.2. *For the n-body problem in $\mathbb{R}^d$, the Poincaré polynomial of $\mathcal{N} \setminus \Delta$ is*

$$\tilde{P}(t) = (1 + t^{d-1})(1 + 2t^{d-1}) \cdots (1 + (n-1)t^{d-1}).$$

In particular, for the planar three-body problem we have

$$\tilde{P}(t) = (1 + t)(1 + 2t) = 1 + 3t + 2t^2.$$

Proof. It suffices to find the Betti number of the unnormalized space $\mathbb{R}^{dn} \setminus \Delta$. To do this, note that the normalization of the center of mass and moment of inertia gives a diffeomorphism

$$\mathbb{R}^{dn} \setminus \Delta \simeq \mathbb{R}^d \times \mathbb{R}^+ \times (\mathcal{N} \setminus \Delta).$$

Now Künneth's theorem from algebraic topology shows that the Poincaré polynomial of a product space is the product of the Poincaré polynomials of the factors. Here, the first two factors are homologically trivial with Poincaré polynomials equal to 1.

The computation for $\mathbb{R}^{dn} \setminus \Delta$ is by induction on n. For $n = 1$ we have

$$\mathbb{R}^d \setminus \Delta = \mathbb{R}^d \setminus \{0\} \simeq \mathbb{R}^+ \times \mathbf{S}^{d-1}$$

and we get the Poincaré polynomial of a sphere, $\tilde{P}(t) = 1 + t^{d-1}$. For $n > 1$ we have a fiber bundle $\pi\colon \mathbb{R}^{dn} \setminus \Delta \to \mathbb{R}^{d(n-1)} \setminus \Delta$ where the projection just forgets the n-th body, $\pi(x_1, \ldots, x_n) = x_1, \ldots, x_{n-1})$. The fiber over a point $(x_1, \ldots, x_{n-1})$ is $\mathbb{R}^d \setminus \{n - 1 \text{ points}\}$ because the n-th body must avoid the other $n - 1$. Now this fiber bundle is not a product but it does satisfy certain topological conditions which guarantee that the Poincaré polynomials multiply. First, there is a cross-section map $\sigma\colon \mathbb{R}^{d(n-1)} \setminus \Delta \to \mathbb{R}^{dn} \setminus \Delta$ with $\pi \circ \sigma = id$. For example, we could let the n-th body of $\sigma(x_1, \ldots, x_{n-1})$ be at the point obtained by translating the barycenter of the other $n-1$ bodies a distance greater than the maximum distance between these bodies in the direction of the first coordinate axis. In addition, the fundamental group of the base acts trivially on the fiber (for $d \neq 2$ the base is simply connected). In any case, we go from the Poincaré polynomial for $(n - 1)$ bodies to the polynomial for n bodies by multiplying by the Poincaré polynomial of the fiber, namely $1 + (n - 1)t^{d-1}$. □

Next we restrict attention to the planar problem and pass to the quotient space $\mathcal{M}$ under the $\mathbf{S}^1$ action. The image of the normalized space $\mathcal{N} \simeq \mathbf{S}^{2n-3}$ is diffeomorphic to the complex projective space $\mathbb{CP}(n - 2)$ and the projection is a nontrivial circle bundle. But when we delete the collision set, the bundle becomes trivial. For example, there is a global cross-section to the circle action consisting of all noncollision configurations where the vector from x_1 to x_2 is the direction of the positive first coordinate axis. It follows that, in the planar case,

$$\mathcal{N} \setminus \Delta \simeq \mathbf{S}^1 \times \mathcal{M}.$$

Proposition 2.11.3. *For the n-body problem in $\mathbb{R}^2$, the Poincaré polynomial of the rotation reduced, normalized configuration space is*

$$P(t) = (1+2t)\cdots(1+(n-1)t).$$

Proof. Since $\mathcal{N} \setminus \Delta$ is the product of a circle and $\mathcal{M}$, we have $\tilde{P}(t) = (1+t)P(t)$. Then Proposition 2.11.2 with $d = 2$ gives the result. □

For example when $n = 3, 4$ we have, respectively,

$$P(t) = 1 + 2t, \quad P(t) = (1+2t)(1+3t) = 1 + 5t + 6t^2.$$

For $n = 3$, the Betti numbers $\beta_0 = 1$ and $\beta_1 = 2$ describe the homology of the shape sphere with the three collision points deleted which is diffeomorphic to the twice punctured plane.

To apply the Morse inequalities to the planar n-body problem first note that we have, after quotienting by rotations, $n!/2$ collinear central configurations. By Proposition 2.9.2, these have Morse index $n-2$. The next result, due to Palmore, uses this information to good effect.

Proposition 2.11.4. *Suppose that all of the central configurations are nondegenerate for a certain choice of masses in the planar n-body problem. Then there are at least*

$$\frac{(3n-4)(n-1)!}{2}$$

central configurations, of which at least

$$\frac{(2n-4)(n-1)!}{2}$$

are non-collinear.

Proof. The simplest lower bound on the number of critical points is obtained by setting $t = 1$ in (2.52):

$$\sum_k \gamma_k \geq \sum_k \beta_k = P(1) = \frac{n!}{2}.$$

But the information about the collinear configurations mentioned above shows that in the Morse polynomial, we have $\gamma_{n-2} \geq n!/2$. On the other hand, the coefficient of t^{n-2} in the Poincaré polynomial $P(t)$ is $\beta_{n-2} = 2 \cdot 3 \cdots (n-1) = (n-1)!$.

Let $R(t) = \sum_k r_k t^k$ be the residual polynomial in the Morse inequality (2.52). Then we have

$$r_{n-2} + r_{n-3} \geq \frac{n!}{2} - (n-1)!.$$

Setting $t = 1$ in (2.52) now gives

$$\sum_k \gamma_k \geq \frac{n!}{2} + 2(r_{n-2} + r_{n-3}) \geq \frac{3n!}{2} - 2(n-1)! = \frac{(3n-4)(n-1)!}{2}.$$

Subtracting $n!/2$ gives the non-collinear estimate. □

For example, when $n = 3$ the Morse estimate gives five critical points, which is exactly right. For $n = 4$ we have at least 24 CC's of including the 12 collinear ones, assuming nondegeneracy. The estimates increase rapidly with n —we expect there to be many CC's.

In the nonplanar case, the reduction of symmetry is more complicated and the quotient space is not a manifold. See [19, 27] for two approaches to the spatial case. We also mention the paper of McCord [18] which gives estimates based on Lyusternik–Schnirelmann theory instead of Morse theory.

Instead of pursuing this, we will just make a few remarks on what Morse theory can tell us about balanced configurations. Recall that these also admit a variational characterization as critical points of $U|_{\mathcal{N}(S)}$, where $\mathcal{N}(S)$ is the space of normalized configurations with respect to the metric based on the symmetric matrix S, $\langle \xi, \eta \rangle = \xi^T \hat{S} M \eta$. Now if we fix a symmetric matrix S with distinct eigenvalues, there is no longer any rotational symmetry and we can have nondegenerate critical points in $\mathcal{N}(S) \setminus \Delta$. The topology of this space is independent of S, so we can use the Poincaré polynomial $\tilde{P}(t)$ from Proposition 2.11.2.

This time there are more collinear configurations. If we fix any one of the d eigenlines of S we will find $n!$ collinear SBC's which are nondegenerate with Morse index $(d-1)(n-1)$. There are d eigenlines for a total of $d\,n!$ collinear SBC's. If we knew their indices, it might be possible to use the information to get strong Morse estimates for the number of non-collinear SBC's. It seems that the proof of Proposition 2.9.2 can be generalized to show that the collinear SBC's corresponding to the largest eigenvalue of S have index $(d-1)(n-1)$ which would give $\gamma_{(d-1)(n-1)} \geq n!$. Using this to estimate the residual polynomial as in the proof of Proposition 2.11.4 gives a lower bound

$$\sum_k \gamma_k \geq (3n-1)(n-1)!,$$

but this exceeds the known count of $d\,n!$ collinear configurations only for $d = 2$.

2.12 Dziobek configurations

In Section 2.9 we studied collinear central configurations. These are at the lower end of the dimension range for an n-body configuration, $1 \leq \dim(x) \leq n-1$. We also saw that the only CC with $\dim(x) = n-1$ is the regular simplex. In this section we consider the highest nontrivial dimension.

Definition 2.12.1. *A* Dziobek *configuration is a configuration of n bodies with* $\dim(x) = n-2$.

The physically interesting examples are collinear configurations of 3 bodies, planar but non-collinear configurations of 4 bodies, and spatial but nonplanar configurations of 5 bodies. They are named after Otto Dziobek who studied the planar

four-body case [10]. We will be interested in finding Dziobek central configurations (DCC's).

We begin by studying the geometry of Dziobek configurations. We will assume that the dimension of the ambient space is $d = n - 2$ so any n-body configuration is given by $x = (x_1, \ldots, x_n)$ with $x_j \in \mathbb{R}^{n-2}$. It is useful to associate with x the so-called $(n-1) \times n$ *augmented configuration matrix*

$$\hat{X} = \begin{bmatrix} 1 & \cdots & 1 \\ \hline x_1 & \cdots & x_n \end{bmatrix}. \tag{2.53}$$

This is just the configuration matrix of Section 2.4 with a row of ones added to the top. Then it is easy to see that $\dim(x) = \operatorname{rank} \hat{X} - 1$. Note that, because of the row of ones, two configurations are translation equivalent if and only if their augmented configuration matrices have the same row space or, equivalently, the same kernel.

For a Dziobek configuration we have $\operatorname{rank} \hat{X} = n - 1$ and $\dim \ker \hat{X} = 1$. Hence there is a nonzero vector $\Delta = (\Delta_1, \ldots, \Delta_n)$, unique up to a constant multiple, such that

$$\begin{aligned} \Delta_1 + \cdots + \Delta_n &= 0, \\ x_1\Delta_1 + \cdots + x_n\Delta_n &= 0. \end{aligned} \tag{2.54}$$

There is a nice formula for a vector Δ satisfying (2.54). Let $\hat{X}_k$ be the $(n-1) \times (n-1)$ matrix obtained from X by deleting the k-th column and let $|\hat{X}_k|$ denote its determinant. Then,

$$\Delta = (|\hat{X}_1|, -|\hat{X}_2|, \ldots, (-1)^{k+1}|\hat{X}_k|, \ldots)^T \tag{2.55}$$

is a solution to (2.54). Moreover, since the determinants are proportional to the volumes of the $(n-2)$-simplices of the deleted configurations, at least one of them is nonzero in the Dziobek case.

Next we will reformulate the dimension criteria above in terms of the mutual distances r_{ij} or rather, their squares $s_{ij} = r_{ij}^2$. Using equations (2.54) we have

$$\sum_j s_{ij}\Delta_j = |x_i|^2 \sum_j \Delta_j - 2x_i \cdot \sum_j x_j\Delta_j + \sum_j |x_j|^2\Delta_j = \sum_j |x_j|^2\Delta_j, \tag{2.56}$$

where i is any fixed index and the sum over j runs from 1 to n (here, $s_{ii} = 0$). The result is independent of i and we denote it by $-\Delta_0$. Define the Cayley–Menger

matrix and determinant by

$$CM(x) = \begin{bmatrix} 0 & 1 & 1 & 1 & \cdots & 1 \\ 1 & 0 & s_{12} & s_{13} & \cdots & s_{1n} \\ 1 & s_{12} & 0 & s_{23} & \cdots & s_{2n} \\ 1 & s_{13} & s_{23} & 0 & \cdots & s_{3n} \\ \vdots & \vdots & \vdots & \vdots & & \vdots \\ 1 & s_{1n} & s_{2n} & s_{3n} & \cdots & 0 \end{bmatrix}, \quad F(x) = |CM(x)|. \tag{2.57}$$

Then we have $CM(x)\Delta = 0$, where now $\Delta = (\Delta_0, \Delta_1, \ldots, \Delta_n)$. Consequently, we have

$$F(x) = |CM(x)| = 0$$

for any Dziobek configuration or, indeed, for any configuration with $\dim(x) \leq n-2$.

In order to find equations for Dziobek central configurations (DCC's), begin by setting $\lambda = m_0\lambda'$ in the standard equations (2.10). After some algebra we find that, for each $j = 1, \ldots, n$,

$$\sum_{i=1}^{n} m_i S_{ij} x_i = 0, \tag{2.58}$$

where

$$\begin{aligned} S_{ij} &= \frac{1}{r_{ij}^3} - \lambda', \quad i \neq j, \\ m_j S_{jj} &= -\sum_{i \neq j} m_i S_{ij}. \end{aligned} \tag{2.59}$$

Proposition 2.12.2. *Let x be a Dziobek central configuration of the n-body problem, let S_{ij} be given by* (2.59) *and let Δ be any nonzero solution of* (2.54)*. Then there is a real number $\kappa \neq 0$ such that*

$$m_i m_j S_{ij} = \kappa \Delta_i \Delta_j. \tag{2.60}$$

Moreover, at least two of the Δ_i are nonzero.

Proof. Equation (2.58) and the second equation of (2.59) show that for each $j = 1, \ldots, n$ the vector

$$(m_1 S_{1j}, m_2 S_{2j}, \ldots, m_n S_{nj})$$

is a solution to equations (2.54). Since the solution is unique up to a constant multiple, there must be constants k_j such that $m_i S_{ij} = k_j \Delta_i$. Since $S_{ij} = S_{ji}$, the vector $(k_1, \ldots, k_n)$ is a multiple $\kappa(\Delta_1/m_1, \ldots, \Delta_n/m_n)$ so we get (2.60) for some real number κ. If $\kappa = 0$ or if only one of the Δ_i were nonzero then all of the S_{ij}, $i \neq j$, would vanish and so all of the r_{ij} would be equal. But this only happens for the regular simplex, which is not a Dziobek configuration. □

Multiplying two of the equations (2.60) gives:

Corollary 2.12.3. *Let x be a Dziobek configuration and let S_{ij} be given by* (2.59). *Then for any four indices $i, j, k, l \in \{1, \ldots, n\}$ we have*

$$S_{ij}S_{kl} = S_{il}S_{kj}.$$

These equations can be used to derive some mass independent constraints on the shapes of CC's. For example, when $n = 4$ we have two independent equations of the form

$$(r_{12}^3 - \lambda')(r_{34}^3 - \lambda') = (r_{13}^3 - \lambda')(r_{24}^3 - \lambda') = (r_{14}^3 - \lambda')(r_{23}^3 - \lambda').$$

Eliminating λ' gives a necessary condition on the distances, in addition to the vanishing of the Cayley–Menger determinant, for a configuration to be central for some choice of the masses.

2.13 Convex Dziobek central configurations

In this section we present an existence proof for convex Dziobek configurations based on ideas of Xia [37]. First we discuss the geometry of the space of convex configurations. Consider the n-body problem in $\mathbb{R}^{n-2}$ as in Section 2.12. The normalized configuration space $\mathcal{N}$ is diffeomorphic to a sphere of dimension $(n-1)(n-2)-1$. The Dziobek configurations form an open subset, but $\mathcal{N}$ also contains configurations with $\dim(x) < n-2$.

For each $x \in \mathcal{N}$, let $\Delta(x)$ be the vector of determinants (2.55) representing, up to a factor, the $(n-2)$-dimensional volumes of its $(n-1)$-body subconfigurations. Then $\Delta\colon \mathcal{N} \to \mathcal{V} \subset \mathbb{R}^n$, where $\mathcal{V}$ is the hyperplane $\Delta_1 + \cdots + \Delta_n = 0$. If x is a Dziobek configuration then at least two of the determinants Δ_i are nonzero and Δ determines a point $[\Delta]$ of the unit sphere $\mathbf{S}(\mathcal{V}) \simeq \mathbf{S}^{n-2}$ in $\mathcal{V}$. The planes $\Delta_i = 0$ divide the sphere into components where the signs of the Δ_i are constant.

The signs of the variables Δ_i provide a geometric classification of Dziobek configurations. Suppose, for example, that $\Delta_n \neq 0$ so that the first $n-1$ bodies span a nondegenerate simplex in $\mathbb{R}^{n-2}$ and the ratios $b_i = -\Delta_i/\Delta_n$, $i = 1, \ldots, n-1$, are the barycentric coordinates of x_n with respect to this simplex [6]. In particular, x_n is in the interior of the simplex if and only if $b_i > 0$ for $i = 1, \ldots, n-1$. This provides a simple characterization of when a Dziobek configuration is *nonconvex*, namely, we must have either exactly one $\Delta_i > 0$ and $\Delta_j < 0$ for $j \neq i$, or else exactly one $\Delta_i < 0$ and $\Delta_j > 0$ for $j \neq i$. Let $\mathcal{N}CD \subset \mathcal{N}$ denote the open set of nonconvex Dziobek configurations.

The complement $K = \mathcal{N} \setminus \mathcal{N}CD$ is a compact set containing all of the convex Dziobek configurations. There will be some point $x \in K$ where $U|_K$ achieves its minimum and we would like to conclude that x is a convex Dziobek central configuration. This entails showing that the minimum does not occur on the boundary ∂K. We will prove this for $n = 4$ and get existence of planar, noncollinear convex central configurations for the four-body problem, a result due to

MacMillan–Bartky [17]. Unfortunately, there seem to be problems extending the proof to higher dimensions. To highlight the difficulties, we will split the proof into two parts. First we consider the part of ∂K consisting of Dziobek configurations. This part of the proof works for all n.

Proposition 2.13.1. *Let $x \in \partial K$ be a Dziobek configuration. Then x is not the minimizer of $U|_K$.*

Proof. We will show that arbitrarily close to x, there are points of K with strictly smaller values of $U|_K$. Instead of working with normalized configurations and $U|_K$, we can forget the normalization and use the homogeneous function $G = I(x)U(x)^2$.

By hypothesis, there is a sequence of nonconvex Dziobek configurations $x^k \to x$. After re-indexing and taking a subsequence we may assume that for all k, the n-th body x_n^k is contained in the interior of the simplex formed by $x_1^k, \ldots, x_{n-1}^k$. Taking the limit we conclude that x_n is contained in the boundary of the closed simplex formed by $x_1, \ldots, x_{n-1}$. Since we are assuming that x is still a Dziobek configuration, $x_1, \ldots, x_{n-1}$ span a nondegenerate $(n-2)$-simplex. After re-indexing again, we may assume that x_n is contained in the facet of this simplex spanned by $x_2, \ldots, x_{n-1}$. Let x_{ik}, $k = 1, \ldots, n-2$, denote the coordinates of the bodies in the ambient space $\mathbb{R}^{n-2}$. After a rotation and translation we may assume $x_{11} > 0$ and $x_{i1} = 0$, $i = 2, \ldots, n-1$. In other words all of the bodies except x_1 lie in a coordinate plane with x_1 strictly to the right.

Consider the distances r_{1k} from x_1 to the other bodies. Since x_n is contained in the closed simplex spanned by $x_2, \ldots, x_{n-1}$, we will have $r_{1n} < r_{1k}$ for some $k \in \{2, \ldots, n-1\}$ and we may assume without loss of generality that $r_{1n} < r_{12}$. Then we will see that moving x_n a little to the left while moving x_2 a little to the right decreases G. Moreover these perturbed configurations are in K.

We will use mutual distance version of the moment of inertia (2.9) and the usual formula for $U(r_{ij})$. Note that if we move x_2, x_n in the direction of the first coordinate axis, the derivatives of the distances r_{ij}, $2 \le i < j \le n$, are all zero. Only r_{12} and r_{1n} change to first order. If we change the first coordinates of x_2, x_n by $\delta x_{21} = m_2^{-1}\xi$ and $\delta x_{n1} = -m_n^{-1}\xi$ for some small $\xi > 0$, a short computation shows that the first-order change in G is

$$\delta G = 2IUm_1 x_{11}\xi(r_{12}^{-3} - r_{1n}^{-3}),$$

where $x_{11} > 0$ is the first coordinate of x_1. Since $r_{1n} < r_{12}$ and $\xi > 0$, we have $\delta G < 0$ as required. □

Next we need to consider boundary points $x \in \partial K$ with $\dim(x) < n-2$. It is easy to see that every configuration with $\dim(x) < n-2$ can be perturbed into both a convex and nonconvex Dziobek configuration, hence all such lower-dimensional configurations are in ∂K. Fix a dimension $k < n-2$ and let $\mathcal{N}_k \subset \mathcal{N}$ be the set of configurations with $\dim(x) \le k$. Since $\mathcal{N}_k \subset \partial K \subset K$ it follows that if $x \in \mathcal{N}_k$ is a minimizer of $U|_K$ then it is also a minimizer of $U|_{\mathcal{N}_k}$ and is therefore a lower-dimensional CC. Therefore, in order to rule out such boundary

points we need to understand how the potential changes when we perturb x to a convex Dziobek configuration. We know from Proposition 2.10.1 that there will be some perturbation to a Dziobek configuration which lowers the potential, but we do not know that this perturbation moves us into K. When $n = 4$, however, the only lower-dimensional configurations are collinear and we have the stronger Proposition 2.9.2.

Proposition 2.13.2. *There exists at least one convex, planar, non-collinear central configuration of the four-body problem for each cyclic ordering of the bodies; hence, at least six in all, up to similarity in the plane.*

Proof. If $x \in \partial K$ is a collinear configuration, then Proposition 2.9.2 shows that every perturbation of x to a non-collinear configuration in $\mathcal{N}$ will lower the potential. In particular, perturbing x into K will lower the potential. On the other hand, Proposition 2.13.1 shows that the non-collinear boundary points also admit potential-lowering perturbations into K. So the minimizer of $U|_K$ is in the interior as required.

Note that there are six components of Dziobek configurations with Δ's having the convex sign patterns

$$(+,+,-,-), \quad (+,-,+,-), \quad (+,-,-,+),$$

and the three more with the signs reversed. These correspond to the distinct cyclic orderings. If K_0 is the closure of any one of these, we can apply the same argument to find a CC in its interior. We only need to note that the required potential-lowering perturbations can be made into K_0. □

In [37] it is claimed that the analogous result holds for $n = 5$, but as noted above, more information about the behavior of planar five-body CC's under perturbations into Dziobek configurations seems to be needed.

Given that convex Dziobek configurations exist, one can ask about their possible shapes. It is possible to use equations (2.60) together with the positivity of the masses and the signs of the Δ_i to derive some simple geometrical constraints, see [17, 30].

Finally, we can use the existence of at least six local minima to improve the Morse estimates for the planar four-body problem. Recall that Proposition 2.11.4 gives the existence of at least twenty four CC's, including the twelve collinear ones (assuming that all critical points are nondegenerate). The twelve collinear CC's have index 2 which is the maximum possible, and the six convex Dziobek configurations are minima so $\gamma_0 \geq 6$ if they are nondegenerate. The Morse inequalities become

$$\gamma_0 + \gamma_1 t + \gamma_2 t^2 = 1 + 5t + 6t^2 + (1+t)(r_0 + r_1 t),$$

where $\gamma_0 \geq 6$ and $\gamma_2 \geq 12$. It follows that $r_0 \geq 5$ and $r_1 \geq 6$. Setting $t = 1$ gives a lower bound for the total number of CC's of

$$\gamma_0 + \gamma_1 + \gamma_2 \geq 12 + 2(5+6) = 34.$$

This lower bound seems to be sharp although there can be as few as 32 in degenerate cases, see [12, 33].

2.14 Generic finiteness for Dziobek central configurations

In this section we will present a proof that there are at most finitely many similarity classes of Dziobek central configurations for generic choices of the masses; the proof is based on [22]. We will also sketch a proof that these central configurations are generically nondegenerate.

Proposition 2.14.1. *For generic choices of the masses, there are only finitely many Dziobek central configurations up to similarity. In fact there is a mass-independent bound on the number of such configurations valid whenever the number is finite.*

In particular, this applies to planar CC's of the four-body problem and spatial but nonplanar CC's of the five-body problem. For the four-body problem, the only non-Dziobek central configurations are the regular tetrahedron and the collinear CC's. So in this case it follows that the total number of CC's is generically finite. However, there is a stronger result [14]: the number of CC's is finite for *all* choices of positive masses and is at most 8472. This is proved by completely different methods which required extensive algebraic computations. Similar methods were applied to the spatial five-body problem in [13] with the result that the generic conditions on the masses mentioned in Proposition 2.14.1 are made explicit. For the planar five-body problem, Albouy and Kaloshin have recently proved generic finiteness with explicit genericity conditions, see [4]. It is still open whether or not there exist exceptional choices of five positive masses which admit infinitely many CC's, but Roberts has an example involving masses of different signs [29]. The problem of finiteness for planar CC's was singled out by Steve Smale as the sixth of eighteen problems for twenty-first century mathematics [35]. But for $n > 5$ even generic finiteness is open.

The rest of this section is devoted to the proof of Proposition 2.14.1. The key point is to find the dimension of the algebraic variety defined by the equations for Dziobek central configurations. If the dimension of the space of central configurations is the same as the dimension of the space of normalized mass parameters, then the generic finiteness will follow from general theorems of algebraic geometry. For example, in Figure 2.7, Euler's quintic equation defines a two-dimensional surface. The projection of the surface to the two-dimensional normalized mass space necessarily has zero-dimensional fibers, at least for generic masses. In this case, all of the fibers are finite.

We begin with equations (2.60) relating the quantities S_{ij} from (2.59) and the Δ_i variables. However, we will make a few modifications. First of all, it is theoretically advantageous to work with complex, projective algebraic varieties

which are defined by homogeneous polynomial equations. Define a new variable r_0 such that $\lambda' = r_0^{-3}$ so that

$$S_{ij} = r_{ij}^{-3} - r_0^{-3}.$$

Let $p = n(n-1)/2$ be the number of mutual distance variables r_{ij}. We will think of the vector $r = (r_0, r_{12}, \ldots, r_{34}) \in \mathbb{C}^{p+1}$ as homogeneous coordinates for a point $[r] \in \mathbb{CP}(p)$, the complex projective space. Passing from r to $[r]$ can be viewed as an alternative way of normalizing the size of the configuration.

Next we suppress the mass variables from equations (2.60) by defining new variables $z_i = \Delta_i/m_i$. After clearing denominators we get polynomial equations

$$r_0^3 - r_{ij}^3 = \kappa z_i z_j r_0^3 r_{ij}^3. \tag{2.61}$$

The following proposition shows that by introducing another variable z_0 we can get a set of equations which are separately homogeneous in the variables r and $z = (z_0, z_1, \ldots, z_n) \in \mathbb{C}^{n+1}$. We will view z as a set of homogeneous coordinates for a point $[z] \in \mathbb{CP}(n)$.

Proposition 2.14.2. *Suppose r_{ij} are the mutual distances of a Dziobek central configuration for some choice of masses $m_i > 0$. Let $r_0^{-3} = \lambda'$, and let $[r] \in \mathbb{CP}(p)$ be the corresponding point in the projective space. Then there is a point $[z] \in \mathbb{CP}(n)$ such that*

$$z_0^2(r_0^3 - r_{ij}^3) = z_i z_j r_{ij}^3. \tag{2.62}$$

Moreover, the Cayley–Menger determinant vanishes, $F(r) = 0$.

Proof. It follows from Proposition 2.12.2 and the definition of r_0 that there exist $z_i, \kappa \in \mathbb{R}$ such that (2.61) holds. Since $\kappa \neq 0$ we can define $z_0 \in \mathbb{C}$ so that $\kappa z_0^3 = r_0^{-3}$ and then we get equations (2.62). □

Equations (2.62) and the Cayley–Menger determinant are separately homogeneous with respect to the variables r and z so they define a projective variety in the product space $\mathbb{CP}(p) \times \mathbb{CP}(n)$. As usual, we need to exclude the collision configurations. Let

$$\Sigma = \{([r], [z]) \in \mathbb{CP}(p) \times \mathbb{CP}(n) : z_0 r_0 \prod_{i<j} r_{ij} = 0\}.$$

Then we can define the variety

$$V = \{([r], [z]) \in \mathbb{CP}(p) \times \mathbb{CP}(n) \setminus \Sigma : \ F(r) = 0 \text{ and } (2.62) \text{ hold } \},$$

which contains all of the Dziobek central configurations. We will also work with the subvarieties obtained by setting some of the $z_i = 0$. Let

$$V_k = \{([r], [z]) \in V : z_{k+1} = \cdots = z_n = 0\}.$$

These are *quasi-projective* varieties, that is, they are difference sets $V = X \setminus Y$ where X, Y are projective varieties. Much of the theory of complex, algebraic geometry applies to such difference sets. We will use [8, 26, 31] as references for this theory. One important point is that every quasi-projective variety has a projective closure, defined as the smallest projective variety containing V. In general, this is smaller than the variety X.

The following result is crucial for proving the generic finiteness theorem we are after. It shows that the variety V containing the Dziobek configurations has the same dimension as the normalized mass space.

Proposition 2.14.3. *The variety V satisfies* $\dim V = n-1$. *More generally,* $\dim V_k = k-1$, *for all* $k \geq 2$.

Proof. Let $\pi_2 \colon \mathbb{CP}(p) \times \mathbb{CP}(n) \to \mathbb{CP}(n)$ be the projection. The proof for V consists of analyzing the fibers and image of the mapping $\pi_2 \colon V \to \mathbb{CP}(n)$. Suppose $[z] \in \pi_2(V)$ and let $([r], [z]) \in V$. By definition of Σ we have $z_0 r_0 \neq 0$ so there will be a representative r of $[r]$ with $r_0^3 z_0^2 = 1$. Then r_{ij} satisfies

$$g_{ij} = (z_i z_j + z_0^2) r_{ij}^3 - 1 = 0. \tag{2.63}$$

It follows that $z_i z_j + z_0^2 \neq 0$ on $\pi_2(V)$, and that the mapping $\pi_2 \colon V \to \mathbb{CP}(n)$ has finite fibers. If we can show that the projective closure $W = \overline{\pi_2(V)}$ has dimension $\dim W = n-1$, general results from algebraic geometry will give $\dim V = n-1$ as well.

The main point is to show that there exists a nonzero homogeneous polynomial $H(z)$ which vanishes on $\pi_2(V)$. This implies $\dim W \leq n-1$. We have $p+1$ equations for the p variables r_{ij}, namely, equations (2.63) and the Cayley–Menger determinant. To construct $H(z)$, begin by taking the resultant with respect to r_{12} of the Cayley–Menger determinant $F(r)$ and the polynomial g_{12}. The result is a polynomial involving z and the variables r_{ij} but with r_{12} eliminated. Now take the resultant with respect to r_{13} of this new polynomial and g_{13}. Continuing in this way, we can eliminate all of the variables r_{ij} obtaining a homogeneous polynomial $H(z)$ in the z variables alone. It is conceivable that $H(z)$ is identically zero, and the next step is to show this is not the case.

Recall that the vanishing of the resultant is a necessary condition for two polynomials in a single variable to have a common complex root. The polynomials may involve other variables which can be viewed as parameters. If the parameters are such that the leading coefficient of at least one of the two polynomials is nonzero, then the vanishing of the resultant is also sufficient for the existence of a common root. It follows that if $H(z) = 0$ for some $z \in \mathbb{C}^{n+1}$ such that

$$z_i z_j + z_0^2 \neq 0, \quad 1 \leq i < j \leq n, \tag{2.64}$$

then there do exist $r_{ij} \in \mathbb{C}$ such that equations (2.63) and the Cayley–Menger condition hold. Therefore, to show that $H(z)$ is not identically zero, it suffices to

find a single point z such that (2.64) hold, but for which the required r_{ij} do not exist.

To this end, choose z such that $z_0 = 1, z_i = 0, 3 \le i \le n$. Then for $3 \le i, j \le n$ we have $z_i z_j + z_0^2 = 1$ and the equations $g_{ij} = 0$ reduce to $r_{ij}^3 = 1$. So these r_{ij} and their squares s_{ij} are all third roots of unity. On the other hand, if we choose z_1, z_2 so that

$$z_1 z_2 + z_0^2 = 1/\sqrt{8}$$

then $r_{12}^3 = \sqrt{8}$ and s_{12} is twice a third root of unity. We will show that with this z, the Cayley–Menger determinant does not vanish.

Lemma 2.14.4. *Let $\omega_{ij} \in \mathbb{C}$, $0 \le i < j \le n$, be third roots of unity. Then*

$$\begin{vmatrix} 0 & 1 & 1 & 1 & \cdots & 1 \\ 1 & 0 & 2\omega_{12} & \omega_{13} & \cdots & \omega_{1n} \\ 1 & 2\omega_{12} & 0 & \omega_{23} & \cdots & \omega_{2n} \\ 1 & \omega_{13} & \omega_{23} & 0 & \cdots & \omega_{3n} \\ \vdots & \vdots & \vdots & \vdots & & \vdots \\ 1 & \omega_{1n} & \omega_{2n} & \omega_{3n} & \cdots & 0 \end{vmatrix} \neq 0.$$

Proof. The determinant can be expanded as a sum of monomials in the ω_{ij} with integer coefficients. Each monomial is equal to an integer multiple of $1, \omega$ or ω^2 where $\omega = -\frac{1}{2} + \frac{\sqrt{3}}{2}i$. Therefore the determinant is of the form $\alpha + \beta\omega + \gamma\omega^2$ where α, β, γ are integers. An expression of this form vanishes if and only if it is a multiple of the minimal polynomial of ω, $1 + \omega + \omega^2$; that is, if and only if $\alpha = \beta = \gamma$. A necessary condition for this is that $\alpha + \beta + \gamma$ be divisible by 3. Now the sum $\alpha + \beta + \gamma$ is the value of the determinant with all $\omega_{ij} = 1$ which turns out to be $(-1)^n 4$. So the determinant cannot vanish. □

It follows that our homogeneous polynomial $H(z)$ is not identically zero. Therefore the subvariety $Z = \{[z] : H(z) = 0\} \subset \mathbb{CP}(n)$ has dimension $n - 1$. The the projection $\pi_2(V)$ is contained in Z. In fact,

$$\pi_2(V) = \{[z] \in Z : (2.64) \text{ hold}\}.$$

Since $\pi_2(V) \neq \emptyset$, at least some of the irreducible components of Z intersect the set where (2.64) holds. Let W denote the union of these irreducible components (W will be the zero set of those factors of $H(z)$ which are not divisible by any of the polynomials in (2.64)). Then $\dim W = n - 1$ and the complement $W \setminus \pi_2(V)$ is a lower-dimensional subvariety. It follows that W is the projective closure of $\pi_2(V)$ and that $\dim W = \dim V = n - 1$, as claimed.

The proof for V_k is similar, but we use the projection $\pi_2 \colon V_k \to \mathbb{CP}(k)$ where we view $\mathbb{CP}(k)$ as the subset of $\mathbb{CP}(n)$ with $z_{k+1} = \cdots = z_n = 0$. Again we need to see that the resultant $H(z)$ does not vanish identically on $\mathbb{CP}(k)$. This follows because the point z with $H(z) \neq 0$ which we constructed above is actually in $\mathbb{CP}(k)$, $k \ge 2$. □

So far, we have discussed the variety V of Dziobek central configurations without fixing the masses. Next we discuss the mapping from V to the normalized mass space. A nonzero mass vector $m = (m_1, m_2, \ldots, m_n)$ determines a point in the projective space $[m] \in \mathbb{RP}(n-1) \subset \mathbb{CP}(n-1)$. We will think of $\mathbb{CP}(n-1)$ as the normalized mass space. A generic mass vector will mean $[m] \in \mathbb{CP}(n-1) \setminus B$, where B is a proper subvarienty of $\mathbb{CP}(n-1)$. Note that if B is such a proper subvariety then $B \cap \mathbb{RP}(n-1)$ is also a proper subvariety. This follows since any complex polynomial which vanishes identically on $\mathbb{RP}(n-1)$ also vanishes identically on $\mathbb{CP}(n-1)$.

Relations between the variables $([r], [z]) \in V$ and the masses are derived from the fact that the vector

$$\Delta = (\Delta_0, \Delta_1, \ldots, \Delta_n) = (\Delta_0, m_1 z_1, \ldots, m_n z_n)$$

is in the kernel of the Cayley–Menger matrix $CM(r)$ from (2.57). Let $K \subset \mathbb{CP}(p)$ be the subvariety of projective vectors $[r]$ such that $\operatorname{rank} CM(r) < n$. If $[r] \in K$ then r_{ij} cannot be the mutual distance of a Dziobek configuration. Consider the decomposition of V into irreducible components. Call an irreducible component W a *Dziobek component* if $W \not\subset K$. To study generic finiteness for Dziobek configurations it suffices to consider each Dziobek component separately.

If $W \subset V$ is a Dziobek irreducible component, then outside the proper subvariety $W \cap K$, the vector Δ is uniquely determined up to a constant multiple. There are two cases depending on whether or not some of the variables z_i vanish identically on W, a possibility we will denote by $z_i \equiv 0$. If $z_i \not\equiv 0$ for all i then the subset $W_0 = \{([r], [z]) \in W : z_i = 0 \text{ for some } i\}$ is a proper subvariety of W. The uniqueness of Δ implies that $[m]$ is uniquely determined for $([r], [z]) \in W \setminus (W_0 \cup K)$. This means that we have a rational *mass mapping* $W \to \mathbb{CP}(n-1)$ assigning to each point of $W \setminus (W_0 \cup K)$ a unique, projective mass vector (in algebraic geometry, a rational map can be multivalued on a proper subvariety). Since $\dim W = n - 1 = \dim \mathbb{CP}(n-1)$ it follows that a generic $[m]$ has a finite number of preimages in W. More precisely, either the mass mapping takes W into a proper subvariety of the mass space or not. In the first case the generic mass point $[m]$ has no preimages in W. In the latter case, we say that the mapping is *dominant* and the generic point $[m]$ has a nonzero but finite number of preimages, the number being bounded by some bound which is independent of $[m]$.

On the other hand, if some $z_i \equiv 0$ on W we may assume without loss of generality that W is a component of V_k from Proposition 2.14.3. Since $z_{k+1} = \cdots = z_n = 0$, the $(n-k)$ masses $m_{k+1} = \cdots = m_n$ are arbitrary. But other masses are unique up to a constant factor. Then Proposition 2.14.3 shows that

$$\tilde{W} = \{([r], [z], [m] : ([r], [z]) \in W, CM(r)\Delta = 0\}$$

is a subvariety of the product $\mathbb{CP}(p) \times \mathbb{CP}(n) \times \mathbb{CP}(n-1)$ of dimension $(k-1) + (n-k) = n-1$. Projection onto the mass space defines a rational map

$\tilde{W} \to \mathbb{CP}(n-1)$, and the same reasoning as before shows that a generic mass point has a finite number of preimages in W. This completes the proof of generic finiteness.

The generic nondegeneracy of DCC's follows from another nice fact about rational maps of varieties. Consider a dominant rational map between varieties of the same dimension. Then for a generic $[m]$ in the range space, all of its preimages are smooth points (meaning that the variety is locally a complex manifold) and the mapping is a local diffeomorphism. If this holds for a map of complex manifolds then it also holds for the real parts. Applying this theory to the real part of the varieties $\tilde{W}$ in $\mathbb{RP}(p) \times \mathbb{RP}(n) \times \mathbb{RP}(n-1)$ shows that the variety of DCC's looks like a finite covering map near a generic real $[m]$.

On the other hand, consider Dziobek CC's as critical points of U in $\mathcal{M}$, the quotient space of $\mathcal{N}$ under the action of the rotation group. Since we are working in $\mathbb{R}^{n-2}$, the Dziobek configurations have top dimension and the quotient space is locally a manifold. The implicit function theorem shows that DCC has a unique smooth continuation to nearby masses with the map to mass space a local diffeomorphism if and only if it is a nondegenerate critical point in $\mathcal{M}$. So generic masses admit only nondegenerate DCC's.

2.15 Some open problems

We will close these notes by mentioning some open questions about central configurations. Perhaps the simplest one to state, if not to solve, is Smale's sixth problem about finiteness of the number of central configurations in the plane for fixed positive masses [35]. As noted in the last section, even the weaker question of generic finiteness is open for $n > 5$. One could also consider the same problem in higher dimensions or for S-balanced configurations with both the masses and the symmetric matrix S fixed. The generic finiteness problem seems more tractable in light of Roberts' example of a continuum of solutions for fixed nonpositive masses, and the difficulties preventing Albouy and Kaloshin from handling all positive masses in the five-body case. Perhaps opening up the problem to allow SBC's might make a positive mass counterexample possible.

Another type of open problem is about the Morse indices of CC's and SBC's. As noted in Section 2.10, not much is known about the Morse indices of non-collinear CC's and even about collinear SBC's. Good results about this would improve the Morse theoretical estimates of the total number of critical points. It was a lack of information about the Hessian in directions normal to the subspace occupied by the configurations which prevented us from extending the existence proof for convex Dziobek configurations to $n > 4$ bodies. The most natural conjecture, that the normal blocks of the Hessian are negative semi-definite, is not true in general. There are planar CC's for which the potential increases in certain normal directions [20, 24].

As far as we know, the convex Dziobek configurations of the four-body problem are unique given the ordering of the bodies, but no proof has been given. The problem of counting convex Dziobek configurations could be posed for $n > 4$ once the existence problem is solved.

Another group of open questions concerns a topic not treated in these notes, namely the dynamical stability of relative equilibrium and homographic motions. Given a planar CC we saw that we have a simple relative equilibrium solution where the bodies rigidly rotate around their center of mass. In rotating coordinates this becomes an equilibrium and one can ask about its linear stability. In particular, one can ask if there is any relation between the eigenvalues at the equilibrium point and the Morse index of the critical point. All of the known examples of linearly stable relative equilibria correspond to critical points which are local minima. Is this always the case? In light of Albouy–Chenciner's theory of higher-dimensional relative equilibria, one can generalize the problem to ask for the relationship between the properties of an SBC as a critical point and as an equilibrium point of the reduced equations of motion. In fact, the problem of linear stability of higher-dimensional relative equilibria seems to be completely open.

Bibliography

[1] A. Albouy, *Recherches sur le probléme des configurations centrales*, preprint (1997).

[2] A. Albouy, *Mutual distance in celestial mechanics*, Lecture Notes from Nankai University, Tianjin, China, preprint (2004).

[3] A. Albouy and A. Chenciner, *Le problème des n corps et les distances mutuelles*, Inv. Math. **131**, (1998) 151–184.

[4] A. Albouy and V. Kaloshin, *Finiteness of central configurations of five bodies in the plane*, Annals of Math. **176**, (2012) 535–588.

[5] V.I. Arnold, *Mathematical Methods of Classical Mechanics, 2nd ed.*, Springer-Verlag, New York, (1989).

[6] M. Berger, *Geometry I*, Springer-Verlag.

[7] A. Chenciner, *The Lagrange reduction of the N-body problem, a survey*, `arXiv:1111.1334`, (2011).

[8] D. Cox, J. Little, and D. O'Shea, *Ideals, varieties, and algorithms. An introduction to computational algebraic geometry and commutative algebra*, Springer-Verlag, New York, (1997).

[9] H.S.M. Coxeter, *Regular Polytopes*, Dover, New York, (1973).

[10] O. Dziobek, *Über einen merkwürdigen Fall des Vielkörperproblems*, Astron. Nach. **152**, (1900) 33–46.

[11] L. Euler, *De motu rectilineo trium corporum se mutuo attrahentium*, Novi Comm. Acad. Sci. Imp. Petrop. **11**, (1767) 144–151.

[12] M. Hampton, *Concave Central Configurations in the Four Body Problem*, thesis, University of Washington (2002).

[13] M. Hampton and A. Jensen, *Finiteness of spatial central configurations in the five-body problem*, Cel. Mech. Dyn. Astr. **109**, (2011) 321–332.

[14] M. Hampton and R. Moeckel, *Finiteness of relative equilibria of the four-body problem*, Inventiones Mathematicae **163**, (2006) 289–312.

[15] J.L. Lagrange, *Essai sur le problème des trois corps*, *Œuvres* **6**, (1772).

[16] R.C. Lyndon, *Groups and Geometry*, London Mathematical Society Lecture Notes Series **101**, Cambridge University Press (1985).

[17] W.D. MacMillan and W. Bartky, *Permanent Configurations in the Problem of Four Bodies*, Trans. Amer. Math. Soc. **34**, (1932) 838–875.

[18] C.K. McCord, *Planar central configuration estimates in the n-body problem*, Ergod. Th. and Dynam. Sys. **16**, (1996) 1059–1070.

[19] J.C. Merkel, *Morse theory and central configuration in the spatial N-body problem*, J. Dyn. Diff. Eq. **20**, (2008) 653–668.

[20] R. Moeckel, *On central configurations*, Math. Zeit. **205**, (1990) 499–517.

[21] R. Moeckel, *Relative equilibria with clusters of small masses*, Jour. Dyn. Diff. Eq. **9**, (1997).

[22] R. Moeckel, *Generic Finiteness for Dziobek Configurations*, Trans. Amer. Math. Soc. **353**, (2001) 4673–4686.

[23] R. Moeckel, *Celestial Mechanics – especially central configurations*, available at http://www.math.umn.edu/∼rmoeckel/notes/Notes.html.

[24] R. Moeckel and C. Simó, *Bifurcations of spatial central configurations from planar ones*, SIAM J. Math. Anal. **26**, (1995) 978–998.

[25] F.R. Moulton, *The Straight Line Solutions of the Problem of n Bodies*, Ann. of Math. **12**, (1910) 1–17.

[26] D. Mumford, *Algebraic Geometry I, Complex Projective Varieties*, Grundlehren der Mathematische Wissenschaften 221, Springer-Verlag, Berlin, Heidelberg, New York (1976).

[27] F. Pacella, *Central configurations of the n-body problem via equivariant Morse theory*, Arch. Rat. Mech. **97**, (1987) 59–74.

[28] J. Palmore, *Classifying relative equilibria*, I: Bull. AMS, **79** (1973) 904-908; II: Bull. AMS, **81** (1975) 489–491; III: Lett. Math. Phys. **1**, (1975) 71–73.

[29] G. Roberts, *A continuum of relative equilibria in the five-body problem*, Phys. D **127**, (1999) 141–145.

[30] D. Schmidt, *Central configurations in* $\mathbb{R}^2$ *and* $\mathbb{R}^3$, in Hamiltonian Dynamical Systems, Contemporary Math. **81**, (1988) 59–76.

[31] I.R. Shafarevich, *Basic Algebraic Geometry 1, Varieties in Projective Space*, Springer-Verlag, Berlin, Heidelberg, New York (1994).

[32] M. Shub, *Appendix to Smale's paper: Diagonals and relative equilibria*, Lecture Notes in Math. **197**, (1971) 199–201.

[33] C. Simó, *Relative equilibria in the four-body problem*, Cel. Mech. **18**, (1978) 165–184.

[34] S. Smale, *Problems on the nature of relative equilibria in celestial mechanics*, Lecture Notes in Math. **197**, (1971) 194–198.

[35] S. Smale, *Mathematical problems for the next century*, Mathematical Intelligencer **20**, (1998) 7–15.

[36] Z. Xia, *Central configurations with many small masses*, J. Differential Equations **91**, (1991) 168–179.

[37] Z. Xia, *Convex central configurations for the n-body problem*, J. Differential Equations **200**, (2004) 185–190.

Chapter 3

Dynamical Properties of Hamiltonian Systems with Applications to Celestial Mechanics

Carles Simó

3.1 Introduction

Our goal is to study some properties of the *dynamics of the N-body problem*. As is well known, the *Newtonian model of N punctual masses*, $m_i, i = 1, \ldots, N$, located at $q_i(t) \in \mathbb{R}^d$, moving under their mutual gravitational attraction is described by the equations

$$\ddot{q}_i = \sum_{j=1, j\neq i}^{N} (q_j - q_i)/r_{i,j}^3, \quad r_{i,j}^2 = ||q_j - q_i||_2^2, \quad i = 1, \ldots, N. \tag{3.1}$$

The system has several *first integrals*. The centre of mass ones, in a suitable reference moving linearly with constant velocity, are $\sum_{i=1}^N m_i q_i = 0$, $\sum_{i=1}^N p_i = 0$, where the related momenta are defined as $p_i = m_i \dot{q}_i$. Furthermore, defining the kinetic energy as $T(p) = \sum_{i=1}^N ||p_i||_2^2/m_i$ and the potential one as $U(q) = \sum_{1\leq i<j\leq N} m_i m_j / r_{i,j}$, one has the energy integral $T(p) - U(q) = H(q,p) = h$. The total angular momentum $\sum_{i=1}^N m_i q_i \wedge \dot{q}_i$ is another first integral. In general, no more first integrals exist. Of course, q and p above refer to the vectors in $\mathbb{R}^{Nd}$ which contain all the components of positions and momenta. System (3.1) can be put in *Hamiltonian formulation*: $\dot{q}_i = \partial H/\partial p_i$, $\dot{p}_i = -\partial H/\partial q_i$. The pairs (q_i, p_i)

© Springer Basel 2015

J. Llibre et al., *Central Configurations, Periodic Orbits, and Hamiltonian Systems*,
Advanced Courses in Mathematics - CRM Barcelona, DOI 10.1007/978-3-0348-0933-7_3

are canonically conjugated. In the present case, the Hamiltonian has Nd degrees of freedom (d.o.f.), despite the fact that the centre of mass integrals reduces them to $(N-1)d$, and the angular momentum gives additional reduction. For applications we shall consider the cases $d = 2$ and $d = 3$. The equations are analytic except on the collision set, when at least one of the values of $r_{i,j}$ equals zero.

In many problems it is interesting to consider that some of the bodies have a negligible mass. They are influenced by massive bodies but have no action on them. These are the *restricted* N-body problems.

The N-body problem belongs to the general class of Hamiltonian systems. In these systems and in all kinds of dynamical systems, the ultimate goal is *to describe the main mechanisms leading to a fairly global description of the dynamics*, how it depends on parameters and, if it is possible to act on the system (either with additional forces or by changing parameters), how to have some control on the behaviour of the system. In the present case we shall be interested in *conservative systems*, either in the continuous version described by a Hamiltonian or in the discrete version. Next we make some comments on the passage from continuous systems to discrete ones and vice-versa.

3.1.1 Continuous and discrete conservative systems

The associated discrete version is given by *symplectic maps*: $F\colon (x, y) \to (X, Y)$, where $X = F_1(x, y)$, $Y = F_2(x, y)$, with x, y, X, Y belonging to some set in $\mathbb{R}^d$ and such that the 2-form $dx \wedge dy = \sum_{i=1}^{d} dx_i \wedge dy_i$ is preserved: $dX \wedge dY = dx \wedge dy$. We can replace working in $\mathbb{R}^d \times \mathbb{R}^d$ by a formulation in symplectic manifolds but, to have a simpler presentation, we prefer to work explicitly using coordinates and refraining from extensions.

It is a simple matter to obtain discrete maps from a flow led by $\dot{x} = f(x)$, where f is a vector field (v.f.) in some open set U of $\mathbb{R}^n$. Assume Σ is a hypersurface, given as points $x \in U$ such that $g(x) = 0$, where $g\colon U \to \mathbb{R}$. We require that it satisfies the *transversality condition*. We say that Σ is transversal to the v.f. if the scalar product $(f, \nabla g)$ is different from zero in Σ. The geometrical meaning is clear: the flow of f (that we shall denote as φ_t^f or simply as φ_t) crosses transversally the section Σ. In many examples one simply takes as g one of the coordinates (either equal to zero or to a constant). In that case, Σ is usually not the full coordinate hyperplane, but the part of it satisfying the transversality condition. Then, given a point $Q \in \Sigma$ we define a map, the so-called *Poincaré map* $\mathcal{P}$, as the first return of Q to Σ: $\varphi_{t(Q)}(Q) \in \Sigma$ with a minimal value of $t(Q) > 0$. Note that, eventually, some Q can never return to Σ for any $t > 0$. This implies that Σ has to be reduced to a suitable subset. We also note that the return time $t(Q)$ depends on the starting point. We denote as $\mathcal{P}(Q) := \varphi_{t(Q)}(Q)$ the image of Q under the Poincaré map $\mathcal{P}$.

In the case of a Hamiltonian H with m d.o.f. (hence x has dimension $2m$) fixing a transversal section Σ and the level of energy h, the Poincaré map associated

to Σ defines a map in $\Sigma \cap H^{-1}(h)$, of even dimension $2(m-1)$. This map is symplectic.

Given a discrete map $x \to F(x)$ in $V \subset \mathbb{R}^n$, there is also a simple way to produce a v.f. such that it has, as associated Poincaré map, the initial map, provided F is close to the identity, say $F(x) = x + \varepsilon G(x)$ with ε small enough (see later). For concreteness we shall assume that G is a real analytic function. We want to define a non-autonomous periodic v.f. of period 1 in t. Let us consider, for instance, and for a given $k > 1$, the function $\psi_k(t) = c \int_0^t s^k(1-s)^k \, ds$, where the constant c is selected to have $\psi_k(1) = 1$. Then we define the flow starting at the point x after a time $t \in [0,1]$ as $\varphi_t(x) = x + \varepsilon \psi_k(t) G(x)$, that is, we are using an Hermite-like interpolation, because $\psi_k^j(0) = 0$ for $j = 0, \ldots, k$, $\psi_k(1) = 1$, and $\psi_k^j(1) = 0$ for $j = 1, \ldots, k$. Other interpolations can also be used. For other values of t it is defined by periodicity: $\varphi_t(x) = \varphi_{(t)}(x)$ where $(t) = t - [t]$, being $[t]$ the largest integer less than or equal to t. Clearly $\varphi_0(x) = x$, $\varphi_1(x) = F(x)$. Now we should define the v.f. at (y, τ) for $\tau \in [0,1]$. To this end we look for z such that $\varphi_\tau(z) = y$. It follows immediately, from the implicit function theorem, that a solution exists if $|| \operatorname{Id} + \varepsilon DG||_\infty > 0$. Finally the v.f. is $f(y,\tau) = \varepsilon \frac{d\psi_k}{dt}(\tau) G(z)$.

We note that this is a slow v.f., having the parameter ε as a factor. It is usually referred to as the *suspension* of the map F. We can consider if it is possible to approximate it by an autonomous v.f. This follows from a general theorem on averaging, that we present in a wider context: the case of v.f. depending on time in a quasiperiodic way.

Theorem 3.1.1. *Let*

$$\dot{z} = \varepsilon f(z, \theta, \varepsilon), \tag{3.2}$$

where f is analytic in (z,θ) for $z \in \Omega \subset \mathbb{C}^n$, $\Omega = D + \Delta$, a Δ-neighbourhood of D in $\mathbb{C}^n$, D a compact in $\mathbb{R}^n$, and $\theta \in \mathbb{T}^p + \Delta$, $p \geq 2$, where $\mathbb{T}^p$ is a p-dimensional torus. Assume f in (3.2) *is bounded in ε for $|\varepsilon| \leq \varepsilon_0$ and $\theta = \omega t$, where $\omega \in \mathbb{R}^n$ is a vector of frequencies satisfying the Diophantine condition* (DC)

$$|(k, \omega)| \geq b|k|^{-\tau}, \quad \forall k \in \mathbb{Z}^p \setminus \{0\}, \tag{3.3}$$

where $b > 0$, $\tau > p-1$ and $|k| = \sum_{i=1}^p |k_i|$. Then, if ε_0 is small enough, for a fixed ε with $|\varepsilon| \leq \varepsilon_0$, there exists a change of variables $z = h(w, \theta, \varepsilon)$, analytic in (w,θ) for $w \in D + \Delta/2$, $\theta \in \mathbb{T}^p + \Delta/2$, such that the new equation is $\dot{w} = \varepsilon(g(w,\varepsilon) + r(w,\theta,\varepsilon))$ and the remainder satisfies an exponentially small bound

$$|r|_{\Delta/2} < c_1 \exp(-c_2/\varepsilon^{c_3}), \tag{3.4}$$

where c_1, $c_2 > 0$, $c_3 = 1/(\tau+1)$. The constants c_1, c_2 depend only on $|f|_\Delta$, the dimensions and the constants in (3.3). *Furthermore, $|g|_{\Delta/2} < 2|f|_\Delta$. Here $|f|_\Delta$ denotes the sup norm of f in $D + \Delta$, $\mathbb{T}^p + \Delta$ for the fixed value of ε.*

Remark 3.1.2. (i) In the periodic case (it would be $p = 1, \tau = 0$), there is no need of analyticity with respect to t; just integrable is enough. Then $c_3 = 1$, see [36].

(ii) The optimal number of averaging steps (i.e., up to which order in ε one should cancel the quasiperiodic dependence) is $\approx \varepsilon^{-c_3}$.

(iii) If f is a Hamiltonian v.f., the change to w can be made canonical. Hence, the averaged system, skipping the remainder r, is also Hamiltonian, see [51].

(iv) If f has been obtained by suspension of a map F, we can produce an autonomous v.f., like g, which interpolates F except by exponentially small terms.

The basic idea of the proof is to obtain the change $z = h(w, \theta, \varepsilon)$ by means of *sequence of changes*. This methodology is common to many topics in dynamical systems. First we try to cancel the *purely quasiperiodic* terms in f, that is, the terms in $\tilde{f} = f - \bar{f}$, where $\bar{f}$ denotes the average with respect to θ. Writing the suitable condition for the change, one has to solve a PDE to obtain the quasiperiodic coefficients in this first change. To solve it with control on how the coefficients of the change behave is where the *analyticity with respect to* θ and the DC (3.3) play their roles. In the periodic case one has to do just an integration, and this is why to be integrable in t is enough in that case.

Once the terms in $\tilde{f}$ have been skipped, one has to check the contribution that the change makes in ε^2. Here is where the *analyticity with respect to* z plays a role, to bound the derivatives in a slightly smaller strip, passing from half width Δ to Δ_1. Then we proceed to cancel the purely quasiperiodic terms which appear with ε^2 as factor, and so on, to cancel the non-autonomous terms in ε^k, $k = 3, \ldots$ At every step, to be able to bound the contributions made by the change to higher order in ε, one has to reduce the size of the analyticity domain, introducing a decreasing sequence for the half widths of the successive domains $\Delta_2 > \cdots > \Delta_k > \cdots$.

After every change one has a bound on the remainder. If for a given ε we do too many changes, as we want to keep an analyticity domain of positive half width, the differences $\Delta_{k-1} - \Delta_k$ are small. This implies bad estimates for the derivatives and an increase on the size of the remainder. This is why, for every ε, there is an optimal order. Simpler estimates give then the bound in (3.4). See [41] for details and examples.

These kind of bounds on remainders are relevant to bound errors on approximations done, for instance, with normal forms (see Subsection 3.3.2). The variables can be scaled in the domain of interest and the role of ε is played by the size of the domain.

Finally we stress that the passage from flows to maps and vice-versa, when the map or some power of it is close enough to the identity, allows a more complete understanding and representation of key phenomena.

In what follows we shall consider that all v.f. and maps are in the analytic category.

3.1.2 Comments on the contents

Setting aside the two-body problem and subclasses with some special symmetry, the simplest N-body problem is the planar circular restricted three-body problem which has two d.o.f. (see Section 3.4). The next simplest problem can be the planar general three-body problem. Even restricting to a fixed value of the angular momentum it has three d.o.f. The dimension can be reduced by fixing energy and using a Poincaré section. In the first case we obtain symplectic 2D maps, easy to visualize. In the second case we have symplectic 4D maps, not so easy to visualize. There are key objects of codimension one (see Subsection 3.3.4) and homoclinic/heteroclinic phenomena due to the intersection of two objects of dimension two in dimension four. The invariant tori (see Subsection 3.3.3) do not separate the phase space, and slow escape from points as close as we like to invariant tori (Arnold diffusion or general diffusion, see Subsection 3.3.5), avoiding a large set of nearby tori, can occur.

For these reasons we devote Section 3.2 to introducing several simple but paradigmatic examples in the 2D case, with the hope that they will make it easier to grasp the main ideas in higher dimension. See also slides (B) for several examples with low dimensional conservative systems.

Section 3.3 is devoted to presenting some general theoretical results. But it is also relevant to see how to use the ideas of the proofs in concrete examples. In many cases, effective computation is based on implementation of the proof, either by symbolical or numerical methods or, quite frequently, by a combination of both.

Finally Section 3.4 presents some applications to Celestial Mechanics, with a variety of goals.

Concerning references, most of the basic results can be found in classical standard books. A few of them appear in the list of references, and no explicit mention to them is made in the text. Some references to concrete topics are scattered throughout the text and they are given at the end of these notes. The reader can also, at the end of the references, look at the list of slides of several talks given in the past and that, in turn, refer to some animations.

3.2 Low dimension: same key examples of 2D symplectic maps to see the kind of phenomena to face

Invariance of $dx \wedge dy$ in dimension 2 is equivalent to area preservation. We shall denote as APM the area preserving maps. The simplest non-trivial APM which come to mind are the quadratic ones: $x, y \in \mathbb{R}$ and F_1, F_2 are polynomials of degree

two. These maps were widely studied by M. Hénon [20]. See also slides (E) and slides (G). They are relevant because:

(i) the number of parameters can be reduced to only one, and they have a very simple geometrical interpretation;

(ii) they appear in a natural way as a very good approximation in some parts of $\mathbb{R}^2$ when we consider arbitrary APM; in particular when we study Poincaré maps of Hamiltonian systems with two d.o.f.;

(iii) the following problems can all be understood thanks to our knowledge of the quadratic case: (a) the existence of invariant curves diffeomorphic to $\mathbb{S}^1$; (b) the role of the invariant manifolds of hyperbolic fixed or periodic points and how they lead to the existence of chaos; and (c) the geometrical mechanisms leading to the destruction of invariant curves.

We shall illustrate some of these features in this section.

3.2.1 The Hénon map

In the initial formulation the map (except in some degenerate cases) can be written, thanks to the APM character, shift of origin and scaling, as $F\colon (x, y) \to (1 - ax^2 + y, -x)$. Hence, this family of maps depends on a single parameter a. The geometric interpretation is simple: it is the composition of the map $(x, y) \to (x, y + 1 - ax^2)$ (one of the so-called de Jonquières maps) and a rotation of angle $-\pi/2$. Figure 3.1 shows, for $a = -1/2$, the square $[-3, 3]^2$ (in red), the first image (in green) and part of the next two images (in blue and magenta, respectively). One can ask whether all points will escape for future iterations. To give an answer to this question, we plot in black the set of points which remain bounded for all iterations and the selected value of a.

However, we shall use another representation of that map, see [52], given by

$$F_c \begin{pmatrix} x \\ y \end{pmatrix} \to \begin{pmatrix} x + 2y + \frac{c}{2}(1 - (x + y)^2) \\ y + \frac{c}{2}(1 - (x + y)^2) \end{pmatrix}, \tag{3.5}$$

which depends on c that can be assumed to be positive. It has two fixed points: H at $(-1, 0)$, hyperbolic $\forall c > 0$, and $E = (1, 0)$, elliptic for $0 < c < 2$ and hyperbolic with reflection for $c > 2$. The reversor $S(x, y) = (x, -y)$ allows us to obtain $F_c^{-1} = SF_cS$.

Doing the change of scale $(\xi, \eta) = (x, 2y/\sqrt{c})$ one obtains a map $\sqrt{c}$-close to the identity. According to Section 3.1 it can be approximated by the time-$\sqrt{c}$ flow of the v.f. $d\xi/dt = \eta$, $d\eta/dt = 1 - \xi^2$, with Hamiltonian $K(\xi, \eta) = \eta^2/2 - \xi + \xi^3/3$. It is, of course, a trivial matter to improve K to any power of $\sqrt{c}$. This v.f. has the same fixed points as F_c and a separatrix on the level $K = 2/3$.

Next we show iterates of some initial points under F_c for $c = 0.2$ and $c = 0.762$, see Figure 3.2.

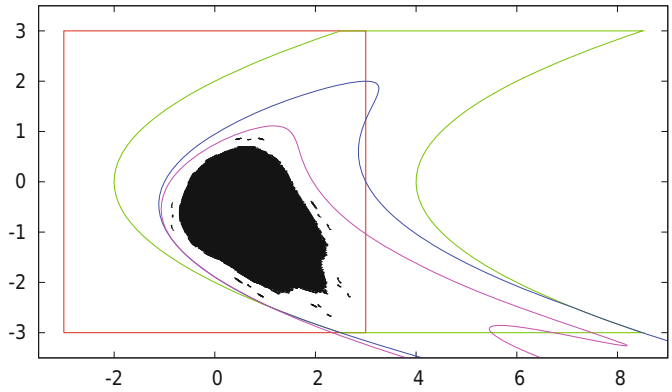

Figure 3.1: The square $[-3, 3]^2$ (in red) and the first three images of it under the Hénon map with $a = -0.5$, shown in green, blue and magenta, respectively. The last two have parts outside the frame shown here. In black we display the invariant set of points which remain bounded under all iterations.

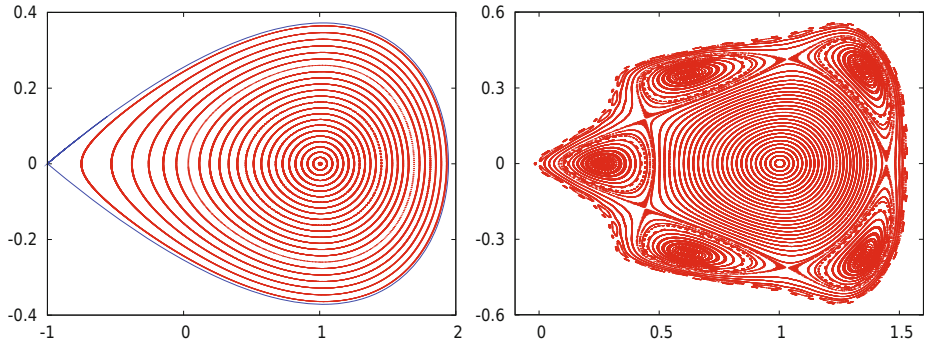

Figure 3.2: Some iterates under F_c. *Left:* for $c = 0.2$. *Right:* for $c = 0.762$. We have taken initial points on $y = 0$ and plotted 5,000 iterates of each one after a transient of 10^6 iterates. Points outside the displayed domain escape to infinity close to the left branch of W^u_H. When looking at the figure in the electronic version it is suggested to magnify the right plot to see the details. The same applies to several other plots in the next figures, without explicit mention.

An important characteristic of points whose orbit is an invariant curve (IC) is the *rotation number* ρ. It measures the average value of the fraction of revolution that the point turns in each iterate. We can look at the curves around the elliptic point E in previous plots and take polar coordinates. Let θ_k be the angle of the k-th iterate, but considered in the lift $\mathbb{R}$ instead of $\mathbb{S}$. Note that in this example

the points turn clockwise. Then, we define

$$\rho = \frac{1}{2\pi} \lim_{k\to\infty} \frac{\theta_k}{k}. \tag{3.6}$$

It always exists and does not depend on the initial point on the curve.

On the left plot in Figure 3.2 one can see a pattern which looks like the phase portrait of a one d.o.f. Hamiltonian, with a foliation by periodic solutions and a separatrix in blue. It seems that, as in the case of one d.o.f. systems, the map is *integrable*. That is, there exists a non-constant function $C(x, y)$ preserved by the map: $C(F(x, y)) = C(x, y)$. In fact there is a Cantor set (of positive measure) of ICs with $\rho \notin \mathbb{Q}$, an infinite number of periodic orbits of elliptic and hyperbolic type and the right-hand sides of the manifolds of H do not coincide. What happens is that the differences with respect to the flow case are extremely small, in agreement with (3.4). We shall see details on this smallness in the part about invariant manifolds of Section 3.2.1.

The right-hand plot in Figure 3.2 displays a typical behaviour of a *not close to integrable APM*. Certainly there are many ICs (again a Cantor set) around the point E, but at some distance one can see big *period-5 islands* around elliptic periodic points of period 5, and one can guess the existence of period-5 hyperbolic points. Close to them there are *chaotic orbits*, still surrounded by some more ICs, (rotational, that is, they make the full turn around E) and, finally, some little islands before reaching a place where most of the points *escape*.

Some comments on invariant curves

The plots in Figure 3.2 raise several questions: (1) do ICs really exist for F_c? (2) what is the structure of the set of ICs? (3) how are they destroyed? (4) what happens after an IC's destruction?

First we introduce the so-called *twist maps*. These are integrable maps defined in some annular domain $r_d < r < r_u$, having a foliation by ICs, given by

$$T(r, \alpha) = (r, \alpha + a(r)), \tag{3.7}$$

and satisfying the *twist condition*

$$da(r)/dr \neq 0. \tag{3.8}$$

Of course, one can have the form (3.7) after a diffeomorphism. The curves can have a shape different from circles, like ellipses, to be star-shaped or not.

A key result is the *Moser twist theorem*.

Theorem 3.2.1. *Consider a perturbation $F_\varepsilon = T + \varepsilon P$ of a twist map T. Then, if we have an invariant curve of T which has Diophantine rotation number γ, this curve, with a small deformation, subsists for F_ε provided ε is sufficiently small.*

The Diophantine condition, in the present case, is like (3.3) with frequencies γ and 1: $|k_1\gamma + k_0| \geq b|k|^{-\tau}$, $\forall (k_1, k_0) \in \mathbb{Z}^2 \setminus \{0\}$, where $|k|$ denotes some norm of $k = (k_1, k_0)$.

Let us comment a little on the three conditions: (a) it must be a perturbation of a twist map T; (b) the rotation number γ must be Diophantine; and (c) it must be close enough to T, that is, ε must be small.

Assume that the Fourier representation of the IC of T which has $\rho = \gamma$ is $r(\alpha) = \sum_{j\in\mathbb{Z}} a_j \exp(\mathrm{i}\, j\alpha)$ in the present polar coordinates we are using (typically, for a given problem, the twist map will not be given in the form (3.7), and to put it explicitly in this form can be cumbersome). Let $r_\varepsilon(\alpha) = \sum_{j\in\mathbb{Z}} b_j \exp(\mathrm{i}\, j\alpha)$ be the representation of the desired IC, invariant under F_ε. The invariance condition is expressed, in (r, α), as $F_\varepsilon(r_\varepsilon(\alpha), \alpha) = (r_\varepsilon(\alpha + 2\pi\gamma), \alpha + 2\pi\gamma)$. It is clear that we can fix the origin of angles in an arbitrary way.

We try to pass from the coefficients a_j to b_j by making a sequence of changes (similar to the case of Theorem 3.1.1) such that, after the k-th change, one has an approximation of the IC under F_ε with $\rho = \gamma$ with an error $\mathcal{O}(\varepsilon^{2^k})$. That is, a Newton method in the space of Fourier series. The equation to be solved at each step is of the form $G(\alpha + 2\pi\gamma) - G(\alpha) = R(\alpha)$, the so-called *homological equation*, where $R(\alpha)$ is related to the error of the previous approximation and has zero average, a necessary condition in order to make it possible to solve the equation.

Using Fourier representations for G and R, say $G = \sum_{j\in\mathbb{Z}} g_j \exp(\mathrm{i}\, j\alpha)$ and $R = \sum_{j\in\mathbb{Z}} r_j \exp(\mathrm{i}\, j\alpha)$, $r_0 = 0$, it is straightforward to obtain $g_j = r_j/(\exp(\mathrm{i}\, j2\pi\gamma) - 1)$, $j \neq 0$. But, of course, if $j\gamma$ is close to an integer, the previous denominator is close to zero. This is known as the *small denominators problem*. The DC allows us to control the behaviour of the coefficients of G, so that if R is analytic in some complex strip around real values of α, G is also analytic (perhaps in a slightly narrower strip).

The problem is then that the error in the next approximation does not have zero average and we will not be able to solve the next homological equation. But this average can be canceled by modifying the initial independent term a_0 (or, equivalently, by selecting a proper value for g_0) and this is possible, thanks to the twist condition, by applying the implicit function theorem. It is convenient to express the twist condition as $d\rho/da_0 \neq 0$; that is, in terms of the average of the initial curve. Finally the smallness of ε is necessary to have convergence in the Newton procedure. Note that, for a fixed γ, the larger is the twist condition, the larger are the admissible values of ε.

In Section 3.3.3 we shall talk about generalizations to higher dimension, both for symplectic maps and for Hamiltonian flows. The key ideas for the proofs are the same.

Using *normal form* tools (see Section 3.3.2) it is easy to prove that, what seem to be ICs in Figure 3.2 are really ICs, at least close to the point E. Furthermore, it is clear that the structure of the set of ICs is Cantorian, because so is the structure of the set of Diophantine numbers for values of b, τ bounded from below, see (3.3).

It is interesting to see what happens when the twist condition is *not satisfied*. Figure 3.3 shows, for the map (3.5), with $c = 1.35$, the evolution of ρ as a function of x for initial points of the form $(x, 0)$. It is clear that ρ is only defined for ICs and periodic orbits (or islands) and, in the present case, it seems that this occurs for most of the initial values of x. One can prove that this behaviour, with a local minimum at $x = 1$ and a local maximum on each side, appears only for $c \in (c_1, c_2)$, $c_1 = 5/4$, $c_2 \approx 1.4123$. For $c \in (0, c_1)$ one has a local (in fact, global) maximum at $x = 1$ (the point E).

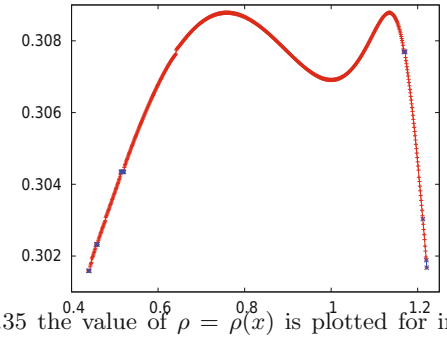

Figure 3.3: For $c = 1.35$ the value of $\rho = \rho(x)$ is plotted for initial points on $y = 0$. In blue the points with $\rho \in \mathbb{Q}$. Note that now, to the left or to the right of $x = 1$, the function ρ is no longer monotonous.

The twist condition is lost near the maxima. Let ρ_M be the value of ρ at a given maximum M. Assume that there exist rationals $p/q < \rho_M$ with q not too large. They give rise to the typical islands structure, with q islands on each family, on both sides of the IC with $\rho = \rho_M$ (or close to it). The interaction of these two families of islands, with $\rho = p/q$, gives rise to the so-called *meandering curves*, see [43], which cannot be written with the radius as a function of the angle seen from the point E. The curves have some folds (or meanders) but it is still possible to apply Moser's Theorem 3.2.1 to prove that they exist. Figure 3.4 shows an example of meandering ICs for $c = 1.3499$ and a magnification including some nearby orbits.

Some comments on invariant manifolds of hyperbolic points

Beyond the IC of an APM, there are other very important invariant objects which play a key role in dynamics (this is also true for more general maps and flows in any dimension, see Section 3.3.4). They are the *stable and unstable manifolds of the hyperbolic fixed or periodic points*. They can be seen as the non-linear generalisation of the invariant subspaces of the differential of the map at the fixed point. On the left-hand plot in Figure 3.2, for $c = 0.2$, the branches $W^{u,+}$ and $W^{s,-}$ (the ones which start to the right of $x = -1$) seem to be coincident, but they are not.

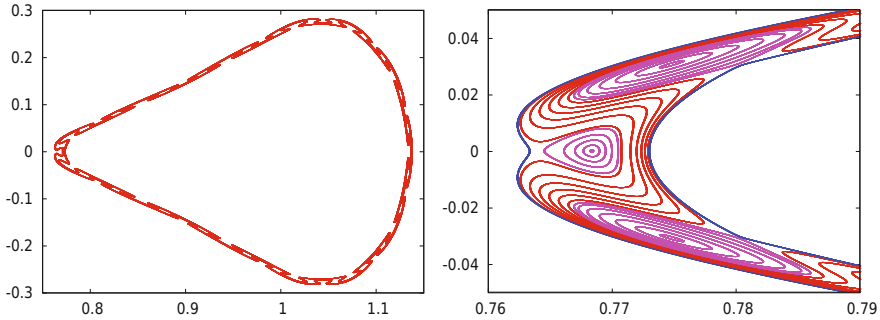

Figure 3.4: *Left:* We show a couple of orbits for $c = 1.3499$, sitting on a domain in which ρ passes through a maximum. These orbits are on invariant curves known as meanders. *Right:* A magnification of the left. Beyond different meanders in red, one can see two typical invariant curves (inner and outer) in blue and islands, in magenta, which belong to two different chains of islands of rotation number 4/13.

Figure 3.5, left, shows a magnification when they return to the vicinity of the point $(-1, 0)$, after going clockwise around E under F_c (red points), or counterclockwise under F_c^{-1} (blue points). We see tiny oscillations with a size $\mathcal{O}(10^{-3})$. The right-hand plot in Figure 3.5 shows the manifolds for $c = 0.77$ with large oscillations. The points in $W^u \cap W^s$ are known as *homoclinic points* (or biasymptotic points). Some of them, on $y = 0$, can be seen to the right of the plot. The successive nearby returns of the manifolds produce infinitely many homoclinic points. Depending on the location of a point with respect to a given homoclinic, after passing close to H under iteration by F_c, will follow close to the positive, $W^{u,+}$, or to the negative, $W^{u,-}$, branches of W^u. And similarly for the stable branches using F_c^{-1}.

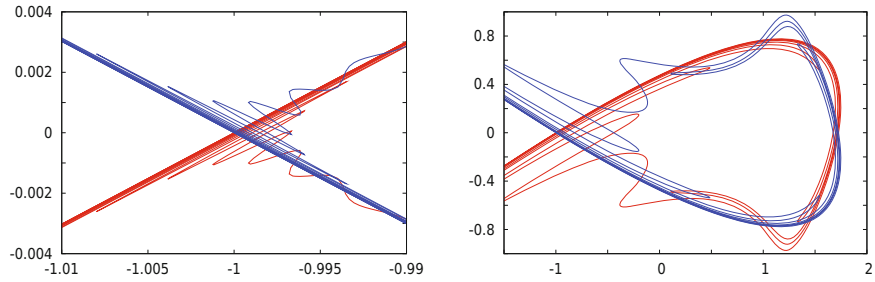

Figure 3.5: *Left:* a magnification of Figure 3.2 showing that the manifolds do not coincide. *Right:* part of the invariant manifolds of the hyperbolic point H for $c = 0.77$ (the unstable manifold in red, the stable one in blue). One has $W_H^s = S(W_H^u)$. The splitting of the manifolds is now clearly visible. It is increasing with c. Note that the domain around the point E which is not covered by the oscillations of the manifolds, becomes smaller. Compare with the non escaping set of points in Figure 3.2 right, for a nearby value of c.

A measure of the lack of coincidence of W^u and W^s is the *splitting angle*. This is defined as the angle between manifolds at a given homoclinic point. In the present case of quadratic APM, we can measure the angle at the first intersection of the manifolds with $y = 0$ to the right of $x = 1$ and see how it behaves as a function of c. For concreteness, we denote this angle as $\sigma(c)$. In Figure 3.6, left and middle, we represent the value of $\sigma(c)$ in different scales. In the left-hand plot, despite the splitting being different from zero for any $c > 0$, we see that only for $c > 0.2$ does it start to be visible. To make visible what happens for small c, we display, in the middle plot, $\log(\sigma)$ against $\log(c)$. Note that already for $c = 0.05$ the value of $\sigma(c)$ is below 10^{-15} and, hence, it is negligible for any practical application.

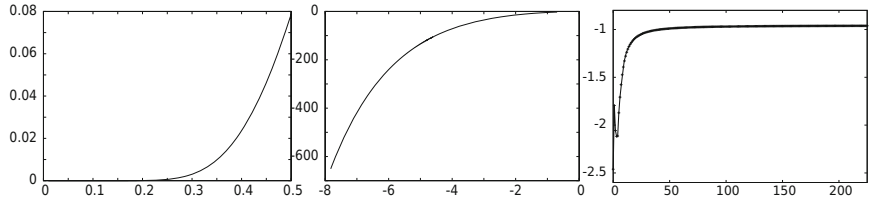

Figure 3.6: Different representations of the splitting angle $\sigma(c)$ between the manifolds at the first intersection with $y = 0$, $x > 1$. *Left:* σ, as a function of c, showing that σ seems negligible for $c < 0.2$. At that value of c, the first digits are $\sigma(c) = 6.21463426856826630097675406749853074250 03 \ldots \times 10^{-5}$. *Middle:* $\log(\sigma)$ as a function of $\log(c)$, which allows to see how small $\sigma(c)$ is for c approaching zero. *Right:* the values of $\log_{10}(\omega_{2m}(2\pi^2)^{2m}/(2m+6)!)$ versus m, to give evidence of the Gevrey character of $\Omega(h)$ (see text).

Concerning the right-hand plot in Figure 3.6 we need some preliminaries. Let $\lambda(c)$ be the *dominant eigenvalue* at the point H, which is equal to $1+c+\sqrt{2c+c^2}$ for F_c. An essential parameter in the theoretical study of the problem is $h(c) = \log(\lambda(c))$, because using suitable representations of the manifolds, it is possible to show that the splitting has upper bounds of the form $\exp(-\eta/h)$, where η is related to the *imaginary part of the singularity of the separatrix of the limit flow*, as mentioned before in Figure 3.2. This type of result is true for general analytic APM close to the identity map, see [10, 11]. In fact, for the present problem one can prove a more precise result. The splitting angle has the form

$$\sigma(c) = \frac{9}{2} \times 10^6 \pi^2 h(c)^{-8} \exp\left(-\frac{2\pi^2}{h(c)}\right) \times \Omega(h). \tag{3.9}$$

The term $\Omega(h)$ can be expanded in powers of h^2, say $\Omega(h) = \sum_{m\geq 0} \omega_{2m} h^{2m}$, and can be bounded by $\omega_0 + \mathcal{O}(h)$. The constant term can be determined numerically and the first digits of ω_0 are 2.48931280293671. Note, however, that the series defining $\Omega(h)$ is divergent. But for every value of h it provides a good approxima-

tion if we truncate the summation at the appropriate place. There is numerical evidence that the series is of *Gevrey-1 class*.

A formal power series $\sum c_k t^k$ is said to be of Gevrey-β class if the series $\sum c_k (k!)^{-\beta} t^k$ is convergent. We can compute the series $\sum_{m\geq 0} \omega_m h^{2m}/(2m)!$ obtained from $\Omega(h)$ using $\beta = 1$. From a numerical determination of $\Omega(h)$, for different values of h, one can obtain the coefficients ω_{2m}. See [12] for methodology and examples. In the right-hand plot in Figure 3.6 we display $\log_{10}(\omega_{2m}(2\pi^2)^{2m}/(2m+6)!)$ as a function of m, which seems to tend to a constant. This gives evidence of the Gevrey-1 character of $\Omega(h)$ we mentioned. But to prove this fact is an open problem.

See slides (H) for the role of the splitting phenomena in the measure of the chaotic domain in different problems.

On the destruction of invariant curves

As mentioned in the part about invariant submanifolds in Section 3.2.1, if ρ is too close to a rational (in the Diophantine sense), or if the twist condition is too weak, or if the perturbation ε with respect to an integrable map is too large, the IC does not exist. These analytic properties also have a nice geometric interpretation.

To illustrate the mechanism leading to the destruction of ICs we consider Figure 3.7. It has been produced for $c = 0.618$ (left) and $c = 0.63$ (right) and it only shows the left-hand part of the set of points which have bounded orbits. The case of Figure 3.7 is similar to the one on the Figure 3.2 right, but now the main islands are 6-periodic instead of 5-periodic.

On the left-hand plot one can see medium size islands with $\rho = 3/19$ (one of them with its central elliptic point on $y = 0$) and two symmetrical islands, in the same family, with $\rho = 4/25$, as well as several satellite islands, then tiny islands (e.g., with $\rho = 17/107, 39/245, 11/69, 19/119, 21/131, 13/81, \ldots$) and ICs. In particular, some ICs are still present between the two chains of medium size islands. Some other ICs, surrounding the main period-6 islands (not displayed), appear as the rightmost curves shown.

On the right-hand plot we display in black two chains of islands of rotation numbers $3/19$ and $4/25$, corresponding to the ones in the left plot, but now they are smaller. Consider the associated hyperbolic periodic orbits, the one with rotation number $4/25$ being visible on the x-axis and the two symmetric points belonging to the hyperbolic periodic orbit of rotation number $3/19$ being close to $x = -0.2$ off the x-axis. The manifolds of these periodic orbits give rise to *heteroclinic connections*, that is, intersections of the stable and unstable manifolds of two different objects. The manifolds $W^u_{4/25}, W^s_{4/25}$ are shown in red and green, respectively. The manifolds $W^u_{3/19}, W^s_{3/19}$ are shown in blue and magenta, respectively. Note that $W^u_{4/25}$ and $W^s_{3/19}$ (and, symmetrically, $W^s_{4/25}$ and $W^u_{3/19}$) have *transversal* heteroclinic intersections. This produces an obstruction to the existence of the ICs which could separate the chains of islands. This is the basis of the so-called *obstruction mechanism* [38].

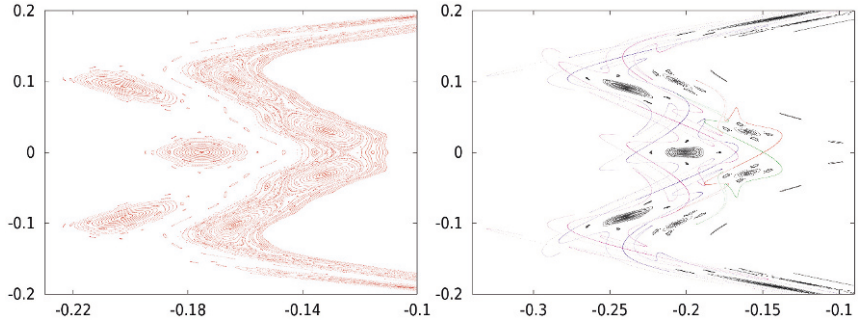

Figure 3.7: *Left:* A part of the set of non escaping points for the map F_c and $c = 0.618$. *Right:* similar plot for $c = 0.63$, displaying also several invariant manifolds of periodic hyperbolic points leading to heteroclinic intersections. See the text for details.

Indeed, if we consider a curve formed by a piece of invariant manifold of the inner hyperbolic periodic point (the one of period 25) until the heteroclinic point, followed by a piece of invariant manifold of the outer hyperbolic periodic point (the one of period 19), from the heteroclinic point to the periodic one, the ICs will have to cross it. This is impossible because of the invariance. In fact, one concludes that ICs with $\rho \in (3/19, 4/25)$ cannot exist. But ICs with ρ in that interval are found for $c = 0.618$. Hence, the geometrical mechanism responsible for the destruction is the existence of heteroclinic connections which obstruct the possible curves.

Anyway, there are invariant objects with ρ in the above mentioned interval. It is proved that they should be at the outer part of the manifolds of the hyperbolic periodic orbit with $\rho = 4/25$ and at the inner part of the manifolds of the hyperbolic periodic orbit with $\rho = 3/19$. The heteroclinic intersections of these manifolds create *gaps* which forbid the existence of points of the invariant object in them. As a consequence, the invariant object which remains for some irrational $\rho \in (3/19, 4/25)$ is a *Cantor set* [29, 30]. Points which were located inside an IC for $c = 0.618$ and, hence, without possible escape, can now, for $c = 0.63$, find a gap of the Cantor set and escape under iteration. It looks like some random process and, certainly, the probabilities are related to the size of the gaps in the Cantor set.

3.2.2 The standard map

Looking at the right-hand plot in Figure 3.2 we clearly see the period-5 islands around period-5 elliptic points and, as already said, we can guess the existence of period-5 hyperbolic points. We also see ICs close to the island, some of them inside, which have $\rho > 1/5$, and others outside, which have $\rho < 1/5$. If instead of iterations under F_c we iterate using F_c^5 we will check that the inside curves turn

a little clockwise and the outside ones turn a little counterclockwise. We can ask: what happens for an APM if we have two ICs turning by iteration a small amount in opposite directions?

This is the contents of the so-called *last geometric theorem by Poincaré*. Between the two curves, invariant under a map M, there should appear fixed points, generically isolated and alternatively elliptic and hyperbolic. Typically, one point of each type appears. But if the map is the q-th power of some other map $\tilde{M}$, with rotation number p/q, $(p,q)=1$, then there are q fixed points of each type under M, which are q-periodic under $\tilde{M}$.

The structure of the islands is reminiscent of the phase portrait of a pendulum, whose Hamiltonian is $H(x,y)=y^2/2+\cos(x)$ using suitable coordinates. From a quantitative point of view (the width of the islands) we recall that the maximal distance between upper and lower separatrices in a pendulum with Hamiltonian $H(x,y)=y^2/2+\delta\cos(x)$ is $4\sqrt{\delta}$. But we keep the presentation in the scaled version, i.e., with the coefficient of the cosine equal to 1. The equations are $\dot{x}=y$, $\dot{y}=\sin(x)$. One can think of a discrete model which, in the limit, behaves as the pendulum. The simplest approach would be to use an explicit Euler method with step h, which gives the map $(x,y)\to(x+hy, y+h\sin(x))$. Unfortunately, that map is not an APM, but can be made symplectic using a symplectic Euler method: $(x,y)\to(\bar{x},\bar{y})$, $\bar{y}=y+h\sin(x)$, $\bar{x}=x+h\bar{y}$. If we do not like to have the parameter h in both variables, we simply replace hy by a new variable z, rename z again as y, introduce $k=h^2$, and we obtain

$$SM_k:\begin{pmatrix} x\\ y\end{pmatrix}\to\begin{pmatrix} \bar{x}=x+\bar{y}\\ \bar{y}=y+k\sin(x)\end{pmatrix}, \tag{3.10}$$

a popular map known as a *standard map* [7]. It is clear that we can look at the variables (x,y) in $\mathbb{S}\times\mathbb{R}$ or in $\mathbb{T}^2$. It has fixed points located at $(0,0)$, hyperbolic, and at $(\pi,0)$, elliptic, that we denote again as H and E. Figure 3.8 displays the phase portrait (in $\mathbb{T}^2$) for $k=0.5$ and $k=1$.

On the left-hand plot it is hard to see that the stable and unstable manifolds of H do not coincide. A study like the one in the invariant manifolds part of Section 3.2.1 reveals similar properties. But the strongest difference between these plots is that in the left one there exist rotational ICs, that is, ICs going from the left vertical boundary to the right one (in this representation; in fact these boundaries are identified). These curves are absent in the right plot. Hence, if we consider the map in $\mathbb{S}\times\mathbb{R}$, there is no obstruction to the dynamics in the y direction for $k=1$. There are points with an initial value $y\in[0,2\pi)$ whose iterates can go arbitrarily far away in the y direction (despite the fact that for that value $k=1$ will require many iterates).

The critical value up to which one has rotational ICs is the so-called *Greene's critical value* $k_G\approx 0.971635$; see [19]. The "last" rotational IC which is destroyed has $\rho=(\sqrt{5}-1)/2$, the golden mean. This is not a surprise; it is the number in $(0,1)$ with best Diophantine properties. The obstruction method using hyperbolic

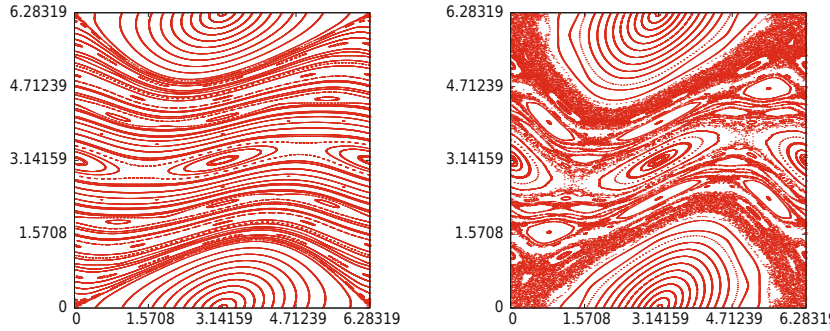

Figure 3.8: Phase portrait of (3.10). *Left:* for $k = 0.5$, still quite well ordered. *Right:* for $k = 1$, already with a big amount of chaos. Beyond the main elliptic island around E one can see several islands in both cases. The largest chaotic zone appears around the invariant manifolds of H.

periodic orbits with rotation numbers of the form F_{n-1}/F_n and F_n/F_{n+1}, F_n being the n-th Fibonacci number, plus a suitable extrapolation, allows us to determine k_G accurately. Note also that for $k > k_G$ but close to k_G, the rotational IC with $\rho = (\sqrt{5}-1)/2$ is replaced by a Cantor set with "small holes". This supports the claim about the large number of iterates needed to have y far away from the initial location. *Renormalization theory* [26, 27] provides the framework to understand those things in detail. For large values of k the standard map has interesting *statistical properties*. But they can be strongly affected by the role of the islands, see [32].

On the other hand, the Hamiltonian $H(x, y) = y^2/2 + \cos(x)$ can be replaced by more complex ones to obtain generalized standard maps. Adding terms in y^3 and $y\cos(x)$ allows us to explain the asymmetry which can be seen in Figure 3.2, right between the inner part and the outer part of the islands and the related inner, and outer splittings of the manifolds of the associated periodic hyperbolic points [52], in contrast with the symmetries of a pendulum. Replacing $y^2/2$ by $-by + y^3/3$ allows us to reproduce a limit flow of the meandering curves, as shown in Figure 3.4, and other more complicated changes give rise to labyrinthine ICs with funny shapes [43].

3.2.3 Return maps: the separatrix map

A useful device to understand the dynamics when some hyperbolic invariant object $\mathcal{A}$ has orbits homoclinic to it are the *return maps*. Assume that we have an initial point in a given domain $\mathcal{D}$ close to a point homoclinic to $\mathcal{A}$. Then it approaches $\mathcal{A}$ under iteration, close to $W^s_{\mathcal{A}}$, and after the passage near $\mathcal{A}$ moves away, close to $W^u_{\mathcal{A}}$, and returns to $\mathcal{D}$. Can we describe how the return is produced?

To illustrate with an example we have used a modified Hénon–Heiles potential. In a pioneer example Hénon and Heiles in 1964 used a Hamiltonian with two d.o.f. (a model of the motion of a star in a galaxy with cylindrical symmetry) [21]. The Hamiltonian they derived is

$$HH(x, y, p_x, p_y) = (x^2 + y^2 + p_x^2 + p_y^2)/2 + x^3/3 - xy^2, \tag{3.11}$$

and a careful study of the behaviour of nearby orbits of the system (3.11) lead to the detection of chaotic motion, giving evidence of the lack of integrability, a fact that was proved theoretically later and that was relevant to face integrability problems from an algebraic point of view; see [34] and references therein. Later on the family with Hamiltonian $HH_c(x, y, p_x, p_y) = (x^2 + y^2 + p_x^2 + p_y^2)/2 + cx^3 - xy^2$ was introduced, and the case $c = 0$,

$$HH_{c=0}(x, y, p_x, p_y) = (x^2 + y^2 + p_x^2 + p_y^2)/2 - xy^2, \tag{3.12}$$

that we shall use as illustration, presents some interesting particularities. Like many other simple models it has a symmetry with respect to simultaneous change of sign of y and t.

One can fix the value of the energy and use $y = 0$ as a Poincaré section. The Poincaré map $\mathcal{P}$ has a fixed point H which corresponds to a hyperbolic periodic orbit of (3.12). The invariant manifolds on $HH_{c=0}^{-1}(0.115)$ are shown in Figure 3.9. There exist homoclinic points and the symmetry implies that the upper branch of W_H^s can be obtained from the lower branch of W_H^u.

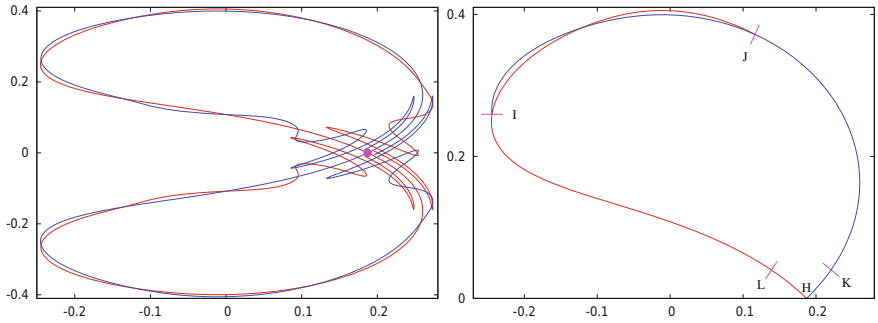

Figure 3.9: *Left:* the invariant manifolds (W^u in red, and W^s in blue) of the hyperbolic simple periodic orbit of the modified Hénon–Heiles Hamiltonian located inside the domain of admissible conditions on the Poincaré section $y = 0$, for the level of energy $h = 0.115$. The variables displayed are (x, p_x). *Right:* a magnification of the upper part showing the location of sections I, J, K, and L mentioned in the text. The periodic orbit appears marked as H on the section.

Our goal is to describe the return to a suitable domain $\mathcal{D}$ as a model for a general setting. In Figure 3.9 on the right there is a homoclinic point in the segment

market as I, whose image under $\mathcal{P}$ is the segment marked as J. A suitable domain can be a strip around the parts of the manifolds between I and J. Note that in the present case, due to the symmetry, we consider in Figure 3.9 (right) only the upper part in the (x, p_x) variables. It can happen that, after passage near H, a point moves to the lower part. Hence, it is convenient to consider $\mathcal{D}$ as the union of two strips, symmetric the one with the other, and that we can denote as $\mathcal{D}_+$ and $\mathcal{D}_-$, according to the sign of p_x, and define $\mathcal{D} = \mathcal{D}_+ \cup \mathcal{D}_-$.

In general, there is no symmetry and then $\mathcal{D}_-$ is not obtained from $\mathcal{D}_+$ by symmetry, and even some of the branches of the manifolds can escape, as it happens for (3.5).

If we take the part of W^u_H from H to the homoclinic point which appears in J, followed by the part of W^s_H between the homoclinic and H, and add the symmetric part (on $p_x < 0$) we have a *figure-eight pattern* which appears in many problems. This occurs, e.g., in the manifolds of the hyperbolic fixed point of (3.10). Looking at the map in $\mathbb{S} \times \mathbb{R}$ in suitable coordinates, one has also a figure-eight pattern [53].

First we assume that a point is located in $\mathcal{D}_+$ below W^s_H (the line in blue). After passing close to H it will return to $\mathcal{D}_+$. We follow an elementary method to find the return map. If the splitting is small enough we can assume that the upper branches of the manifolds are coincident and consider a nearby integrable map in the domain bounded by the branches of the manifolds. Let φ_t be the flow of a Hamiltonian v.f. with one d.o.f. in (x, p_x) with Hamiltonian $\mathcal{H}$ such that $\varphi_{2\pi}$ coincides with this integrable map. In particular, points in I move to points in J under $\varphi_{2\pi}$, and we can redefine the strip $\mathcal{D}_+$ as the set $\cup_{t\in[0,2\pi]}\varphi_t(I)$. The manifolds $W^{s,u}_H$ under that Hamiltonian v.f. coincide and form the separatrix of $\mathcal{H}$. As additional variable in $\mathcal{D}_+$, transversal to that separatrix, we take the level h of $\mathcal{H}$, assuming $\mathcal{H}$ is positive inside the separatrix and equal to zero on it.

For concreteness, let us denote as λ the dominant eigenvalue of the differential of the map $\varphi_{t=1}$ at H. It is clear that the dominant eigenvalue for $\varphi_{t=2\pi}$, close to the one of the initial map, say μ, is $\lambda^{2\pi}$ and that for the Hamiltonian v.f. is $\log(\lambda)$. If λ is close to 1 then $\log(\lambda)$ will be close to zero. For simplicity, we denote $\log(\lambda)$ as λ^*. In terms of the dominant eigenvalue of the initial map one has $\lambda^* \approx \log(\mu)/(2\pi)$.

As all the orbits in the domain bounded by the separatrix are periodic under the flow, when a point in $\mathcal{D}_+$ returns to it, it has the same value of h. But t has changed by the period, which behaves like $c - \log(h)/\lambda^*$, where c is a constant (essentially equal to the time to go from section L to section K). The map would be $(t, h) \mapsto (t + c - \log(h)/\lambda^* \,(\mathrm{mod}\, 2\pi), h)$.

Now we return to our original map. The only change is due to the lack of coincidence of W^s_H and W^u_H. If we consider the variable h defined as an energy with respect to W^u_H, when continuing the motion close to W^s_H the energy should be considered with respect to that manifold. There is a jump in energy due to the splitting. Note that, using a normal form around H, it is possible to define in a natural way an energy in a neighbourhood of this point, and to transport that

function along both manifolds, by backward or forward iteration, see [11], and also [50] in a general context. The two energies do not coincide in $\mathcal{D}_+$. The difference is the jump just mentioned. Let us denote it as $s(t)$ (it has a weak dependence on h that we neglect). The simplest expression for $s(t)$ is a sinusoidal oscillation $\varepsilon \sin(t)$ which measures the location of W^u_H with respect to W^s_H. Then the return map becomes

$$\begin{pmatrix} t \\ h \end{pmatrix} \to \begin{pmatrix} \bar{t} = t + c - \log(\bar{h})/\lambda^* \,(\mathrm{mod}\ 2\pi) \\ \bar{h} = h + \varepsilon \sin(t) \end{pmatrix}. \tag{3.13}$$

It is clear that the map is not defined if $\bar{h} = 0$ because then the point is in W^s_H. On the other, hand we have not considered the case $h < 0$. Then the process is similar, but we land on the lower domain $\mathcal{D}_-$. Beyond the variables (t, h) one has to consider a sign σ equal to ± 1 in $\mathcal{D}_\pm$. Using also the sign and renaming the variables as ξ, η, with $\xi \in [0, 2\pi)$ and η small, the map (3.13) becomes

$$SepM\colon \begin{pmatrix} \xi \\ \eta \\ \sigma \end{pmatrix} \to \begin{pmatrix} \bar{\xi} = \xi + c - \log(|\bar{\eta}|)/\lambda^* \,(\mathrm{mod}\ 2\pi) \\ \bar{\eta} = \eta + \varepsilon \sin(\xi) \\ \bar{\sigma} = \sigma \times \mathrm{sign}(\bar{\eta}) \end{pmatrix}, \tag{3.14}$$

a map known as a *separatrix map*. In a general case the jump $\varepsilon \sin(\xi)$ is replaced by a function $s(\xi)$. In the asymmetric cases one uses different jump functions $s_\pm(\xi)$ according to σ. The parameter ε, related to the size of the jump or splitting has, typically, exponentially small upper bounds as a function of some physical parameter, like the energy in the case of system (3.12). But in other cases, if the dominant eigenvalue at H tends to a constant $\lambda_0 > 1$ when some parameter γ tends to zero, it can be, simply, a power of γ.

For simplicity, we concentrate on the symmetric case and to points passing only through $\mathcal{D}_+$. Then $\sigma = 1$ and we discard it in (3.14). Now we assume that η is close to some fixed value, η_0, write $\eta = \eta_0 + \zeta$ and $\log(\bar{\eta}) = \log(\eta_0) + \log(1 + \bar{\zeta}/\eta_0) \approx \log(\eta_0) + \bar{\zeta}/\eta_0$, keeping only linear terms in $\bar{\zeta}$. This is a good approximation if $\bar{\zeta}/\eta_0$ is small. If we assume, also, that λ is close to 1, then λ^* is small. In the (ξ, ζ) variables the map becomes $(\xi, \zeta) \mapsto (\bar{\xi} = \xi + c_1 + b_1\bar{\zeta},\ \zeta + \varepsilon \sin(\xi))$, where $c_1 = c - \log(\eta_0)/\lambda^*$, $b_1 = -1/(\eta_0 \times \lambda^*)$, and we do not write explicitly that ξ is taken mod 2π. Finally, define new variables $u = \xi, v = c_1 + b_1\zeta$ and the map becomes

$$\begin{pmatrix} u \\ v \end{pmatrix} \to \begin{pmatrix} \bar{u} = u + \bar{v} \\ \bar{v} = v + b_1 \varepsilon \sin(u) \end{pmatrix}. \tag{3.15}$$

Comparing (3.15) with (3.10) we see that they are identical if we set $k = b_1\varepsilon = -\varepsilon/(\eta_0 \times \lambda^*)$. Therefore, we can expect to find invariant curves in the separatrix map at a distance $\eta_0 > \varepsilon/(k_G \times \lambda^*)$ from the location of the invariant manifolds in $\mathcal{D}_+$. A similar reasoning applies in the outer part, when the invariant curves make the full turn around the figure eight. This gives also an estimate of the width of

the zone with chaotic dynamics around the split manifolds. The estimate is quite realistic if ε is very small and λ is close to 1. This occurs, for instance, in a case like the Hamiltonian (3.12) because then, on a level of energy h, λ^* and ε are, respectively, of the order of h and exponentially small in h. See [47] for a study of several cases, with different number of d.o.f., either resonant or not.

As final comments in this subsection one has to add that it is very important to derive return maps in higher dimensions, like Hamiltonian systems with ≥ 3 d.o.f. or symplectic maps in dimension ≥ 4. But the formulas that one obtains can be far from simple, due to quasiperiodicity and resonances. To derive, from these return maps, bounds on the distance at which one can find invariant tori, speed of diffusion, etc, is an open problem. See slides (J) for other open problems associated to some classes of global bifurcations.

3.3 Some theoretical results, their implementation and practical tools

In this section we recall some general results and also provide tools to make them explicit.

3.3.1 A preliminary tool: the integration of the ODE, Taylor method and jet transport

In the case of an analytic Hamiltonian (or general) v.f. like $\dot{x} = f(t, x)$, $x(t_0) = x_0$, $(t_0, x_0) \in \Omega \subset \mathbb{R} \times \mathbb{R}^n$ or $\Omega \subset \mathbb{C} \times \mathbb{C}^n$, one should use integration methods of the initial value problem for ODE. For instance, having in mind to compute Poincaré iterates.

A quite convenient method is the *Taylor method*. That is, to obtain the Taylor expansion $x(t_0 + h)$ for suitable values of h. If $x(t_0 + h)$ has components x_i, $i = 1, \ldots, n$, we look for a representation

$$x_i = \sum_{s=0}^{N} a_i^{(s)} h^s, \tag{3.16}$$

for suitable N, h, and use it as a one-step method. For further reference we denote as $a^{(s)}$ the vector with components $a_i^{(s)}$.

The point is how to compute the coefficients of the expansion in an easy way to high order. For a very large class of functions the evaluation of f can be split

into simple expressions

$$\begin{aligned} e_1 &= g_1(t,x), \\ e_2 &= g_2(t,x,e_1), \\ &\vdots \\ e_j &= g_j(t,x,e_1,\ldots,e_{j-1}), \\ &\vdots \\ e_m &= g_m(t,x,e_1,\ldots,e_{m-1}), \\ f_1(t,x) &= e_{k_1}, \\ &\vdots \\ f_n(t,x) &= e_{k_n}. \end{aligned}$$

Each one of the expressions e_j contains a sum of arguments, a product or quotient of two arguments or an elementary function (like sin, cos, log, exp, $\sqrt{\ },\ldots$) of a single argument. The basic idea is to compute in a recurrent way the power series expansion (up to the required order) of all the e_j. The g_j have to be seen as operations with (truncated) power series. Hence, we can proceed as follows:

(i) Input: t and the components of x_0, that is, the coefficients of order zero in (3.16).

(ii) Step s, $s \geq 0$: from the arguments of g_j up to order s we obtain the order s terms of e_j; in particular for $f_j(t,x)$, which gives the order $s+1$ for x_j (dividing by $s+1$). This is repeated up to the required value of N.

(iii) The values of N, h can be selected so that the truncation error $\sum_{s>N} a_i^{(s)} h^s$ is bounded, for every component, by some small ε negligible in front of the (unavoidable) round off error.

Under reasonable assumptions, like $c_1\gamma^s \leq ||a^{(s)}|| \leq c_2\gamma^s$, $0 < c_1 < c_2$, (which implies radius of convergence $\rho = 1/\gamma$) in the limit when $\varepsilon \to 0$, say $\varepsilon = 10^{-d}$, with d large, one can take h such that the last term satisfies $||a^{(N)}||h^N = \varepsilon$. It turns out, concerning efficiency, that the optimal value of h tends to $\rho \times \exp(-2)$ (independently of the equation, and where ρ refers to the radius of convergence around the current point x_0), and $N \approx d\log(10)/2$ when $\varepsilon \to 0$.

To carry out step (ii) above is immediate for arithmetic operations. As an example for elementary functions we consider the case of powers, that we should use to integrate (3.1). Let $u(t) = \sum_{s\geq 0} u_s t^s$, $u_0 \neq 0$, $\alpha \in \mathbb{R}$, and we want to compute $v(t) = u(t)^\alpha = \sum_{s\geq 0} v_s t^s$. Then,

$$v_0 = u_0^\alpha, \quad v_s = -\frac{1}{s u_0} \sum_{k=0}^{s-1} v_k u_{s-k}[k - \alpha(s-k)],$$

for $s > 0$, the determination being fixed by the one used for v_0. This follows easily from $v(t) = u(t)^\alpha$ by taking logarithms and differentiation with respect to

t. Similar recurrences can be obtained for any elementary function. If f contains special functions (e.g., Bessel functions) it is enough to add the ODE satisfied by these functions to the system to be integrated.

Computing to order N has a cost $\mathcal{O}(N^2)$. This is true for the most expensive elementary operations and functions, and it is the basis of the optimal estimates given above, see [22] and slides (A).

In the autonomous case, to obtain the image of a point for a Poincaré map $\mathcal{P}$ through a section Σ given by $g(x) = 0$ when g changes from < 0 to > 0, assume that we have a time t^* such that $g(\varphi_{t^*}(x_0)) < 0$ and $g(\varphi_{t^*+h}(x_0)) > 0$, for the current value of h. Finding $\mathcal{P}(x_0)$ reduces to solving a 1-dimensional equation, $g(\varphi_{t^*+\delta}(x_0)) = 0$, for the variable δ. This is easily done by using Newton's method.

Assume now that we look for a periodic solution. It can be written as a fixed point of a Poincaré map: $G(x_0) = \mathcal{P}(x_0) - x_0 = 0$, for $x_0 \in \Sigma$. Again this can be solved by Newton's method, but this requires that one knows the differential map $D\mathcal{P}(x_0)$. To this end we integrate, together with the v.f. f, the first order variational equations $\dot{A} = Df(\varphi_t(x_0))A$, $A(0) = \mathrm{Id}$. There are two points to take into account, see [40]:

(i) The admissible variations of x_0 should be confined to the tangent space to Σ at that point. Furthermore, if the system has first integrals, like in the Hamiltonian case, this gives additional constraints for x_0 and the admissible variations if we fix the levels of these integrals.

(ii) The return time to Σ depends on the initial point. If instead of leaving from x_0 we leave from $x_0 + \xi$, ξ being an arbitrarily small admissible variation, the landing time in Σ has to be corrected by terms $\mathcal{O}(||\xi||)$. This is relevant to computing $D\mathcal{P}(x_0)$.

In some cases (see Subsection 3.3.4) we can be interested in having an approximation of the Poincaré map not restricted to first order terms in the variations of $x_0 \in \Sigma$, but to higher order: we would like to have the Taylor expansion of $\mathcal{P}(x_0+\xi)$ to some given order in ξ. To this end, one can integrate the higher order variational equations, restrict the domain of definition to Σ and to the levels of the current first integrals, or proceed in a different, easier, way, using *jet transport*, described along the following lines.

This can be also applied to obtain the image of a neighbourhood of a point x_0 under φ_t, to see how it depends on parameters (useful to analyze bifurcations), etc.

Assume the initial conditions are $x_0+\xi$, where ξ are some variations and we want to obtain $\varphi_t(x_0+\xi)$ at order m in ξ. It is enough to replace all the operations described above to compute e_j, in order to obtain the coefficients in (3.16), done with numbers, by operations with polynomials in ξ up to order m. This applies to arithmetic operations, elementary functions, special functions, etc. Hence, instead of the vectors a^s of numerical coefficients in (3.16) we deal with tables containing the numerical coefficients, up to order m, of n polynomials in the ξ variables.

If we return to the case of the Poincaré map, we had to solve $g(\varphi_{t^*+\delta}(x_0)) = 0$, for the variable δ. Now δ will depend on ξ, but this is not a problem for Newton's method. We simply apply it by replacing numbers by polynomials in ξ.

We remark that the jet transport can be implemented in an efficient way. It is also possible to produce rigorous estimates of the tails at every step, and to obtain intervals which contain the correct values of all the coefficients. This allows us to convert a purely numerical simulation into a Computer Assisted Proof (CAP). See, e.g., [24].

3.3.2 Normal forms

To study many systems, a useful trick is to try to reduce them to an expression as simple as possible, according to the topics of interest. If we study a discrete map around a fixed point, it would be nice to be able to reduce it to a linear map. In general, this is not possible. Furthermore, we can be interested also in the dependence with respect to parameters, to analyze possible bifurcations.

For concreteness we face a Hamiltonian in n d.o.f., in Cartesian coordinates, around a fixed point (located at the origin) that we assume totally elliptic: the eigenvalues are $\exp(\pm \mathrm{i}\omega_j)$, $j = 1, \ldots, n$. In canonically conjugate variables (x_i, y_i), $i = 1, \ldots, n$, we write it as $H = \sum_{k\geq 2} H_k$, where H_k denote the homogeneous terms of order k and $H_2 = \sum_{i=1}^{n} \omega_i (x_i^2 + y_i^2)/2$. In principle, we try to make a change of variables to cancel the terms H_k, $k > 2$. To keep the Hamiltonian character of the v.f. we shall use canonical transformations. These can be easily obtained as the flow of an auxiliary Hamiltonian, G, with respect to an auxiliary time s until, say, $s = 1$. If you do not want to use a "so big time $s = 1$" simply scale $(x, y) \to \varepsilon(u, v)$, divide the Hamiltonian by ε^2 obtaining $H_2(u, v) + \varepsilon H_3(u, v) + \varepsilon^2 H_4(u, v) + \cdots$, and then the final value of s will be ε. But this is equivalent to the previous approach. What makes the change close to the identity is the smallness of (x, y), not the fact of using $s = 1$.

As we want to cancel, first, the terms in H_3, we shall represent G also as a sum of homogeneous parts, starting at order 3, $G = \sum_{k\geq 3} G_k$.

To transform the function H under the change we write $dH/ds = \{H, G\}$, where

$$\{H, G\} = \sum_{i=1}^{n} \frac{\partial H}{\partial x_i}\frac{\partial G}{\partial y_i} - \frac{\partial H}{\partial y_i}\frac{\partial G}{\partial x_i}$$

denotes the Poisson bracket. Note that the bracket of homogeneous polynomials of degrees d_1 and d_2 has degree $d_1 + d_2 - 2$. Higher order derivatives are obtained by doing, successively, the Poisson bracket with G once and again. Trying to cancel (if it is possible to cancel) the terms H_k, $k \geq 3$, we determine the homogeneous parts G_k. But it turns out that to obtain these parts it is much simpler to use complex coordinates. We introduce

$$\begin{pmatrix} x_i \\ y_i \end{pmatrix} = \frac{1}{\sqrt{2}} \begin{pmatrix} 1 & \mathrm{i} \\ \mathrm{i} & 1 \end{pmatrix} \begin{pmatrix} q_i \\ p_i \end{pmatrix}, \quad i = 1, \ldots, n.$$

Then H_2 becomes $\sum_{j=1}^{n} \mathrm{i}\,\omega_j q_j p_j$. The transformed Hamiltonian is

$$\varphi_{s=1}^{G}(H) = H + \{H, G\} + \frac{1}{2!}\{\{H, G\}, G\} + \frac{1}{3!}\{\{\{H, G\}, G\}, G\} + \cdots \quad (3.17)$$

Assume we have determined G_j, $j < m$, and we want to cancel all the possible terms to order m in (3.17). There are terms or order m in (3.17) which come from H_m or involving G_j, $j < m$, which are already known and that we denote, together, as K_m. For definiteness, assume $K_m = \sum_{a,b,|a|+|b|=m} K_{a,b}\, q^a p^b$, where a denotes a multiindex with n non-negative components a_i, $|a| = \sum_{i=1}^{n} a_i$, and $q^a = \Pi_{i=1}^{n} q_i^{a_i}$, as usual. Similarly for b and p^b. The only unknown part comes from G_m, that we also write as $G_m = \sum_{a,b,|a|+|b|=m} G_{a,b}\, q^a p^b$ and we would like to have

$$0 = \{H_2, G_m\} + K_m = \sum_{a,b,|a|+|b|=m} \mathrm{i}\,(\omega, b-a) G_{a,b}\, q^a p^b + \sum_{a,b,|a|+|b|=m} K_{a,b}\, q^a p^b, \quad (3.18)$$

where $(\omega,\, b-a)$ denotes the scalar product $\sum_{j=1}^{n} \omega_j (b_j - a_j)$. As $K_{a,b}$ is known, one easily determines $G_{a,b}$, provided $(\omega,\, b-a) \neq 0$. But it is clear that if $b_j = a_j$ for all j, then the term $K_{a,a}$ must be left on the transformed Hamiltonian, independently of ω. These are called the *unavoidable resonances* which appear at even orders. Furthermore, if ω is *resonant*, i.e., there are integers c_j, $j = 1, \ldots, n$, such that $(\omega,\, c) = 0$, other terms should be kept in the transformed Hamiltonian when $b - a = c$. These are the additional resonant terms.

The normalization process can be continued to any order. But, in general, unless the Hamiltonian is integrable, the formal normal form is not convergent. One can expect that it belongs to some Gevrey class (see the invariant manifolds part in Section 3.2.1), but I am not aware of *concrete general results* in that direction.

After we have transformed the Hamiltonian up to order M, we can skip the terms of higher order and denote the contribution up to order M as HNF_M, the *normal form to order* M. We recall that a Hamiltonian system with n d.o.f. is said to be *integrable* (in the Liouville–Arnold sense) if there exist n first integrals, F_j, $j = 1, \ldots, n$, an involution, $\{F_i, F_j\} = 0$, and functionally independent almost everywhere. If ω is non-resonant then the HNF_M is integrable, because one can take $F_j = q_j p_j$, $\forall j$.

Now consider the resonant case. By construction, $\{H_2, HNF_M\} = 0$ and, therefore, except in the degenerate case in which they are not independent, if $n = 2$ one has HNF_M integrable. In general this is not true if $n > 2$. The system can be far from integrable even in a small vicinity of a totally elliptic point. But it can take a long time to have numerical evidence of the existence of chaos, even if it occurs for most of the initial conditions.

A celebrated theorem by Arnold says that, for an integrable system, if the set of points in the phase space corresponding to fixed values of the first integrals $F_1^{-1}(c_1) \cup F_2^{-1}(c_2) \cup \cdots \cup F_n^{-1}(c_n)$ is compact, then it is an n-dimensional torus

$\mathbb{T}^n$. Around a given torus one can introduce the so-called *action-angle variables* (I, φ), $I \in \mathbb{R}^n$, $\varphi \in \mathbb{T}^n$. The integrable system can be written, then, as depending only on I: $H = H_0(I)$, the integration is elementary and the frequencies on the given torus have the expression $\omega_j = \partial H_0/\partial I_j|_{F=c}$, $j = 1, \ldots, n$. If the system is perturbed to $H = H_0(I) + \varepsilon H_1(I, \varphi)$ we can study how the properties of $H_0(I)$ change under the effect of the perturbation. See Subsections 3.3.3 and 3.3.5 in this direction.

But we want to point out that it is also possible to try to produce a normal form for the perturbed Hamiltonian around the given torus if the frequencies on it, ω_j, satisfy a non-resonant condition. This can push the perturbation to higher order in ε, making easier the applicability of general results.

Up to now we have considered, around a fixed point, the totally elliptic case. If the quadratic term H_2 contains some hyperbolic part $H_2 = \sum_{i=1}^{n_e} \omega_i(x_i^2+y_i^2)/2+ \sum_{j=n_e+1}^{n} \lambda_j x_j y_j$, one can use similar ideas to obtain approximations of the central manifold and of the Hamiltonian reduced to it. We return to this in Subsection 3.3.4.

3.3.3 Stability results: KAM theory and related topics

There is a natural generalization of the idea of twist map to higher dimension. Consider a map T defined, in suitable coordinates, in a product of n annuli, with radii $r_i \in (r_{d,i}, r_{u,i})$, $0 < r_{d,i} < r_{u,i}$, $i = 1, \ldots, n$, of the form $T(r, \alpha) = (r, \alpha + a(r))$, where $r \in \mathcal{R} = \Pi_{i=1}^n (r_{d,i}, r_{u,i})$ has components $r_1, \ldots, r_n$, $\alpha \in \mathbb{T}^n$ and a is a map from $\mathcal{R}$ to $\mathbb{R}^n$ which can be denoted as *translation*. The map T is an integrable symplectic map, and $\mathcal{R} \times \mathbb{T}^n$ is foliated by tori invariant under T. Nothing else but what we saw for (3.7) in the part about ICs in Section 3.2.1.

The differential of the translation with respect to the radii, $D_r a(r)$ is known as *torsion*.

Then the KAM theorem for symplectic maps has the following statement, completely analogous to Theorem 3.2.1.

Theorem 3.3.1. *Consider a perturbation $F_\varepsilon = T + \varepsilon P$ of the integrable symplectic map T in $\mathcal{R} \times \mathbb{T}^n$, and assume that for $r = r^*$ the vector $a(r^*)$ satisfies a DC, that the torsion is non-degenerate and ε is small enough. Then the map F_ε has also invariant tori in $\mathbb{T}^n$, close to $r = r^*$, and on them the action of F_ε is conjugated to the one of T on $r = r^*$, that is, a translation by $a(r^*)$.*

In the present case, the DC is slightly different from the one in (3.3). Beyond the translations $a_i(r)$, $i = 1, \ldots, n$, one has to add the value 1, as it is obvious thinking on the suspension. So, it reads as

$$\left| (\sum_{i=1}^{n} k_i, a_i) + k_0 \right| \geq b|k|^{-\tau}, \quad \forall k \in \mathbb{Z}^{n+1} \setminus \{0\},$$

where k denotes now $(k_1, \ldots, k_n, k_0)$. The role of the DC, the non-degeneracy of

the torsion, is analogous to the twist condition, and the smallness of ε plays the same role.

A result similar to Theorem 3.3.1 holds in the case of Hamiltonian systems.

Theorem 3.3.2. *Let $H_0(I)$ be an integrable Hamiltonian, for which there exist invariant tori, and assume that for some given torus, labelled by I^*, the frequencies $\omega(I^*) = \partial H_0(I)/\partial I|_{I=I^*}$ satisfy a DC (in the sense of* (3.3)*) and are non-degenerate, so that the differential $\partial\omega/\partial I|_{I=I^*}$ is regular. Then if ε is small enough, a perturbed Hamiltonian $H(I,\varphi) = H_0(I) + \varepsilon H_1(I,\varphi,\varepsilon)$ has a nearby invariant torus with the same frequencies.*

These results usually do not give estimates on how small ε should be or, if any, they are very pessimistic. However, normal form techniques (see Subsection 3.3.2) can help to start the iterative process in a very good approximation, so that the difference with the initial guess and the true torus, if it exists, is sufficiently small.

For the effective computation of invariant tori there exist different methods.

A quite classical method is the Lindstedt–Poincaré (LP) method. In principle, it is formal because one looks for the invariant tori without paying too much attention to the DC (despite the fact that this can also be implemented). Assume that we look for 2D tori around a totally elliptic point (assumed to be located at the origin) in a Hamiltonian system with $n = 2$ d.o.f. Let $\omega_1(0)$, $\omega_2(0)$, be the frequencies at the fixed point. The linear system will have, for the q, p variables, a representation as linear combinations of $\cos(\omega_1(0)t + \psi_1)$ and $\cos(\omega_2(0)t + \psi_2)$, where ψ_1, ψ_2 represent some phases, and these terms have amplitudes α_1, α_2. Due to symmetries and the freedom to select the origin of time, the phases for the different variables can be put in simple form.

We wish to satisfy the equations $\dot{q} = \partial H/\partial p$, $\dot{p} = -\partial H/\partial q$ by expanding in powers of the amplitudes α_1, α_2 and integration of the coefficients of these powers with respect to time. However, it turns out that at some order we can find on the right-hand side of the equations terms which are not purely quasiperiodic, i.e., they are constant. The solution consists in allowing the frequencies to depend also on the amplitudes. So $\omega_i = \omega_i(0) + \sum_{j_1,j_2} c_{i,j_1,j_2}\alpha_1^{j_1}\alpha_2^{j_2}$, $i = 1, 2$, and a suitable choice of these c_{i,j_1,j_2} coefficients cancels the constant terms.

An often used method is based in writing the coordinates of the points of the unknown torus as Fourier series in some angles, and then imposing the invariance conditions. For concreteness we consider the case of symplectic maps. The flow case can be reduced to this one via a Poincaré map. Assume that we look for a d-dimensional torus in which the dynamics is conjugated to $\theta \mapsto \theta + \alpha$, for $\theta \in \mathbb{T}^d$ and a translation vector $\alpha \in \mathbb{R}^d$ satisfying the DC. Let x be the coordinates in the phase space and F the discrete map. The invariance condition is

$$F(x(\theta)) = x(\theta + \alpha). \tag{3.19}$$

It is clear that one has freedom to select the origin of the angles θ_i and that eventual symmetries can reduce the number of coefficients to be determined.

To begin with the process, we can assume that we have obtained some approximation by direct numerical simulation, or that we start near a fixed (or periodic) point and use the linear approximation or an approximation obtained by an LP method. If we are interested in a family of invariant tori, one can use continuation methods, but taking into account that the values of α should satisfy the DC. Hence, there will be gaps in the family, despite the fact that they can be very small in some cases. Let c denote, generically, the coefficients of the Fourier expansion, truncated at a suitable order. From a grid of values of θ one can obtain initial values of x. They are mapped to $F(x)$ and the images can be Fourier analyzed to obtain the new Fourier coefficients $\hat{c}$. Let L be the action of the translation by α on the initial Fourier coefficients. According to (3.19), we should require $L(c) - \hat{c} = 0$. This is the equation that follows from (3.19) and has to be solved, usually by Newton's method. The differentials of the Fourier synthesis and analysis are elementary and the one of F can be obtained by computing DF (this can be, typically, the differential of a Poincaré map). See [23] for an efficient implementation with similar and extended ideas, which works even with a very large number of harmonics.

The number of harmonics to be used depends on the shape of the torus. One can use in the grid in θ (and, therefore, in x) a number of points larger than the number of components of c. In that way one can check the behaviour of coefficients in $\hat{c}$ which have not been used as c coefficients in the representation of the solution we search, and see if they can be neglected. Otherwise, one increases the number of harmonics. This can be done at successive iterations of Newton's method in a dynamic way.

It is also possible not to fix α a priori and determine it together with the coefficients c. Note that, in case α is close to resonant, one can have convergence problems. For other quite different problems, like looking for invariant tori in PDE, this method requires a huge number of Fourier coefficients if the discretisation dimension is large. Other methods, working directly in the phase space like the synthesis of a return map, see [39, 42], can give the desired results.

There is a fact, concerning invariant tori and which applies also to the computation of some periodic orbits, which can produce difficulties. This is the instability present in partially normally hyperbolic tori or, in a simpler case, in linearly unstable periodic orbits. Given a point x, and assuming it approximately located in an invariant torus, the instability can produce that $F(x)$ is far away from the torus. This produces convergence problems.

The solution consists in using *parallel shooting*. Instead of taking a single Poincaré section, say Σ, one can use several of them, say $\Sigma_0 = \Sigma, \Sigma_1, \Sigma_2, \ldots, \Sigma_{m-1}$, and the corresponding *partial Poincaré maps*:

$$\mathcal{P}_1 \colon \Sigma_0 \mapsto \Sigma_1, \quad \mathcal{P}_2 \colon \Sigma_1 \mapsto \Sigma_2, \quad \ldots \quad \mathcal{P}_m \colon \Sigma_{m-1} \mapsto \Sigma_0.$$

Hence, the full Poincaré map can be written as $\mathcal{P} = \mathcal{P}_m \circ \cdots \circ \mathcal{P}_2 \circ \mathcal{P}_1$. Then we look for Fourier representations in each one of the intermediate sections. This

produces a much larger set of equations, but it has the advantage that each one of the partial maps $\mathcal{P}_j$ is much less unstable.

In the case of highly unstable periodic orbits things are simpler. We only need one point in each intermediate section, say $x_0 \in \Sigma_0$, $x_1 \in \Sigma_1$, ..., $x_{m-1} \in \Sigma_{m-1}$. The conditions are simply $\mathcal{P}_1(x_0) - x_1 = 0$, $\mathcal{P}_2(x_1) - x_2 = 0$, ..., $\mathcal{P}_m(x_{m-1}) - x_0 = 0$. The system to be solved is large but the differential has a simple block structure and the condition number is much better.

3.3.4 Invariant manifolds

Another basic ingredient of the dynamics are the invariant manifolds. In contrast with the tori of maximal dimension, responsible for the regular behaviour, the invariant manifolds are, typically, responsible for the chaotic part of the dynamics. We comment first on invariant stable and unstable manifolds of fixed points of APM F. The components will be denoted as F_1, F_2.

Assume a fixed point is located at the origin with dominant eigenvalue $\lambda > 1$, and having an unstable linear subspace E^u and a stable one E^s. Then the *unstable manifold Theorem* ensures the existence of an unstable manifold $W^u_{\rm loc}$ in a neighborhood of the origin, invariant under F, tangent to E^u at the origin and such that for a point p on it, the iterates under F^{-1} tend to the origin. In fact, only the points in $W^u_{\rm loc}$ remain on the neighborhood for all iterations. This is a local result. Then the global unstable manifold W^u is obtained by iteration of $W^u_{\rm loc}$ under F. A similar result gives the stable manifold, obtained by exchanging F and F^{-1}. In the analytic case, as we assume, the manifolds are analytic.

Let u and s be local coordinates along the unstable and stable eigenvectors. For the linear map DF, the manifold W^u is just $s = 0$. We can try to find a representation of W^u for F as the *graph of a function*: $s = g(u) = \sum_{j\geq 2} a_j u^j$. The invariance condition reads $F_2(u, g(u)) = g(F_1(u, g(u)))$. The coefficients a_j are determined in a recurrent way by identifying the left-hand and right-hand coefficients of u^j.

An alternative representation of W^u is the *parametrization method*. Let us use z as a parameter. In the linear case, a point with $u = z$ is mapped to $u = \lambda z$. Now it is not necessary to use coordinates adapted to the eigenspaces. If we use (x, y) as coordinates around the fixed point and represent the parametrization as $(p_1(z), p_2(z))$, the invariance condition is simply

$$F(p_1(z), p_2(z)) = (p_1(\lambda z), p_2(\lambda z)). \tag{3.20}$$

That is, we look for a conjugacy on the manifold between F and its linear part. We search now for the parametrization as $p_1(z) = \sum_{j\geq 2} a_j z^j$, $p_2(z) = \sum_{j\geq 2} b_j z^j$ in (3.20). Note that the parametrization can be normalized so that the vector of coefficients of order 1 has Euclidean norm equal to 1. As before, the coefficients of order $j > 1$ are obtained in a recurrent way. This is the method used for many of the examples displayed before.

A first practical question, given a parametrization to order N (a similar question can be posed for the graph method), is up to which value of z, say $z_{\max}$, one can use the representation. The idea is quite simple: given a tolerance ε we can compute the point B of parameter z and also the point A of parameter z/λ. One should have $F(A) = B$, according to (3.20). Hence, we can check up to which value of z one has $||F(A) - B|| < \varepsilon$. This gives the admissible domain for z. Then, a *fundamental domain* $\mathcal{FD}$ is parametrized by $z \in (z_{\max}/\lambda, z_{\max}]$. Any point on the manifold can be found as an iterate of a point in $\mathcal{FD}$. A similar domain, with $z < 0$, has to be found for the other branch of the manifold.

To obtain points in the manifold for $z > z_{\max}$ we simply divide the current parameter by λ as many times as required until a value less than $z_{\max}$ is obtained. Assume one has to divide k times. Then we compute the point of parameter z/λ^k and iterate it k times under F. In this way it is possible to reach points away from the fixed one, to detect foldings of the manifold, to reach the vicinity of a homoclinic or heteroclinic point, etc. The selected values of z at which the computation is done can be chosen to satisfy conditions such as having the distance between two consecutive points in W^u or the angle between three consecutive points below some prefixed values.

Why do we need approximations beyond the linear one? The answer depends on the purpose. If we want to produce a long part of the manifold and, especially, if λ is close to 1, we can require many iterates. On the other hand, if F is not given explicitly but follows from a Poincaré map, we need jet transport to have a local Taylor expansion. In any case, there is an optimal choice to obtain the "cheaper order" (cheaper can mean in terms of CPU time, of personal time, or a combination of both).

If we are interested in locating a homoclinic point, and no symmetry is available for this, the problem reduces to finding two parameters, z_u and z_s, and well as two integers, k_u and k_s, to be used for the unstable and stable manifolds, respectively, such that $F^{k_u}(p_u(z_u)) = F^{-k_s}(p_s(z_s))$, where p_u, p_s denote the respective parametrizations. It is possible to find suitable values of k_u, k_s and then to solve for z_u, z_s using Newton's method. A similar method can be used for heteroclinic points, for tangencies, etc.

The ideas are similar in higher dimension. One can look for d-dimensional invariant manifolds, $d > 1$, using either graph or parametric methods. This is specially necessary, for instance, if we look for an unstable manifold with quite different eigenvalues. A low order representation will take the initial points along the direction of the maximal eigenvalue. Beyond using high order local expansions, to decrease the problem, one can use different devices depending on the problem.

To look for the invariant unstable manifold of an invariant curve in a symplectic 4D map, a parametrization using a parameter z, which measures the distance to the curve, and an angle θ along the curve are useful. The fundamental domain, in that case, is diffeomorphic to an annulus. See an example in Subsection 3.4.2 in a different context, and another one in Subsection 3.4.5 concerning a family of invariant curves.

The idea extends to any dimension with increasing complexity. See [2, 3, 4] for a nice global approach.

A different problem appears when we consider symplectic maps in dimension 4 (or higher) or problems reducible to them. Consider again the case of a fixed point but assume that, together with an eigenvalue $\lambda > 1$ and its inverse, there is a couple of eigenvalues of modulus 1. They give rise to the *centre manifold* of the point. In general, when we consider a given neighborhood of the point, the manifold has some degree of differentiability which depends on the neighborhood. Furthermore, there is no uniqueness in general.

The difficulty comes from the fact that the dynamics on that manifold is not known. It can contain, simultaneously, invariant curves, periodic points and chaotic zones. It is said to be a *normally hyperbolic invariant manifold* (NHIM) if the hyperbolicity normal to the manifold is stronger than the hyperbolicity that can be found inside the manifold.

One can recur to normal forms to obtain an approximation of all the dynamics around the point and, in particular, the centre manifold. A similar idea is to use a *partial normal form*, see [42]. Assume we have a Hamiltonian

$$H = \lambda q_1 p_1 + \frac{1}{2}\omega_1(q_2^2 + p_2^2) + \frac{1}{2}\omega_2(q_3^2 + p_3^2) + \sum_{k\geq 3} H_k(q_1, q_2, q_3, p_1, p_2, p_3), \quad (3.21)$$

where, as usual, H_k denotes a homogeneous polynomial of degree k.

We proceed as in the case of normal form above, but trying only to cancel all the terms such that the total degree in (q_1, p_1) is equal to 1. Using again complexification, as in the case of the normal form, for the couples (q_2, p_2) and (q_3, p_3), the current denominators to obtain the successive terms in the Hamiltonian G used to transform H are of the form

$$(k_1 - l_1)\lambda + \mathrm{i}\,(k_2 - l_2)\omega_1 + \mathrm{i}\,(k_3 - l_3)\omega_2,$$

with modulus bounded from below by $|\lambda|$, even if ω_1 and ω_2 are resonant. It is clear that, denoting the new variables as $Q_1, Q_2, Q_3, P_1, P_2, P_3$, if we set $Q_1 = P_1 = 0$ this is the desired centre manifold. Hence, setting these variables to zero we have a Hamiltonian with two d.o.f., which gives the reduction to the centre manifold of the initial Hamiltonian. The process is formal, there is no convergence in general, but one can obtain a good approximation in a suitable domain. One can check up to which distance of the fixed point the approximation satisfies some tolerance condition. See [42] for an example around the collinear point L_2 in the spatial circular restricted three-body problem.

3.3.5 Instability, bounds and detection

In the case of a Hamiltonian with $n \geq 3$ d.o.f., in principle, there is no way to avoid diffusion. The maximal dimensional tori have dimension n, that is, codimension $n-1$ in a fixed level of energy, and they do not separate the phase space. For instance,

initial conditions as close as we like to $L_{4,5}$ in the spatial circular restricted three-body problem (see the beginning of Section 3.4), which are totally elliptic fixed points, can go far away from these points. But normal forms, or averaging, lead to the so-called Nekhorosev estimates [37], showing that one needs an extremely large time if one starts close enough to the libration point. See also [14] for a rather detailed approach. Similar things happen for $(2n-2)$-dimensional symplectic maps.

Consider a perturbation $H(I,\varphi) = H_0(I) + \varepsilon H_1(I,\varphi,\varepsilon)$ of an integrable Hamiltonian H_0. The basic idea of the bounds is similar to the averaging Theorem 3.1.1, trying to cancel, around an arbitrary torus labelled by the action I^*, the dependence with respect to φ. But now the frequencies of the unperturbed Hamiltonian $\omega(I) = DH_0$ may not satisfy the DC and, on the other hand, the perturbation will produce that the frequencies change. Hence, the passage through resonances or through other frequencies not satisfying the DC is unavoidable.

First one should examine what is the effect of a resonance. We refer to Subsection 3.2.2 where we commented on the width associated to a pendulum like structure. A perturbation $\mathcal{O}(\varepsilon)$ can give rise to variations $\mathcal{O}(\sqrt{\varepsilon})$ due to the presence of a simple resonance. This happens if the frequencies change, reach a resonance and then go away from it. But then one can put the following question. Assume that in the variation of some action there is a term, due to the perturbation, like $\dot{I}_j = \varepsilon\cos((k,\varphi))$, where (k,φ) is a linear combination of the angles, and the related combination of the frequencies satisfies $(k,\omega) = 0$. One expects that the frequencies will change with time and one will escape from resonance, but it can happen that the *frequencies are locked at resonance up to order* m for some $m > 0$. That is, $\frac{d^k}{dt^k}(k,\omega) = 0$ for $k = 0,1,\ldots,m$, and $\frac{d^{m+1}}{dt^{m+1}}(k,\omega) \neq 0$. Then, during a long time, the term $\cos((k,\varphi))$ will be close to constant and the action can change by a large amount. If the locking occurs at all orders, the change in I_j will be $\mathcal{O}(\varepsilon t)$. To prevent this locking is why Nekhorosev introduced the so-called *steepness condition*, which prevents the order of the locking exceeding a maximal value. Then one has the Nekhorosev result: under steepness of some order, the variation of the actions $||I(t) - I(0)||$ does not exceed a bound $\mathcal{O}(\varepsilon^b)$ during a time interval $|t| < \mathcal{O}(\exp(c\varepsilon^{-a}))$, where the positive constants a, b, c depend on the order of steepness and properties of H_0, assuming that the norm of H_1 is bounded.

Around a given point, or a given torus (in particular, a periodic orbit) it can happen that there are many KAM tori. The above description of the Nekhorosev estimates puts a bound on how fast escap from the vicinity of these tori can be. Typically, one refers to this fact as *stickiness of the invariant tori*. Perhaps the escape is so slow that it has no relevance during the time interval in which we are interested, or even during the period of validity of the model. This suggests that we introduce the concept of *practical stability*. Assume that the studied object has $I = I^*$. Then, for fixed values of (ε, T), where ε is moderately small and T is large, we say that there is (ε, T)-practical stability if there exists $\rho = \rho(\varepsilon, T)$, such that points with initial conditions at $t = 0$ satisfying $||I(0) - I^*|| < \rho$ evolve with time

satisfying $||I(t) - I^*|| < \varepsilon$ for all $t \in [0, T]$; that is, we require stability only for finite time. See [14].

Clearly, for any v.f. with Lipschitz constant L, (ε, T)-practical stability is found if $\rho \leq \varepsilon \exp(-LT)$, as follows from Gronwall's Lemma. But this gives *extremely small* values of ρ, completely useless for any practical application. More realistic values would be $\rho = 0.01$ for $\varepsilon = 0.02$ and $T = 10^9$, depending on the practical example in mind. See, e.g., [9] for a nice approach to KAM and practical stability simultaneously.

Another relevant point is how to detect the existence of chaos and quantify it in a concrete example. There are many different approaches. We comment on the Lyapunov exponents.

To measure the instability properties of a fixed point (of a continuous or discrete system) it is enough to look at the differential of the v.f., or of the map at that point. How to proceed for a general orbit? The idea is to look for the rate of increase (if any) of the distance between the orbits of nearby points. In the limit, this becomes the rate of increase of an initial displacement, ξ, under the differential of the iterates of the map or under the action of the first order variational flow. For concreteness we consider the case of discrete maps.

Let x_0 be an initial point on a manifold $\mathcal{M}$ on which it acts a map F, and let $x_1 = F(x_0), \ldots, x_k = F(x_{k-1}), \ldots$ be the orbit of x_0. We can define, if it exists,

$$\Lambda = \sup_{\xi} \lim_{k \to \infty} \frac{\log(||DF^k(x_0)\xi||)}{k}, \tag{3.22}$$

where ξ is taken from the vectors with unit norm $||\xi|| = 1$ in $T_{x_0}\mathcal{M}$, the tangent space to $\mathcal{M}$ at the point x_0. One can prove that the limit in (3.22) exists for almost every $x_0 \in \mathcal{M}$ and for almost every $\xi \in T_{x_0}\mathcal{M}$, and it is known as *maximal Lyapunov exponent*.

In the Hamiltonian case (or in the symplectic one) it is easy to prove that, for initial points in invariant tori of maximal dimension, the limit exists and is equal to zero. Typically, $||DF^k(x_0)\xi||$ behaves linearly in k in that case, which gives the desired limit. For generic unstable orbits one expects positive values of Λ. The geometrical reason is clear: every time that the iterates pass close to an hyperbolic object, the unstable component will increase at a geometric rate. For an integrable system, if, for instance, unstable and stable manifolds coincide, when returning near the hyperbolic object, this expansion is canceled due to the iterations which occur close to the stable manifold. But the existence of transversal homoclinic (or heteroclinic points) prevents this from occurring.

One of the basic questions is how to have an estimate of the limit. In practice the number of iterations should be finite (and there is also the effect of round off, which is another issue). A simple approach is to proceed to the computation in (3.22) using a different presentation. Let us define the *Lyapunov sums* as follows. Let x_0, ξ_0 be the initial point and vector, and set $S_0 = 0$. Then, at the k-th iterate,

we use the following algorithm:

$$x_k = F(x_{k-1}), \quad \eta_k = DF(x_{k-1})\xi_{k-1}, \quad \xi_k = \eta_k/||\eta_k||, \quad S_k = S_{k-1} + \log(||\eta_k||). \tag{3.23}$$

Hence, we normalize the tangent vector after every step and add the log of the normalization to the current value of the sum S. It is clear that the limit slope of S_k, as a function of k, should coincide with Λ, as defined in (3.22). Hence, we can proceed as in (3.23) and, from time to time (say, after mN iterates, $m = 1, 2, \ldots$), fit a line to three different subsamples of the current sample (e.g., last 30%, last 50% and last 70%) and accept the average of the slopes as value of Λ if they differ by less than a prescribed tolerance. Otherwise, keep iterating until the next multiple of N, provided this does not exceed a maximal value.

A problem is that, in case $\Lambda = 0$, the convergence can be slow; for instance, $\log(k)/k$ is below 10^{-5} only for $k \geq 1,416,361$. An alternative approach, which tends in a faster way to the limit and also smoothes out the oscillations due to the quasiperiodic effects (in the case of orbits), can be found in [8]. One can look for the systematic use of that method in [25] for a family of 2D symplectic maps in $\mathbb{S}^2$. Another idea, if one is interested only in deciding whether the orbit is regular or chaotic, is to stop computations and consider the orbit as chaotic if S_k exceeds some threshold.

3.4 Applications to Celestial Mechanics

In this section we present several applications to illustrate theoretical and computational approaches to simple examples in Celestial Mechanics. One can have a look at slides (C), concerning the role of dynamical systems in Celestial Mechanics. Most of the applications deal with the restricted three-body problem (RTBP). We shortly recall it.

The RTBP studies the motion of a particle P_3 of negligible mass under the gravitational attraction of two massive bodies, P_1 and P_2, of masses m_1 and m_2, respectively. They are known as primaries or as primary and secondary. We assume that the primaries move in a plane along circular orbits around their centre of masses. We can normalize $m_1+m_2 = 1$ and $d(P_1, P_2) = 1$ and express the dynamics in a rotating frame (the so called synodical frame) with unit angular velocity. The problem depends on a unique parameter $\mu = m_2$. In this frame P_1 and P_2 are kept fixed at $(\mu, 0, 0)$ and $(\mu - 1, 0, 0)$.

The equations of motion are

$$\ddot{x} - 2\dot{y} = \Omega_x, \quad \ddot{y} + 2\dot{x} = \Omega_y, \quad \ddot{z} = \Omega_z, \tag{3.24}$$

where

$$\Omega(x, y, z) = \frac{1}{2}(x^2 + y^2) + \frac{1-\mu}{r_1} + \frac{\mu}{r_2} + \frac{\mu(1-\mu)}{2},$$

$r_1^2 = (x-\mu)^2 + y^2 + z^2$, and $r_2^2 = (x+1-\mu)^2 + y^2 + z^2$. The function

$$J(x, y, z, \dot{x}, \dot{y}, \dot{z}) = 2\Omega(x, y, z) - (\dot{x}^2 + \dot{y}^2 + \dot{z}^2)$$

is a first integral, its value being known as Jacobi constant and it is usually represented as C. The related 5D energy manifolds are defined as

$$\mathcal{M}(\mu, C) = \left\{(x, y, z, \dot{x}, \dot{y}, \dot{z}) \in \mathbb{R}^6 | J(x, y, z, \dot{x}, \dot{y}, \dot{z}) = C\right\} \tag{3.25}$$

and their projections on the configuration space are known as *Hill's regions*, bounded by the zero velocity surfaces (ZVS) (the zero velocity curves, ZVC, in the planar case).

The problem has five equilibrium points (also known as libration points):

(i) Three of them, say L_1, L_2 and L_3, are collinear (or Eulerian) on the x-axis, of centre×centre×saddle type and, hence, they have a 4D centre manifold which contains the so-called horizontal and vertical periodic orbits of Lyapunov type (to be denoted as hpo_L and vpo_L), invariant 2D tori and other periodic orbits (like the halo orbits, depending on the value of C), as well as chaotic regions.

(ii) Two of them, say L_4 and L_5, are triangular (or Lagrangian) at $x = \mu - 1/2$, $y = \pm\sqrt{3}/2$, $z = 0$. The term $\mu(1-\mu)/2$ in Ω is added to have $C(L_{4,5}) = 3$. Let μ_j be the value of μ for which the ratio of frequencies in the plane, $\left[(1 \pm (1 - 27\mu(1-\mu))^{1/2})/2\right]^{1/2}$, is j. The points are totally elliptic for $0 < \mu < \mu_1 = (9 - \sqrt{69})/18$ and the 2:1, 3:1 resonances (leading to instability) show up for $\mu_2 = (45 - \sqrt{1833})/90$ and $\mu_3 = (15 - \sqrt{213})/30$. Associated to the planar frequencies there are the so-called short and long period periodic orbits. The vertical frequency, giving rise also to a family of vpo_L, is equal to 1.

3.4.1 An elementary mission around L_1

First we consider the planar case. Assume that P_1 and P_2 are Sun and Earth, respectively. The distance between them, 1.5×10^8 km, and the period, 1 year, are scaled to 1 and 2π units, respectively, as said before and we take $\mu = 3.0404326 \times 10^{-6}$ (it includes Moon's mass). We want to carry out the following steps:

(i) Compute a periodic orbit of the system, around the Earth, with a period of 1 day (a geostationary orbit) and check that it is close to circular. Call it PO_1.

(ii) Compute some periodic orbits around L_1 (of the hpo_L family), which are symmetrical with respect to the x-axis. Check that they are unstable. We call them, in general, PO_2.

(iii) Compute the left branches of the stable manifolds of the previous orbits until they reach some suitable value of x (e.g., $x = -0.999$).

(iv) Now assume an spacecraft is moving in the "parking" orbit PO_1. At some point of the orbit we give an impulsion Δv, in the direction of the velocity at that point, with the goal of reaching a point of the stable manifold of one of the hpo_L. Determine the hpo_L which are reachable in that way from the parking orbit, at which place one should give the impulsion and which is the size Δv.

This allows us to obtain an elementary approach to a space mission. Later, one can consider the effect of perturbations of other bodies, the separate effects of Earth and Moon, change to a non-planar target orbit, the fact that the target orbit is, approximately, quasiperiodic instead of periodic, to optimize with respect to fuel consumption and with respect to transfer time from departure to a vicinity of the target orbit, etc. For information about the methodology for the design and control of missions around libration points see [15, 16, 17, 18]. We detail the steps to find the solution in the present example.

Step 1: First we compute a periodic orbit around the Earth with period $\tau = 2\pi/366.25$. We start with initial data $(x_0, 0, 0, \dot{y}_0)$ and require $\varphi_\tau(x_0, 0, 0, \dot{y}_0) = (x_0, 0, 0, \dot{y}_0)$. In fact, it is much simpler to ask for the image at $t = \tau/2$ to be of the form $(x_1, 0, 0, \dot{y}_1)$, and then symmetry completes the task. We have two known data $x_0, \dot{y}_0$ and two conditions $y_1 = 0$, $\dot{x}_1 = 0$. After a few attempts one can use Newton's method to find the solution $x_0 \approx -0.999714471273, \dot{y}_0 \approx 0.103463316596$. One can check that the monodromy matrix has a double eigenvalue equal to 1 (as expected: energy preservation and time shift) and the other eigenvalues are $\exp(\pm\alpha \mathrm{i}\,)$, $\alpha \approx 0.034228998$. The difference with respect to a circular orbit is less than 350 m. For further reference we denote this orbit as $\gamma(t)$.

Step 2: Now we face the hpo_L around L_1. First we locate L_1 by imposing $\Omega_x = 0$ as it follows from (3.24). Starting at $x = \mu - 1 + (\mu/3)^{1/3}$, Newton's method converges quickly for μ small. Then we can compute the eigenvalues at that point, which turn out to be λ, λ^{-1}, $\exp(\pm\omega \mathrm{i}\,)$, with $\lambda \approx 2.532659199$, $\omega \approx 2.086453579$. Hence, the maximal eigenvalue of the nearby periodic orbits, when they tend to L_1, is $\exp(2\pi\lambda/\omega) \approx 2052.671203$.

This large instability suggests, again, that we look for the initial data for the hpo_L on the Poincaré section $y = 0$ for a fixed x_0 with $\dot{x}_0 = 0$, and leaving $\dot{y}_0$ as the only unknown variable. The condition to be satisfied is then that the next intersection with $y = 0$ (to the left of L_1) should have $\dot{x} = 0$. This is easily solved by Newton's method. From the half orbit we recover the full orbit by symmetry, the monodromy matrix and, hence, dominant eigenvalue and eigenvector. The instability becomes milder when the size increases. For instance, for the smallest orbit in Figure 3.10 on the left the dominant eigenvalue is 2050.987058, while the largest one is 923.004416. Standard continuation techniques are used to generate these orbits.

Step 3: With the previously computed data it is simple to produce the left branches of the stable manifolds $W^{s,-}_{PO}$ of the hpo_L until they intersect the value $x = -0.999$.

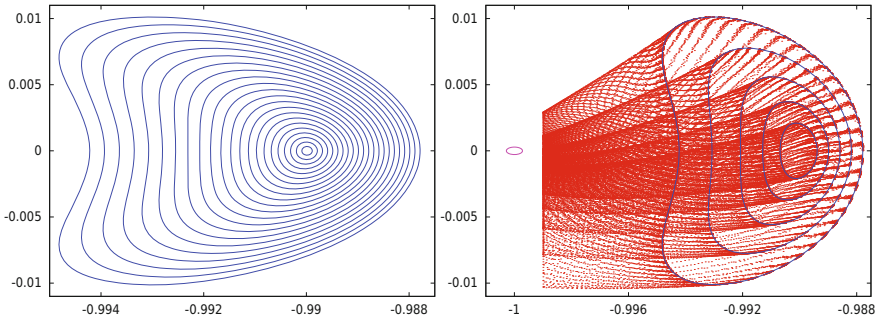

Figure 3.10: *Left:* some orbits in the family hpo_L around L_1. The initial values of x, on $y = 0$, are of the form $x_{L_1} + k \times 10^{-4}$ for $k = 1(1)22$. *Right:* For some of the orbits, concretely for $k = 6(4)22$, we plot also the left branches of $W^s_{PO_k}$ until they reach $x = -0.999$. In both plots the variables x, y are shown.

It is enough to use the linear approximation of the manifold in the Poincaré section $y = 0$. An example is shown in Figure 3.10 to the right. To compute the manifolds 200 points have been taken in a fundamental domain, equally spaced in logarithmic scale. The intersections for the orbits with $k = 8(2)22$, i.e., for the indices ranging from 8 to 22 with step 2 (see Figure 3.10) are shown in red in Figure 3.11 on the right, using $y, \dot{y}$ as variables.

Step 4: The last step is how to reach $W^{s,-}_{PO_k}$ for a given k leaving from the parking orbit. It is suggested to give an impulsion Δv from a given point $\gamma(t^*)$ in the orbit, in the direction of the velocity $\dot{\gamma}(t^*)$ at that point. The first question is to compute what is the size of the new velocity. We simply require that the value of the Jacobi constant with this velocity equals the one of the target PO_k. Let $|v|$ be the modulus obtained for this velocity. Then, $\Delta v = |v| - |\dot{\gamma}(t^*)|$, and the components of the new velocity are proportional to the ones of $\dot{\gamma}(t^*)$. This allows us to compute the trajectories $\psi(t, t^*)$ leaving from the parking orbit until they reach $x = -0.999$. Depending on t^* it can happen that $\psi(t, t^*)$ reaches $x = -0.999$ or it goes first far away to the left, spending too much time. These trajectories are skipped. A sample of the possible $\psi(t, t^*)$ trajectories for several t^* values is shown in magenta in Figure 3.11 on the left, where the parking and target orbit (with $k = 14$) are in red, and $W^{s,-}_{PO_{14}}$ is shown in blue.

Finally, on the right-hand part of Figure 3.11 we show, in the $(y, \dot{y})$ variables, the information that has been obtained in $x = -0.999$: the intersections of $W^{s,-}_{PO_k}$ for $k = 8(2)22$, in red, and the intersections of $\psi(t, t^*)$ when one changes t^*, for the Jacobi levels of PO_k, $k = 10(4)22$, in blue. The intersections of a given red curve with the corresponding blue one are the candidates for the transfer. The values of Δv are quite close. They range from 0.040286 for $k = 10$, to 0.041246 for $k = 22$ (i.e., impulsions ranging from 1.203 to 1.232 km/s).

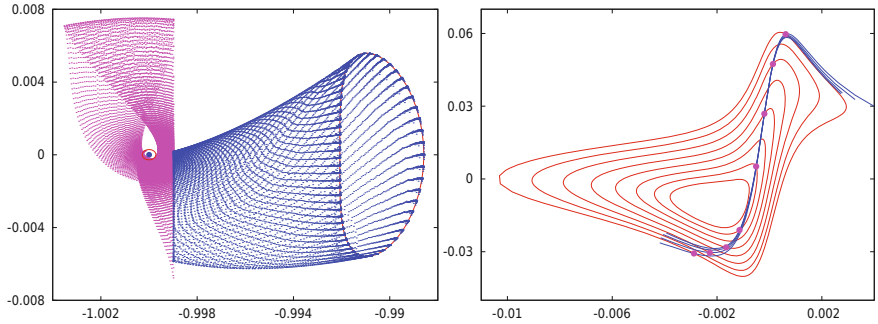

Figure 3.11: *Left:* The parking orbit and an example of a possible target hpo_L (with $k = 14$), both in red, the branch $W^{s,-}_{PO_{14}}$ in blue, and some of the possible trajectories $\psi(t, t^*)$ departing from the parking orbit (see text) in magenta. Plot done using x, y variables. *Right:* The intersections of $W^{s,-}_{PO_k}$ for $k = 8(2)22$ with $x = -0.999$, in red, and the intersections with the same plane of $\psi(t, t^*)$ for different values of t^* on the Jacobi levels of PO_k, $k = 10(4)22$, in blue. Note that these four blue curves are quite close and similar. The possible places for the transfer are the intersections of a $W^{s,-}_{PO_k}$ curve with the corresponding blue curve. They are marked in magenta. For each k shown here two possible places are obtained. This plot is done using $y, \dot{y}$ as variables.

3.4.2 Escape and confinement in the Sitnikov problem

This is an example to study escape/capture on a given problem of Celestial Mechanics using a very simple model. Two massive bodies of equal mass are moving on the $z = 0$ plane on elliptic orbits of eccentricity e around the common centre of mass, located at $(0, 0, 0)$, with semimajor axis $a = 1$, while a body of negligible mass moves along the z-axis. The standing equations are

$$\ddot{z} = -\frac{z}{(z^2 + r(t)^2/4)^{3/2}}, \quad r(t) = 1 - e\cos(E), \quad t = E - e\sin(E), \tag{3.26}$$

where E denotes the eccentric anomaly of the primaries. For $e = 0$ the problem has one d.o.f. and, hence, it is integrable. As a first order system we have $\dot{z} = v$, $\dot{v} = z(z^2 + r(t)^2/4)^{-3/2}$, with the obvious symmetries $S_1 \colon (z, v, t) \leftrightarrow (z, -v, -t)$, $S_2 \colon (z, v, t) \leftrightarrow (-z, v, -t)$, and $S_3 \colon (z, v, t) \leftrightarrow (-z, -v, t)$. We can introduce E as new time variable (denoting $' = d/dE$) and introduce a Hamiltonian formulation:

$$H(z, E, v, J) = (1 - e\cos(E))\left[\frac{1}{2}v^2 - (z^2 + (1 - e\cos(E))^2/4)^{-1/2}\right] - J.$$

A suitable Poincaré section for the representation of orbits is $\Sigma = \{z = 0\}$, using (v, E) as local coordinates. Thanks to the symmetry and to avoid strong deformations we shall use, instead, $(\hat{v}, E)$, where $\hat{v} = |v|(1 - e\cos(E))^{1/2}$.

If the infinitesimal mass escapes to infinity, the massive bodies move in $\mathbb{S}^1$ (eventually, after regularization of binary collisions using Levi–Civita variables).

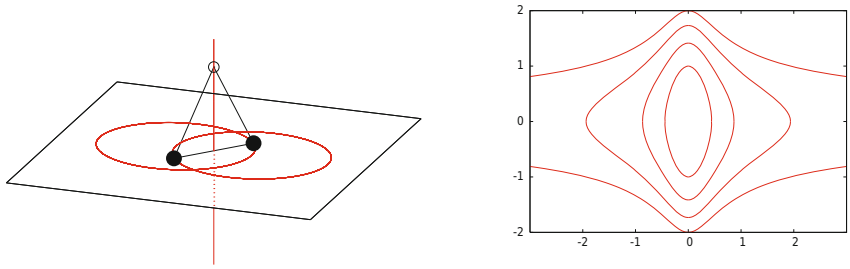

Figure 3.12: *Left:* A representation of the Sitnikov model. *Right:* For $e = 0$ plots of the orbits in the (z, v) variables for values of H equal to -1.5, -1.0, -0.5 and 0.

One talks of a periodic orbit at infinity. A celebrated Theorem by Moser states the following.

Theorem 3.4.1. *The problem has periodic orbits at both z plus and minus infinity, with invariant manifolds (orbits going to or coming from infinity parabolically). For e small enough the manifolds intersect Σ in curves diffeomorphic to circles. These curves have transversal intersection, implying the existence of heteroclinic orbits from $+\infty$ to $-\infty$ and vice-versa.*

As a consequence one has non-integrability, embedding of the shift with infinitely many symbols, existence of oscillatory solutions, escape/capture domains, etc. The PO at ∞ is parabolic or, topologically, weakly hyperbolic. The linearized map around the PO is the identity. To study the vicinity of these orbits we introduce McGehee variables (q, p) defined as $z = 2/q^2, \dot{z} = -p$. Then the equations of motion become

$$q' = \Psi q^3 p, \quad p' = \Psi q^4 \left(1 + \Psi^2 q^4\right)^{-3/2}, \quad \Psi = (1 - e\cos(E))/4. \tag{3.27}$$

If $e = 0$ the invariant manifolds are given as $p = \pm q(1 + q^4/16)^{-1/4}$. We shall denote as $W^{u,s}_{\pm}$ the intersections of unstable/stable manifolds of $\pm\infty$ with Σ. Due to S_3, $W^u_{\pm}$ coincide and also $W^s_{\pm}$ coincide, but W^s_+, W^u_- have $v > 0$, while W^s_-, W^u_+ have $v < 0$. Due to S_1, W^u_+ and W^s_- are symmetric with respect to $E = 0$.

We look for a parametric representation of the manifolds of the PO as

$$p(E, e, q) = \sum_{k\geq 1} b_k(e, E) q^k = \sum_{k\geq 1} \sum_{j\geq 0} \sum_{i\geq 0} c_{i,j,k} e^i \,\mathrm{sc}(jE)\, q^k, \tag{3.28}$$

where $b_k(e, E)$ are trigonometric polynomials in E with polynomial coefficients in e, $c_{i,j,k}$ are rational coefficients, and sc denotes sin or cos functions.

Note that the problem can be reduced to obtain invariant manifolds of fixed parabolic points of discrete maps (think about the intersection of the manifolds with $E = 0$). In this context McGehee proved that the invariant manifolds are

analytic except, perhaps, at $q = 0$, see [31]. In fact, a result of Baldomà and Haro [1] shows that, generically, the 1-dimensional manifolds of fixed parabolic points are of some Gevrey class (see the part on invariant manifolds in Section 3.2.1).

From (3.27) and (3.28) the invariance of the manifolds can be written as

$$\Psi q^4 \left(1 + \Psi^2 q^4\right)^{-3/2} = \sum_{k\geq 1} \frac{db_k}{dE}(e, E) q^k + \sum_{k\geq 1} b_k(e, E) \Psi k q^{k+2} \sum_{m\geq 1} b_m(e, E) q^m. \tag{3.29}$$

Equating coefficients of powers of q in (3.29) leads to the recurrence

$$\binom{-\frac{3}{2}}{m} \left(\frac{1 - e\cos(E)}{4}\right)^{2m+1} = b'_n(e, E) + \frac{1 - e\cos E}{4} \sum_{k=1}^{n-3} k b_k(e, E) b_{n-2-k}(e, E), \tag{3.30}$$

where $m = n/4 - 1$, defined only for n multiple of 4.

To solve the recurrence in (3.30) we first note that for the unstable manifold of $+\infty$ we have $b_1 = 1$. One has $b_1 = -1$ for the stable manifold. For a given value of n we can split the function b_n as $\tilde{b}_n + \bar{b}_n$, where $\bar{b}_n$ denotes the average and $\tilde{b}_n$ the periodic part. Given $b'_n(e, E)$ equal to some known function (computed from the previous coefficients) allows us only to compute the periodic part $\tilde{b}_n$. The average $\bar{b}_n$ is computed previous to the solution of the equation for $b'_{n+3}(e, E)$, to have a zero average function when we integrate. An essential fact is that $b_2 = b_3 = b_4 = 0$. One has also $b_6 = b_7 = b_{10} = 0$, but this is not so relevant.

Now it is a simple task to implement the computation of the coefficients to high order. Using high order is important, because this allows us to have a good representation for large values of q. A large q allows us to start the numerical integration, to obtain the intersection W^u_+ of the manifold with $z = 0$, at a moderate value of z. For instance, using terms up to order $n = 100$ one checks that the representation is good (error of the order of 10^{-16}) for $q = 1/3$. Then the numerical integration can be started at $z = 2/q^2 = 18$.

Figure 3.13 shows some results for different values of e, displaying W^u_+ and W^s_-, and using the $(\hat{v}, E)$ variables as polar coordinates. Note that the use of $(|v|, E)$ would give curves extremely elongated to the right for e close to 1. Concretely, if the eccentricity is equal to $1 - \delta$ then the horizontal variable in the plots reaches values $\approx 2/\sqrt{\delta}$. The values of the splitting angle at $E = 0$ and $E = \pi$ on the section Σ are shown as a function of e in Figure 3.14. Note the quite different behaviour when $e \to 1$. This gives evidence of the transversality for all values of e.

Summarizing, the steps to obtain the manifolds W^u_+ and W^s_- and, hence, the splitting angle, are the following:

(i) introduce McGehee coordinates to pass from (3.26) to a formulation around the periodic orbits at infinity, as given by (3.27);

(ii) look for a suitable representation, as the one in (3.28), in which the manifold is expressed as function of a distance to infinity (q) and a periodic time variable

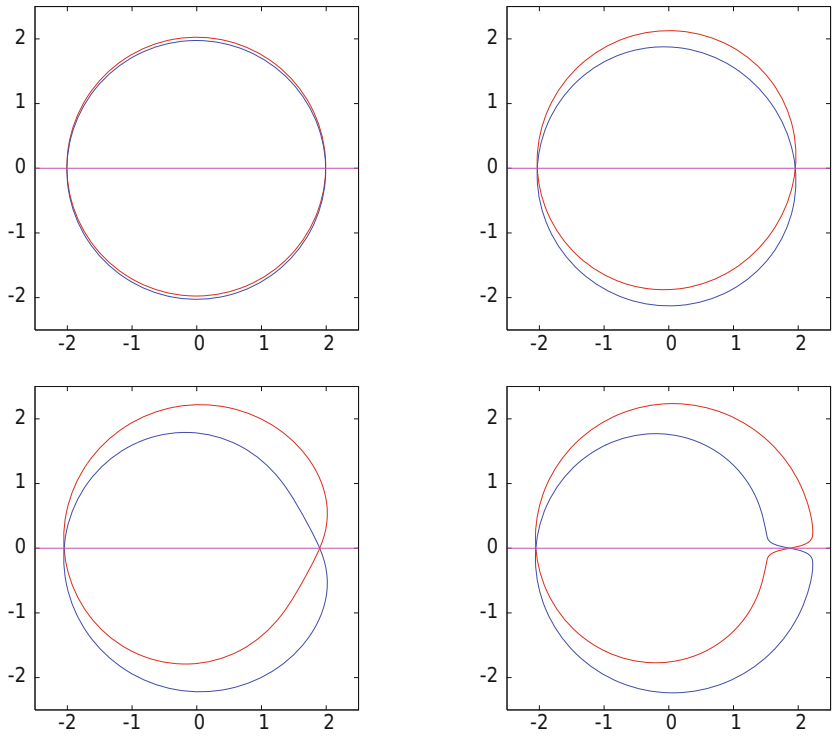

Figure 3.13: The manifolds W^u_+, in red, and W^s_-, in blue, for different values of e. *Top left:* for $e = 0.1$. *Top right:* for $e = 0.5$. *Bottom left:* for $e = 0.9$. *Bottom right:* for $e = 0.999$. In all cases we use $(\hat{v}, E)$ as polar coordinates.

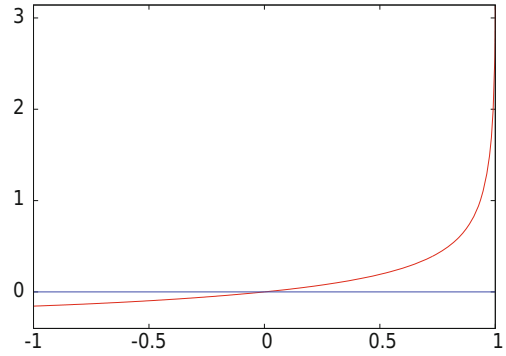

Figure 3.14: The splitting angle of the manifolds W^u_+ and W^s_- in Σ. For positive values on the horizontal axis the splitting angle at $E = 0$ is shown as a function of e. For the negative ones, the splitting angle at $E = \pi$ is shown as a function of $-e$.

(E); write the invariance condition (3.29) and derive the recurrences, as given in (3.30);

(iii) analyze the properties of the recurrences (symmetries, powers of e in the coefficients of the trigonometric polynomials, etc); design and implement routines to obtain the desired numerical coefficients; and

(iv) select a suitable value of q for the current maximal order of the expansion, evaluate (3.28) for a sample of values of E for every desired value of e, and carry out the numerical continuation until $z = 0$.

It is important to stress that, for other similar problems (RTBP planar or spatial, general, etc), to decide if an observed body will be captured or will escape, it is enough to obtain the manifolds and decide the actual position with respect to them. The case of the planar RTBP with a comparison between theoretical predictions and numerical results can be found in [28] and the related slides (I).

3.4.3 Practical confinement around triangular points

As mentioned at the beginning of Section 3.4, the triangular libration points are linearly stable in the 3D RTBP if μ is small enough. But, what can be said about nonlinear stability? For the 2D case, nonlinear stability is proved for $\mu \in [0, \mu_1)$ except for the couple of values μ_2, μ_3. A possible approach is to reduce to the study of a symplectic 2D map and to apply Moser theorem. There is an exceptional value for which the twist condition is not satisfied, but can be recovered as a *weak twist* to higher order via normal forms.

In the 3D case, in principle, there is no way to avoid diffusion. Hence, initial conditions as close as we like to $L_{4,5}$ can go far away from that point. But normal forms, or averaging, lead to the already mentioned Nekhorosev estimates, showing that one needs an extremely large time if one starts close enough to the libration point as discussed in Subsection 3.3.5.

But these results, concerning domains of practical stability in the 3D case, give at most small regions around the triangular points. On the other hand one has found the so-called Trojan (and Greek) asteroids, for the Sun-Jupiter system, far away from $L_{4,5}$, even with relatively high inclination. Hence, it seems that the domain of practical stability for long times is much larger than what is given by theoretical predictions. It would be nice to search for the confining mechanisms.

A side problem is why Trojan-like bodies are not found in the Earth-Moon case. Certainly the Sun is guilty for that, the orbits equivalent to $L_{4,5}$ for the Earth-Moon system being unstable even in simple models of the Earth-Moon-Sun motion. But this does not exclude the possibility that stable orbits exist with moderate inclination.

Here we present some results which can help to understand the main mechanisms, see [48]. For different reasons, many computations are done with initial

conditions on the ZVS using (z, α, ρ) as parameters for a fixed μ, as follows:

$$x = \mu + (1+\rho)\cos(2\pi\alpha), \quad y = (1+\rho)\sin(2\pi\alpha), \quad z = z_0 \geq 0, \quad \alpha \in (0, 1/2),$$
$$\dot{x} = \dot{y} = \dot{z} = 0. \tag{3.31}$$

As for $\mu = 0$ one must be in $1-1$ resonance, it is convenient to look, starting at the ZVS, for initial conditions at rest, in the synodical frame, in the moment that an elliptic orbit with semimajor axis equal to the unity passes through the apocentre in the sidereal frame. That is, for values of $(z, R = 1+\rho)$ related by

$$\begin{gathered} z = \left[4(1+R^2)^{-2} - R^2\right]^{1/2} \quad \text{or} \\ \psi = 1 - \tfrac{1}{2}w + \tfrac{3}{2^5}w^2 - \tfrac{1}{2^8}w^3 - \tfrac{25}{2^{13}}w^4 + \tfrac{33}{2^{16}}w^5 + \mathcal{O}(w^6), \end{gathered} \tag{3.32}$$

where $w = z^2$, $\psi = \psi(z) = R^2$. This suggests that we make plots using the variables

$$(\alpha,\ \gamma = 1 + \rho - \sqrt{\psi(z)},\ z). \tag{3.33}$$

It is clear that L_5 corresponds to $\rho = 0$, $\alpha = 1/3$, $z = 0$. By symmetry, similar results are obtained for L_4. Also, by symmetry, it is enough to look for $z \geq 0$. For the limit case, $\mu = 0$, one would have $\gamma = 0$.

Some reasons to start at the ZVS are:

(i) Most of the i.c. non-leading to escape are on 3D tori. Hence, we scan a set of positive measure in the full phase space (not fixing the Jacobi constant C).

(ii) The results obtained can be used as a seed to obtain the relevant objects involved in the practical confinement, either starting at the ZVS or not.

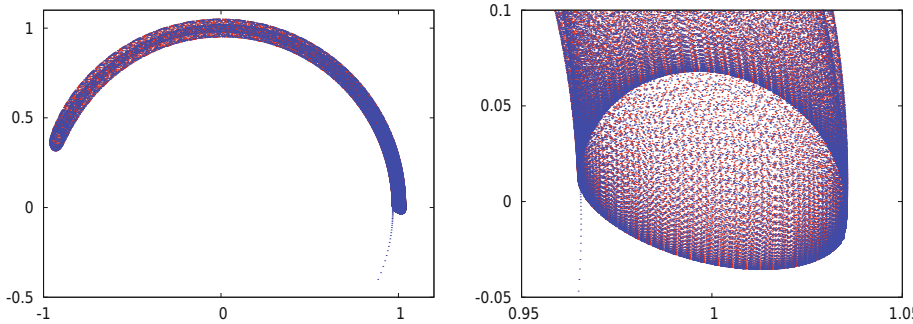

Figure 3.15: Example of a transition for $\mu = 0.0001$, $\alpha = 0.05$, $z = 0.3$. The two tori (confined in red, escaping in blue) have values of ρ which differ in 10^{-10}. We show the projections on (x, y) of the Poincaré section through $z = 0$. *Left:* a global view. *Right:* a magnification. The separating unstable 2D torus or invariant curve in the section belongs to $W^{u,s}_{L_3}$. Note that the points in red are partially hidden by the ones in blue.

First, we show some results concerning the *quasi-boundary* between escape and practical confinement. Figures 3.15 and 3.16 display, for a small value $\mu = 10^{-4}$ of the mass parameter, two different kinds of objects which appear on the quasi-boundary. We should mention that the relevant objects have codimension 1 in the full phase space. In the present case they have dimension 5. Typically, they are $W^{u,s}$ of central objects of dimension 4. These objects can be the centre manifolds of fixed points of centre×centre×saddle type or the centre manifolds of 1-parameter families of periodic orbits of centre×saddle type (the parameter being, e.g., the value of the Jacobi constant). But it is clear that these $W^{u,s}$ do not coincide: there is some splitting. This is the reason why they are named quasi-boundaries.

We note, for instance, that in the upper left plot of Figure 3.16 beyond the blue curve commented on the caption, one can guess another invariant curve (in the Poincaré section, a 2D torus in the phase space) on top of the plot. The separation between confined and escaping orbits is close to a double heteroclinic connection between the lower curve in blue and the upper one in red. But the related branches of these two partially normally invariant curves do not match exactly. There is some tiny splitting between the branches.

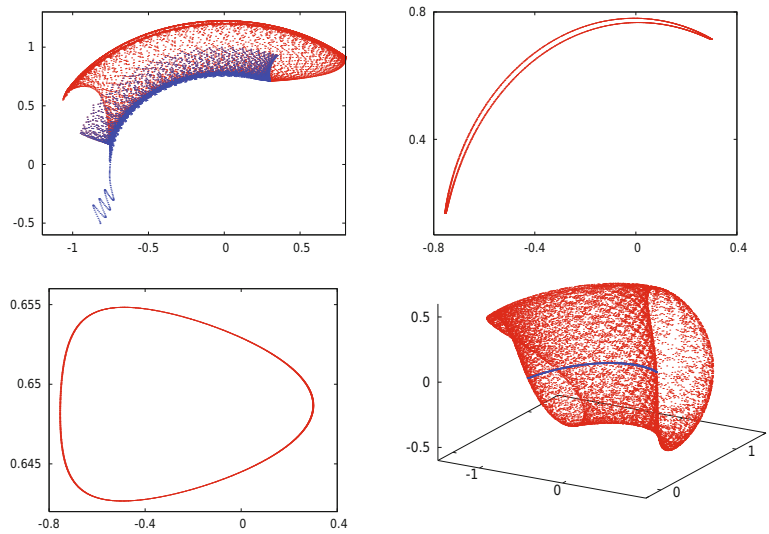

Figure 3.16: Similar to Figure 3.15 but starting at $\alpha = 0.4$, $z = 0.6$. Now the separating unstable 2D tori are not in $W^{u,s}_{L_3}$. *Top:* initial part of Poincaré iterates with many iterates in blue, giving evidence of the lower unstable 2D torus and points escaping from it (*left*), and the separating lower unstable invariant curve alone (*right*) projected on (x, y). *Bottom:* The same curve projected on $(x, \dot{z})$ (*left*), and the related 2D separating unstable torus in a (x, y, z) projection (*right*).

In Figure 3.17 we display a general view of the boundary. See comments on the caption. Typically, the transitions have been detected after a maximum

integration time equal to $10^6 \times 2\pi$ (in special cases 10, 10^2 or 10^3 times larger) and with a resolution of 10^{-6} in ρ; see slides (D) for other values of μ.

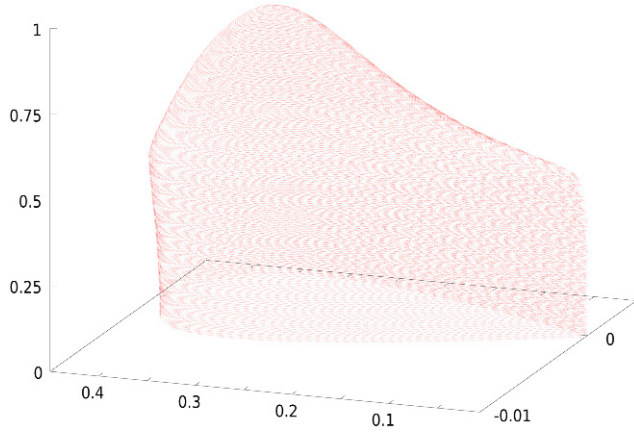

Figure 3.17: A 3D view of the detected boundaries of practical stability starting at the ZVS for $\mu = 10^{-4}$, shown in the (α, γ, z) variables. The inner (resp., outer) part corresponds to $\gamma < 0$ (resp. $\gamma = 0$). Note the sharp change on the behaviour of the boundary which occurs between $z = 0.4$ and $z = 0.5$.

We can make a rough scan of the boundaries for different values of μ, both for the planar and spatial RTBP. We say rough in the sense that, typically, the maximal time to look for escaping has been reduced to $10^5 \times 2\pi$ time units and that the grid we scan uses $\Delta\rho = 10^{-4}$, then $\Delta\alpha$ equal to 2×10^{-4} in the planar case (5×10^{-4} in the spatial one) and $\Delta z = 5 \times 10^{-3}$ in the spatial case. The results are shown in Figure 3.18. Note that the effect of the resonances is less important in the spatial case. This is due to the fact that, for some values of μ, the resonances destroy stability in the planar case, but still a large set of initial conditions is stable in the spatial case. The change of the frequencies when z increases is responsible for the minima being shifted to larger values of μ.

From now on we concentrate on a fixed value $\mu = 0.0002$. The reasons for this choice are the following:

(i) μ being small, the boundaries are sharper;

(ii) it should be also possible to obtain some information by means of perturbation theory;

(iii) it is close to the Titan-Saturn mass ratio.

This small value of μ, however, raises a problem: the escape is relatively slow and, hence, the integration time is large. The methodology used (for the L_5 case) is as follows:

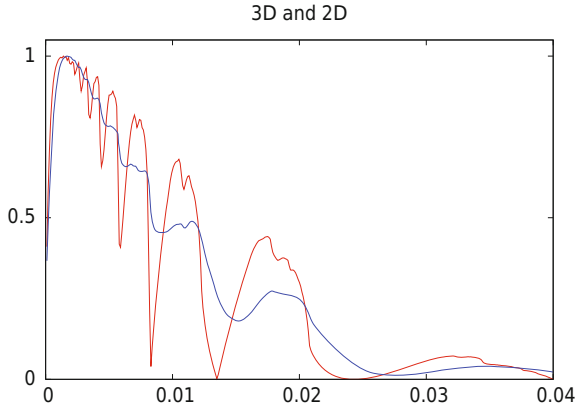

Figure 3.18: Statistics as a function of μ starting at the ZVC (planar case, in red) and at the ZVS (spatial case, in blue). This is normalized to the maximum, which for the planar case occurs at $\mu = 0.0014$ with 282757 points, and for the spatial case it occurs for $\mu = 0.0017$ with 19014882 points. Note the sharp effect of the resonances in the planar case. Similar patterns are found for the Hénon map and in many other examples, see [46]. In the spatial case the effect of the resonances is milder and delayed. In both cases some stability subsists even for $\mu > \mu_1$.

(i) Define some escape criterion (e.g., the (x, y) projection of the orbit enters some wedge near the negative y-axis, or the orbit comes too close or too far from the primary, or too close to the secondary).

(ii) Scan a set of initial conditions for short time (e.g., $10^4 \times 2\pi$, using some grid with small steps $\Delta\alpha$, $\Delta\rho$, δz). Look at every initial point on the grid, for fixed z, as a pixel. Keep the pixels non leading to escape.

(iii) Repeat for longer time (e.g., $5 \times 10^4 \times 2\pi$) for the pixels at a distance (counted in the sup norm) less than d pixel units from the ones which already escaped (typically, we take $d = 5$). The tested points are marked depending on whether they escape or they remain. Iterate the scan until no more points have to be tested: all the ones at distance less than or equal to d from escaping points have been tested and remain. Repeat two more times for longer and longer integration time ($25 \times 10^4 \times 2\pi$, $10^6 \times 2\pi$).

(iv) Eventually do additional refinements of ρ for fixed α, z.

Figures 3.19 and 3.20 show some results for $\mu = 0.0002$ displaying, for different values of z, the set of non-escaping points starting on the ZVS and the boundaries of the domain. See the captions for the variables used to represent the results. Note that the domain of practical stability contains, for the planar case $z = 0$, stable points quite close to the L_3 ($\alpha \approx 0$). In the spatial case there are stable orbits which reach z as large as 0.865 and, as the value of ρ for these orbits reaches ≈ -0.181 they have a maximum inclination exceeding 46 degrees.

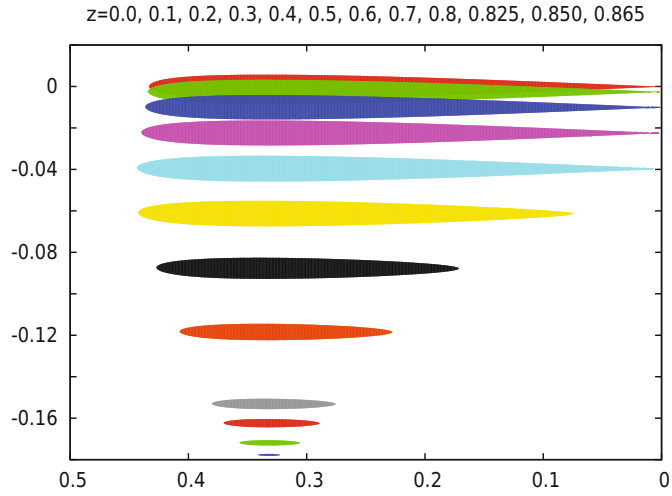

Figure 3.19: For $\mu = 0.0002$ the subsisting points, starting at the ZVS for 12 different z values, given on the top of the plot. The coordinates used for the representation are (α, ρ).

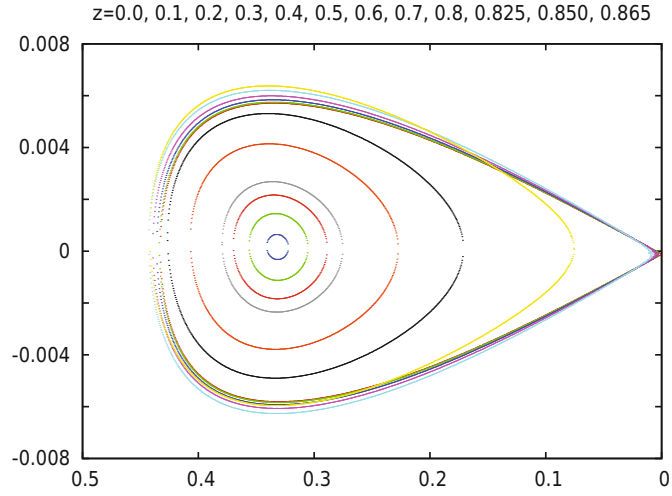

Figure 3.20: Boundaries of the domains shown in Figure 3.19 using the paraboloid like corrections. That is, as vertical variable one has used γ, as defined in (3.33) instead of ρ.

Some sections of the boundary for $\mu = 0.0002$, for several values of α, are shown in Figure 3.21.

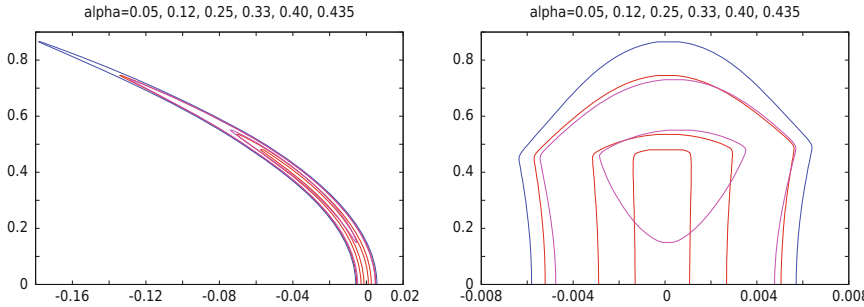

Figure 3.21: Some sections of the boundary starting at the ZVS for different values of α. *Left:* in the (ρ, z) variables. *Right:* using the (γ, z) variables. The curves for $\alpha = 0.05, 0.12, 0.25$ are plotted in red, and are easily seen on the right-hand plot going away from $(0, 0)$ and each line encircling the previous one. The curve for $\alpha = 0.33$ is displayed in blue. This is the largest one. Finally the curves for $\alpha = 0.40$ and $\alpha = 0.435$ are plotted in magenta. Last one does not reach $z = 0$.

Still many things must be completed even for this small μ for which the boundaries tend to be rather sharp, because they are associated to relatively small splitting. The problem becomes more rough for the Sun-Jupiter case, because then one starts to see the effect of some island-like structure. For the Earth-Moon case the behaviour is quite wild due to the strong effect of resonances. The Earth-Moon mass ratio is not far from the 3:1 resonance value μ_3.

3.4.4 Infinitely many choreographies in the three-body problem

In the Newtonian N-body problem with all masses equal to 1, we can consider very simple solutions in the planar case, the like N-gon relative equilibrium solutions. Due to the homogeneity one can scale time and distance so that it is enough to consider solutions with period 2π. The N bodies move on a circle of radius R such that

$$2R^3 = \Sigma_{j=1}^{N-1} (2\sin(j\pi/N))^{-2}.$$

It is clear that all the bodies move on the same path in the plane. Hence, the following is a natural question: are there other periodic solutions such that all bodies with equal masses move on the plane along the same path? At the end of the twentieth century a solution with 3 bodies on the same planar curve, different form a circle, was proved to exist by Chenciner–Montgomery [6]. Also, Moore [33] found the same orbit in a previous numerical work in a different context, a few years before. The path of this solution is the very popular figure eight curve and is displayed in Figure 3.22.

Immediately, one can pose the question for $N > 3$ and for other shapes of the path. These solutions are called *choreographies* because of the dancing-like

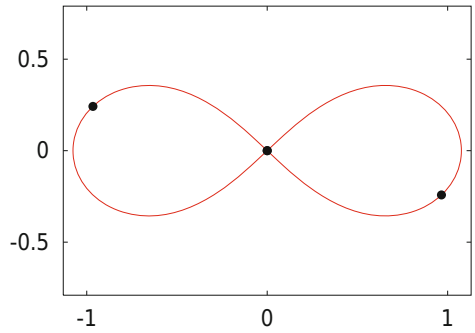

Figure 3.22: The figure eight solution of the three-body problem. The initial positions of the bodies are marked as black points. For concreteness, we can assume that at $t = 0$ the body located at the origin moves to the right, up. This forces the motion of the other two.

motion of the bodies seen in animations, see [5, 45]. More precisely, they should be called *simple* choreographies because they are on the same curve; we use the term *k-choreographies* for bodies moving on k different curves. Slides (F) provide some examples and links to animations. One can also introduce the notion of *relative* choreographies if they are seen as choreographies in a uniformly rotating frame. Two choreographies which differ only by a rotation, by scaling, change of orientation, symmetry, etc, should be seen as the same.

Returning to simple choreographies in a fixed frame (or *absolute* choreographies) what one tries to find is some 2π–periodic function $\psi\colon \mathbb{S}^1 \mapsto \mathbb{R}^2$ such that if the body j is located at $q_j(t) = \psi(t - (j-1)2\pi/N)$ for $j = 1, \ldots, N$, we have a solution to the equations of motion.

Another natural question arises: are there other choreographies of the three-body problem different from the figure eight?

A simple observation is that at some $t > 0$, relatively small, the three bodies in Figure 3.22 will be in an isosceles configuration. Such a configuration is defined, for instance, assuming that at some moment of time the bodies 2 and 3 have positions and velocities given by

$$x_3 = x_2, \quad y_3 = -y_2, \quad \dot{x}_3 = -\dot{x}_2, \quad \dot{y}_3 = \dot{y}_2. \tag{3.34}$$

The conditions for m_1 are determined from the centre of mass integrals. This isosceles triangle has a symmetry axis passing through m_1.

Assume that after some time τ the bodies pass through another isosceles configuration, concerning positions, with the body m_2 in the symmetry axis defined by the positions of m_3 and m_1, and that the velocities are close to satisfy the isosceles condition. Let β be the angle between the former symmetry axis (the x-axis) and the new one. A refinement is done to satisfy the full isosceles conditions

with good accuracy (see the end of this subsection). Then, after rotating positions and velocities at τ by an angle $-\beta$, we have an isosceles configuration with the same symmetries concerning velocities than the initial one. The only change is a circular permutation of the bodies with change of orientation. Then the action of the semi-direct product of $\mathbb{Z}_2$ and $\mathbb{Z}_3$ (symmetry and permutation of the bodies) produces a relative choreography with period $T = 6\tau$ and rotation 6β. If β is $k\pi, k \in \mathbb{Z}$, we have an absolute choreography, symmetric with respect to the x-axis.

This has been applied to $\approx 10^9$ initial conditions. Near 3×10^5 relative choreographies have been found and, by continuation of each one of them with respect to the angular momentum, many (345 up to now) absolute, non-equivalent, choreographies have been found. It is clear that several relative choreographies can lead, by continuation, to an absolute choreography equivalent to another one found previously, and these are not counted. It is checked that some of these new three-body choreographies seem to belong to families. An example is shown in Figure 3.23. See [44] for other families.

Figure 3.23 suggests to try to continue the family for an increasing number of loops. Now the continuation has to be done with respect to integers and not in a continuous way. But using extrapolation of the data from the previous loops it has been possible to continue the family without any problem (using quadruple precision and high order extrapolation) until the solution shown in Figure 3.24. The natural conjecture is that there are infinitely many choreographies in this family.

There is an easy description of that solution. One of the bodies (say, the red one) moves close to an elongated ellipse while the other two (green and blue) move in a close binary, with its centre of mass close to an ellipse. When the three bodies approach the centre of mass there is an exchange: the blue body moves close to an elongated ellipse and the red and green form a binary in turn. At the end of this we have traveled 1/3 of the period. The bodies return to the initial position with a cyclic permutation RGB $\to$ GBR. One should stress that when they approach the centre of mass the bodies are not close to triple collision. Preliminary results seem to indicate that the minimal value of the moment of inertia along the orbit is strictly decreasing with the number of binary loops, tending to a positive constant.

It should be mentioned that, among the 345 absolute choreographies available, one can identify several families. It is not excluded that some of these families contain infinitely many elements. But it can also happen that a couple of families merge together in a saddle-node bifurcation.

The steps for that application are as follows:

(i) To obtain initial data in isosceles configuration one can prescribe some negative energy. Then we give values of (x_2, y_2) and determine the positions of the other masses. Because of the symmetries we can select $x_2 > 0$, $y_2 < 0$. A bound on the domain is obtained because the kinetic energy should be

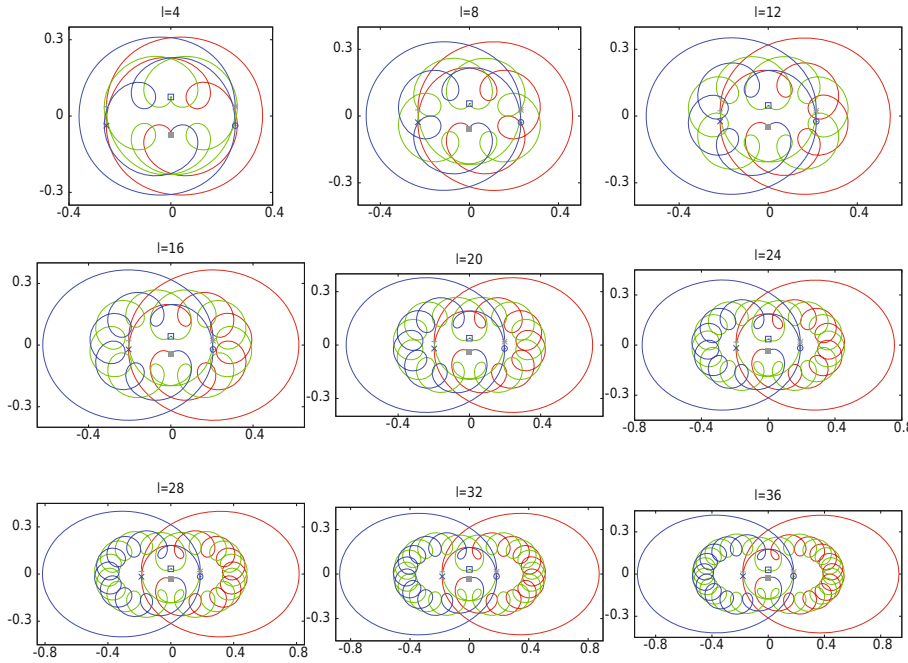

Figure 3.23: Choreographies of the three-body problem belonging to a family. The paths of the three bodies during 1/3 of the period are shown in different colors. The positions of the bodies in the initial isosceles configuration and the ones after 1/6 of the period are also shown. To display the solutions with the same scale in x and y variables, the coordinates have been exchanged. Now, for these choreographies, the symmetry axis is the vertical one and for this family both isosceles configuration (at $t = 0$ and after 1/6 of the period) are symmetrical the one from the other with respect to the horizontal axis. Counting the little inner loops (for instance, the ones in red) the number increases from 1 to 9 from top to bottom and from left to right. The value ℓ on top of each plot refers to the total number of small loops, either in red, blue or green.

non-negative. The possible values of $(\dot{x}_2, \dot{y}_2)$ are parametrized by an angle $\gamma \in [0, 2\pi]$.

(ii) Then, we proceed to the integration of (3.1) with the selected initial conditions, looking for a passage near another isosceles configuration. A maximal time is used (e.g., 5 units) and the attempt is stopped if the bodies move too far or they become too close. If a candidate is obtained a refinement is done by Newton's method, to have a good approximation to an isosceles symmetry after 1/6 of the period. For the refinement we fix γ and leave (x_2, y_2) as free variables to satisfy the isosceles condition for the velocities when it is satisfied by the positions.

(iii) Next we carry out continuation by changing the angular momentum, looking

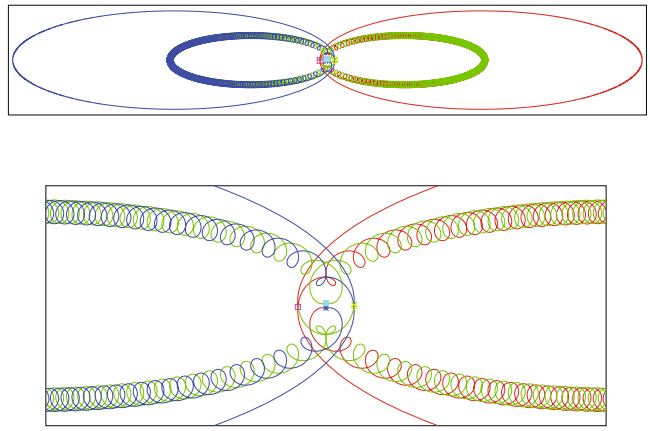

Figure 3.24: *Top:* a choreography of the three-body problem of the same family of the ones shown in Figure 3.23. In each of the binary portions the bodies in the binary make 200 revolutions around the centre of mass of the binary, while the third body moves close to an elongated ellipse. Only 1/3 of the orbit is shown. The remaining parts are obtained by cyclic permutations. *Bottom:* a magnification of the central part of the top.

for an absolute choreography. Continuation is stopped if the bodies approach a collision. The new absolute choreographies are stored in a list. If they are already in the list, they are discarded. Later, for our present goal, we select the ones which belong to the family as shown in Figure 3.23.

(iv) Finally the family is continued with respect to the number of loops. An extrapolation based on the previously computed loops allows us to have a very good guess. Newton's method converges in few iterations.

3.4.5 Evidences of diffusion related to the centre manifold of L_3

In this last application we consider the 3D RTBP for a small value $\mu = 0.0002$, like we used in Subsection 3.4.3. Our goal is to give evidence of the diffusion when we consider the unstable dynamics originated by the unstable/stable manifolds of the part $W^c_{L_3,C}$ of the centre manifold $W^c_{L_3}$ of L_3, for a given value C of the Jacobi constant. For concreteness, we use the value $C = 2.95998466228$. To have a feeling of the meaning, let us say that for that value of C the vpo_L in $W^c_{L_3,C}$ has values of z going from -0.2 to $+0.2$.

Beyond the vpo_L, the $W^c_{L_3,C}$ contains 2D tori, the hpo_L, some tiny chaotic domains, and the additional periodic orbits related to these domains. Using the methods of Subsections 3.3.1 and 3.3.3, we can compute both periodic orbits and several tori. It is simpler to represent the tori as ICs of the Poincaré map $\mathcal{P}$ associated to the section $\Sigma := \{z = 0, \dot{z} > 0\}$. In this application we shall use once and again Σ and $\mathcal{P}$. As we fixed also the value of C, we have to consider a discrete

map in a 4D space that we denote as Σ_C.

The ICs are hyperbolic normally to the centre manifold. Hence, we can compute its manifolds, say $W^u_{\mathcal{C}}$, $W^s_{\mathcal{C}}$, for a given curve $\mathcal{C}$. Note that these manifolds are 2D and to visualize them we can compute a section through some codimension-1 manifold in Σ_C (e.g., an hyperplane Π). A suitably chosen Π gives as $W^u_{\mathcal{C}} \cap \Pi$ a closed curve, say $\mathcal{C}_u$. In a similar way we can obtain $\mathcal{C}_s$. Of course, these two curves in $\Sigma_C \cap \Pi$, which is 3D, do not intersect generically, as opposite to $W^u_{\mathcal{C}}$ and $W^s_{\mathcal{C}}$ which are 2D in the 4D space Σ_C, for which one expects to have intersections, but not necessarily located in Π. But we can have a feeling of their relative position by looking at $\mathcal{C}_u$ and $\mathcal{C}_s$.

Figure 3.25 illustrates what has been said. In the left plot several ICs are shown, as well as the point corresponding to the vpo_L. Note that the largest IC is quite close to the hpo_L. The 2D torus corresponding to this last IC has values of z which range in the small interval $[-0.017, 0.017]$. The hpo_L, which is contained in $z = 0$, is located outside the largest IC shown at a distance ≈ 0.004. The right plot displays $\mathcal{C}_u$ and $\mathcal{C}_s$ for several ICs, using as Π the hyperplane defined by $y = -\sqrt{3}(x - \mu)$. One detects, visually, that for tori close to the vpo_L the curves are quite close. The difference increases going outside, away from the vpo_L, and decreases again when approaching the hpo_L. This will be one of the relevant facts to explain the results obtained.

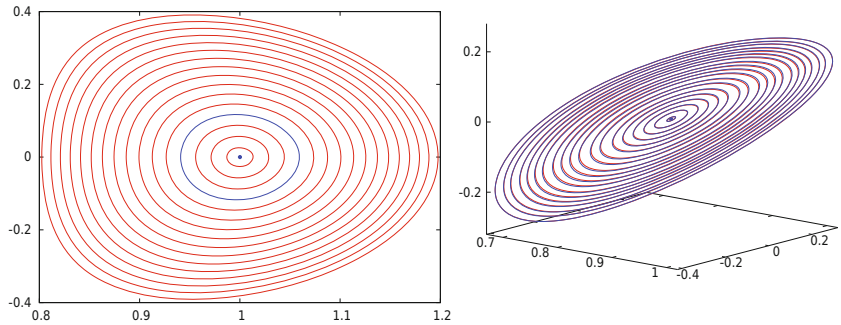

Figure 3.25: *Left:* invariant curves obtained as intersections with Σ of some tori in the $W^c_{L_3,C}$ for $C = 2.95998466228$ projected on the (x, y)-plane. The vpo_L orbit for this value of C has $z \in [-0.2, 0.2]$ and corresponds to the blue point. The blue curve will be used in the computations reported here. *Right:* sections with $y = -\sqrt{3}(x - \mu)$ of the Poincaré sections of the unstable (red) and stable (blue) manifolds of some of the tori. For the 3D view we use the $(y, \dot{y}, \dot{z})$ variables.

Figure 3.26 shows the projection in (x, y) of the first 10^5 iterates under $\mathcal{P}$ starting at a point close to the blue curve, say $\mathcal{C}_b$, in Figure 3.25, left. The first iterates follow closely the upper part of $W^u_{\mathcal{C}_b}$ and return near $\mathcal{C}_b$ close to the upper part of $W^s_{\mathcal{C}_b}$ (or of some other nearby curve). As it is well known, next iterates can continue going up or down, as happens after every return near $\mathcal{C}_b$, in a quasirandom

way. For completeness, the manifolds of vpo_L are also shown (displayed in blue).

This behaviour suggests that, at the successive returns near $W^c_{L_3,C}$, the Poincaré iterates can approach different tori (2D in the phase space) on that centre manifold. That is, a typical mechanism of diffusion thanks to chains of heteroclinic connections of different tori.

But there are also tori (3D for the Hamiltonian flow, 2D for $\mathcal{P}$) close to these manifolds. Among these tori one finds the ones close to the boundary of the practical stability domain for L_5, as seen in Subsection 3.4.3. Looking at Figure 3.19 one checks that they reach values of α very close to 0 (the value of α for L_3) up to $z = 0.4$. The successive points can remain for a large number of iterations, say 10^6 and even 10^8 in some tests, close to one of these tori, to one of the tori in the symmetric domain around L_4, or even tori which visit a vicinity of both L_5 and L_4 (with an (x, y) projection of the iterates in Σ similar to the red points in Figure 3.26). The tori are very sticky, see Subsection 3.3.5. As a consequence, the orbit of a point should consist of passages from the vicinity of the W^u of one of the ICs to the vicinity of the W^s of another IC (or, perhaps, the same one) with long stays near tori of one of the three types described.

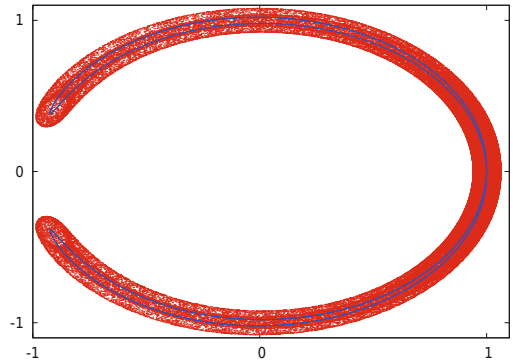

Figure 3.26: Starting at a point very close to the invariant curve in blue in Figure 3.25 we have computed the first 10^5 intersections with Σ. The plot shows the projections on the (x, y)-plane. As a reference, we also show in blue the initial part of the manifolds of the vpo_L. The lack of coincidence of these last manifolds is not seen with the present resolution.

To have evidence of this expected behaviour, we have taken 1920 points close to $\mathcal{C}_b$ (the blue curve in Figure 3.25 left). For every initial point we record the first 5×10^6 Poincaré iterates, except if some kind of escape is detected. A typical escape occurs when, going the iterates to the left, either near the upper or lower part of Figure 3.26, they approach the location of the secondary. After this encounter, the successive iterates can move close to the primary, escape far away or even return several times near the secondary. Anyway, only for 37 of the 1920 initial conditions escape was detected. Certainly the initial conditions will lead to escape if the number of Poincaré iterates is largely increased, at least on this level of the

Jacobi constant. See later for some tests with initial data taken near the vpo_L.

To visualize the diffusion and to display a moderate amount of data we have computed passages of the Poincaré iterates through a narrow slice around $x = 0$. Only from time to time an iterate falls in the slice. For instance, among the $1920 \times 5 \times 10^6$ computed Poincaré iterates (and except for the few iterates lost because of escape) only $\approx 3.2 \times 10^6$ fall in the slice $|x| < 10^{-3}$. The passage can occur in the upper part going from right to left (inner transition) or from left to right (outer transition), and also from right to left (outer transition) or from left to right (inner transition) in the lower part (see Figure 3.26).

The variables used in Σ are $(x, y, \dot{x}, \dot{y})$. Due to the symmetries, the inner upper and inner lower transitions are symmetrical, with the changes $(x, y, \dot{x}, \dot{y}) \leftrightarrow (x, -y, -\dot{x}, \dot{y})$, and the same occurs for the outer ones.

Using only the points falling into the slice up to a maximum of 10^5 iterates for all the initial conditions, the results (inner and outer upper transitions) are shown in Figure 3.27 left. The blue points, P_- to the left and P_+ to the right, correspond to the intersections with $x = 0$ of the manifolds of the vpo_L. The point P_- is the first intersection of $W^u_{\text{vpo}_L}$ with $x = 0$, and P_+ is the first intersection of $W^s_{\text{vpo}_L}$ with $x = 0$. The y coordinate of P_- is smaller than the one of P_+. In both cases we refer to the manifolds of vpo_L as seen in Σ. Compare with the section through $x = 0$ of the upper part of the blue curves in Figure 3.26. Note also that in Figure 3.27 we display $y - 1$ as horizontal coordinate, while $\dot{y}$ is used for the vertical one.

To see the behaviour when the number of iterates increases, the right part of Figure 3.27 shows the evolution when we consider iterates in the slice after a maximal number of iterations going from 10^5 to 8×10^5 and, later, to 5×10^6 (from green to blue and then to red). The points are plotted in the reverse order. So, blue points hidden red ones and green points hidden blue ones. In magenta we show the location of P_-. To prevent from too heavy files we take the narrower slice $|x| < 10^{-4}$ and only show iterates when moving in the upper part to the left, that is, upper inner transitions.

It is interesting to display statistics of the process. A simple measure is the evolution of the distance of the iterates to the point P_-, marked in magenta in Figure 3.27 right. We use the slice $|x| < 10^{-3}$ and all the Poincaré iterates (up to 5×10^6 for the 1920 initial points, except for 37 points which escape, after escape is detected). Then we compute the distances $r_{k,i}$ to P_- in the $(y, \dot{y})$ variables, where i is the index of the initial point and k the number of the Poincaré iterate. One takes samples of the $r_{k,i}$ for all the indices i and for ranges of k of the form $((j-1)M, jM]$, $j = 1, \ldots, 100$, with $M = 50,000$. The samples can be labelled by the final value of k. The Figure 3.28 displays, on the left, the behaviour of the average distance as a function of the final value of k in the range of values of k in the sample, while the behaviour of the standard deviation is shown on the right. For these computations both inner transitions (upper and lower) have been taken into account, in order to have larger samples (the total number of inner transitions amounts to 1643007).

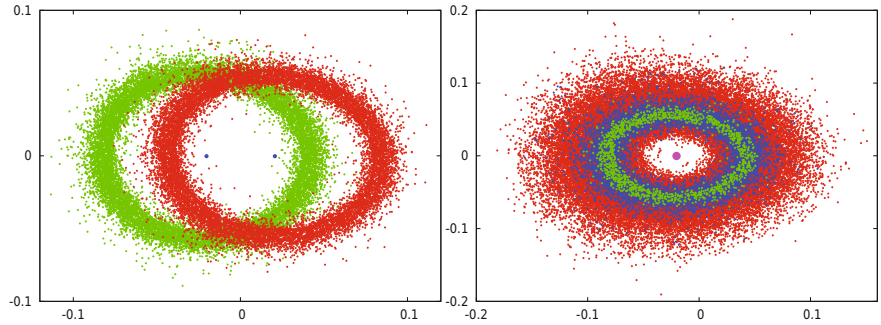

Figure 3.27: For the set of points described in the text we show the $(y-1, \dot{y})$ projections using different slices and times, for $y > 0$ (for $y < 0$ it is similar). *Left:* the slice is defined as $|x| < 10^{-3}$ and we restrict to the first 10^5 Poincaré iterates of the initial points. In green (resp., red) the points when the iterates move to the left (resp., to the right) when looking at them projected on (x, y). We also show the location of $P_{\pm}$, as described in the text. *Right:* points in the upper inner transitions. In red (resp., blue, green) we plot the points on the slice for a number of Poincaré iterates up to 5×10^6 (resp., up to 8×10^5, up to 10^5).

The results deserve some discussion. We can consider a diffusion process but, as the rate of diffusion is related to the passage from some 2D torus (invariant curve in the Poincaré section) to a nearby one, from the comments preceding Figure 3.25, the rate of diffusion is not constant. It increases going away from the vpo_L and then it decreases again when approaching the hpo_L. From the left plot in Figure 3.28 it seems that the average is still in a range where the diffusion rate is increasing. This asymmetry is what produces the increase of the average. Note that the value of the distance to P_- for the first iterates which fall in the slice has an average of ≈ 0.0597. Concerning the standard deviation, one should mention that it takes a not so small value (≈ 0.005) for $k = 50,000$ (the first displayed point). One of the reasons for this is that, looking at the green points in Figure 3.27, one checks that they are scattered around an ellipse, not a circle. Also, after 50,000 iterates the scattering is non-negligible.

One can mention that a good fit of the data for the standard deviation, as a function of the number of Poincaré iterates, k, is of the form $\sigma \approx c(a_0 + a_1 k + a_2 k^2)^{1/2}$ with $a_0, a_1 > 0$, $a_2 < 0$, and c a small positive constant. The negative character of a_2 should be due to the decrease of the diffusion rate when going to the outer curves in Figure 3.25.

Furthermore, when the distance d to P_- reaches a value d^* less than, but not too far from 0.18, the orbits quickly escape. One can check that the upper part of the unstable manifold of the hpo_L has a first intersection with $x = 0$ on a curve, similar to a circle, for which the distance to P_- takes an average value equal to 0.2. Hence, we can consider this as a diffusion process with varying diffusion rate (first increasing, later decreasing, as a function of the distance to P_-) and with

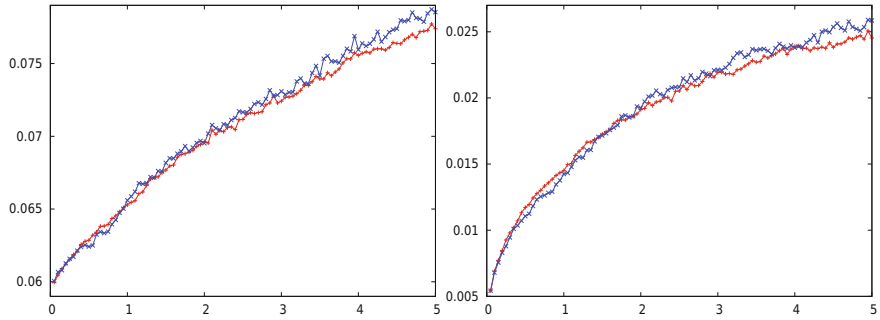

Figure 3.28: The *left* (resp., *right*) plot shows (in red) the evolution of the average (resp., standard deviation) for ranges of k of the form $((j-1)M, jM]$, $j = 1, \ldots, 100$, with $M = 50,000$. The horizontal variable in the plots refers to millions of Poincaré iterates. For comparison, the blue lines show the same results, with a reduced set of initial points, for computations done using quadruple precision. See the text for details.

an absorbing barrier: reaching $d = d^*$ the points disappear from the system.

It is worth commenting also that, as an additional check, preliminary computations concerning diffusion and the related statistics have been carried out using quadruple precision. The size of the sample of initial points has been reduced by a factor of 4. The number of escapes before reaching $N = 5 \times 10^6$ is 9, in good agreement with the previous result. Note that now the samples for the statistics are smaller, which gives slightly larger errors in the determination of average and standard deviation. For comparison, the results are displayed in blue also in Figure 3.28.

Concerning escape, the following experiment has been carried out. A total of 625 initial conditions has been taken in Σ at distances of the order of 10^{-13} from the intersection of the vpo_L with Σ. Poincaré iterates have been computed up to a maximum of 10^9. The first escape is produced after a number of iterates close to 65×10^5. Only 13 points subsist for the full 10^9 iterates, most of them spending a big part of the iterations very close to invariant tori. This is, again, related to the stickiness of these tori. A plot of the number of points which subsist after k iterations, for values of k multiples of 10^7 is shown in Figure 3.29.

Furthermore, taking initial data close to the 9 outermost tori in Figure 3.25 (again using samples of 625 points), one checks that all points escape, and that the average number of iterates for the escape decreases in an exponential way when we approach the outer torus. If the same experiment is done with 625 initial points close to the hpo_L, the result is that all of them escape. In that case, as the orbit lives in $z = 0$, one can count the number of crossings of the orbits through the section $x = 0$, either with $y > 0$ or with $y < 0$, and either with $\dot{x} > 0$ or with $\dot{x} < 0$. The average number of such crossings is 14175. Note that, in contrast with the passage of Poincaré iterates through a slice around $x = 0$, it happens that

there are outer and inner, upper and lower crossings both with $\dot{x} > 0$ and with $\dot{x} < 0$. See [48] for an explanation of this fact.

These results, displayed in Figure 3.29, require a few comments. Up to 64.9 million iterates there is no escape. Only 14 points escape before 10^8 iterates. Then, up to $\approx 3 \times 10^8$ iterates the number of subsisting points is nearly linear in the number of iterates, that is, a rate of decrease close to a constant. Finally, up to $\approx 9 \times 10^8$ the rate of escape is slightly below an exponential one. The last escape was produced around 870 million iterates. To explain these changes is a nice open problem.

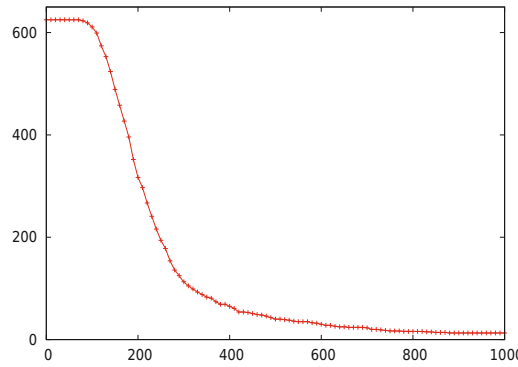

Figure 3.29: Statistics of the number of non-escaping points, starting close to the vpo_L, as a function of the number of Poincaré iterations. For the simulations one has used a sample of 625 initial points. In the horizontal axis the number of iterations is shown in millions.

A basic ingredient for this application is to have an efficient method to compute Poincaré iterates. The steps are the following:

(i) The computation, stability properties and unstable direction of the vpo_L, as fixed point of the Poincaré map, is an easy task. The invariant curves of $\mathcal{P}$ are computed by looking at a representation of the variables $(x, y, \dot{x}, \dot{y})$ as Fourier series in a parametrization angle, using a number of harmonics between 6 and 26, depending on the torus, as explained in Subsection 3.3.3. The symmetries imply that, setting the origin of the angle at the minimal value of x, both x and $\dot{y}$ are even, while y and $\dot{x}$ are odd. In this way, the left plot in Figure 3.25 has been obtained. As a side comment we remark that the rotation numbers are of the order of 10^{-4} and decreasing when going away from the vpo_L. This produces some problems in the condition number of the linear systems to be solved in the Newton iterations.

(ii) The next step is the computation of invariant unstable/stable manifolds of the invariant curves. The reversibility implies that it is enough to compute the unstable ones, the stable being then recovered by the symmetries.

We recall that the manifolds have a parametrization as a function of an angle and a distance to the curve. A fundamental domain is diffeomorphic to a cylinder. Looking for points such that after some number of iterations are on an hyperplane Π requires a continuation method (e.g., to have the starting distance as a function of the angle) or any similar device. This has been used for the right-hand plot in Figure 3.25. The plots in Figure 3.26 follow immediately from the computation of Poincaré iterates.

(iii) To produce Figure 3.27 only requires the computation of Poincaré iterates, detection of the passage through a given slice and whether an inner or outer, upper or lower passage occurs. These are elementary tasks, despite the computational cost being high. The statistics can be produced by elementary means.

Note that the difficulties mentioned in item (i), about the smallness of the rotation number, could be expected a priori. The problem in this region of the phase space is a tiny perturbation of the two-body problem in synodical coordinates. If $\mu \to 0$ the limit is the two-body problem, without the singularities which occur in the case of L_1 and L_2 due to the presence of the secondary, which lead, under suitable scaling, to a limit non-integrable case which is Hill's problem, see [35, 49]. Hence, for $\mu \to 0$, the rotation numbers of the ICs like the ones in Figure 3.25 tend to zero. Concretely they are $\mathcal{O}(\mu)$, in contrast with the hyperbolicity at L_3 and also at the ICs, the vpo_L and the hpo_L, which is $\mathcal{O}(\sqrt{\mu})$. The possible resonances are of a so high order that they become undetectable. The diffusion comes only from the effect of the heteroclinic connections of the manifolds of these ICs. The situation is more complex if there is also a relevant amount of hyperbolicity in the centre manifold itself. See related topics in [13].

Summarizing: one has good evidence of the existence of diffusion associated to the centre manifold of L_3 on levels of the Jacobi constant not too far from the value at that point. Certainly one can produce escape, due to the effect of the secondary and even for μ as small as 0.0002, but the escape time is large. Anyway, there are many topics which require further research.

Acknowledgments

Some of the topics presented in this Chapter have been partially supported by grants MTM2010-16425 and MTM2013-41168-P (Spain), 2009 SGR 67 and 2014 SGR 1145 (Catalonia). The author is grateful to the Centre de Recerca Matemàtica where he was staying during the preparation of the written version of these lectures.

Bibliography

[1] I. Baldomà and À. Haro. "One dimensional invariant manifolds of Gevrey type in real-analytic maps". *Discrete Contin. Dyn. Syst. Ser. B* **10** (2008), 295–322.

[2] X. Cabré, E. Fontich and R. de la Llave. "The parameterization method for invariant manifolds I: Manifolds associated to non-resonant subspaces". *Indiana Univ. Math. J.* **52** (2) (2003), 283–328.

[3] X. Cabré, E. Fontich and R. de la Llave. "The parameterization method for invariant manifolds II: Regularity with respect to parameters". *Indiana Univ. Math. J.* **52** (2) (2003), 329–360.

[4] X. Cabré, E. Fontich and R. de la Llave. "The parameterization method for invariant manifolds III: Overview and applications". *J. Differential Equations* **218** (2) (2005), 444–515.

[5] A. Chenciner, J. Gerver, R. Montgomery and C. Simó. "Simple Choreographic Motions of N Bodies: A Preliminary Study". In *Geometry, Mechanics and Dynamics*, P. Newton, P. Holmes, A. Weinstein, editors, pp. 287–308, Springer-Verlag, 2002.

[6] A. Chenciner and R. Montgomery. "A remarkable periodic solution of the three-body problem in the case of equal masses". *Ann. of Math.* (2) **152** (3) (2000), 881–901.

[7] B.V. Chirikov, "A universal instability of many-dimensional oscillator systems". *Phys. Rep.* **52** (5) (1979), 264–379.

[8] P.M. Cincotta, C.M. Giordano and C. Simó. "Phase space structure of multidimensional systems by means of the Mean Exponential Growth factor of Nearby Orbits". *Physica D* **182** (2003), 151–178.

[9] A. Delshams and P. Gutiérrez. "Effective stability and KAM theory". *J. Differential Equations* **128** (2) (1996), 415–490.

[10] E. Fontich and C. Simó. "The Splitting of Separatrices for Analytic Diffeomorphisms". *Ergod. Th. & Dynam. Sys.* **10** (1990), 295–318.

[11] E. Fontich and C. Simó. "Invariant Manifolds for Near Identity Differentiable Maps and Splitting of Separatrices". *Ergod. Th. & Dynam. Sys.* **10** (1990), 319–346.

[12] V. Gelfreich and C. Simó. "High-precision computations of divergent asymptotic series and homoclinic phenomena". *Discrete and Continuous Dynamical Systems B* **10** (2008), 511–536.

[13] V. Gelfreich, C. Simó and A. Vieiro. "Dynamics of $4D$ symplectic maps near a double resonance". *Physica D* **243** (2013), 92–110.

[14] A. Giorgilli, A. Delshams, E. Fontich, L. Galgani and C. Simó. "Effective stability for a Hamiltonian system near an elliptic equilibrium point, with an application to the restricted three body problem". *J. Diff. Eq.* **77** (1989), 167–198.

[15] G. Gómez, A. Jorba, J. Masdemont and C. Simó. *"Dynamics and Mission Design Near Libration Points. Volume 3: Advanced Methods for Collinear Points"*. World Sci. Pub., Monograph Ser. Math. Vol. 4, Singapore, xiv+187 pp., 2000.

[16] G. Gómez, A. Jorba, J. Masdemont and C. Simó. *"Dynamics and Mission Design Near Libration Points. Volume 4: Advanced Methods for Triangular Points"*. World Sci. Pub., Monograph Ser. Math. Vol. 5, Singapore, xii+262 pp., 2000.

[17] G. Gómez, J. Llibre, R. Martínez and C. Simó. *"Dynamics and Mission Design Near Libration Points. Volume 1: Fundamentals: The Case of Collinear Libration Points"*. World Sci. Pub., Monograph Ser. Math. Vol. 2, Singapore, xx+442 pp., 2001.

[18] G. Gómez, J. Llibre, R. Martínez and C. Simó. *"Dynamics and Mission Design Near Libration Points. Volume 2: Fundamentals: The Case of Triangular Libration Points"*. World Sci. Pub., Monograph Ser. Math. Vol. 3, Singapore, xii+146 pp., 2001.

[19] J.M. Greene, "A method for determining stochastic transition". *J. Math. Phys.* **6** (20) (1976), 1183–1201.

[20] M. Hénon, "Numerical study of quadratic area-preserving mappings". *Quart. Appl. Math.* **27** (1969), 291–312.

[21] M. Hénon and C. Heiles. "The applicability of the third integral of motion: Some numerical experiments". *Astronomical J.* **69** (1964), 73–79.

[22] À. Jorba and Maorong Zou. "A software package for the numerical integration of ODE's by means of high-order Taylor methods". *Experiment. Math.* **14** (1) (2005), 99–117.

[23] À. Jorba and E. Olmedo. "On the computation of reducible invariant tori on a parallel computer". *SIAM J. Appl. Dyn. Syst.* **8** (4) (2009), 1382–1404.

[24] T. Kapela and C. Simó. "Computer assisted proofs for nonsymmetric planar choreographies and for stability of the Eight". *Nonlinearity* **20** (2007), 1241–1255.

[25] F. Ledrappier, M. Shub, C. Simó and A. Wilkinson. "Random versus deterministic exponents in a rich family of diffeomorphisms". *J. Stat Phys.* **113** (2003), 85–149.

[26] R.S. MacKay. "A renormalisation approach to invariant circles in area-preserving maps". *Physica D* **7** (1-3) (1983), 283–300.

[27] R.S. MacKay. *"Renormalisation in area-preserving maps"*. Advanced Series in Nonlinear Dynamics, 6. World Scientific. 1992.

[28] R. Martínez and C. Simó. "The invariant manifolds at infinity of the RTBP and the boundaries of bounded motion". *Regular and Chaotic Dynamics* **19** (2014), 745–765.

[29] J. Mather. "Minimal measures". *Comment. Math. Helv.* **64** (1989), 375–394.

[30] J. Mather. "Action minimizing invariant measures for positive definite Lagrangian systems". *Math. Z.* **207** (1991), 169–207.

[31] R. McGehee. "A stable manifold theorem for degenerate fixed points with applications to Celestial Mechanics". *J. Differential Equations* **14** (1973), 70–88.

[32] N. Miguel, C. Simó and A. Vieiro. "On the effect of islands in the diffusive properties of the standard map, for large parameter values". *Foundations of Computational Mathematics* **15** (2014), 89–123.

[33] C. Moore. "Braids in Classical Gravity". *Physical Review Letters* **70**, (1993), 3675–3679.

[34] J.J. Morales, J.P. Ramis and C. Simó. "Integrability of Hamiltonian Systems and Differential Galois Groups of Higher Variational Equations". *Annales Sci. de l'ENS* 4^e série **40** (2007), 845–884.

[35] J.J. Morales, C. Simó and S. Simón. "Algebraic proof of the non-integrability of Hill's Problem". *Ergodic Theory and Dynamical Systems* **25** (2005), 1237–1256.

[36] A. Neishtadt, "The separation of motions in systems with rapidly rotating phase". *J. Appl. Math. Mech.* **48** (1984), 133–139.

[37] N.N. Nekhorosev, "An exponential estimate of the time of stability of nearly-integrable Hamiltonian systems". *Russian Mathematical Surveys* **32** (6) (1977), 1–65.

[38] A. Olvera and C. Simó. "An obstruction method for the destruction of invariant curves". *Physica D* **26** (1987), 181–192.

[39] J. Sánchez, M. Net and C. Simó. "Computation of invariant tori by Newton–Krylov methods in large-scale dissipative systems". *Physica D* **239** (2010), 123–133.

[40] C. Simó. "Analytical and numerical computation of invariant manifolds". In *"Modern methods in Celestial Mechanics"*, D. Benest and C. Froeschlé, editors, pp. 285–330, Editions Frontières, 1990.

[41] C. Simó. "Averaging under fast quasiperiodic forcing". In Proceedings of the NATO-ARW *"Integrable and chaotic behaviour in Hamiltonian Systems"* (Torun, Poland, 1993), I. Seimenis, editor, pp. 13–34, Plenum Pub. Co., New York, 1994.

[42] C. Simó. "Effective Computations in Celestial Mechanics and Astrodynamics". In *"Modern Methods of Analytical Mechanics and their Applications"*, V.V. Rumyantsev and A.V. Karapetyan, editors, CISM Courses and Lectures **387**, 55–102, Springer, 1998.

[43] C. Simó. "Invariant Curves of Perturbations of Non Twist Integrable Area Preserving Maps". *Regular and Chaotic Dynamics* **3** (1998), 180–195.

[44] C. Simó. "Dynamical properties of the figure eight solution of the three-body problem". In *"Proceedings of the Celestial Mechanics Conference dedicated to D. Saari for his 60th birthday"* (Evanston, 1999), A. Chenciner et al., editors, *Contemporary Mathematics* **292** (2000), 209–228.

[45] C. Simó. "New families of Solutions in N–Body Problems". In *"Proceedings of the 3-rd European Congress of Mathematics"*, C. Casacuberta, R. M. Miró-Roig, J. Verdera, S. Xambó, editors, *Progress in Mathematics series* **201** (2001), 101–115 (Birkäuser, Basel).

[46] C. Simó. "Some properties of the global behaviour of conservative low dimensional systems". In *"Foundations of Computational Mathematics"* (Hong Kong, 2008), F. Cucker et al. editors, pp. 163–189, London Math. Soc. Lecture Notes Series **363**, Cambridge Univ. Press, 2009.

[47] C. Simó. "Measuring the total amount of chaos in some Hamiltonian Systems". *Discrete and Continuous Dynamical Systems A* **34** (2014), 5135–5164.

[48] C. Simó, P. Sousa-Silva and M. Terra. "Practical Stability Domains near $L_{4,5}$ in the Restricted Three-Body Problem: Some preliminary facts". In *Progress and Challenges in Dynamical Systems* **54** (2013), 367–382.

[49] C. Simó and T. Stuchi. "Central Stable/Unstable Manifolds and the destruction of KAM tori in the planar Hill problem". *Physica D* **140** (2000), 1–32.

[50] C. Simó and D. Treschev. "Stability islands in the vicinity of separatrices of near-integrable symplectic maps". *Discrete and Continuous Dynamical Systems B* **10** (2008), 681–698.

[51] C. Simó and C. Valls. "A formal approximation of the splitting of separatrices in the classical Arnold's example of diffusion with two equal parameters", *Nonlinearity* **14** (2001), 1707–1760.

[52] C. Simó and A. Vieiro. "Resonant zones, inner and outer splittings in generic and low order resonances of Area Preserving Maps". *Nonlinearity* **22** (2009), 1191–1245.

[53] C. Simó and A. Vieiro. "Dynamics in chaotic zones of area preserving maps: close to separatrix and global instability zones". *Physica D* **240** (2011), 732–753.

Some classical books:

- V.I. Arnold. *"Les méthodes mathématiques de la mécanique classique"*. Éditions Mir, Moscow, 1976.
- V.I. Arnold and A. Avez. *"Problèmes ergodiques de la mécanique classique"*. Gauthier-Villars, Paris 1967.
- M.W. Hirsch, C.C. Pugh and M. Shub. *"Invariant Manifolds"*. Lecture Notes in Mathematics **583**, Springer-Verlag, Heidelberg, 1977.
- J.K. Moser. *"Stable and random motions in Dynamical Systems: with special emphasis on Celestial Mechanics"*, Princeton University Press, Princeton, 1973.
- C.L. Siegel and J.K. Moser. *"Lectures on Celestial Mechanics"*. Die Grundlehren der mathematischen Wissenschaften, Band 187. Springer-Verlag, New York-Heidelberg, 1971.

Slides of several talks:

(A) *"Taylor method for the integration of ODE"*, number 8.
http://www.maia.ub.es/dsg/2007/.

(B) *"Some properties of the global behaviour of conservative low dimensional systems"*, number 3.
http://www.maia.ub.es/dsg/2008/.

(C) *"On the role of Dynamical Systems in Celestial Mechanics"*, number 4.
http://www.maia.ub.es/dsg/2010/.

(D) *"Domains of Practical Stability near $L_{4,5}$ in the 3D Restricted Three-Body Problem"*, number 8.
http://www.maia.ub.es/dsg/2012/.

(E) *"Quadratic Area Preserving Maps in R^2"*, number 5.
http://www.maia.ub.es/dsg/2013/.

(F) *"The dances of the N bodies"*, number 7.
http://www.maia.ub.es/dsg/2013/.

(G) *"The role of Michel Hénon in detecting regular and chaotic dynamics in conservative systems"*, number 8.
http://www.maia.ub.es/dsg/2013/.

(H) *"Measure of the chaotic domain in simple Hamiltonian systems"*, number 7.
http://www.maia.ub.es/dsg/2014/.

(I) *"Splitting, return maps and confined motion in the planar RTBP: Theory and praxis"*, number 1.
http://www.maia.ub.es/dsg/2015/.

(J) *"Experiments looking for theoretical predictions"*, number 2.
http://www.maia.ub.es/dsg/2015/.